Departament de Ciències Experimentals i de la Salut
Facultat de Ciències de la Salut i de la Vida
Universitat Pompeu Fabra

Characterization of the role of the CPEB family of RNA-binding proteins in neurodegeneration

Héctor Anta Rodríguez

TESI DOCTORAL UPF / 2016

Dissertation presented to obtain the degree of Doctor of Philosophy.

This work was carried out under the supervision of Dr. Pilar Navarro Medrano and Dr. Raúl Méndez de la Iglesia, in the Institut Hospital del Mar d'Investigacions Mèdiques (IMIM), and the Institute for Research in Biomedicine (IRB Barcelona).

Dr. Pilar Navarro Medrano   Dr. Raúl Méndez de la Iglesia   Héctor Anta Rodríguez
(Thesis co-director)   (Thesis co-director)   (PhD candidate)

A mis padres, por su cariño y apoyo incondicional

A mi abuela Nati y mi tío Jose, por haber tenido la suerte de teneros en mi vida

Acknowledgements

Dejando la ciencia a un lado, me gustaría dedicarle esta tesis a mi pequeña gran familia del PRBB (y fuera del PRBB), tanto a todos los que pasasteis por mi vida en los primeros años como a los que seguís estando aquí. Con vosotros he vivido mil y una aventuras (¡y sigo haciéndolo!). Habéis sido como una segunda familia, de verdad. Se podría decir que con vosotros el experimento siempre salía porque ¡vosotros siempre habéis sabido cómo activar mis terminales sinápticos!. Vera, Rius, Cindy, Adrien, Bing, Quique, Charlie, Rosh, Nancy, Eva, Irene, David, Albert, Marta, Judith... ¡Gracias por estos 4 años!

Eva, esta tesis no habría sido lo mismo sin ti. Gracias por tu esfuerzo y paciencia, por haber estado siempre ahí y por toda tu comprensión, cariño y ayuda constante, tanto científica como emocionalmente. Gracias por ser como tú eres y por haber recorrido este camino junto a mí. He tenido que esperar un año para contestarte... Y te digo que sí... Tu también has estado a la altura en mi tesis, ¡y mucho más!.

Gracias a Montse, Jose y Paqui (SCT IMIM) por todo lo que me habéis ayudado y por hacerme reír cada día de una forma diferente; a Carmen, por ser de esas personas entrañables que saben hacerse querer; y a Sonia, por saber cómo echarme del laboratorio cuando se hacían las 8 de la tarde "en punto".

No podía olvidarme de vosotros, "Los Guitarrones". La verdad es que da gusto haber podido crecer rodeado de todos y cada uno de vosotros. Carlos, Diego, Adrián, Pepe, Bea, Héctor... Gracias. No podría haber imaginado una compañía mejor que la vuestra durante tantos años. Sanabria lleva vuestro nombre. Sin vosotros no habría sido lo mismo.

Lotillo "Murray", qué decir que no sepas... Has sido un apoyo insustituible desde que alcanza mi memoria... No tengo palabras para expresar cuánto valoro una amistad como la tuya. Podría escribir un libro más largo que esta tesis (quizá dos) con todo lo que he vivido contigo. Muchas gracias por haber estado, y seguir estando, siempre ahí.

Con cariño a mis "Sésiles", así como a Suso, Bárbara y Unai. Gracias por un montón de recuerdos que atesoro, así como por los buenos momentos que me habéis seguido dando durante este PhD, aunque estemos algo desperdigados.

Mónica, Iván, Gonzalo, Raquel... Lo malo de haberme ido a Barcelona es que he tenido que dejar en Madrid a personas tan maravillosas como vosotros. Aunque hayamos estado algo separados físicamente, habéis estado ahí y habéis sido una parte muy importante de esta tesis. ¡Gracias!

A Rafa y María. Nunca podré agradeceros lo suficiente la suerte que tengo de teneros, todo lo que me habéis ayudado y lo bien que me habéis acogido. Soy fan vuestro, ya os lo he dicho muchas veces. ¡No cambiéis!

Por último, a toda mi familia, en especial a mis padres Ángel y Montse, así como a Mary, Eugenio, Patricia, mis abuelos Celso y Nati y sobre todo a mi tío Jose. Cada uno de vosotros me habéis inspirado de una forma diferente y muy especial, y si a alguien le tengo que dedicar este trabajo, sin duda alguna es a vosotros. Gracias por vuestro apoyo emocional incondicional, por todos los buenos momentos que me habéis hecho pasar, y sencillamente por haber sido como solo vosotros sabéis ser. La verdad es que he tenido una gran suerte por haberos tenido en mi vida. Todo lo que soy, sin duda alguna os lo debo a vosotros. Nunca sabré agradecéroslo lo suficiente. ¡Gracias!

Abbreviations

3'-UTR: 3'-untranslated region

5'-UTR: 5'-untranslated region

Aβ: amyloid beta

ABCE1: ATP binding cassette subfamily E member 1.

ActD: actinomycin D

AD: Alzheimer's disease

AMPA: α-amino-3-hydroxy-5-methyl-4-isoxazol propionic acid

APA: alternative cleavage and polyadenylation

APP: amyloid precursor protein

Arc: activity-regulated cytoskeleton associated protein

ARE: AU-rich element

A site: acceptor site

ASP: Anchor-specific primer

BACE1: beta-site APP cleaving enzyme 1

BDNF: brain-derived neurotrophic factor

BSA: bovine serum albumin

CA3: cornu ammonis 3

CaMKII: Ca^{2+}/calmodulin dependent protein kinase II

CD: cordycepin

CDS: coding sequence

CFIm: pre-mRNA cleavage factor I

CFIm25: pre-mRNA cleavage factor I 25 kDa subunit

CFIm68: pre-mRNA cleavage factor I 68 kDa subunit

CFIIm: pre-mRNA cleavage factor II

CHX: cycloheximide

Clp1: pre-mRNA cleavage complex II protein Clp1

CNS: central nervous system

CPE: cytoplasmic polyadenylation element

CPEB: cytoplasmic polyadenylation element binding

CPSF: cleavage and polyadenylation specificity factor

CREB1: cAMP responsible element binding protein 1

CSF: Cerebrospinal fluid

CSTF: cleavage stimulation factor

CTD: C-terminal domain

CX: cortex

DG: dentate gyrus

DSE: downstream sequence element

E17.5: embryonic day 17.5

ECM: extracellular matrix

eEF: eukaryotic elongation factor

eIF: eukaryotic initiation factor

E-LTP: early phase long term potentiation

EOAD: early-onset Alzheimer's disease

eRF: eukaryotic release factor

E site: exit site

EST: expressed sequence tag

FXS: fragile X syndrome

GMP: guanosine Monophosphate

GTP: guanosine triphosphate

HP: hippocampus

IF: immunofluorescence

IHF: immunohistofuorescence

IRES: internal ribosome entry site

KI: knock-in

KO: knock-out

LCD: low complexity domain

L-LTP: late phase long term potentiation

LOAD: late-onset Alzheimer's disease

LTD: long-term depression

LTP: long-term potentiation

m^{7}GpppN: methylguanosine

MAPK: mitogen-activated protein kinase

MEF: murine embryonic fibroblast

miRNA: microRNA

MMP: matrix metalloproteinase

mRNA: messenger RNA

MTT: 3-(4,5-dimethylthiazol-2-yl)-2,5-diphenyltetrazolium bromide

NES: nuclear export signal

NFTs: neurofibrillary tangles

NLS: nuclear localization signal

NMDA: N-methyl-D-aspartate

NTD: N-terminal domain

PA: plasminogen activator

PABP: polya(A)-binding protein

PAI-1: plasminogen activator inhibitor 1

PAP: poly(A) polymerase

PAS: poly(A) signal

PAT assay: poly(A) tail length assay

PBS: phosphate buffererd saline

Pcf11: pre-mRNA cleavage complex II protein Pcf11

PKA: protein kinase A

PSD95: post-synaptic density protein 95

PSEN1: presenilin 1

PSEN2: presenilin 2

P site: peptidyl site

RACE: rapid amplification of cDNA ends

RBP: RNA-binding protein

RNA Pol II: RNA polymerase II

RRM: RNA recognition motif

SAM: S-adenosylmethyonine

SD: standard deviation

SEM: standard error of the mean

TBS: Tris buffered saline

tPA: tissue-type plasminogen activator

uAUG: upstream AUG codon

uORF: upstream open reading frame

uPA: urokinase-type plasminogen activator

uPAR: uPA receptor

USE: upstream element

WB: western blot

WT: wild type

ZZ domain: Zinc-binding domain

Abstract

Alzheimer's disease (AD) is the most common type of dementia in the elderly. It is associated to a progressive loss of memory, problems in learning and behaviour changes. This disease is characterized by the accumulation of extracellular amyloid β (Aβ) aggregates and intracellular deposits of hyperphosphorylated Tau protein. Both aggregates trigger neuronal apoptosis and glial inflammation, leading to the cognitive decline found in AD patients. Interestingly, the serine protease tissue plasminogen activator (tPA), which is induced by Aβ, has been found to play a dual, dose-dependent role in the disease. Physiological levels of tPA confers neuroprotection through plasmin generation and Aβ degradation. In contrast, high doses of tPA activate intracellular signalling pathways in neurons and glial cells, inducing neuronal apoptosis and inflammation. However, the molecular mechanisms that govern the regulation of tPA expression in AD have still not been fully elucidated. In this work, we demonstrate that Aβ-induced tPA expression is regulated by translational control. In particular, our results show that CPEB1 and CPEB4, two members of the cytoplasmic polyadenylation element binding protein (CPEB) family of RNA-binding proteins, control local tPA synthesis in response to Aβ. Specifically, Aβ promotes tPA mRNA translation in the dendritic spines through synaptic polyadenylation and synaptic cleavage and polyadenylation, a mechanism that is impaired in the absence of CPEB1 or CPEB4. Our results also demonstrate that the pre-mRNA 3'-end processing machinery required for the efficient cleavage and polyadenylation of mRNAs is also present in the synaptic terminals. Finally, we have found that, similarly to tPA, CPEB4 is upregulated in the synaptic terminals in response Aβ and *in vivo* in the brain of AD patients.

Resumen

La enfermedad de Alzheimer (EA) es la demencia más común en la tercera edad. Está asociada a una pérdida progresiva de memoria, problemas de aprendizaje y cambios de comportamiento. Esta enfermedad se caracteriza por la acumulación de agregados extracelulares de proteína β-amiloide (Aβ) y depósitos intracelulares de proteína Tau hiperfosforilada. Ambos agregados inducen apoptosis neuronal e inflamación mediada por las células de la glia, lo cual desencadena el declive cognitivo característico de los enfermos de EA. En este sentido, se ha demostrado que una serina proteasa, el activador del plasminógeno tisular (del inglés "tissue plasminogen activator", tPA), cuya expresión se induce por Aβ, juega un doble papel clave en la enfermedad en función de sus niveles. Por un lado, unos niveles fisiológicos de tPA pueden ser neuroprotectores a través de la generación de plasmina, con la consiguiente degradación del Aβ. Por otro lado, unos niveles altos de tPA activan cascadas de señalización intracelular en neuronas y células de la glia, lo que induce apoptosis neuronal e inflamación. Los mecanismos moleculares que rigen la regulación de la expresión de tPA en la EA no se conocen con claridad. En este trabajo, demostramos que la expresión de tPA inducida por Aβ está regulada por control traduccional. En concreto, nuestros resultados muestran que CPEB1 y CPEB4, dos miembros de la familia CPEB de proteínas de unión a RNA (del inglés "cytoplasmic polyadenylation element binding, CPEB), controlan la síntesis de tPA en respuesta a Aβ. Concretamente, el Aβ promueve la traducción del ARNm de tPA en las espinas sinápticas a través de poliadenilación sináptica, y procesamiento y poliadenilación alternativos sinápticos, un mecanismo que se ve interrumpido en ausencia de CPEB1 o CPEB4. Nuestros resultados también demuestran que la maquinaria de procesamiento de los extremos 3' del pre-ARNm necesaria para llevar a cabo este proceso está presente en los terminales sinápticos. Por último, hemos encontrado que, al igual que tPA, CPEB4 se sobreexpresa en los terminales sinápticos en respuesta a Aβ, así como en el cerebro de pacientes con EA.

TABLE OF CONTENTS

INTRODUCTION

1. General mechanisms for gene expression regulation

1.1. The transcription process and the importance of the CTD of RNA Pol II

Eukaryotic gene expression is a tightly controlled process. The expression of protein-coding genes starts with the synthesis of the pre-mRNA by the RNA Polymerase II (RNA Pol II). During transcription, a cap is added to the mRNA in the 5'-end, the introns are removed in the process of splicing and its 3'-end is cleaved and polyadenylated, a process which is known to be coordinated by the C-terminal domain (CTD) of the RNA Pol II. Finally, the mRNA is transported to the cytoplasm, where it will be translated into protein. However, as we will discuss in next sections, this process is not so simple, as the newly generated mRNAs can have other fates, such as subcellular localization, degradation or translational repression.

The RNA Pol II is a protein complex of 12 subunits. Its largest subunit, Rbp1, contains a unique CTD, consisting of a repetition of 7 residues in tandem, Tyr^1-Ser^2-Pro^3-Thr^4-Ser^5-Pro^6-Ser^7 (Corden et al., 1985) with increased number of repetitions depending on the organism's complexity, ranging from 26 in yeast (Allison et al., 1985) to 52 in mammals (Corden et al., 1985). In general, the heptapeptides can be phosphorylated at 5 different positions in different combinations depending on the transcriptional state of the RNA Pol II, (pre-initiation, initiation, elongation or termination). When the RNA polymerase is in the pre-initiating stage, its CTD is not phosphorylated (Laybourn and Dahmus, 1989). However, the transcriptionally active RNA Pol II goes through different phosphorylation stages. The generalized model of CTD modification proposes that during initiation, Ser5 is phosphorylated by CDK7, a member of the TFIIH complex. As the mRNA is elongated, Ser2 is phosphorylated by CDK9 or pTEFb, while phosphatases gradually remove the phosphorylations from Ser5. As a result, in the initiation steps the CTD is mainly phosphorylated in Ser5 and

during elongation in both Ser2 and Ser5. Finally, during the termination steps, the CTD is phosphorylated in Ser2 only **(Figure 1)** (for review, see Egloff and Murphy, 2008). However, other modifications, such as Ser7 modifications have been identified (Chapman et al., 2007; Egloff et al., 2007).

In addition to the roles in the regulation of mRNA transcription, the CTD of the RNA Pol II is known, depending on its phosphorylation state, to serve as a loading platform to mRNA processing factors as RNA Pol II elongates the mRNA (reviewed in Hsin and Manley, 2012). Therefore, coupled to transcription, the mRNA will be processed (McCracken et al., 1997a). This mechanism will be important for the mechanism of 3'-end formation and alternative cleavage and polyadenylation, which will be discussed later on in this chapter.

Once transcribed and processed, the mature mRNA, bound to multiple RNA-binding proteins (RBPs), will be transported to the cytoplasm, where it will be translated, localized, stored or degraded, depending on the RBPs bound to it. This will be determined by *cis*-acting regulatory elements present in the mRNA. The structure of the mRNA, as well as different *cis*-acting regulatory elements it may contain, will be discussed in the following sections.
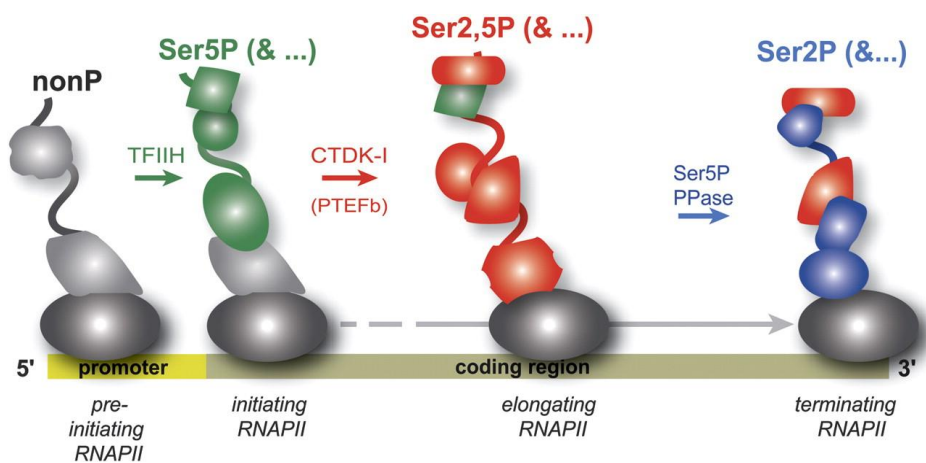
Figure 1. The phosphorylation pattern of RNA Pol II CTD changes during transcription. Schematic representation of the different phosphorylations of RNA Pol II (grey oval). Ser5P modifications are shown in green, double Ser2P and Ser5P in red, and Ser5P in blue (see text for more details). Image taken from Phatnani and Greenleaf, 2006.

4

1.2. The structure of mRNA

As previously mentioned, mRNA is synthesized from DNA in the nucleus as a pre-mRNA. Then, in order to acquire its mature structure, a cap of 7-methyl guanosine is added to the 5'-end, the introns are removed by the spliceosome, and finally, the 3'end is cleaved and polyadenylated by the cleavage and polyadenylation machinery. The main functional elements present in the newly generated mRNA, from 5'-end to 3'-end are: the 7-methylguanosine cap (m^{7}GpppN), the 5'-Untranslated region (5'-UTR), the coding sequence (CDS), the 3'-Untranslated Region (3'-UTR) and the poly(A) tail (**Figure 2**). Moreover, the 5'-UTR and the 3'-UTR contain *cis*-acting elements that will be recognized by different RBPs. The structure of the RNA, some of these *cis*-acting elements present on it, as well as how they are generated, are further detailed in next sections of this chapter.
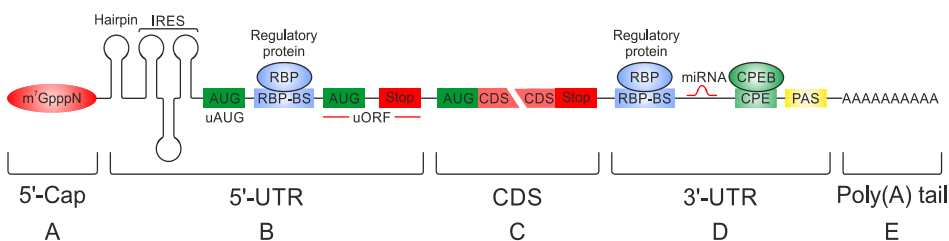
Figure 2. Major regulatory elements of the mRNA. *Structure of the mRNA from 5' (left) to 3' (right). (A) The 5'-Cap structure (red oval) is shown. (B) In the 5'-UTR, hairpin structures that can negatively affect translation are shown first, followed by an Internal ribosome entry site (IRES), that can mediate CAP-independent translation. The 5'-UTR also contains upstream AUGs (uAUGs, dark green) and upstream Open Reading Frames (uORF, from a uAUG, to a stop codon shown in red), which negatively affect translation by recruiting ribosomes upstream the CDS. Finally, RNA Binding Protein Binding Sites (RBP-BS) recognized by RBPs (shown in blue) can be found. (C) The coding sequence (CDS) is the ORF of the mRNA sequence that is translated into protein, which starts with an AUG codon and finishes in a stop codon. The CDS was split in two parts to make it shorter. (D) The 3'-UTR contains RBP binding sites (RBP-BS, in blue) and binding sites for micro RNAs (miRNA, red curves). One specific RBP-BS is the CPE that is recognized by CPEB (in green). Finally, the end of the 3'-UTR usually contains at least one poly(A) signal (PAS, shown in yellow), which is recognized by the cleavage and polyadenylation machinery, which cleaves the mRNA and produces the poly(A) tail. (E) The poly(A) tail is shown. For simplicity, only 10A are shown.*

1.2.1. The 5'-Cap, the 5'-UTR and the coding sequence

The 5'-Cap

Coupled to transcription, when the mRNA is only around 25 nucleotides long, the cap machinery adds a 7-methylguanosine (m^7GpppN) cap to the first transcribed nucleotide in the 5'-hydroxyl group (Rasmussen and Lis, 1993) (**Figure 2A**). This capping occurs in three steps. First, a RNA triphosphatase removes the γ phosphate of the first nucleotide (pppN, being N the nucleotide and p the phosphates) of the nascent mRNA (generating ppN). Then, a RNA guanyliltransferase uses guanine triphosphate (GTP) as a substrate and transfers a guanine monophosphate (GMP) group to the cap (generating GpppN). Finally, a mRNA (guanine-N7) methyltransferase transfers a methyl group from S-adenosylmethyonine (SAM) to the N7 position of the guanine (generating m^7GpppN) (Shuman, 1995). This process requires the RNA Pol II CTD to be phosphorylated in Ser5 (Cho et al., 1997; Ho et al., 1998; McCracken et al., 1997b).

The presence of the cap is not only critical for ensuring the stability of the mRNA (Furuichi et al., 1977; Shimotohno et al., 1977). It has also been reported to be necessary for the processes of splicing (Edery and Sonenberg, 1985; Inoue et al., 1989; Izaurralde et al., 1994; Konarska et al., 1984; Ohno et al., 1987), cleavage and polyadenylation (Cooke and Alwine, 1996; Flaherty et al., 1997; Gilmartin et al., 1988), transport to the cytoplasm (Hamm and Mattaj, 1990; Izaurralde et al., 1995) and translation (Both et al., 1975; Muthukrishnan et al., 1975; Rhoads, 1988; Shatkin, 1985).

The 5'-UTR

The 5'-UTR is located upstream the coding sequence. The main regulatory elements present in the 5'-UTR are: secondary structures (loops), binding sites for RNA binding proteins, and upstream initiation codons and open reading frames (uAUGs and uORFs, respectively) (**Figure 2B**).

6

Secondary structures (hairpins) are major 5' regulatory elements. They are usually located near the cap and are very effective in inhibiting translation (more effective the closer to the cap they are) by limiting the access of the preinitiating complex to the mRNA. Additionally, special secondary structures called Internal Ribosome Entry Site (IRES) may also mediate cap-independent translation.

The 5'-UTR also contains sequences that are recognized by RNA-Binding proteins (RBPs), either the ones found in the general translation machinery, or others that selectively target specific mRNAs, such as Mushasi, HuR or SXL.

Finally, the 5'-UTR may also contain uORFs and uAUGs, which consist of a full ORF or an initiation codon without an in-frame downstream stop codon, both located upstream the main CDS. They mainly affect translation by hampering the access of the ribosome to the main ORF. For review on this section, see Araujo et al., 2012.

<u>The coding sequence</u>

The CDS consists on the sequence that will be translated into protein. It starts from the codon AUG and finishes with one of the three stop codons UAA, UAG or UGA. This coding sequence is flanked by the 5' and 3' untranslated regions (5'-UTR and 3'-UTR) (**Figure 2C**).

1.2.2. The 3'-UTR

The 3'-UTR is located downstream the CDS and contains different sequences that are recognized by RBPs, which in general affect the subcellular localization, stability, translation efficiency or processing of the mRNA. Moreover, the 3'-UTR contains sequences recognized and regulated by microRNAs (miRNAs). Finally, this region also contains critical sequences required for the cleavage and polyadenylation of the pre-mRNA, and also for the translational control

through cytoplasmic polyadenylation, as we will discuss in next chapters (**Figure 2D**) (for review see Matoulkova et al., 2012).

Some of the *cis*-acting sequences present in the 3'-UTR that will be described in detail are the cytoplasmic polyadenylation element (CPE), which is targeted by the cytoplasmic polyadenylation element binding proteins (CPEBs), the poly(A) signal (PAS), the AU-rich elements (AREs), the auxiliary upstream element (USE) and the downstream element (DSE).

It is important to mention that in general, mRNAs with shorter 3'-UTRs can be generated through alternative cleavage and polyadenylation (APA) of the mRNA. In this regard, different RBPs, such as CPEBs or cleavage stimulation factor 64 (CSTF64), can contribute to this process (Bava et al., 2013; Takagaki et al., 1996). Alternative cleavage and polyadenylation is a widespread mechanism of translational regulation that indirectly controls mRNA translation efficiency. Recent studies have demonstrated that when two potential isoforms of the same 3'-UTR are possible, the longer one showed lower translation efficiency. Accordingly, the shorter 3'-UTRs are usually selected by highly proliferative cells (e.g. cancer cells) (Sandberg et al., 2008), while the longer ones, more prone to miRNA or RBP-mediated regulation, are chosen by arrested or more differentiated cells (Ji et al., 2009).

1.2.3. The poly(A) tail and the mechanism of 3'-end formation

During transcription, before mRNA transcripts are released and transported to the cytosol, they are processed at the 3'-end by a two-step mechanism. First, the mRNA is cleaved by an endonucleolytic reaction. Then, a poly(A) polymerase (PAP) adds a poly(A) tail immediately after the cleavage site (**Figure 2E**). This process is critical, because the poly(A) tail promotes the transport of the mRNA to the cytoplasm (Huang and Carmichael, 1996), increases the stability of the mRNA by protecting it from the activity of the 3'-5' nucleases

(Ross, 1995; Sachs, 1990) and enhances translation by interacting with the m^{7}GpppN cap through poly(A)-binding protein (PABP) (Sachs, 1990).

The mechanism of 3'-end formation through cleavage and polyadenylation, which could appear to be simple, actually requires the action of several molecules (at least 14 in mammals), as well as different *cis*-acting signals present in the 3'-UTR of the mRNA.

The first *cis*-acting signal discovered to be associated with 3'-end processing was the PAS (Proudfoot and Brownlee, 1976). It is located in the 3'-UTR, at 10-30 nucleotides upstream the cleavage site. Human expressed sequence tag (EST) analysis revealed that in the vast majority of the mRNAs, it consists on the hexamers AAUAAA (58%) or AUUAAA (15%), even though a significant number of mRNAs may contain other 10 potential non-canonical hexameric PAS (Beaudoing et al., 2000). The second *cis*-acting signal is the DSE. This signal is located downstream the cleavage site and has been observed as a U-rich sequence (UUUUU) (Chou et al., 1994; Gil and Proudfoot, 1987) or a GU-rich element (YGUGUUYY, being Y a pyrimidine) (McLauchlan et al., 1985). The last *cis*-acting signal is the USE. This sequence does not have a specific consensus sequence, but it often consists on a U-rich sequence, UGUA or UAUA (Hu et al., 2005).

There are several proteins and protein complexes required for 3'-end cleavage and polyadenylation (**Figure 3**). RNA Pol II transcribes the mRNA and its CTD serves as a scaffolding platform to different proteins depending on its phosphorylation state as described in section 1.1. Coupled to transcription, the cleavage and polyadenylation specificity factor (CPSF) complex, comprised by CPSF30, CPSF73, CPSF100, CPSF160 and Fip1, recognizes the PAS. The cleavage stimulation factor (CSTF) complex, comprised by CSTF50, CSTF64 and CSTF77, recognizes the DSE. The cleavage factor I (CFIm) complex, comprised by CFIm25 and CFIm68, recognizes the USE (Brown and Gilmartin, 2003). The Cleavage

Factor II (CFIIm) complex, composed by Clp1 and Pcf11, recognizes the CTD of the terminating RNA polymerase (phosphorylated in Ser2 but not phosphorylated in Ser5) (for review see Charlesworth et al., 2013; Elkon et al., 2013; Jurado et al., 2014).

Once the recognition of the *cis*-acting signals takes place, CPSF73 mediates the cleavage and CPSF100 recruits PAP that adds the poly(A) tail, which will be coated by poly(A) binding proteins (PABP) to protect the mRNA from degradation and promote its export and translation (for review see Charlesworth et al., 2013; Elkon et al., 2013; Jurado et al., 2014).
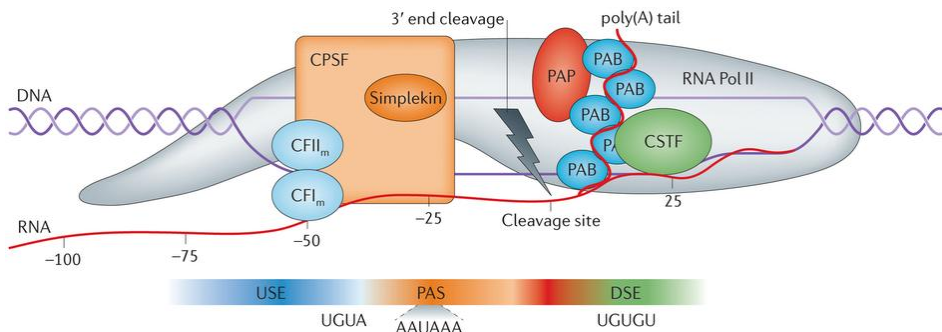
Figure 3. Main complexes, proteins and functions of the 3'-end formation machinery. During transcription, RNA Pol II elongates the mRNA and its CTD serves as a scaffold. The CPSF complex (CPSF30, CPSF 73, CPSF100, CPSF160 and Flp1) recognizes the PAS. The CFIm complex (CFIm25 and CFIm68) recognizes the USE. The CSTF complex (CSTF50, CSTF64 and CSTF77) recognizes the DSE. The CFIIm complex (Clp1 and Pcf11) recognizes the CTD of RNA Pol II. CPSF73 mediates the cleavage, PAP elongates the poly(A) tail and PABP will bind to it. Image taken from (Elkon et al., 2013).

1.3. Molecular mechanisms of mRNA translation

Once the mRNA has been transcribed and processed, it is transported to the cytosol where it will be translated. Translation represents the process by which the mRNA is translated into protein, a tightly controlled process which involves the action of several proteins and protein complexes. The process of translation can be divided in 3 phases: initiation, elongation and termination.
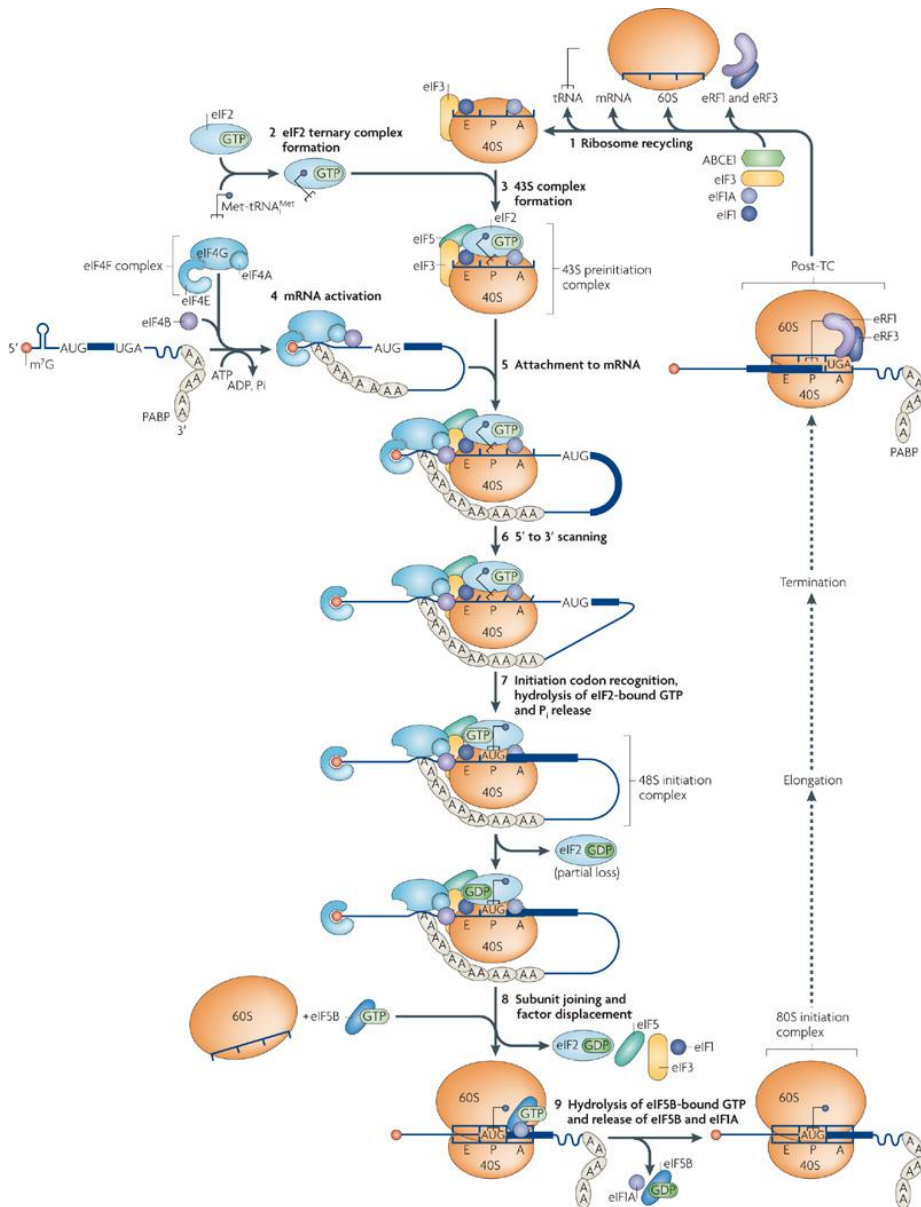
Figure 4. Model of the eukaryotic translation initiation. *In the canonical pathway, the previously used ribosomes are recycled, releasing the 40S and 60S subunits (1). The ternary complex eIF2-GTP-Met-tRNA^Met is formed (2) and located in the P site of the ribosome, together with other eIFs, forming the 43S pre-initiation complex (3). The mRNA is activated in an ATP-dependent manner and the eIF4F complex is formed and targeted to the mRNA (the subunit eIF4E binds the cap and eIF4G PABP) (4). The 43S preinitiation complex binds to the mRNA (5) and scans it (6). When an AUG codon is found, the eIF2-bound GTP is hydrolyzed (7), the eIFs (except eIF1A) will be released and the 60S subunit, together with GTP-eIF5B, will be recruited (8). After the hydrolysis of the eIF5B-bound GTP and the release of eIF5B and eIF5A, the 80S initiation complex is formed and translation starts. Image taken from Jackson et al., 2010.*

11

1.3.1. Initiation

The initiation is the process in which the initiator tRNA (Met-tRNA) and the ribosomal subunits 40S and 60S are positioned on the initiation codon AUG, which signals the beginning of the coding sequence (steps 1-9 from **Figure 4**). In general, initiation is considered the rate-limiting step, and is the preferred step of regulatory intervention in the process of translation.

First, Met-tRNA and GTP-bound eukaryotic initiation factor 2 (eIF2) are loaded onto the 40S ribosomal subunit together with other eIFs (eIF1, eIF1A, eIF3 and eIF5) to form the 43S preinitiation complex. This preinitiation complex will bind to the mRNA by recognizing the m^7GpppN cap (or an IRES loop). Cap recognition is mediated by the interaction of eIF3 with the eIF4F complex, which is comprised by eIF4E (which recognizes and bind the cap), eIF4A (a helicase that favors the binding to the RNA) and eIF4G (a scaffolding protein that keeps together eIF4E, eIF4A and eIF3). eIF4G also interacts with the PABP, forming a closed-loop (**Figure 7**). When the 43S complex binds the mRNA, it scans it until it finds an AUG codon. Then, the eIF5 will catalyze the hydrolysis of the eIF2-bound GTP. This will release the initiation factors (including the GDP-eIF2 that loses affinity after the hydrolysis of the GTP), the small subunit will be displaced one codon forward, and the 60S subunit will bind, forming the translation competent 80S ribosome, leaving the Met-tRNA in the ribosomal P site. Then, translation starts. Finally, eIF2B mediates guanine nucleotide exchange on eIF2, recycling it for next round. (For review, see Gebauer and Hentze, 2004; Jackson et al., 2010; Pestova et al., 2001).

1.3.2. Elongation

In comparison to initiation, the elongation process is relatively simple. During elongation, an aminoacylated tRNA (aa-tRNA) enters the acceptor site (A site) of the ribosome, together with a GTP-bound eukaryotic elongation factor 1 (eEF1). The recognition of the specific codon stimulates GTP hydrolysis and the

12

release of eEF1-GDP from the A site. At the same time, the ribosome suffers a structural change that induces the contact of the 3'-ends of both the aa-tRNA of the A site and the polypeptide-containing tRNA of the peptidyl site (P site). At this point, both peptides shift positions (from A to P and from P to E) and the polypeptide is transferred to the aa-tRNA, therefore increasing the polypeptide length in one amino acid. eEF2-GTP then enters the A site, hydrolyzes the GTP and the ribosome advances one position, being now ready to receive a new aa-tRNA (**Figure 5**) (Dever and Green, 2012; Richter and Coller, 2015).
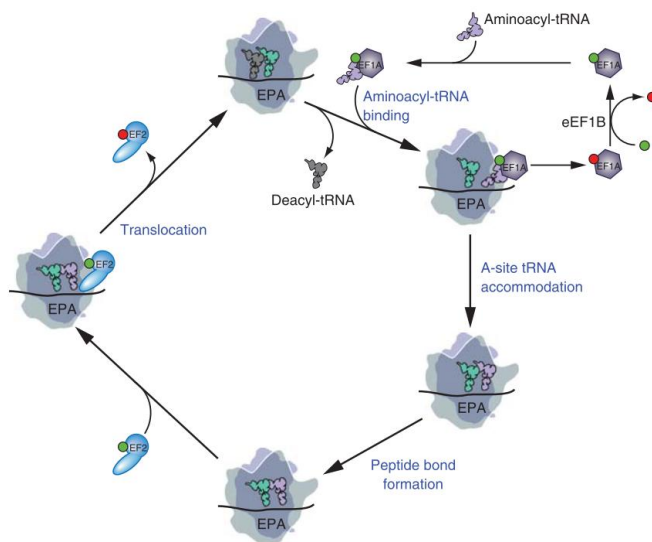
Figure 5. The translation elongation process. *During elongation, an aa-tRNA enters the A site of the ribosome bound to eEF1-GTP. If the codon detected is correct, GTP is hydrolyzed, eEF1 released and the aa-tRNA is accommodated and establish contact with the aa-tRNA of the P site. The tRNAs enter in a hybrid formation in which both acceptor sites of the P and A sites move to the E and P site, respectively, which forms the peptide bond. eEF2-GTP binds and the hydrolysis of its GTP mediates the translocation of the ribosome one position. The ribosome is ready now for a new cycle of translation. Figure taken from Dever and Green, 2012.*

1.3.3. Termination

The termination phase starts when the translating ribosome reaches a stop codon (UAA, UAG or UGA). Then, the ester bond in the peptidyl-tRNA is hydrolyzed and the finished protein is released. This process is mediated by two eukaryotic release factors (eRFs) proteins: eRF1, which mediates high fidelity

recognition of the stop codon and then catalyzes the hydrolysis of the bond between the peptide and the peptidyl-tRNA; and eRF3, a GTPase required for the binding. During termination, the eRF1/eRF3/GTP complex binds the A site, GTP is hydrolyzed and eRF3 is released. Finally, the ATPase ABCE1 binds and facilitates the conformation of eRF1 in an active configuration, which allows it to hydrolyze the peptidyl bond (**Figure 6**) (Dever and Green, 2012).
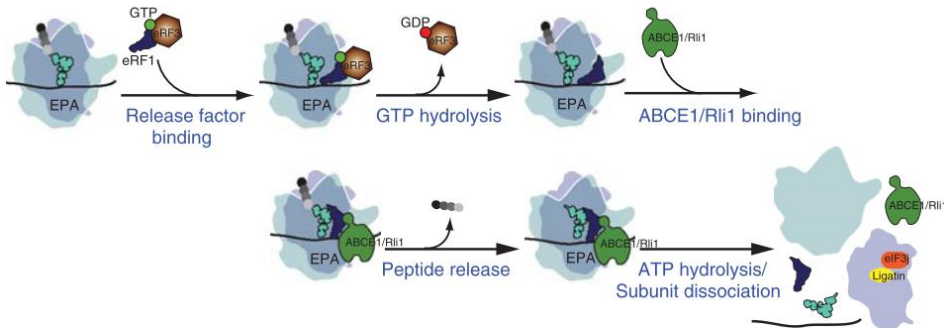
Figure 6. The translation termination process. During termination, the eRF1-eRF3-GTP complex binds to the A site of the ribosome and recognizes the stop codon. GTP is hydrolyzed and eRF3 is released. Finally, the ATPase ABCE1 binds and promotes the configuration of eIF1 in an active configuration that releases the peptidyl bond. Finally ATP hydrolysis promotes subunit dissociation and then the ribosomes are ready for a new round of translation (recycling). Image taken from Dever and Green, 2012.

1.3.4. Ribosome recycling

After the termination phase, the 80S ribosome is split again into the 40S and 60S subunits. This step is critical, because it allows the cell to prepare the 40S subunit for a new round of translation. Importantly, this event can take place after successful protein synthesis, but also after a failed synthesis (e.g. if the ribosome is stalled due to a damaged mRNA or a hairpin on it) or when a "vacant" (empty) ribosome is loaded (a mechanism that takes place during nutrition stress conditions to prevent new protein synthesis). The mechanisms involving recycling are not fully understood, but it is assumed that ABCE1 participates in the splitting (Dever and Green, 2012; Nürenberg and Tampé, 2013) (**Figures 4 and 6**).

14

1.3.5. The closed-loop model of translation

The interactions of the different elements of the mRNA are critical for the correct translation of that specific mRNA. It is widely known that when both cap and poly(A) tail are present in a mRNA, they act synergistically to enhance translation (Gallie, 1991). It is also known that eukaryotic initiation factor 4G (eIF4G) binds to PABP (Imataka et al., 1998) and the cap-binding protein eIF4E (Mader et al., 1995). Accordingly, the closed loop is a model in which the mRNA bends forming a loop by establishing contact between the poly(A)-bound PABP and the cap-bound eIF4E, using as a scaffold eIF4G (Imataka et al., 1998; Tarun et al., 1997; Wells et al., 1998) (**Figure 7**). This enhances translation through the enhanced recruitment of the 40S subunit. Moreover, beyond the translation initiation process, the release factors eRF1 and eRF3 are proposed to optimize the recycling steps by forming a bridge eRF1-eRF3-PABP that bends the 3'-UTR and enhances the translation by allowing the direct re-initiation of the ribosomes (Uchida et al., 2002) (**Figure 7**).
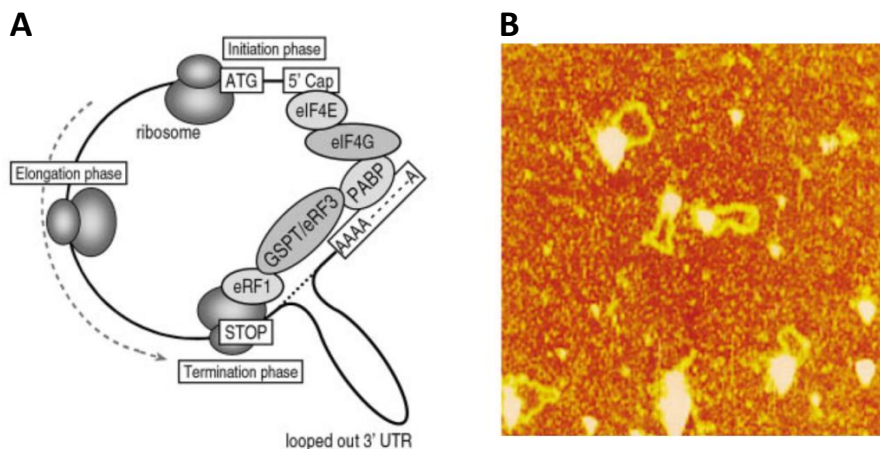
Figure 7. The closed-loop model of translation. *(A) Schematic diagram of the closed-loop model. The 5'Cap binding protein eIF4E and the poly(A) binding protein PABP are both recognized by eIF4G, which results in the formation of an mRNA loop that enhances translation. In addition, during ribosomal termination, eRF3 interacts with both eRF1 and PABP by forming an additional 3'-UTR loop that bends the 3'-UTR and favors the direct re-initiation of the ribosomes. Image taken from Uchida et al., 2002. (B) Evidence of the formation of the closed loop model by atomic-force microscopy. In the picture, looped mRNA with its edges bound by a protein complex can be seen. Adapted from Wells et al., 1998.*

2. Regulation of mRNA translation through cytoplasmic polyadenylation

In general, we can distinguish between two types of translational control: global and mRNA-specific. On the one hand, global translational control takes place by specific regulation of the abundance, post-translational modifications and competitors of the different factors that control the stages of translation (described in chapter 1). As a result, the cell regulates the whole process of translation, thus affecting all the mRNAs or a small group (i.e. it is non-mRNA-specific). On the other hand, in the mRNA-specific translational control, translation is regulated mainly by miRNAs and RBPs, which affect the translation of a specific subset of mRNAs without affecting the rest of mRNAs. Additionally, mRNA-specific translational control takes place locally in polarized cells or tissues, such as oocytes, embryos or neurons, with the aim to restrict the protein synthesis in space and/or time (e.g. local protein synthesis in the synaptic terminals in response to an excitatory neurotransmission) (Gebauer and Hentze, 2004).

In addition to the roles of the poly(A) tail in the protection of mRNAs from degradation, the regulation of the length of the poly(A) tail is an important mechanism of translational control. Cytoplasmic polyadenylation was discovered several decades ago as a conserved mechanism of regulation taking place in the oocytes and early embryos of different eukaryotes (both invertebrates and vertebrates) including worms, frogs and mice (Fox et al., 1989; McGrew et al., 1989; Paris et al., 1988; Vassalli et al., 1989). Even though a lot of progress is being done in other model organisms and systems, the molecular mechanisms of translational repression by deadenylation and cytoplasmic polyadenylation have been best characterized in the meiotic progression of *Xenopus* oocytes by the cytoplasmic polyadenylation element binding protein 1 (CPEB1).

16

Xenopus oocytes are transcriptionally inactive. Therefore, in order to carry out the early protein synthesis required for meiotic progression, they contain specific maternal mRNAs that are stored in a repressed state in the cytoplasm. With the aim to block their premature translation, they contain short poly(A) tails (around 20 nucleotides long). Then, when the oocytes are fertilized or during maturation, the poly(A) tails of these mRNAs are elongated up to 150 nucleotides long, inducing their translation. Therefore, short poly(A) tails are associated with translational repression and long poly(A) tails with translational activation (Mendez and Richter, 2001).

As it will be further described in the following sections, CPEBs regulate translation by recognizing specific sequences in the 3'-UTR of specific mRNAs: the cytoplasmic polyadenylation elements (CPEs), which are AU-rich sequences, typically with the consensus sequence UUUUUAU. As a result, they recruit interacting proteins and form repression complexes, in which the mRNA will be deadenylated and its translation repressed. Phosphorylation leads to changes in the recruitment of interacting proteins and then, the poly(A) tail is elongated and the mRNA subsequently translated. This process requires additional *cis*-acting sequences, such as the PAS. Again, this process has been better characterized for CPEB1, and it still needs to be further characterized how other CPEBs may regulate translation.

In this chapter the mechanisms of mRNA-specific translation regulation through cytoplasmic polyadenylation will be discussed, focusing on the translation regulation mediated by the CPEB family of proteins.

2.1. The CPEB family of proteins

The CPEB family of proteins is a group of RNA binding proteins. Phylogenetically, we can find 4 paralogs in vertebrates (CPEB1, CPEB2, CPEB3 and CPEB4). CPEB1 is the most distant and CPEB2, CPEB3 and CPEB4 are closer between them. This is the reason why sometimes they are considered two independent sub-families (Theis et al., 2003). It is important to mention that even though it was first proposed that the two CPEB subfamilies were able to bind different sequences on the target mRNA (Huang et al., 2006), now it is known that all CPEBs are able to target CPE sequences and hence they can possess overlapping regulatory functions (Igea and Méndez, 2010; Novoa et al., 2010; Ortiz-Zapater et al., 2011). Moreover, different orthologs of CPEBs can be found in other species, but in different number. As examples, *Aplysia californica* has 1 CPEB (CPEB) (Si et al., 2003a), *C. elegans* has 4 (Cbp-1, Cpb-2, Cpb-3 and Fog-1) (Luitjens et al., 2000) and *Drosophila* has 2 (Orb, closer to CPEB1 and Orb2, closer to CPEB2-4) (Keleman et al., 2007; Lantz et al., 1992) (**Figure 8A**).

The structure of CPEBs is highly conserved. Specifically, their most conserved region is the CTD. This CTD contains two RNA Recognition Motifs (RRM) placed in tandem (Hake et al., 1998) and one Zinc-binding domain (ZZ domain) (Merkel et al., 2013), which had been previously described as a standard Zn Finger (Hake et al., 1998). The RRMs, mainly RRM1, participate in mRNA recognition and specificity (Hake et al., 1998; Huang et al., 2006), while the ZZ domain facilitates mRNA recognition without conferring sequence specificity (Huang et al., 2006) and can also mediate protein recognition (Merkel et al., 2013). This means that the ZZ domain may facilitate both mRNA binding and recruitment of cytoplasmic polyadenylation factors (Merkel et al., 2013), hence forming repression or activation complexes, as will be discussed in next section.
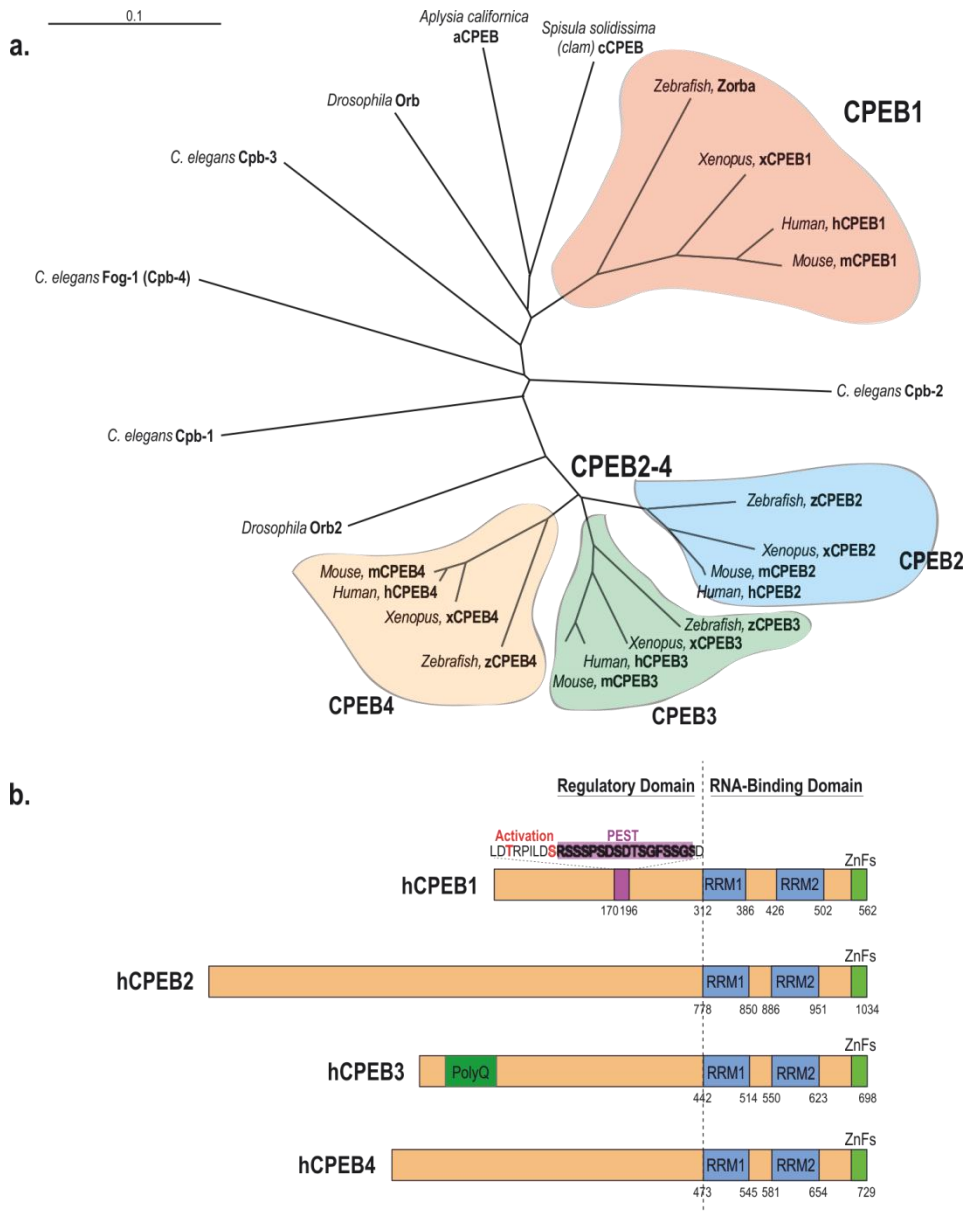
Figure 8. Phylogeny and structure of the CPEB family of proteins. *(A) Unrooted phylogenetic tree of the CPEB family of proteins of the most studied species. It can be seen that the vertebrate CPEB1 is the most distant, while CPEB2, CPEB3 and CPEB4 are closer between them. The members of the family in other invertebrate species are also shown. (B) Structure of the human CPEBs. The C-terminal domain is highly conserved and modular, and contains 2 RNA recognition motifs (RRM1, RRM2) and one Zn finger (ZnF). The N-terminal regulatory domain is highly variable. CPEB1 contains an activation domain followed by a PEST degradation motif, and CPEB3 a polyQ. Figure adapted from Fernández-Miranda and Méndez, 2012.*

The N-terminal domain (NTD) of CPEBs is more variable, and different regulatory sequences can be found depending on the CPEB member and the species. For example, human CPEB1 contains an activation sequence with two potential phosphorylation sites, followed by a PEST degradation motif, which is involved in fast protein degradation (Rogers et al., 1986). In the case of *Xenopus* oocytes, CPEB1 is rapidly degraded after its hyperphosphorylation mediated by Cdc2 and Plx1 through the ubiquitin-proteasome system, which is an important step for meiotic progression and is dependent on its PEST domain (Mendez et al., 2002; Reverte et al., 2001; Setoyama et al., 2007). Moreover, CPEB3 contains a glutamine-rich sequence (polyQ) in the N-terminal domain (**Figure 8B**), which could be involved on its oligomerization. This PolyQ (with more repetitions) is also found in *Aplysia* CPEB, Orb1 and Orb2, and is thought to confer them functional prion-like properties. This, as we will discuss later, will give them the ability to self-aggregate, with important implications in memory formation (Si et al., 2003a). The polyQ is also known to be present in other prion-like proteins, which favors their aggregation under certain pathological conditions, as is the case of huntingtin when it contains the polyQ expansion that leads to Huntington's Disease (Davies et al., 1997; DiFiglia et al., 1997; Scherzinger et al., 1997).

2.2. CPEBs-mediated translational repression and activation through cytoplasmic polyadenylation

As we will discuss in this section, CPEBs mediate translational regulation mainly through two mechanisms: mRNA translational repression, and cytoplasmic polyadenylation with subsequent mRNA translation under specific stimuli.

In general, the mechanism of translational repression involves the deadenylation of the mRNA target and the disruption of the "closed-loop", which blocks the translation of that specific mRNA. In 2008, the requirements for mediating translational repression in *Xenopus* oocytes were established

(Piqué et al., 2008). Concretely, the process of translational repression requires the presence of different sequences of the 3'-UTR to be located in a specific conformation. At least two CPE sequences need to co-exist at no more than 50 nucleotides of distance. These sequences are targeted by CPEB1, which probably forms a dimer that disrupts the cap-eIF4E-eIF4G-PABP-poly(A)-mRNA complex by two mechanisms: first, the unphosphorylated CPEB1 recruits PARN, a deadenylase, that competes with the polymerase Gld2 and overtakes it, resulting in the removal of the poly(A) tail (Kim and Richter, 2006); and second, CPEB1 interacts with PABP, which will not bind the poly(A) tail (Kim and Richter, 2007) (**Figure 9A**).

Two additional models have been proposed for explaining CPEB-mediated translational repression in early stage *Xenopus* oocytes. According to them, the structure of the "closed loop" is altered through the inhibition of the binding between eIF4E and eIF4G through an intermediate protein that interacts with CPEB1. The first model states that this protein can be maskin, which interacts with CPEB1 and eIF4E, impairing the binding of the latter to eIF4G and blocking translation (Stebbins-Boaz et al., 1999) (**Figure 9B**). Alternatively, the second model states that the interacting protein is the eIF4E transporter (eIF4E-T). eIF4E-T is a eIF4E protein involved in the nucleocytoplasmic transport of eIF4E (Dostie et al., 2000) and in the formation of P-bodies and the localization of eIF4E in P-bodies (Andrei et al., 2005; Ferraiuolo et al., 2005). According to this model, eIF4E-T interacts with CPEB1 and eIF4E1b, a close homolog of eIF4E. However, eIF4Eb, which binds to the cap poorly, binds eIF4E-T instead of eIF4G and forms a complex with the helicase RCK/Xp54 and the proteins P100 and Rap55 (Andrei et al., 2005; Minshall et al., 2007). In this case, translation is inhibited because eIF4Eb binds eIF4E-T instead of eIF4G (**Figure 9C**).
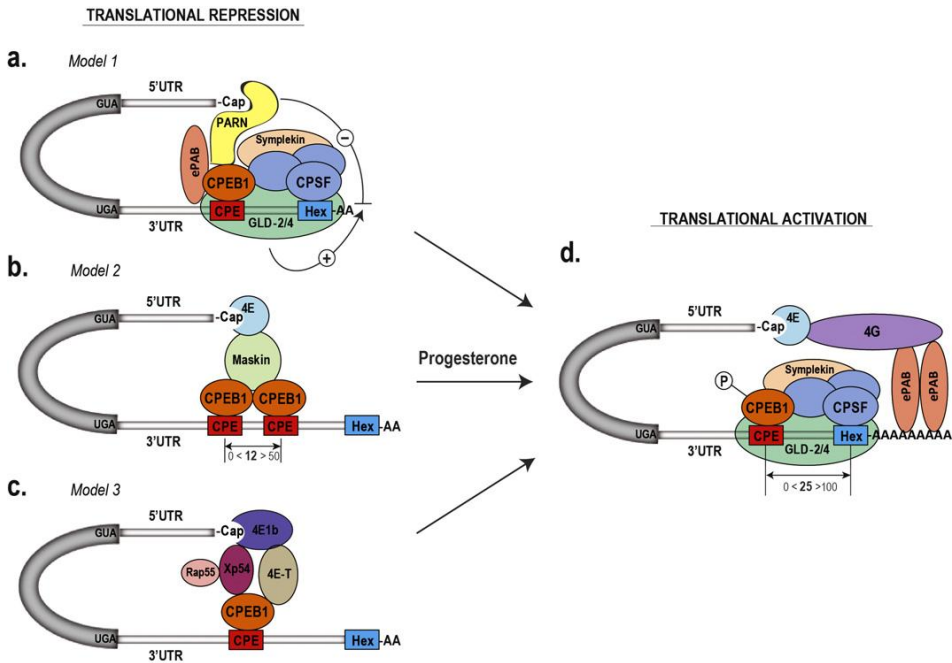
Figure 9. Models of CPEB1-mediated translational repression and activation. Some of the CPEB1 partners involved in CPEB1-mediated repression (A-C) and activation (D) in Xenopus oocytes are shown. (A) Repression complex formed by the interaction of CPEB1 with the polymerase Gld2 and the more active deadenylase PARN that compete with the first and deadenylates the mRNA. ePAB does not bind the poly(A) tail and is sequestered by CPEB1. (B) Repression complex formed by the interaction of CPEB1 and eIF4E through maskin. The interaction of maskin and eIF4E avoids the binding of eIF4G to eIF4E. (C) Repression complex formed by the interaction of CPEB1 with RCK/Xp54, eIF4E-T and eIF4E1b, which will not bind eIF4G. (D) Following progesterone stimulation, CPEB1 is phosphorylated, Gld2/4 mediates mRNA polyadenylation, ePAB binds to the poly(A) tail, and binds to eIF4E through eIF4G, forming the "closed-loop" model. The distance between CPEs required for mediate repression and between CPE and PAS (Hex) to mediate CPEB1-mediated polyadenylation are shown in B and D, respectively. Image taken from Fernández-Miranda and Méndez, 2012.

The translation repression models 2 and 3 presented here are mutually exclusive and it is still not clear whether they represent different repression complexes that are formed for specific mRNAs, or for different moments of cell cycle progression, or whether they are intermediary complexes that are formed until the final one is produced. Moreover, these models are based in studies with *Xenopus* oocytes, and it is not clear which one is present in mammalian somatic cells. For example, the mammalian ortholog of maskin (TACC3) does not contain the motif required for eIF4E binding. In addition, eIF4E1b, which

interacts with eIF4E-T, is an isoform expressed only in oocytes, eggs and early embryos of *Xenopus*, Zebrafish and mice (Minshall et al., 2007). Moreover, RCK/XP54 can be found in repressed somatic mRNAs independently of CPEB1 (Minshall et al., 2009). On the other hand, CPEB, PARN, Gld2, symplekin (Udagawa et al., 2012) and Neuroguidin (a neuronal substitute for maskin) (Jung et al., 2006) have been detected in somatic cells, concretely in neurons, where they can mediate repression and polyadenylation through cytoplasmic polyadenylation as it will be described in next sections. This suggests that model 1, or the combination of model 1 with others, is potentially the more feasible in somatic cells.

Independently of which model or combination of models of translational repression takes place, it is known that in resting *Xenopus* oocytes, in which the mRNAs are in a repressed state, progesterone stimulation leads to the remodeling of the repression complexes into a form that sustains new polyadenylation and subsequent translational activation of the specific mRNAs being regulated (**Figure 9D**). Two *cis*-acting sequences are necessary for this process: the PAS (see chapter 2) (Sheets et al., 1994), located near the polyadenylation site and targeted by the CPSF complex, and the CPE (Dickson et al., 1999), usually separated around 20-30 nucleotides, and at no more than 100 nucleotides (Piqué et al., 2008). In *Xenopus* oocytes, CPEB1 is phosphorylated by Aurora-A (Mendez et al., 2000a) upon progesterone stimulation, which promotes its switch from a repressor into an activator, and recruits CPSF (Mendez et al., 2000b). Then, both proteins recruit the poly(A) polymerase Gld2 to mediate poly(A) elongation, at the same time that CPEB1 loses affinity for the deadenylase PARN, which is expelled from the complex. This produces the translation of early genes and triggers meiotic progression.

CPEBs are not only important in *Xenopus* oocytes. They have also been shown to possess important functions during mouse oogenesis. In fact, *Cpeb1* KO mice

(both males and females) are sterile. It is caused because the gametogenesis stops at pachytene as the mRNAs regulated by CPEB1 are not translated (Tay and Richter, 2001) and also because CPEB1 is also required for G2 to M transition to finish meiosis (Tay et al., 2003).

Finally, besides in vertebrates, the role of CPEBs during development has also been studied in invertebrates, especially in *Drosophila*, where Orb has been proved to be essential for the proper meiotic division. In addition, Orb participates in the anteroposterior mRNA localization in the embryo (e.g. oskar localization to the posterior pole) (Chang et al., 1999; Christerson and McKearin, 1994; Lantz et al., 1994; Roth and Schüpbach, 1994; Tay et al., 2003). Besides its roles in localization, Orb also cooperates with other proteins, such as PAP or Wispy, to control the translation of different mRNAs, like oskar and cortex, respectively (Benoit et al., 2008; Swan and Schüpbach, 2007).

2.3. CPEBs-mediated translational control in somatic cells

As detailed in the previous section, most of the molecular studies with CPEBs have been performed in *Xenopus* oocytes. However, it is also known that somatic cells, especially polarized cells, tightly control mRNA translation. In this regard, CPEBs have been linked to important cell functions, such as control of cell proliferation, senescence, cancer, metabolism and neuronal synaptic plasticity.

First, CPEBs have been shown to possess important functions in proliferation, senescence and cancer. CPEB1 is important for M-phase entry and cell proliferation in cancer cell lines, and depletion of CPEB1 and CPEB4 together leads to synergic proliferation inhibition, pointing to overlapping functions (Novoa et al., 2010). Moreover, it has been suggested a role for CPEB1 as a tumor suppressor gene, taking into account that *Cpeb*1 KO mouse embryonic fibroblasts (MEFs) are immortalized by the deregulation of important genes,

24

such as TP53 and myc (Groisman et al., 2006; Groppo and Richter, 2011) and that *Cpeb1* KO primary human keratinocytes also bypass senescence (Burns and Richter, 2008). Accordingly, CPEB1 downregulation has also been linked with higher malignancy in gliomas (Skubal et al., 2016). CPEB1 inhibition has also been associated to epithelial-to-mesenchymal transition and metastasis through the regulation of MMP9 expression in breast cancer (Nagaoka et al., 2016). In contrast, a pro-tumoral role has been described for CPEB4, which is upregulated in pancreatic ductal adenocarcinoma (PDAC) and gliomas. CPEB4 is responsible for the reprogramming of gene expression in cancer that leads to the translational activation of hundreds of mRNAs, including tissue plasminogen activator (tPA) mRNA (Ortiz-Zapater et al., 2011), which supports invasion, migration and angiogenesis (Díaz et al., 2002; Ortiz-Zapater et al., 2007; Paciucci et al., 1998). Of note, tPA not only plays a key role in PDAC progression (Díaz et al., 2002; Ortiz-Zapater et al., 2007; Paciucci et al., 1998) but also in neurodegenerative diseases such as Alzheimer's disease (Ledesma et al., 2000; Medina et al., 2005; Melchor et al., 2003; Oh et al., 2014; Pineda et al., 2012; Tucker et al., 2000), as it will be discussed in the following chapters. Finally, overexpression and loss of activity of CPEB3 has been positively correlated with malignancy in gliomas. The loose of activity appears to be caused by the expression of a splice variant (Skubal et al., 2016).

In addition, CPEBs have also been shown to play important roles in metabolic regulation. As examples, it has been shown that CPEB1 deficient human fibroblasts have increased levels of anaerobic glycolysis, known as Warburg effect, due to insufficient TP53 mRNA translation that leads them to bypass senescence (Burns and Richter, 2008; Burns et al., 2011; Groppo and Richter, 2011). *Cpeb1* KO mice also show aberrant insulin signaling and glucose metabolism and become insulin-resistant, through the upregulation of the negative regulators of insulin functions PTEN and Stat3 (Alexandrov et al., 2012). Finally, CPEB1 has been linked to mitochondrial energy production in

neurons, as it controls NDUFV2 mRNA translation, which encodes for a key component of the electron transport chain complex I (Oruganty-Das et al., 2012). The reduction of ATP production reduces neuronal dendritic branching, showing that CPEB1 regulation in the mitochondria is necessary for neuronal development (Bestman and Cline, 2008). Finally, CPEB2 has been proposed to respond to oxidative stress. It was shown to suppress HIF1α translation under normoxic conditions and to allow its translation during hypoxia. This is because CPEB2 forms a covalent interaction with NPGPx using a thiol-based redox system that puts CPEB2 in a conformation state that allows it to repress HIF1α translation. During oxidative stress, this interaction is lost and CPEB2 cannot bind HIF1α, therefore allowing its translation (Chen et al., 2015).

However, one of the most interesting areas in which the CPEBs have been found to be involved is in the control of synaptic plasticity in the central nervous system (CNS). Since the understanding of CPEBs roles in the CNS is one of the main objectives of this PhD work, all the current knowledge regarding this topic will be will be broadly described in chapter 3.

2.4. Beyond polyadenylation: CPEBs role in alternative 3'end formation

In addition to the previously mentioned functions of CPEBs, CPEB1 has been recently linked to the process of nuclear polyadenylation (Bava et al., 2013).

In somatic cells, CPEB1 has been shown to continuously shuttle between nucleus and cytoplasm (Ernoult-Lange et al., 2009; Lin et al., 2010). The nuclear localization signal (NLS) of CPEB1 is complex (not consensus) and not well understood, but 2 nuclear export signal (NES) motifs have been detected (Ernoult-Lange et al., 2009). The localization of CPEB in the nucleus may take place to target CPE-containing mRNAs and ensure their translational repression before reaching the cytoplasm (Lin et al., 2010). Additionally, the presence of CPEB1 in the nucleus has been linked to the process of nuclear alternative

cleavage and polyadenylation (Bava et al., 2013) (**Figure 10**). In this regard, the presence of CPEB1 can mediate the shortening of the 3'-UTR of different mRNAs, which in general can change their translation efficiency, as has been discussed in this chapter. According to this model, the nuclear function of CPEB1 is to recruit CPSF to a PAS. Under normal circumstances, the CPSF complex is directed to the stronger PAS (sPAS), usually distal (i.e. located at the end of the 3'-UTR). However, when there is a CPE located at no more than 100 nucleotides (upstream or downstream) of an additional weaker non canonical PAS (wPAS), which is usually located upstream the sPAS, CPEB1 can target that CPE and recruits the cleavage machinery to the wPAS. As a result, an mRNA with a shorter 3'-UTR will be generated.
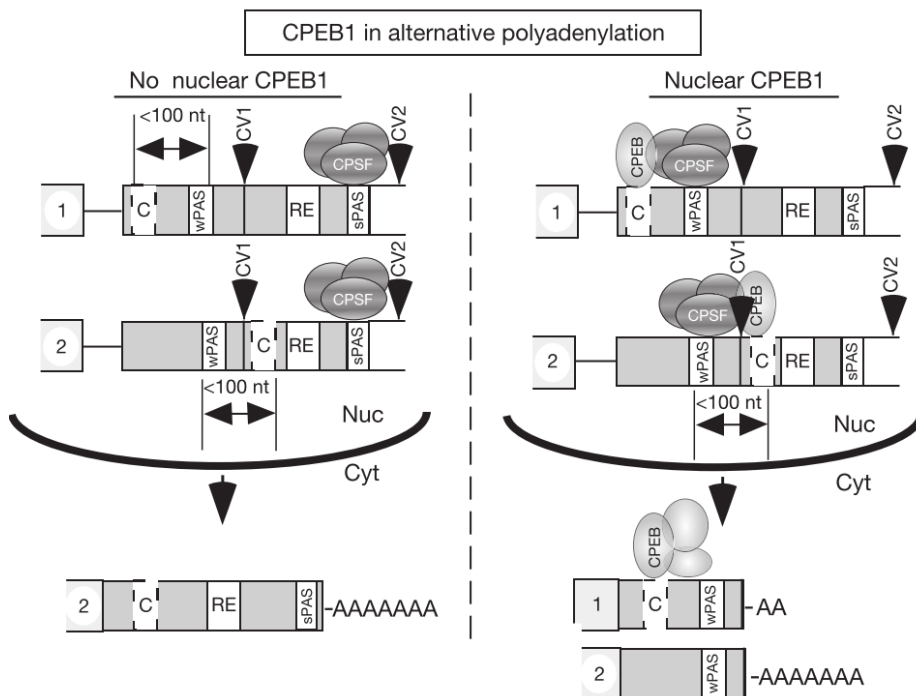
Figure 10. Molecular mechanism of CPEB1-mediated alternative cleavage and polyadenylation. In the absence of nuclear CPEB1 (left panel), the CPSF complex targets the stronger PAS (sPAS) and mediates the downstream cleavage of the mRNA (CV2 site). When CPEB1 (CPEB) is present in the nucleus (right panel), if the mRNA contains a CPE sequence (C) located at no more than 100 nucleotides from another upstream, weaker PAS (wPAS), it directs the CPSF to that point, mediating an upstream cleavage of the mRNA (CV1 site) generating mRNAS with a shorter 3'-UTR that will be subsequently controlled by CPEB1 in the cytoplasm or will escape the regulation depending on the sequences present after the cleavage. Image taken from Bava et al., 2013.

After the nuclear cleavage, the resulting mRNA will be subsequently controlled in the cytoplasm by translational repression/cytoplasmic polyadenylation. This regulation will depend on the organization of the 3'-UTR sequences of the newly generated mRNA. If CPEs were located downstream the cleavage site, the mRNA could escape the cytoplasmic control by CPEB1 (**Figure 10**). This mechanism of alternative 3'-end formation mediated by CPEB1, originally described in 2013 (Bava et al., 2013), has also been proved to take place during liver cirrhosis for the mRNAs of CPEB4 and VEGF (Calderone et al., 2015).

Moreover, under certain circumstances, the presence of the nuclear CPEB has also been shown to participate in nuclear alternative splicing (Bava et al., 2013).

3. Role of CPEBs in the Central Nervous System

3.1. Memory formation: From short-term to long-term memory

All the brain processes, such as emotions, learning and memory, are possible because of the complex synaptic network of all the neurons that comprise the brain. In addition, the ability to process external information and new experiences and to translate it into learning is possible through continuous changes in cell connectivity (*i.e.* synaptic plasticity). Memory can be divided in terms of duration into short-term memory and long-term memory. Short-term memory is the retention of information for latter use without altering the synaptic network, whereas long-term memory implies a substantial change in the neural pathways that can persist from days to years. The difference is that while short-term memory relies on the modification of pre-existing proteins (*e.g.* phosphorylation) and changes in the strength of the preexisting synapses, long-term memory requires new transcription and new protein synthesis, as well as the growth of new synaptic connections. In fact, the use of translation inhibitors blocks long-term memory formation (Davis and Squire, 1984). Similarly, the use of transcription inhibitors during learning is also known to block long-term memory formation, even though their toxicity make the results difficult to interpret (reviewed in Alberini, 2009).

Long-lasting memories require durable changes in synaptic strength, either reinforcement (Long Term Potentiation, LTP) or debilitation (Long-Term Depression, LTD). As with memory, the early phase of LTP (E-LTP) does not require protein synthesis, while the latter (L-LTP) does. Consequently, the molecular mechanisms which govern the phenomenon of memory establishment are very complex. In fact, neurons have adapted biological pathways in a special and complex way, which is especially evident in the synaptic terminals. A single neuron contains thousands of synaptic connections, but every single synapse can work independently of the others. In this regard,

when a synaptic input takes place, a neuron is able to recognize whether that specific synapse has been previously stimulated (experienced) or not (naïve). This is because after the stimulation, individual synapses undergo biochemical and morphological changes and become "tagged" (reviewed in Kandel, 2001; Mayford et al., 2012; Richter and Klann, 2009; Shepherd and Huganir, 2007; Sutton and Schuman, 2006). Then, in order to convert initial stimuli that initiate short-term memory (E-LTP) in specific synapses into long-lasting memory (L-LTP), neurons use different synaptic kinases, such as protein kinase A (PKA), Ca^{2+}/calmodulin dependent protein kinase II (CaMKII), CaMKIV, mitogen-activated protein kinase (MAPK) or protein kinase C (PKC), as well as phosphatases (such as PP1 or calcineurin), which trigger a retrograde signaling cascade to the nucleus that leads to the activation of nuclear transcription factors (**Figure 11**). One of the most studied is CAMP responsible element binding protein 1 (CREB1), even though other transcription factors, such as serum response factor (SRF), the proto-oncogene c-Fos, epidermal growth factor receptor (EGFR) or nuclear factor κB (NF-κB) have also been proposed to participate in the mechanism of memory acquisition.

Once produced, the newly synthesized mRNAs can be transported to the synapses and translated locally specifically in the stimulated synapses. This can happen in the synapse that was activated and triggered the initial retrograde signal to the nucleus, or in other synapses activated soon after the first one, even if the strength of the activation was low and not able to trigger LTP under normal conditions. In addition, the L-LTP also promotes the growth of new synapses (**Figure 11**). Therefore, the equilibrium between the strength and repetition of the synaptic inputs, together with the equilibrium between kinases and phosphatases that will activate the new transcription and local synaptic translation, will determine the acquisition of long-term memory (reviewed in Kandel, 2012; Kandel et al., 2013). These synaptic changes have been associated with the mechanism of memory formation.

30
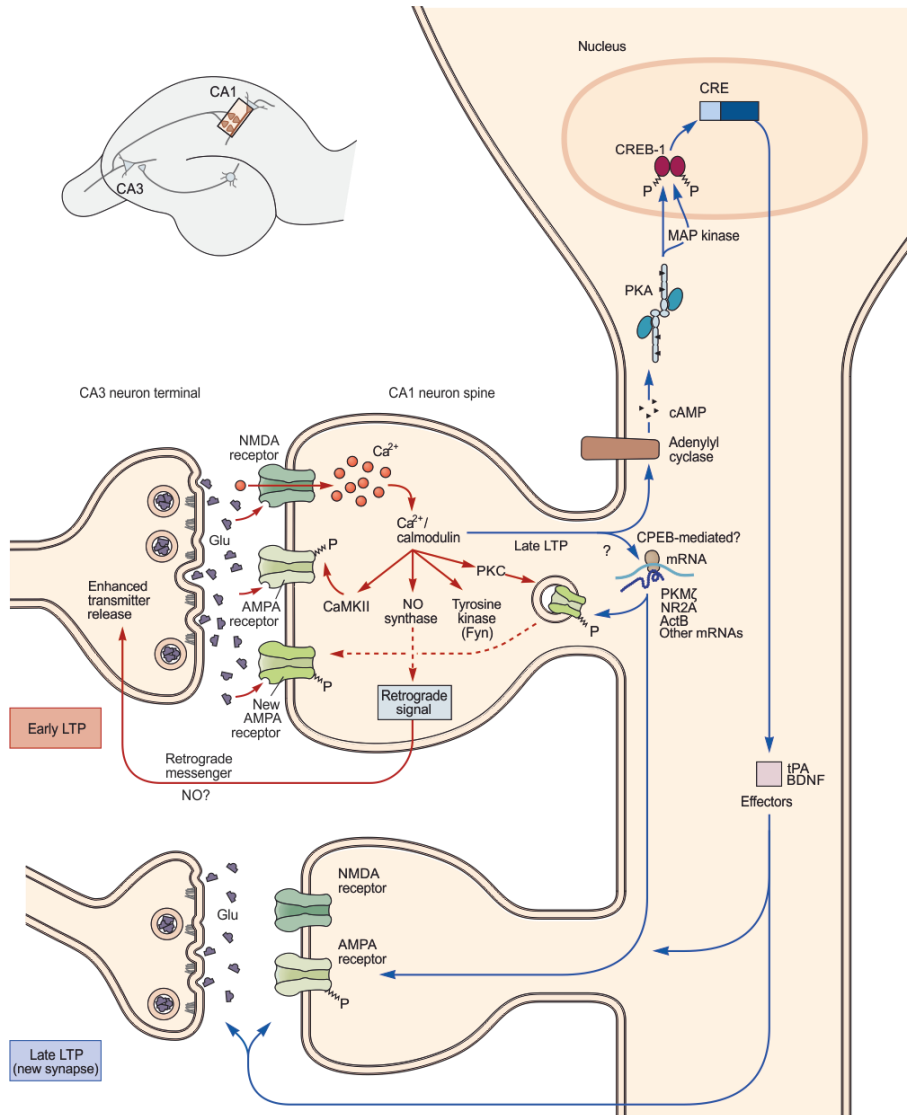
***Figure 11. Molecular mechanisms of short-term and long-term memory formation through the activation of CREB**. A single stimulation induces early LTP in the postsynaptic compartment by stimulating the activation of the NMDA receptors (early LTP, red box). This generates a Ca^{2+} influx in the postsynaptic compartment, which activates second messengers, such as PKC and CaMKII. With repeated stimulations, the activation recruits an adenylate cyclase, which generates cAMP and activates PKA. This activates a MAP kinase that goes to the nucleus and activates CREB-1 by phosphorylation. This mediates the transcription of genes containing the CRE promoter, which are known to mediate the growth of new synapses (Late LTP, blue box) and the modulation of the stimulated ones. Repeated activation of the synapses also stimulates the local, synaptic translation of mRNAs that are generated in the nucleus and transported to the dendrites, which participate in the modulation of synaptic strength. One important candidate is PKMζ, a constitutively active form of PKC, which promotes a long lasting increase in the number of AMPA receptors in the surface. In addition, it is believed that there may exist a retrograde signaling pathway from the postsynaptic to the presynaptic compartment, which would participate in the control of the neurotransmitter release. Image adapted from Kandel et al., 2013.*

31

However, an additional layer of regulation is required. In *Aplysia*, a model organism that has been extensively studied in neuroscience, it is known that, in addition to an initial cascade that initiates long-term synaptic plasticity and growth, there is a need for a second event which stabilizes this biochemical and morphological changes over time. This requires both protein synthesis in the soma and local mRNA translation in the active synapses. In fact, neurons show a tightly controlled mechanism of mRNA targeting in the soma with subsequent transport to the dendrites, where translation can occur. In this regard, the fact that mRNAs are targeted in the soma strongly suggests that they remain dormant while they are transported to the dendrites and thus, they are only translated in stimulated synapses. This suggests that these neurons may recruit a protein which is able to repress and activate translation in the dendrites (Martin et al., 1997).

Local protein production is a mechanism designed to control the local synaptic strength. It is now known that dendrites contain all the proteins required for mRNA translation, including polyribosomes (Steward and Levy, 1982), translation factors, rRNAs, tRNAs, endoplasmic reticulum and the Golgi apparatus (Gardiol et al., 1999). Consequently, local protein synthesis has been observed in isolated dendrites (Torre and Steward, 1992). Moreover, different mRNAs are dendritically localized. Most of these mRNAs participate in the modulation of the synaptic transmission, such as activity-regulated cytoskeleton-associated protein (Arc), CaMKII, brain derived neurotrofic factor (BDNF), tissue plasminogen activator (tPA), and even some subunits of the AMPA and NMDA receptors. In fact, it is now known that the strength of the synaptic response can be regulated both by activity-induced receptor trafficking to the dendrites and by dendritic mRNA translation (Shepherd and Huganir, 2007). The dendritic targeting of mRNA and the localized translation may possess significant advantages. First, mRNAs can be located silenced at the synapses and thus be translated when and where needed. In addition, the

presence of the proteins coded by those mRNAs is avoided in parts of the neurons in which they are not required. Moreover, the information regarding the final location of the protein is present in the mRNA 3'-UTR. As a consequence, it is not required to alter the sequence and structure of the protein to target that specific location. Finally, the newly synthesized proteins may contain unique features (e.g. minimal post-translational modifications) that can be used with additional regulatory purposes (Holt and Bullock, 2009). One example of a key locally translated protein associated with memory maintenance that is being actively studied is PKMζ, a variant of PKC lacking its regulatory domain. Its mRNA is known to be produced in the soma (and upregulated after a synaptic stimulus), transported to the synapses and translated after synaptic stimulation, contributing to memory establishment through its persistent activity, mainly through the regulation of receptor trafficking (Glanzman, 2013; Sacktor, 2012) (**Figure 11**). In addition, it contains CPEs on its 3'-UTR and, according to the CPE code (Piqué et al., 2008) could be regulated by the CPEBs.

3.2. CPEBs: key proteins for memory formation and local mRNA translation at the synapses

Without any doubt, the best characterized example of CPEB-mediated cytoplasmic polyadenylation and translational control in somatic cells takes place in neurons, a mechanism that is critical for synaptic plasticity. Unlike other tissues, all the CPEBs have been described to be expressed in the CNS. More precisely, all of them can be detected in the hippocampus (Theis et al., 2003; Wu et al., 1998), a brain area critical for the formation of new memories. In this section, the current knowledge regarding the role of CPEBs in the CNS is summarized, giving a special emphasis to their synaptic roles. However, it is important to mention that even though a lot of progress is being done, some of the molecular mechanisms regarding the CPEBs-mediated neuronal and

synaptic regulation, as well as their distinctive and overlapping functions remains not fully elucidated. Moreover, up to date, there are not any article showing specific roles of CPEB2 in the CNS, and the knowledge regarding CPEB4 functions is limited.
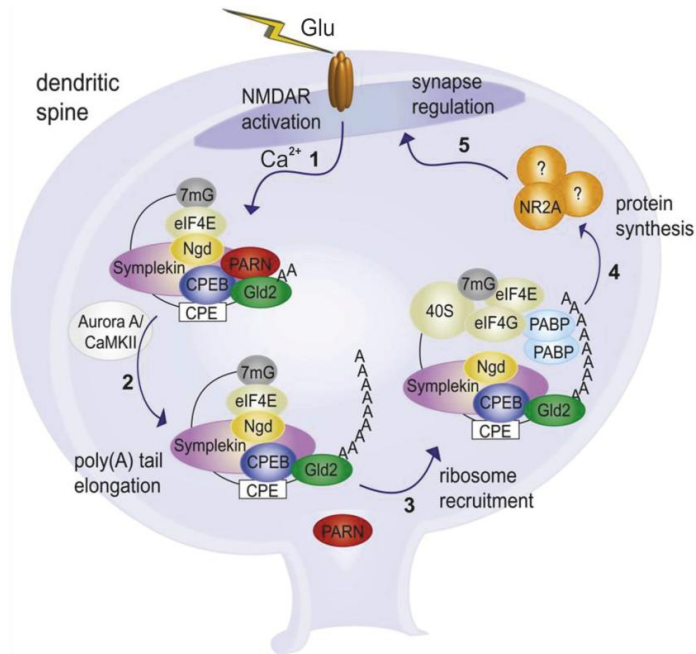
Figure 12. *Role of CPEB1 in the synapse. Diagram showing the molecular mechanism of CPEB1-mediated translation at the synapse. CPEB1 can target and transport mRNAs in repression complexes to the proximity of the synaptic terminals. In response to the activation of the NMDA receptor mediated by glutamate release in the presynaptic terminals, there is a calcium influx in the spine, which activates CaMKII. CaMKII (but could also be Aurora A) phosphorylates CPEB1, which promotes the expulsion of PARN from the repression complex. As a result, Gld2 elongates the poly(A) tail and translation of important mRNAs involved in synaptic modulation takes place. Some examples are NR2A, tPA, BDNF, CAMKII or PMKζ. Adapted from Udagawa et al., 2012.*

3.2.1. Role of CPEB1 in the synapse

CPEB1, one of the most studied members of the CPEB family, is directly involved in memory formation. In *Cpeb1* KO mice, theta burst-induced LTP is severely reduced in the Schaffer collateral-CA1 pathway (Alarcon et al., 2004). Moreover, it was shown that even though *Cpeb1* KO mice have normal learning capacity, they have a deficit in hippocampal extinction, a type of memory in which behavioral responses become extinct when not reinforced, which

probably relies on a different molecular mechanism compared to other types of memory, such as acquisition (Berger-Sweeney et al., 2006).

Regarding the molecular mechanisms by which CPEB1 acts, the first evidence was published in 1998 (Wu et al., 1998). In this work, it was demonstrated that CPEB1 is expressed in the rodent brain, especially in cortex and hippocampus, and is also highly enriched in the postsynaptic terminals. Moreover, the work proposed that CaMKII mRNA, which is also found in the dendrites and translated upon synaptic stimulation (Ouyang et al., 1997), is targeted and polyadenylated by CPEB1, a mechanism that requires the CPEs. CPEB1 was later discovered to control the local synaptic translation of other mRNAs important to synaptic function in response to synaptic stimulation (**Figure 12**), such as cytoskeletal actin (Fukazawa et al., 2003; Liu and Schwartz, 2003), early growth response 1 (EGR1) (Simon et al., 2004), tPA (Shin et al., 2004) or c-fos (Zearfoss et al., 2008). However, among all mRNAs described to be controlled by CPEB1, one of the most important is GluN2A. Its mRNA is present in the dendrites, contains CPEs, and in response to a pattern of stimulation that resembles LTP is translated (Udagawa et al., 2012). Consequently, the resulting protein can be inserted in the membrane, working as a new functional NMDA receptor (**Figure 12**), which can contribute to synaptic modulation (Swanger et al., 2013). In these cases, together with CPEB1, the protein in charge of repressing the mRNAs would be Neuroguidin, which is the equivalent of maskin in neurons (Jung et al., 2006). As expected, the other components of the polyadenylation machinery that were described in *Xenopus* oocytes have also been found in dendrites (Huang et al., 2002; Jung et al., 2006; Mendez and Richter, 2001; Udagawa et al., 2012).

Importantly, in addition to control synaptic polyadenylation, CPEB1 has been involved in the synaptic transport of mRNAs. In this regard, CPEB1 has been shown to target CaMKII and other mRNAs, such as MAP2, to associate with the

dynein and kinesin motors, and to bidirectionally transport these mRNAs through the dendrites (Huang et al., 2003). This means that CPEB1 can control the spatiotemporal translation of mRNAs and that the mRNAs can be on the move in dendrites, but only translated in the vicinity of a stimulated synapse (Krichevsky and Kosik, 2001).

3.2.2. Role of CPEB2 in the synapse

Even though it is known that all CPEBs are present in the brain, the functions of CPEB2 have not been fully elucidated. CPEB2 is expressed in a wide variety of brain areas and different splice variants have been detected in different neuronal cell types in the hippocampus. In primary cultures of hippocampal neurons, CPEB1 and CPEB2 show similar patterns in neurons and astrocytes, and some validated targets for CPEB2 are also CPEB1 targets, pointing to potential overlapping functions (Turimella et al., 2015).

3.2.3. Role of CPEB3 in the synapse

Recently, CPEB3 has been studied in the mammalian synapse, based on previous results with its homologous Orb2 and *Aplysia* CPEB (apCPEB). Like apCPEB and Orb2, vertebrate CPEB3 also possesses a polyQ domain on its NTD, even though it is slightly shorter (**Figure 13**). In *Aplysia*, the presence of the polyQ tail in the NTD makes apCPEB able to aggregate and form highly stable long-lived aggregates that get accumulated in activated synapses (Si et al., 2003a, 2003b). In fact, *Aplysia* CPEB has been described to form amyloid-like fibers (Heinrich and Lindquist, 2011; Raveendra et al., 2013), a critical mechanism for synaptic plasticity (Miniaci et al., 2008; Si et al., 2010). In *Drosophila*, Orb2 has also been found to form this amyloid-like fibers (Majumdar et al., 2012). In fact, its polyQ domain is critical for long term memory (Keleman et al., 2007). Apparently, during long-term memory, the isoform Orb2B mediates translation through its RRM, and Orb2A, through its

polyQ domain and independently of its RRM, mediates the formation of heterologous Orb2A:Orb2B amyloid-like fibrils, a process that involves Orb2A polyQ (Krüttner et al., 2012; Majumdar et al., 2012).
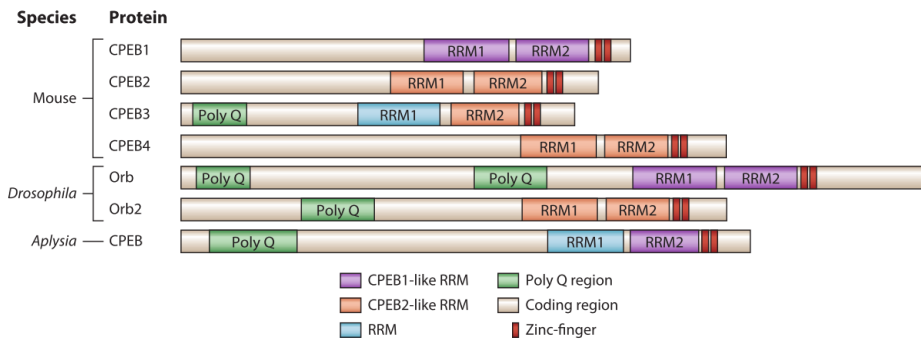
Figure 13. CPEB3 is proposed as a functional candidate for Orb, Orb2 and Aplysia CPEB. *Comparison of the homology of sequences between mouse CPEBs and its homologs in Drosophila and Aplysia. As it is observed, only CPEB3 contains the polyQ tail in the N-terminal domain, which is also present in Orb, Orb2 and Aplysia CPEB. Figure adapted from Ivshina et al., 2014.*

Based on these previous results with invertebrates, and given the presence of a polyQ tail of its NTD, the vertebrate CPEB3 was proposed to function in a similar way (**Figure 13**). Indeed, it has been shown that CPEB3 is also able to form aggregates in response to synaptic stimulation, which means that it could be considered a prion with physiological roles (Stephan et al., 2015). The aggregation of CPEB3 has been proposed to be negatively controlled by SUMOylation (Drisaldi et al., 2015). However, other lines of evidence propose that by default, CPEB3 represses translation, and that upon activation of the NMDA receptor, it is cleaved by calpain 2, which makes it able to bind RNA but not to repress it (Wang and Huang, 2012). The protein synthesis controlled by CPEB3 has been proposed to be regulated by Neuralized1, an E3 ubiquitin ligase, in a proteolytic-independent way, a process that had only been proposed to take place in yeast (Spence et al., 2000). When this ligase is downregulated through the overexpression of a dominant negative form, the expression of GluA1 and GluA2 is altered *via* CPEB3 and the synaptic efficiency reduced, whereas its overexpression results in enhanced hippocampal-

dependent memory and an increase in the number of synapses (Pavlopoulos et al., 2011).

Regarding CPEB3 roles in memory, initial studies demonstrated that CPEB3 KO mice showed enhanced hippocampal-dependent memory, through the upregulation of important plasticity-related proteins, as PSD95 and the subunit GluA1 of the NMDA receptor (Chao et al., 2013), which was previously described to be CPEB3 targets (Huang et al., 2006). However, a more recent study with conditional *Cpeb3* KO mice showed defects in synaptic plasticity and impaired memory. The authors argued that this contradiction could have been caused by compensatory mechanisms that took place in the previous work originated by the use of a total KO mouse model (Fioriti et al., 2015).

3.2.4. Role of CPEB4 in the synapse

Currently, even though CPEB4 is known to be located in the synapses, little is known regarding its specific synaptic role. *Cpeb4* KO mice do not show signs of hippocampal memory impairment even though they contain abnormally enlarged spines (Tsai et al., 2013). Moreover, out of the synapses, CPEB4 is known to shuttle between nucleus and cytoplasm and it is retained in the nucleus during brain ischemia, thus acting as a pro-survival protein (Kan et al., 2010).

3.3. CPEBs in neurodegenerative diseases

Up to date, the only neurodegenerative disease in which the CPEBs (in particular CPEB1) have been proved to be involved in, is in the fragile X syndrome (FXS). This disease is a common form of inherited mental retardation and one of the leading forms of autism, which is produced by the inactivation of the *Fmr1* gene by an CGG repeat expansion on its 5'-UTR. The normal function of the gene product, FMRP, is to act as a translational repressor, modulating the translation of different dendritic mRNAs, which is critical for

different forms of synaptic plasticity. When FMRP is not functional, there is an increased protein synthesis (around 10-20%) in the postsynaptic dendrites and the synaptic function is altered (for review, see Santoro et al., 2012). It was demonstrated that *Fmr1 -/- Cpeb1 -/-* mice showed a significant amelioration of the symptoms associated with FXS compared to *Fmr1 -/- Cpeb1 +/+* animals and that the depletion of CPEB1 in adults rescued the working memory deficits. This points to a model in which CPEB1 exerts a positive translational regulation and FMRP a negative regulation, a phenotype that is compensated when both proteins are depleted (Udagawa et al., 2013). CPEs are present in one third of the nearly 1000 mRNAs targeted by FMRP, which suggests that both proteins could co-regulate some mRNA targets (Darnell et al., 2011; Udagawa et al., 2013).

In addition, CPEB4 has been identified as a pro-survival protein involved in the response to brain ischemia (Kan et al., 2010). Moreover, a recent study showed that while *Cpeb4* KO animals are normal, mice expressing only the N-terminal low complexity domain (LCD) of CPEB4 (LTD-CPEB4), form LCD-CPEB4 aggregates that accumulate in the nucleolus, thus affecting rRNA biogenesis as well as producing an increased expression of stress-related genes, such as DRR1. As a result, mice display: increased neonatal death, mobility deficits derived from impaired motor axon branching and reduced neuromuscular junction formation (a typical event that precedes neuronal death). Therefore, this report links the accumulation of aggregated LCDs, which are also present in other neurodegenerative diseases mediated by other proteins, with neurodegeneration of motor neurons and CPEB4 (Shin et al., 2016).

Apart from these reports, there are no other publications showing association between CPEBs and other neurodegenerative diseases. Nevertheless, one interesting candidate of study is Alzheimer's Disease (AD). This idea comes from the evidence that CPEB1 has been described to interact with the amyloid

precursor protein (APP), which anchor it to the neuronal membranes (Cao et al., 2005). Moreover, CPEB1 and CPEB4 are known to target the mRNA of the tissue plasminogen activator (tPA) (Ortiz-Zapater et al., 2011; Shin et al., 2004), a protein that, as we will explain in next chapters, plays a key role in the disease.

4. Alzheimer's Disease

Alzheimer's Disease (AD) is the most common type of dementia in the elderly. This neurodegenerative disease was first described by Alois Alzheimer in 1907. It is characterized by the accumulation of extracellular aggregates of amyloid beta (Aβ) peptide (senile plaques) and intracellular, aberrantly phosphorylated Tau protein (neurofibrillary tangles, NFT), which is a microtubule associated protein (Alzheimer, 1907; Glenner and Wong, 1984; Lee et al., 1991). The classical clinical symptoms of the early phase of the disease include memory impairment, deterioration of the language and visuospatial deficits (Esteban-Santillan et al., 1998; Greene et al., 1996; Kirk and Kertesz, 1991; Pillon et al., 1993; Price et al., 1993), followed by seizures, gait disturbances, and motor and sensory abnormalities in the late phase (McKhann et al., 1984). As the disease progresses, several conditions may lead to death, such as infections, nutritional disorders, fractures, wounds or epilepsy (Chandra et al., 1986).

4.1. Types of Alzheimer's Disease

In general terms, we can distinguish between two types of AD: late-onset AD (LOAD) and early-onset AD (EOAD).

4.1.1. Late-onset AD (LOAD)

This is the most frequent form of AD. It develops after the age of 65 and it is considered to be associated with a mixture of environmental and genetic factors that affect Aβ catabolism and clearance in the elderly. Even though several risk factors, such as smoking, diabetes or obesity have been linked to LOAD (Arvanitakis et al., 2004; Beydoun et al., 2008; Cataldo et al., 2010), the main risk factors are the female chromosomal sex, the presence of the apolipoprotein ε4 (APOE-ε4) allele (associated with lipid transport alterations), and especially the age (Riedel et al., 2016).

4.1.2. Early-onset AD (EOAD)

In contrast to LOAD, which is a complex disorder with complex etiology, EOAD is considered to be a genetically determined form of AD, with a heritability ranging from 92 to 100% (Wingo et al., 2012). This form of AD, which develops before the age of 65, is very rare and accounts for 5% of total AD cases. This form of AD is similar to the LOAD, except for the fact that it appears before and progresses faster (Jacobs et al., 1994).

Mutations in 3 genes were initially discovered to play a role in EOAD: amyloid precursor protein (APP), presenilin-1 (PSEN1) and presenilin-2 (PSEN2), which in general accelerate the generation of Aβ, and therefore the onset of the disease. In addition, the presence of the APOE-ε4 allele is also considered a risk factor for this form of AD (St Clair et al., 1995). However, these mutations together can only explain up to 10% of the cases of EOAD (Wingo et al., 2012). Of note, this form of AD allowed the discovery and cloning of APP, PSEN1 and PSEN2, which was crucial for the understanding of the molecular mechanisms of the disease.

4.2. The onset of Alzheimer's Disease: the amyloid cascade hypothesis

Although AD seems to have a multifactorial origin, one of the most accepted causes of the disease is the "amyloid cascade hypothesis". According to this model, when there is lack of protection, compensation mechanisms and/or clearance of Aβ in the ageing brain, the generation and subsequent accumulation of this peptide in small oligomeric aggregates, as well as bigger fibrillar aggregates triggers pathophysyological changes that lead to AD. Different lines of evidence support this hypothesis: Aβ is known to be neurotoxic both *in vivo* and *in vitro* and all the known mutations associated with AD are known to increase the levels of Aβ. Moreover, most people suffering from trisomy 21 (Down's syndrome), and hence having 3 APP copies,

develop physiopathological features of AD. Finally, mice that overexpress human APP accumulate plaques and have memory deficits (reviewed in Cummings, 2004; Hardy and Selkoe, 2002).

In the brain, Aβ is generated from the transmembrane protein APP by proteolytic cleavage mediated by two secretases: β-secretase (Beta-Site APP Cleaving Enzyme 1, BACE1); and γ-secretase (conformed by presenilins PSEN1 and PSEN2 in the core, and the accessory proteins APH-1, Nicastrin and PEN2). Under normal conditions, APP is preferentially proteolyzed first by an α-secretase, a group of membrane bound proteases of the ADAM (a disintegrin and metalloproteinase) family. This releases a soluble peptide (APPsα) and a membrane-bound C-terminal fraction (APP-CTFα), which is degraded by the lysosomes or is further proteolyzed by the γ-secretase complex, releasing small hydrophobic fragments called P3 fragments (Non-amyloidogenic pathway, **Figure 14**). Alternatively, APP can be proteolyzed following the amyloidogenic pathway. When APP follows this alternative processing pathway, it is first proteolyzed by β-secretase in the residue 1 of the final Aβ, which generates the soluble APPsβ and the membrane-bound APP-CTFβ that is subsequently proteolyzed by the γ-secretase complex in the residues 40 or 42, releasing $Aβ_{1-40}$ or $Aβ_{1-42}$, the major forms of neurotoxic Aβ found in AD (Amyloidogenic pathway, **Figure 14**) (reviewed in De Strooper et al., 2010).

Once Aβ is produced, it eventually aggregates and triggers the subsequent events that lead to neuronal death and dementia, specifically synaptic loss and then neuronal cell death. However, before this takes place, it affects synaptic plasticity at the early stages of the disease (reviewed in Selkoe, 2002; Small et al., 2001). Additionally to the toxic effects mediated directly by Aβ, the aggregation of this peptide also induces the activation of the astrocytes and glial cells, which will produce inflammation and oxidative stress. Finally, aggregated amyloid beta has the ability to imbalance the kinase/phosphatase

pathways, which will lead to the aggregation and accumulation of intracellular, insoluble deposits of hyperphosphorylated Tau protein in the neurons (which disrupts the microtubule trafficking and leads to cell death). Moreover, Aβ promotes other events, such as lipid peroxidation and excitotoxicity (reviewed in Cummings, 2004; Hardy and Selkoe, 2002; De Strooper et al., 2010). It is important to highlight that Aβ accumulation can start 20 years before the appearance of the clinical symptoms of the disease (Bateman et al., 2012).

Even though the amyloid cascade hypothesis is nowadays the most accepted model for explaining the onset of AD, different lines of evidence support an alternative hypothesis called "the Tau hypothesys". According to it, AD is originated by different causes, mainly hyperphosphorylation, that promote Tau dissasembly from the microtubules. However, this can also occur through mutations that alter its function or isoform expression. Tau is normally soluble. However, these specific circumstances make it to disassemble from the microtubules, forming insoluble aggregates (NFTs) which sequester normal Tau, microtubule associated protein 1 (MAP1), MAP2, and ubiquitin. The exact mechanisms of Tau aggregation in the absence of specific mutations have not been fully elucidated yet but it is thought to be produced mainly through Tau hyperphosphorylation. However, other processes, such as protease action or exposure to polyanions like glycosaminoglycans have been reported. The insoluble structures formed after Tau aggregation directly damage cytoplasmic functions and indirectly interfere with axonal transport through the loss of the microtubular network, thus leading to cell death. In addition, once cells die, aggregated Tau is released, which can activate microglial cells that will contriibute to exacerbate the damage. For reviews on this section, see Iqbal and Grundke-Iqbal, 2008; Maccioni et al., 2010; Mohandas et al., 2009; Mudher and Lovestone, 2002.
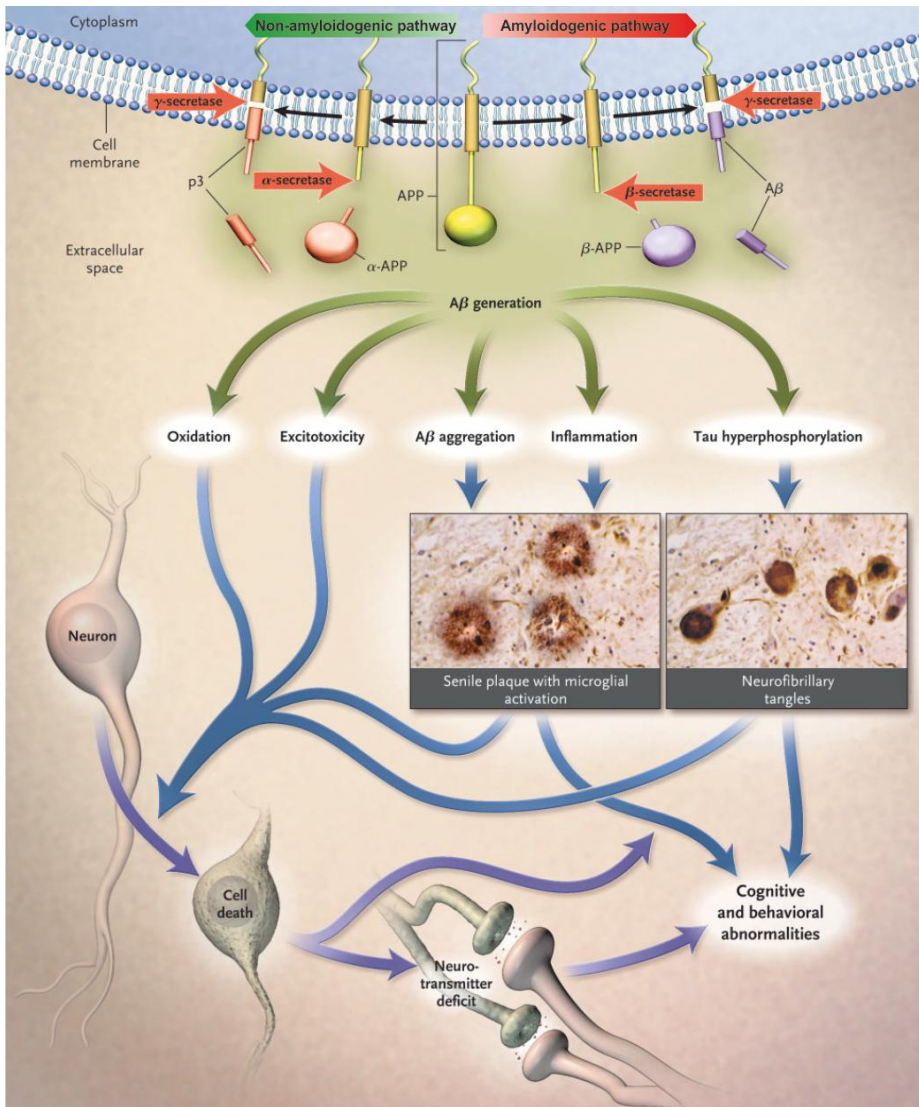
***Figure 14. Schematic diagram of the onset of Alzheimer's Disease**. AD originates from an incorrect proteolytic processing of APP. In the non-amyloidogenic pathway (from APP to the left, shown in green), APP is cleaved first by α-secretase complex, generating APPsα, which is then cleaved by the γ-secretase complex, thus releasing a mixture peptides of different lengths, called in general p3. In the amyloidogenic pathway (from APP to the right, shown in red), APP is first cleaved by β-secretase complex, generating APPsβ, which is then cleaved by γ-secretase in position 40 or 42, thus generating $A\beta_{1-40}$ or $A\beta_{1-42}$. Aβ will aggregate and mediate reduction in synaptic efficiency and activation of the glial cells that will lead to inflammation and progressive synaptic and dendritic neuronal injury, which produces oxidative stress and excitotoxicity. Moreover, alterations in the kinase and phosphatase pathways lead to Tau hyperphosphorylation and accumulation of NFTs with subsequent breakage of the microtubular transport. All together will produce neuronal loss and cell dysfunction with neurotransmitter deficits that will lead to dementia. Figure adapted from Cummings, 2004 with information from De Strooper et al., 2010.*

45

4.3. Mouse models of Alzheimer's disease

During the past years, different mouse models for the study of AD have been developed. However, it is important to bear in mind that none of the current genetically engineered AD mouse models fully recapitulate the comprehensive neuropathology of the human AD brain. However, all these animal models have offered great advantage toward the understanding of particular proteins, processes and lesions derived from AD pathogenesis (Radde et al., 2008). The most common animal models overexpress mutated forms of APP or combinations of mutations in APP and tau. However, as we will discuss, two promising *knock-in* (KI) animal models have emerged very recently.

Transgenic mice overexpressing human APP only show subtle changes in Aβ levels. However, a robust increase in Aβ levels and AD-like pathology occurs when they overexpress human APP containing some of the typical mutations found in familial AD (FAD), which are usually located inside the APP sequence or in PS1 and/or PS2 of the γ-secretase complex. These mutations in general favor the processing of APP by β-secretase and/or increases the γ-secretase processing of APP. Therefore, the classical mouse models of AD overexpress human APP and/or human PS1 or PS2, harboring different mutations, typically under the control of platelet-derived growth factor (PDGF), Thy-1 or the hamster prion promoter (PrP). In general, the accumulation of more mutations is associated with faster disease onset. Some examples include: PDAPP (Games et al., 1995), Tg2576 (Hsiao et al., 1996), J20 (Mucke et al., 2000), APP23 (Sturchler-Pierrat et al., 1997), TgCRND8 (Chishti et al., 2001), APPDutch (Herzig et al., 2004), PS/APP (Holcomb et al., 1998) and 5XFAD (Oakley et al., 2006).

Although mutations in APP and/or presenilins cause classic AD with senile plaques, they fail to develop NFTs. In order to overcome this limitation, different models were created to develop NFTs by overexpressing mutant Tau containing different mutations that make it dissociate from the microtubules

46

and aggregate. Some examples of these mouse models are: JNPL3 (Lewis et al., 2000), rTg4510 (Santacruz et al., 2005) or hTau (Andorfer et al., 2003).

To study the interaction between plaques and NFTs, other models containing APP and/or PSEN and/or Tau mutations have been developed, as it is the case of APPSwe-Tau (Tg2576 x JNPL3)(Lewis et al., 2001) or 3XTg (Oddo et al., 2003).

It is important to mention that the use of transgenic mouse models has several drawbacks, including the effects associated to the overexpression of mutant proteins, the side effects produced by the site in which the transgene is randomly inserted, or the potential phenotypes produced by the overproduced, non-Aβ fragments, such as sAPP or CTFβ. To solve this problem, different single APP KI mouse models (APP$^{NL-F/NL-F}$ and APP$^{NL-G-F/NL-G-F}$) have emerged in the last years (Saito et al., 2014). For their generation, the endogenous mouse APP was humanized. Then, the mutations Swedish (KM670/671NL) and Beyreuter/Iberian (I716F) were included, which increase the levels of Aβ generated and the ratio Aβ42/40, respectively (APP$^{NL-F/NL-F}$ mouse model). Finally in order to accelerate the onset of AD, another model (APP$^{NL-G-F/NL-G-F}$) was generated including the Arctic mutation (E694G) in the previous mouse model. These mice accumulate Aβ and show AD-like phenotype without the artefactual features of APP overexpression and have been proved to be promising for the study of AD (Masuda et al., 2016; Saito et al., 2014).

Finally, an alternative way to model AD in mice is the intracranial administration of aggregated Aβ directly in the hippocampus (or other brain areas). This *in vivo* model of AD is widely used because it allows the study of the short-term effects of Aβ in the brain of other mouse models (*e.g.* KO mice) without the requirements of time-consuming crossings with AD mouse models (Eisele et al., 2009; Jean et al., 2015; Tsukuda et al., 2009). In addition, it is a very interesting model, as it recapitulates the pro-inflammatory environment found in AD patients (McLarnon and Ryu, 2008).

5. The plasminogen System and Alzheimer's disease

As explained in the previous chapter, some of the mechanisms that could explain LOAD are proposed to be associated with the impairment of the mechanisms of Aβ clearance. In recent years, it has been shown that some proteolytic enzymes are able to degrade Aβ, which means that the reduction of their activity could be crucial for AD pathogenesis, or even that they could be used as an alternative therapeutic approach, as it is the case of angiotensin-converting enzyme (Hu et al., 2001), neprylysin (Kanemitsu et al., 2003), endothelin-converting enzyme (Eckman et al., 2001), insulin-degrading enzyme (Mukherjee et al., 2000) and plasmin (Tucker et al., 2000). In this chapter, we will focus on the plasminogen system, its physiological roles, and how it can contribute to Alzheimer's disease.

5.1. The plasminogen system and its thrombolytic and tissue remodeling roles

The plasminogen system is a balanced system comprised by plasmin (the key protease of the system), its inactive precursor plasminogen, and different activators and inhibitors that participate in a coordinated way to regulate plasmin generation and activity (**Figure 15**).

Plasmin was first discovered to play important roles in thrombolysis through the degradation of fibrin clots, even though it has also been proved to participate in other cell functions, such as: matrix degradation, cell migration (Moonen et al., 1982; Shea and Beermann, 1992) and neuronal plasticity in the CNS (Pang et al., 2004). In mammals, plasmin can be generated by two different plasminogen activators (PAs): tissue-type plasminogen activator (tPA) and urokinase-type plasminogen activator (uPA). PAs are serine proteases that cleave specific bonds in the zymogen plasminogen to process it into the proteolytically active plasmin. tPA-mediated plasmin generation has been

classically linked to fibrin degradation in the bloodstream (Collen and Lijnen, 1991). In fact, tPA is able to bind to fibrin, which increases its affinity for plasminogen and its catalytic activity. Moreover, several cell receptors, being Annexin II the main receptor in endothelial cells, are able to induce tPA activity (Cesarman et al., 1994; Hajjar and Krishnan, 1999; Hajjar et al., 1994). On the other hand, uPA-mediated plasmin generation has been more linked to pericellular degradation of the extracellular matrix (ECM) and migration (Blasi, 1999). The activity of uPA is stimulated by its receptor uPAR (Ellis and Dano, 1991).

Furthermore, the activity of the PAs is tightly regulated by some inhibitors that block the PAs by direct binding, being the most important one plasminogen activator inhibitor-1 (PAI-1) (van Mourik et al., 1984) and plasminogen activator inhibitor-2 (PAI-2) (Kruithof et al., 1995). Actually, once they are liberated to the bloodstream, tPA and uPA are rapidly inactivated by direct binding to these PAIs (Kruithof et al., 1984).

Finally, once generated, the activity of plasmin can be further regulated by other two inhibitors: α2-antiplasmin (α2-PI) (Collen, 1976; Moroi and Aoki, 1976; Müllertz and Clemmensen, 1976) and α2-macroglobulin (α2-MG) (Ganrot, 1967). By blocking the activity of plasmin that is not bound to fibrin, plasmin inhibitors act as negative regulators of the plasminogen system in order to prevent proteolytic degradation of other important coagulation factors.

Circulating tPA levels under resting conditions are around 5ng/mL, but large amounts can be secreted quickly under certain circumstances. Even though it was described to be released mainly by endothelial cells (Levin and del Zoppo, 1994), tPA can also be released by keratinocytes (Chen et al., 1993; Schmidt et al., 2004), melanocytes (Hashimoto et al., 1986) and different tumor cells (Corte et al., 2005; Ortiz-Zapater et al., 2007). Moreover, as we will discuss in

next chapter, tPA also play important roles in the CNS.
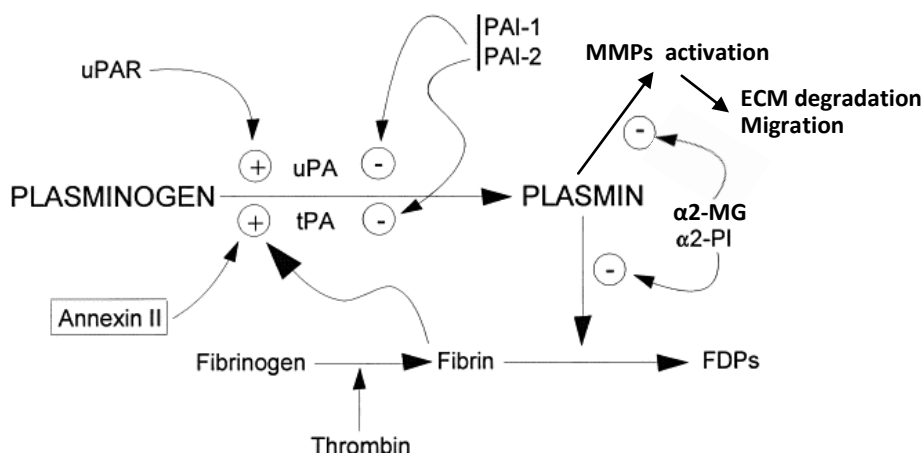
Figure 15. The plasminogen system in the bloodstream. Plasminogen circulates through the bloodstream. Plasmin can be generated from plasminogen through uPA or tPA. Plasmin is able to degrade fibrin, produced from fibrinogen in response to an injury, into fibrin degradation products (FDPs). tPA can bind to fibrin, which increases its catalytic activity and therefore fibrin catalyzes its own destruction. Plasmin is also responsible for the activation of MMPs, which degrade the ECM and facilitates cell migration. Some cell surface receptors, such as uPAR or Annexin II also activate the PAs. The plasminogen activator inhibitors 1 and 2 (PAI-1, PAI-2), among others, control the activity of the PAs. Finally, some proteins such as α2-antiplasmin and α2-macroglobulin can directly control plasmin activity. Adapted from Hajjar and Krishnan, 1999).

5.2. Role of the plasminogen system in the central nervous system

Besides its well-known roles in fibrinolysis and ECM degradation, the plasminogen system has also been demonstrated to play important roles in the CNS both in physiological and pathological conditions. It is important to highlight that, even though both tPA and uPA have been reported to be expressed in the brain, tPA is the major PA of the healthy CNS, whose functions will be described in more detail in this section. However, unlike the tPA system, the uPAR/uPA system is not constitutively expressed and was believed for a

long time to be absent from the normal brain (Sappino et al., 1993). However, now it has been proved to be stress-responsive and both uPA and its receptor uPAR, or uPAR only, have been found to be transiently upregulated in response to different stimuli (injuries) to the CNS. Some examples include inflammation (Gabay and Kushner, 1999), brain ischemia (Rosenberg et al., 1996), multiple sclerosis (East et al., 2005; Gveric et al., 2001), cerebral malaria (Fauser et al., 2000), Alzheimer's disease (Tucker et al., 2000; Walker et al., 2002) or Creutzfeldt-Jacob disease (Deininger et al., 2002). Moreover, it has been found in the brain and cerebrospinal fluid (CSF) from patients infected with HIV (Sidenius et al., 2004) and in the CSF of patients with bacterial meningitis (Winkler et al., 2002).

As introduced before, tPA has been reported to exert both physiological and pathological roles in CNS, through a dual mechanism. On the one hand, tPA can mediate several functions in a catalytic-dependent way, mainly through plasmin generation. However, on the other hand, it has also been demonstrated that tPA possesses catalytically-independent functions (Rogove et al., 1999) and it is able to interact with different receptors, such as Annexin II (Hajjar and Krishnan, 1999). This confers tPA a cytokine-like activity that can be important not only for additional physiological roles, but also for the appearance of toxic side effects, as will be discussed in this chapter.

The regulation of tPA in the CNS is complex and involves transcriptional control, which makes tPA an early immediate gene (Qian et al., 1993); translational control of its mRNA mediated by CPEB1 (Shin et al., 2004) and potentially by CPEB4 (Ortiz-Zapater et al., 2011); and post-translational regulation through its localization in synaptic vesicles and release upon synaptic stimuli (Lochner et al., 2006; Salles and Strickland, 2002); and subsequent inhibition by neuroserpin, a brain-specific inhibitor of tPA (Krueger et al., 1997).

5.2.1. The structure of tPA

tPA is a glycoprotein of 527 amino acids and around 70 kDa (depending on glycosylation). It is synthesized as a single-chain protein but can be hydrolyzed by plasmin or trypsin, thus forming a two-chain structure that remains together bound by a disulfide bond. Structurally, from N-terminal to C-terminal, it is formed by 5 autonomous domains: the fibronectin type I domain (FN1: Ser1 to Lys49), which mediates fibrin affinity; an EGF-like domain (EGF: Ser50 to Asp87); the kringle regions 1 and 2 (KR1 and KR2: Thr88 to Gly176 and Asn177 to Cys261, respectively) and a serine protease domain (SP: Ser262 to Pro527) (Pennica et al., 1983) (**Figure 16**). These domains are involved in the different functions of tPA, including its binding to fibrin (through FN1 and KR2), its rapid clearance in vivo (through FN or EGF), its binding to receptors (through EGF), its catalytic activity (through SP) and its regulation by PAI-1 (through the sequence Lys296-His-Arg-Arg299 inside SP) (Lijnen and Collen, 1991).

Figure 16. The structure of tPA*. tPA is a glycoprotein which contains independent functional domains: A fibronectin type I domain (fibronectin finger), an EGF domain, two kringle domains (Kringle 1 and 2) and one serine protease domain. Taken from Nordt and Bode, 2003.*

52

5.2.2. Physiological roles of tPA

In the CNS, neurons synthesize tPA, which is transported to the growth cones (Lochner et al., 1998) and dendritic spines (Shin et al., 2004) and its expression is known to be upregulated: in the hippocampus after learning and long-term potentiation (LTP) (Qian et al., 1993); in the cerebellum after motor learning (Seeds et al., 1995); in the amygdala after fear and anxiety (Pawlak et al., 2003) and in the hypothalamus (Teesalu et al., 2004). In addition, plasminogen as well as its inhibitors PAI-1 and neuroserpin, are known to be expressed in the CNS (Salles and Strickland, 2002; Teesalu et al., 2004). However, it is thought that the main inhibitor of the activity of neuronal tPA is neuroserpin (Krueger et al., 1997). This hypothesis is confirmed by the fact that the overexpression of neuroserpin in the CNS reduces the activity of tPA (Cinelli et al., 2001). It is important to highlight that, unlike other serpins, the interaction of neuroserpin and tPA seems to be unstable, which means that its inhibitory effect could be only transient (Barker-Carlson et al., 2002)*,* thus pointing to important *in vivo* regulatory relevance. Different physiological roles of tPA have been associated to neuronal tPA, as it will be described in this section and in **Figures 17 and 18**.

Role of tPA in neurite outgrowth and axon regeneration

First, different studies demonstrated that tPA KO neurons have impaired neurite outgrowth, and exogenous addition or overexpression of tPA produces increased neurite outgrowth (Baranes et al., 1998; Lee et al., 2007a; Minor et al., 2009; Pittman and DiBenedetto, 1995). Similar effects are observed in cells with altered expression of neuroserpin (Parmar et al., 2002). Moreover, *in vivo* studies showed that axonal regeneration following injury is reduced in *tPA* KO mice, which improves with exogenous tPA administration (Akassoglou et al., 2000; Siconolfi and Seeds, 2001; Zou et al., 2006).

tPA has been suggested to mediate neurite growth through the proteolytic processing of neurotrophins (Pang et al., 2004). For axonal growth, tPA has

been proposed to control plasmin-mediated proteolysis of ECM components, which facilitates migration (Bukhari et al., 2011; Pittman and DiBenedetto, 1995; Wu et al., 2000). For axonal regeneration, the removal of fibrin aggregates and the macrophage recruitment to remove cell debris appears to be important (Akassoglou et al., 2000; Zou et al., 2006). This mechanism involves the direct binding of tPA to LRP-1 (Cao et al., 2006). Furthermore, the binding to LRP-1 or Annexin II receptors has also been shown to be important in a non-proteolytic way (Lee et al., 2007a; Shi et al., 2009).
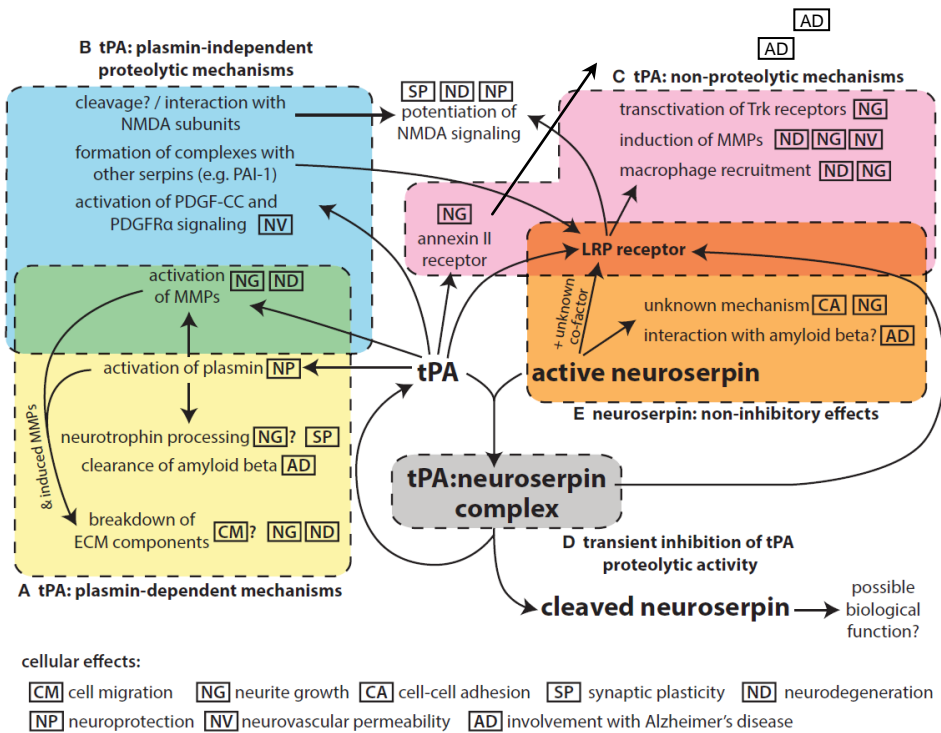
Figure 17. Summary of tPA roles in the CNS. *(A) tPA can act on different substrates indirectly through the generation of plasmin. (B) tPA can also participate in the proteolytic processing of different substrates different from plasmin. (C) tPA has also been demonstrated to interact with different receptors independently of its proteolytic activity. (D) Neuroserpin can transiently regulate tPA activity through direct binding. (E) Neuroserpin could also possess important functions besides the inhibitory regulation of tPA activity. Adapted from Lee et al., 2015). For more information refer to text.*

Role of tPA in memory

Besides its roles in migration and regeneration, tPA has also been found to play important roles in L-LTP. *tPA* KO mice show reduced L-LTP (Frey et al., 1996; Huang et al., 1996) and impaired hippocampal dependent tasks, being the latest partially restored by tPA administration (Pawlak et al., 2002). In addition, the overexpression or administration of tPA increases LTP and spatial memory (Baranes et al., 1998; Madani et al., 1999).

Some authors defend that the mechanism by which tPA participates in memory is through tPA-induced plasmin-mediated maturation of the proBDNF into mature BDNF (mBDNF) (Pang et al., 2004), changing the ratio proBDNF/mBDNF. proBDNF is associated to LTD and mBDNF to LTP, and tPA is released only when neurons are subjected to high-frequency stimulation, which means that tPA mediates different responses to different stimulation patterns. However, a recent study suggested that this effect could be mediated by tPA indirectly by potentiating the NMDA receptor, in a plasmin-independent way (Rodier et al., 2014). Several studies support the idea that tPA can act as a modulator of glutamatergic neurotransmission by controlling the activation of the NMDA receptor by proteolytic cleavage of its NR1 subunit (Fernández-Monreal et al., 2004; Nicole et al., 2001), in GluN2D-containig receptors (Obiang et al., 2012) (**Figure 18A**), direct proteolytic and non-proteolytic modulation of its subunit NR2B (Ng et al., 2012; Norris and Strickland, 2007) (**Figures 18A and 18C**), or indirectly through a signaling involving the low density lipoprotein receptor-related protein 1 (LRP1) receptor, that recruits intracellular PSD95 and modulates NMDA activity (Martin et al., 2008; Samson et al., 2008) (**Figure 18C**). Finally, tPA interaction with the NMDA receptor can control the compensatory increase in the surface density of NR2B receptors that takes place during alcohol dependence (Pawlak et al., 2005), probably activating intracellular signaling cascades (**Figure 18B**).

Even though the different reports point to the same direction, the precise mechanisms are still controversial given the variety of brain areas, experimental procedures and developmental stages considered in the different reports. However, the general outcome of these studies suggest that tPA is a very important neuromodulator.
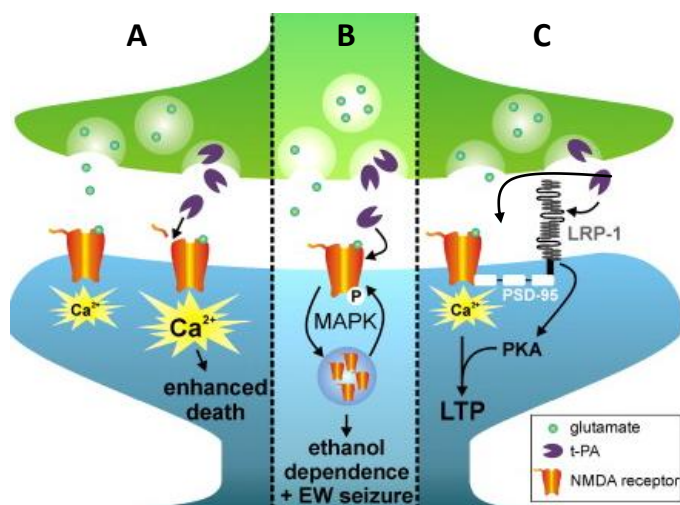
Figure 18. Proposed molecular mechanisms for tPA-mediated glutamatergic synaptic transmission. Besides its indirect roles in synaptic transmission modulation through proBDNF maturation, tPA can be released from the presynaptic compartment and exert different direct functions in the postsynaptic compartment by directly modulating the NMDA receptor activity. (A) tPA can proteolyze the NR1 subunit of the NMDA receptor and modulate its activity, potentiating the synapses and the calcium influx inside the postsynaptic terminal, which can potentiate the synapse or mediate excitotoxic cell death. (B) tPA has been shown to potentiate the development of ethanol dependency through NR2B phosphorylation, MAPK-ERK1/2 activation, and a rise in the number NR2B- containing NMDARs. (C) The tPA receptor LRP1 is known to be tethered to NMDA via PSD95. The interaction of tPA directly with NMDA or with its receptor LRP1 in a non-proteolytic way facilitates NMDAR-dependent L-LTP in the hippocampus through a signal transduction that elevates PKA levels. Even though tPA protein is present in presynaptic vesicles and its mRNA has been proved to be translated in the PSDs (Shin et al., 2004), only the presynaptic tPA is shown for simplicity reasons. Figure adapted from Samson and Medcalf, 2006.

Role of tPA in cerebrovascular regulation

Finally, in the CNS, tPA is also found in the interface between the basement membrane of the endothelial cells and the astrocytes, where it modulates the cerebrovascular tone (Nassar et al., 2004) and the permeability of the blood-

brain-membrane (Polavarapu et al., 2007).

5.2.3. Pathological roles of tPA

Something to consider is that the role of tPA in the CNS is controversial, because even though several studies clearly show its important roles in physiological events such as synaptic plasticity and neuroprotection as described above (Pang et al., 2004; Qian et al., 1993; Seeds et al., 1995; Wu et al., 2015), other studies point to neurotoxic effects of tPA (Chen and Strickland, 1997; Echeverry et al., 2010; Tsirka et al., 1995; Wang et al., 1998). This is very important and, due the thrombolytic properties of plasmin, one year after the publication of an important clinical study in 1995 (The National Institute of Neurological Disorders and Stroke rt-PA Stroke Study Group, 1995), the intravenous administration of recombinant tPA was approved as the standard treatment for ischemic stroke in the first 3h after the onset of the pathology. Some authors stated that it could be extended to 4.5h in selected patients (Hacke et al., 2008), even though it has not been officially approved. However, the toxicity associated with tPA is still a concern, given that a significant number of patients develop intracranial hemorrhage.

Different mechanisms have been proposed for the pathological roles of tPA in the CNS: First, the plasmin generated by tPA or the activation of MMPs can contribute to ECM degradation that promotes neuronal death (Chen and Strickland, 1997; Tsirka et al., 1997; Wang et al., 2003). Second, an excess of potentiation of the NMDA receptor mediated by tPA, besides modulating its activity, can also produce excitotoxicity in some situations (Nicole et al., 2001). In fact, immunotherapy against tPA reduces neuronal damage in stroke models (Gaberel et al., 2013). Third, the interaction of tPA with LRP1 can mediate different events, such as MMP expression (Lee et al., 2007b; Wang et al., 2003), the opening of the blood-brain barrier (Sashindranath et al., 2012; Yepes et al., 2003), or even activation of the microglia (Rogove et al., 1999; Siao and Tsirka,

2002; Zhang et al., 2009). Finally, it has been reported that the non-catalytic interaction of tPA with Annexin II and Galectin1, in a dose-dependent manner, can also induce neuronal apoptosis (Medina et al., 2005) and microglial activation (Pineda et al., 2012) in pathological conditions. This is significantly relevant in the context of neurodegenerative diseases, as it is the case of Alzheimer's disease.

5.2.4. Role of tPA in Alzheimer's disease

As already commented in previous chapters, the plasminogen system is a fine-tuned system that can participate in multiple physiological and pathological processes, including AD. In this regard, it is known that aggregated Aβ stimulates the transcriptional expression of tPA and that, at the same time, tPA can bind to Aβ aggregates (as a substitute for fibrin), which stimulates its affinity for plasminogen and its catalytic activity. This suggests that Aβ can replace fibrin in the role of activating tPA (Kingston et al., 1995). In fact, in brains of AD patients, tPA co-localizes with senile plaques (Medina et al., 2005). The plasmin generated by tPA is therefore able to degrade the Aβ peptide and attenuate its toxicity (Ledesma et al., 2000; Tucker et al., 2000). Actually, when aggregated Aβ is directly injected in the hippocampus of WT mice (which contains high levels of tPA), it is rapidly cleared, but in tPA or plasminogen KO mice, it persists longer and produces neuronal degeneration (Melchor et al., 2003). In addition, the depletion of endogenous tPA in human APP-overexpressing mice (Tg2576 mouse model) is associated with reduced lifespan, increased cerebral Aβ accumulation and worsening of the AD pathology (Oh et al., 2014).

These data indicate that tPA has a physiological neuroprotective role in CNS avoiding Aβ accumulation by its plasmin-mediated degradation. However, in pathological situations like AD, tPA can also play the opposite effect triggering a cell death cascade that contributes to exacerbate the pathology. Indeed,

several reports suggest that the overexpression of tPA induced by Aβ triggers neuronal apoptosis through sustained ERK1/2 activation in a dose-dependent and catalytic-independent manner (Medina et al., 2005). Moreover, increased tPA levels also promote microglial inflammation (Siao and Tsirka, 2002) through activation of ERK1/2, JNK, AKT and p38 pathways which lead to TNFα production (Pineda et al., 2012), contributing to neurodegeneration. The activation of signaling pathways independently of the catalytic activity of tPA is not exclusive of neurons. It has also been reported in other models, such as epithelial cells (Ortiz-Zapater et al., 2007; Roda et al., 2009) and fibroblasts (Hu et al., 2006), leading to the classification of tPA as a new cytokine.

Overexpression and neurotoxic effects of tPA during AD can be a consequence of inefficient plasmin generation, resulting in the reduction of clearance, and increased levels of Aβ aggregates and therefore a continuous stimulus for tPA synthesis by neurons (**Figure 19**). Indeed, plasmin levels are significantly lower in people affected by AD (Ledesma et al., 2000). Several reasons can explain the reduced plasmin levels in these patients. First, lipid rafts composition can be altered during AD progression, resulting in inefficient plasminogen activation, as this event requires intact lipid rafts (Ledesma et al., 2003a). In fact, the generation of plasmin requires the binding of plasminogen to the membrane (Plow et al., 1995) through the interaction with molecules such as Annexin II (Hajjar and Acharya, 2000), α-enolase (Miles et al., 1989), amphoterin (Parkkinen and Rauvala, 1991) or the ganglioside GM1 (Miles et al., 1991), which are enriched in the rafts of neurons (Ledesma et al., 2003b).

On the other hand, it has been reported increased levels of PAI-1 in the CNS related to age, a phenomenon which is worsened during Aβ accumulation (Cacquevel et al., 2007; Melchor et al., 2003). This increase in PAI-1 levels can block the proteolytic activity of tPA, and therefore contribute to the reduction

59

of plasmin levels and increased aggregation of Aβ (Liu et al., 2011). Both models are not mutually exclusive and could take place simultaneously.

In summary, regulation of tPA expression in response to Aβ emerges as crucial event in AD onset and progression. However, little is known about the molecular mechanism regulating Aβ-induced tPA expression. Considering that tPA mRNA is present in the soma and synaptic terminals and targeted by CPEB1 and CPEB4 (Ortiz-Zapater et al., 2011; Shin et al., 2004), and that these proteins control synaptic mRNA translation, they could potentially be novel regulators of the tPA response during AD pathology.
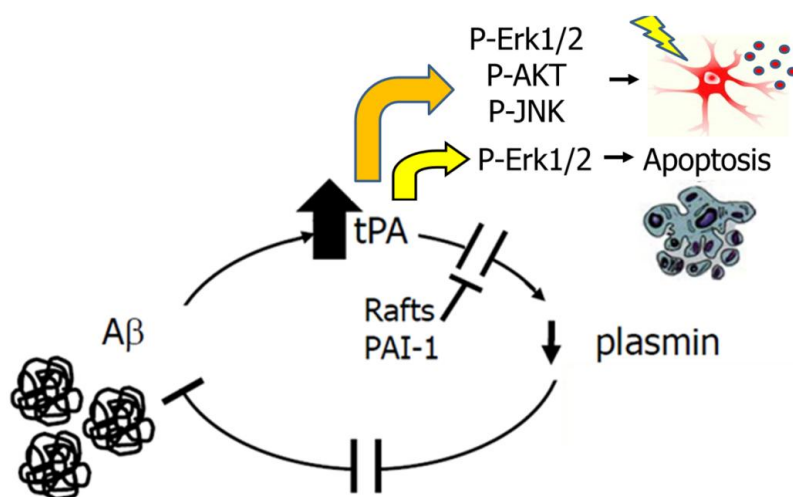
Figure 19. Role of the plasminogen system in AD pathology. The plasminogen system is induced by Aβ during the course of AD pathology. As a result, tPA expression and activity are induced and plasmin generated, which degrades Aβ. However during AD progression, the alteration of the neuronal lipid rafts and/or the overexpression of PAI-1, impair the tPA-mediated conversion of plasminogen into plasmin. Since plasmin is not generated, Aβ is not degraded, and it starts to accumulate. As a result, tPA is induced at a higher extent. Even though a high proportion of this tPA will be catalytically inactive because it will be bound to PAI-1, cell signaling cascades activated by high tPA concentrations, through its interaction with cell surface receptors in a non-catalytic way, will lead to neuronal apoptosis and microglial-mediated inflammation, which contributes to the pathology of AD.

AIMS

AIMS

CPEBs are known to control important cell functions, especially in polarized cells such as neurons, where they regulate different physiological processes such as memory formation. However, different lines of evidence start to show that they can possess important functions during neurodegenerative diseases. Currently, little is known regarding the molecular mechanisms by which CPEBs act in this context. Therefore, unraveling these specific regulation processes mediated could help us to understand and even treat these diseases.

Considering that tPA is overexpressed during AD pathology and that both CPEB1 and CPEB4 are known to target tPA mRNA during glutamate-mediated synaptic plasticity and pancreatic cancer, respectively, in this work we focus on the study of the molecular mechanism by which this overexpression takes place in response to Aβ treatment. Our specific objectives are:

1. Study if neuronal tPA overexpression in response to Aβ treatment is regulated by translational control.

2. Analyze if CPEB1 and/or CPEB4 are implicated in the Aβ-induced tPA overexpression.

3. Study the molecular mechanisms by which CPEB1 and/or CPEB4 control tPA overexpression.

4. Characterize the expression and localization of CPEBs in human samples of AD.

5. Elucidate the implications of CPEBs-mediated translational control in AD pathogenesis using *in vivo* and/or *in vitro* models for AD.

MATERIALS AND METHODS

1. Mice

Mice were maintained in cages in groups of four under pathogen-free conditions with 12h stable light cycles, temperature of 22±2°C and controlled moisture between 40-70%. They were fed *ad libitum* with complete feed. All the procedures were approved by the CEEA (Ethical Committee for Animal Experimentation) of the Barcelona Biomedical Research Park (PRBB) and/or the Barcelona Science Park (PCB).

1.1. Mouse colonies

1.1.1. *Cpeb1* KO mice

The gene targeting strategy for the generation of *Cpeb1* KO mice has been previously described by our group (Calderone et al., 2015). For the generation of the line, the initial targeting vector, containing a FRT-flanked neomycin resistance cassette in the intron 4 of *Cpeb1* gene and 2 LoxP sites flaking exon4, was electroporated in mouse W4 ES cells. The neomycin resistance cassette was removed from the *Cpeb1^{flFrt}* allele of the positive cells through the expression of the FlpO recombinase (Raymond and Soriano, 2007). The positive ES cells were then microinjected in the inner cell mass of developing blastocysts. The excision of exon4 of *Cpeb1* was then achieved by mating the chimeric mice with a CMV-Cre transgenic line, leading to a ubiquitous Cre-mediated recombination that generates a frameshift and loss-of-function in *Cpeb1^{fl}* allele (*Cpeb1$^-$*).

1.1.2. *Cpeb4* KO mice

The gene targeting strategy for the generation of the *Cpeb4* KO mice has been previously described by our group (Calderone et al., 2015). Mouse ES cells carrying a FRT-flanked βGeo cassette (β-galactosidase gene fused to neomycin resistance gene) in intron 1 of *Cpeb4* gene and 2 LoxP sites flanking exon2, were microinjected in the inner cell mass of developing blastocysts. The

resulting chimeric mice were crossed with C57BL/6J mice. The βGeo cassette was then removed from the Cpeb4^{flFrt} allele by mating these mice with pCAG-Flp mice (Rodríguez et al., 2000). The excision of exon2 of *Cpeb4* was then achieved by mating these mice with a CMV-Cre transgenic line, leading to a ubiquitous Cre-mediated recombination that generates a frameshift and loos-of-function in the *Cpeb4^{fl}* allele (*Cpeb4$^-$*).

1.1.3. Brain-specific *Cpeb4 KO* mice

For the generation of the brain-specific conditional *Cpeb4* KO mice, animals of the genotype *Cpeb4$^{fl/fl}$* were crossed with the transgenic line Nes-Cre8 (Petersen et al., 2002; Zimmerman et al., 1994), which expresses Cre recombinase under the control of Nestin promoter and restricts its expression to the central nervous system.

1.1.4. *tPA* KO mice

tPA KO mice were a kind gift from Dr. Peter Carmeliet (VIB Vesalius Research Center, KU Leuven, Belgium) (Carmeliet et al., 1994). To disrupt tPA gene, a targeting vector containing a neomycin resistance gene replacing exon 9 of *tPA* was inserted in ES cells. Positive cells were microinjected in the inner cell mass of developing blastocysts and the chimeric mice were mated.

1.1.5. Wild.type OF-1 mice

Pregnant *wt* OF1 females were purchased to Charles River Laboratories.

1.2. DNA Genotyping

1.2.1. Genomic DNA extraction

Genomic DNA for genotyping was extracted from the tail of ~5 week-old mice or the leg of E17.5 embryos. Both tissues were processed in the same way except for the duration of the initial tissue digestion.

Tissue was digested for 2h (embryonic leg) or 16h (adult tail) at 55°C in 500μL of tail buffer (200mM NaCl, 20mM Tris-HCl, 5mM EDTA, 0.5%[w/v] SDS, pH8) containing 500 μg/mL of proteinase K (Merk Millipore). Samples were centrifuged at 16000g for 10 min and the supernatant transferred to a new tube. 500μL of cold isopropanol was added, and the tubes were mixed by inversion and centrifuged again at 16000g for 10 min. Supernatants were discarded and pellets were washed once with 70% ethanol. Samples were centrifuged for 5 min at 16000g and the pellets resuspended in 250μL of TE buffer (10mM Tris-HCl, 10mM EDTA, pH 8).

1.2.2. Genotyping PCRs

100ng of the DNA obtained was used per PCR reaction. PCRs were performed using BioTaq DNA polymerase Kit (Bioline).

<u>Cpeb1 minus allele (*Cpeb1⁻*)</u>

For the PCR reaction, the forward primer TCTGGTGGTCAGTCATCCTG and the reverse primer CAGAACACTGACAAGATGCTCA were used. After an initial denaturalization step at 94°C for 4 min, samples were subjected to 35 cycles of 94°C for 30s, 60°C for 30s and 72°C for 90s. Finally, they were heated at 72°C for 7min and kept at 4°C. The WT allele produces a 734bp band and the minus (*Cpeb1⁻*) allele a 200bp band.

<u>Cpeb4 minus allele (*Cpeb4⁻*)</u>

For the PCR reaction, the forward primer GTGAGGAAAGCAGTATCTAGGGTC and the reverse primer ACATAGTCACTAACAAACTTGAGG were used. After an initial denaturalization step at 94°C for 4 min, samples were subjected to 35 cycles of 94°C for 30s, 60°C for 30s and 72°C for 90s. Finally, they were heated at 72°C for 7min and stored at 4°C The WT allele produces a 735bp band and the minus (*Cpeb4⁻*) allele a 328bp band.

Floxed *Cpeb4* allele (*Cpeb4^{fl}*)

For the PCR reaction, the forward primer AGTGCTCTGCTGCTGTGCTA and the reverse primer TGGCATCCATGCTTGTGTAT were used. After an initial denaturalization step at 94°C for 4 min, samples were subjected to 35 cycles of 94°C for 30s, 60°C for 30s and 72°C for 60s. Finally, they were heated at 72°C for 7min and stored at 4°C. The WT allele produces a 735bp band and the floxed (*Cpeb4^{fl}*) allele a 600bp band.

Nes-Cre8

For the detection of the Nes-Cre8 transgene, four primers were used: the WT-specific primers (TAGGCCACGAATTGAAAGATCT and GTAGGTGGAAATTCTA GCATCATCC) and the Nes-Cre8-specific primers (GCGGTCTGGCAGTAAAAA CTATC and GTGAAACAGCATTGCTGTCACTT). After an initial denaturalization step at 95°C for 2 min, samples were subjected to 35 cycles of 95°C for 30s, 51°C for 30s and 72°C for 30s. Finally, they were heated at 72°C for 10min and stored at 4°C. The control (WT) band produces a 300bp band and the samples positive for the Nes-Cre8 transgene an additional band of 100bp.

tPA

For the PCR reaction, the forward primers GGAAAGGTGTGACTTACCGTGG CACCCAC and AATGTGTCAGTTTCATAGCC, and the reverse primer CGCTGTG TAACTCTTGCCCATGAGGAC were used. After an initial denaturalization step at 95°C for 5 min, samples were subjected to 40 cycles of 94°C for 1 min, 60°C for 1 min and 72°C for 1 min. Finally, they were heated at 72°C for 10 min and kept at 4°C. The WT allele (*tPA⁺*) produces a 200bp band and the minus (*tPA⁻*) allele a 100bp band.

2. Cell cultures

2.1. Culture of mouse primary hippocampal neurons

Primary hippocampal neurons were cultured as previously described (Dotti et al., 1988; Kaech and Banker, 2006). 24-well or 96-well plates were coated by adding Poly-L-Lysine 1 mg/mL in borate buffer (8.12mM Borax, 77.67mM Boric Acid, pH 8.5) for 16h at 37°C. The coating solution was removed and plates were washed 3 times with MiliQ (MQ) water and filled with plating medium, consisting of Minimum Essential Medium (MEM) supplemented with 0.45% D-glucose (Panreac), 10% heat-inactivated horse serum (Horse Serum, New Zealand Origin, Gibco, Thermo Fisher Scientific) and 100U/mL of Penicillin-Streptomycin (Gibco, ThermoFisher Scientific). The medium was equilibrated overnight before starting the cultures. When required for Immunofluorescence, before adding the Poly-L-Lysine solution, one glass coverslip was placed per well. Coverslips were previously treated with nitric acid 65% for 16h, washed 3 times with water and once with 75% ethanol, dried and autoclaved.

The brains of E17.5 mouse embryos were obtained and the hippocampi were dissected in Hank's Balanced Salt Solution (HBSS) without Ca^{2+} and Mg^{2+} (138mM NaCl, 5.33mM KCl, 0.45mM KH2PO4, 4.16mM $NaHCO_3$, 0.34mM Na_2HPO_4) supplemented with 7mM HEPES pH7.45, 0.45% (w/v) glucose and 100 U/mL of Penicillin-Streptomycin. Hippocampi were pooled and digested with 0.05% trypsin (Gibco) in HBSS for 17 min at 37°C. DNase I (DN25, Sigma-Aldrich) was added to 80 µg/mL and incubated for 1 additional minute at 37°C. After digestion, cells were dissociated with a fire-polished Pasteur pipette and resuspended in 2mL of pre-warmed plating medium. Cells were counted in a Neubauer chamber and plated in the pre-equilibrated plating medium on poly-L-Lysine-coated 24-well plates at a density of 10^5 cells/well for biochemical analysis and $4 \cdot 10^4$ cells/well for Immunofluorescence analysis. For toxicity assays, $1.2 \cdot 10^4$ cells were plated per well in 96-well plates.

Cells were incubated for 4 hours at 37°C and then plating medium was replaced by Neurobasal medium (Gibco, Thermo Fisher Scientific) supplemented with 2% B27, 2mM L-Glutamine (Gibco, Thermo Fisher Scientific) and 100U/mL of Penicillin-Streptomycin. Half of this culture medium was replaced every 3 days. After 3 days in culture, Cytosine β-D-arabinofuranoside (Ara-C, Sigma) was added to a final concentration of 1µM for 48h. After 7 days in culture, L-Glutamine was removed from the culture medium in order to avoid potential excitotoxic effects. Neurons were grown for 15 days before proceeding with the biochemical or imaging analyses.

2.2. Culture of Neuro2A neuroblastoma cell line

Neuro2A cells were cultured in DMEM supplemented with 10% FBS, 2mM Glutamine and 10U/mL of penicillin/streptomycin.

3. Functional synaptosomes and cytosolic fractions

Functional synaptosomal preparation is based on the original protocol of Nagy and Delgado-Escueta, 1984. All the procedures were performed at 4°C. WT, *Cpeb1* KO or *Cpeb4* KO mice were sacrificed by cervical dislocation and the brains obtained, washed in ice-cold PBS and dissected in order to remove the cerebellum and the olfactory bulb. Then, they were homogenized by applying 12 strokes at 245rpm using a 15-mL teflon-glass homogenizer (Potter-Elvehjem, 15mL, Wheaton) containing 12mL of homogenization buffer (0.32M sucrose, 1mM EDTA, 1mg/mL BSA, 5mM HEPES, pH 7.4). An aliquot of this initial homogenate was taken and processed for protein or RNA extraction as described in sections 7 and 8). Homogenates, containing the total brain fraction, were centrifuged at 3000g for 10min. The supernatant was centrifuged again at 3000g for 2 min. The new supernatant (S1), which contains the cytosolic and synaptosomal fractions, was centrifuged at 14000g for 12min. The supernatant (S2), containing the crude cytosolic fraction, was removed and

the pellet (P2) was resuspended in Krebs-Ringer (140mM NaCl, 5mM KCl, 5mM Glucose; 1mM EDTA, 10mM HEPES, pH 7.4) and mixed with ice-cold Percoll (Sigma-Aldrich) to a final concentration of 45% Percoll in a volume of 1mL. Samples were mixed by inversion and centrifuged at 17500g for 2min. The synaptosome-enriched fraction that is found floating in the surface was recovered by removing all the lower fractions with a 27G needle. This synaptosome-enriched fraction was resuspended in 1mL of Krebs-Ringer buffer and centrifuged at 17500g for 30 s for washing it. The supernatant was then removed and the pellet resuspended in HEPES-modified buffer (147mM NaCl, 3mM KCl, 10mM Glucose, 2mM $MgSO_4$, 2mM $CaCl_2$, 20mM HEPES, pH 7.4) containing both protease inhibitors (Complete EDTA-free Protease inhibitor Cocktail tablets, Roche) and 400U/mL of RNAse inhibitors (Ribolock RNAse inhibitor 40U/μL, Thermo Fisher Scientific). This crude synaptosomal fraction is metabolically active, and is able to respond to different treatments for approximately 4 hours. For this reason, this synaptic preparations have been used extensively for *in vitro* studies of the synaptic organization and function (Camoletto et al., 2009; Schubert et al., 2006). These synaptosomes were stimulated *in vitro*, centrifuged at 17500g for 30s and pellets were resuspended in 200μL of RIPA buffer (150mM NaCl, 50mM Tris pH 8, 1%NP40, 0.5% Sodium Deoxycholate, 0.1% SDS, 1mM EDTA) supplemented with protease inhibitors, or in 1mL of TRIzol (Ambion, ThermoFisher Scientific) for the analysis of proteins or RNA, respectively. Alternatively, for some experiments, RNA and protein extracts were obtained without previous stimulation. The stimulation protocol is described in section 4.2.

The cytosolic fraction was prepared through centrifugation at 100.000g for 1h of the crude cytosolic fraction (S2) obtained as described above. The cytosolic fraction will remain in the supernatant (S2'). This cytosolic fraction was used directly for western blot.

A detailed diagram for the preparation the different fractions can be found in results section (**Figure 28A**).

4. Amyloid beta aggregation and treatments

4.1. Aggregation of the Aβ peptide

Amyloid beta (1-40) (Amyloid β-Protein(1-40) Trifluoroacetate salt, H-1194, Bachem) was aggregated in stable soluble and fibrillar forms as described (Ferreira et al., 1997; Lorenzo and Yankner, 1994; Medina et al., 2005; Wogulis et al., 2005). In brief, 1mg of Aβ was resuspended in 2.3mL of Dulbecco's PBS (DPBS), to a final concentration of 100µM. After the initial aggregation, the peptide was aged for 4 days at 37°C, aliquoted, and stored at -80°C until used.

4.2. Aβ treatments of primary neurons and synaptosomes

4.2.1. Aβ stimulation of primary hippocampal neurons

Primary hippocampal neurons were cultured as described in section 2.1 until DIV15. Then, Aβ or the equivalent volume of vehicle solution (DPBS) was added to the cell medium to a final concentration of 10µM. After different time points, ranging from 30min to 16h depending on the experiment, medium was removed and the plates were flash-frozen in liquid nitrogen and stored at -80°C until they were processed for protein or RNA extraction as described in sections 7 and 8.

For specific experiments involving pharmacological inhibitors, 30 minutes before the addition of Aβ, neurons were treated with 5µM Actinomycin D (A1410, Sigma-Aldrich), 20µM Cordycepin (C3394, Sigma-Aldrich) or 100µM Cycloheximide (C4859, Sigma-Aldrich) and then with Aβ 10uM for 8 hours.

4.2.2. Aβ stimulation of synaptosomes

Functional synaptosomes were prepared as described in section 3. After the final resuspension in 1mL of HEPES-Modified medium, synaptosomes were split in 2 tubes in a final volume of 500μL and incubated at 37°C for 10 min. Then, Aβ or the equivalent volume of vehicle (DPBS) was added to a final concentration of 10μM. Stimulation was carried out at 37°C for 30 min. Then, samples were placed on ice, split in 2 tubes (1/3 for protein analysis and 2/3 for RNA analysis) and centrifuged at 17500g for 30s. The supernatant was removed and pellets were processed for protein or RNA analysis as described in sections 7 and 8, respectively.

5. Neuronal toxicity (MTT assay)

Cell toxicity in primary hippocampal neurons was determined by the MTT assay. The MTT assay is normally used for the measurement of cell proliferation based on cell mitochondrial activity. However, considering that neurons are post-mitotic cells, the same assay can be used to determine cell viability following Aβ treatment, as the mitochondrial activity is proportional to the number of viable cells. Primary mouse hippocampal neurons were plated at a cell density of 37500 cells/cm^2 in poly-L-Lysine-coated 96-well plates (12000 cells/well) and maintained in culture until DIV7 as described in section 2.1. Then, aggregated Aβ or the equivalent volume of vehicle solution (DPBS) was added to a final concentration of 10μM. After 48h of treatment at 37°C and 5% CO_2, the cell medium was replaced by the MTT substrate (3-(4.5-dimethylthiazol-2-yl)-2.5-diphenyltetrazolium bromide, Sigma) at 1 mg/mL in Neurobasal/B27 medium (without L-Glutamine) for 3.5 h at 37°C and 5% CO_2. Then, cell medium was removed and the MTT product was extracted from cells with 100μL/well of 20% (v/v) dimethyl sulfoxide (DMSO) in isopropanol. Cell viability was estimated by measuring the absorbance at 570nm. Vehicle-treated neurons were considered 100% of viability.

6. Immunofluorescence

6.1. Immunofluorescence of primary hippocampal neurons

Primary hippocampal neurons were cultured to DIV15 in poly-L-Lysine-coated glass coverslips (in 24-well plates) as described in section 2.1. Growth medium was removed and cells were fixed in fixation solution (4% paraformaldehyde, 4% Sucrose in PBS) at RT for 15 min. Cells were washed 3 times with PBS. Permeabilization was achieved by incubation with 0.3% Triton-X-100 in PBS for 10min at RT. Cells were washed 3 times with PBS and non-specific binding was blocked with 2% Bovine Serum Albumin (BSA) in PBS. Cells were washed twice with PBS and incubated with the primary antibodies overnight at 4°C in 1% BSA in PBS (**Table 1**). Alexa-conjugated secondary antibodies were incubated for 1h at RT in 1% BSA in PBS (TABLE). After 3 additional washes with PBS, samples were quickly washed with MQ water and mounted with Fluoromount-G (SouthernBiotech). Pictures were taken with a Leica SP5 confocal microscope.

6.2. Immunofluorescence of tissue sections

6.2.1. Mouse tissue sections

Mice ranging from 8 to 12 weeks of age were sacrificed by cervical dislocation. Brains were obtained, quickly washed in PBS, cut in 2 sagittal halves and fixed in 10% formalin overnight at 4°C, dehydrated and embedded in paraffin. These formalin-fixed paraffin-embedded (FFPE) tissues were sectioned at 5 to 15μm (depending on the experiment) with a microtome. Sections were dewaxed and rehydrated. Antigen retrieval was performed with citrate buffer (tri-sodium citrate 10mM, pH 6) at 121°C for 15 min in a pressure cooker. Lipofuscin autofluorescence was quenched by incubating the samples 5 min in 70% ethanol and 10min with 0.3% Sudan Black B (SBB, Sigma) in 70% ethanol. Excess of SBB was eliminated by dipping the samples in 70% ethanol (5-10 dips) and washing 3 times with PBS. Non-specific binding was blocked with 2% BSA in PBS

for 1h at RT. Then, primary antibodies were added in 1% BSA in PBS overnight at 4°C (**Table 1**). Samples were washed 3 times in PBS and Alexa-conjugated secondary antibodies were added in 1% BSA in PBS for 1h at RT. Slides were mounted using DAPI Fluoromount-G (SouthernBiotech). For visualization, pictures were taken using a Leica SP5 confocal microscope.

6.2.2. Human brain samples

Human hippocampal samples of AD patients and healthy controls (formalin-fixed-paraffin embedded) were kindly provided by Dr. Eulàlia Marti (Center for Genomic Regulation, CRG, Barcelona) and Dr. Isidre Ferrer (IDIBELL-Hostpital Universitario de Bellvitge, Barcelona). Samples were dewaxed and subsequently processed as described in section 6.2.1 for mouse samples.

Primary antibody	Host	Working dilution	Commercial brand
Anti-Aβ 6E10	Mouse	1:500	BioLegend (SIG 39-320)
Anti-CPEB4	Mouse	1:500	Home-made* (Clone 93c)
Anti-CPEB4	Rabbit	1:400	Abcam (ab83009)
Anti-CPSF30	Rabbit	1:75	Bethyl (A301-584A)
Anti-CPSF59	Rabbit	1:75	Bethyl (A301-359A)
Anti-CPSF68	Rabbit	1:75	Bethyl (A301-356A)
Anti-CPSF73	Mouse	1:100	Santa Cruz (sc-100691)
Anti-CSTF50	Rabbit	1:75	Bethyl (A301-251A)
Anti-CSTF64	Rabbit	1:100	Bethyl (A301-093A)
Anti-CSTF77	Rabbit	1:75	Bethyl (A301-096A)
Anti-MAP2	Chicken	1:1000	Abcam (ab5392)
Anti-PSD95	Mouse	1:500	ThermoFisher (MA1-046)
Anti-RNA Pol II 8WG16	Mouse	1:100	Covance (MMS-126R)
Anti-tPA	Rabbit	1:1000	Home-made serum**
Secondary antibody	Host	Working dilution	Commercial brand
Anti-Mouse/Alexa488	Donkey	1:500	Thermofisher (A21202)
Anti-Mouse/Alexa555	Donkey	1:500	ThermoFisher (A31570)
Anti-Rabbit/Alexa488	Donkey	1:500	ThermoFisher (A21206)
Anti-Rabbit/Alexa555	Donkey	1:500	Thermofisher (A31572)
Anti-Chicken/Alexa-405	Goat	1:500	Abcam (ab175674)

*Table 1. List of primary and Alexa-conjugated secondary antibodies used for Immunocytofluorescence and Inmunohistofluorescence experiments. The host, working dilution and commercial brand are indicated. *This antibody was developed for Dr. Raul Mendez in the Spanish National Cancer Research Centre (CNIO). **This antibody was a kind gift of Dr. Peter Carmeliet (KU Leuven, Belgium).*

7. Western Blot

7.1. Sample processing

7.1.1. Primary hippocampal neurons

Primary hippocampal neurons were grown, stimulated and frozen as described in sections 2.1 and 4.2.1. Samples at -80°C were directly lysed with Laemmli Buffer 1x (2% SDS, 40% glycerol, 5% 2-mercaptoethanol, 0.005% bromophenol blue, 62.5mM Tris-HCl, pH 6.8) and boiled at 98°C for 5min for total protein extraction.

7.1.2. Synaptosomes and subcellular fractions

Subcellular fractions were prepared as described in chapter 3. Total brain extracts or cytosolic extracts were directly quantified with the Pierce BCA Protein Assay Kit (23225, ThermoFisher Scientific). Synaptosomal pellets were resuspended in 200μL of RIPA buffer and quantified. 20μg of each sample were mixed with Laemmli Buffer 4x to a final concentration of 1x, boiled for 5 min at 98°C and processed as described below.

7.1.3. Dissected brain tissue

Hippocampus and/or cortex from adult mice were dissected in ice-cold PBS and homogenized in 1mL of RIPA buffer in a 1mL tissue grinder (Wheaton). Then, they were quantified and processed as described above for the synaptosomes.

7.2. Western blot analysis

Samples were loaded in polyacrylamyde gels of different percentages depending on the sizes of the proteins to analyze and run for 20 min at 80V and then approximately for 1.5h at 140V. Proteins were transferred to a nitrocellulose membrane (Amersham Hybond ECL Nitrocellulose Membrane, GE Healthcare) at 400mA for 75 min at 4°C. Membranes were blocked with TBST

(140mM NaCl, 2.7mM KCl, 25mM Tris, 0.1%[v/v] Tween20, pH 7) containing 10% (w/v) non-fat powdered milk (Central Lechera Asturiana) for 1h at RT. Membranes were incubated with the primary antibodies in 2% milk in TBST overnight at 4°C (**Table 2**). Then, they were washed 3 times with TBST (5 minute per wash) and incubated with the secondary antibodies for 1h at RT in 2% milk 2% milk in TBST (**Table 2**). After 3 washes (of 5 min each) with TBS-T, they were developed with Pierce ECL Western Blot Substrate (Thermo Scientific). Membranes were exposed to a radiography film (Radiographic film Curix, Agfa) and developed with a Film Processor Device (Fuji Medical Film Processor model FPM-100A, Fujifilm).

Primary antibody	Host	Working dilution	Commercial brand
Anti-CPEB1	Rabbit	1:500	Proteintech (13274-1-AP)
Anti-CPEB4	Rabbit	1:500	Abcam (ab83009)
Anti-tPA	Rabbit	1:3000	Home-made serum*
Anti-CPSF30	Rabbit	1:1000	Bethyl (A301-584A
Anti-CPSF73	Mouse	1:100	Santa Cruz (sc-100691)
Anti-CSTF64	Rabbit	1:1000	Bethyl (A301-093A)
Anti-CSTF77	Rabbit	1:1000	Bethyl (A301-096A)
Anti-HistoneH3	Rabbit	1:50000	Abcam (ab1791)
Anti-PSD95	Mouse	1:3000	ThermoFisher (MA1-046)
Anti-RNA Pol II N20	Rabbit	1:500	Santa Cruz (sc-899)
Anti-RNA Pol II 8WG16	Mouse	1:1000	Covance (MMS-126R)
Anti-RNA Pol II Ser2P	Mouse	1:1000	Covance (MMS-129R)
Anti-Synaptophysin	Mouse	1:3000	SySy (101 011)
Anti-αTubulin	Mouse	1:10000	Sigma (T9026)
Anti-Vinculin	Mouse	1:2000	Abcam (ab18058)
Secondary antibody	Host	Working dilution	Commercial brand
Anti-Goat/HRP	Rabbit	1:2000	Dako (P0449)
Anti-mouse/HRP	Rabbit	1:2000	Dako (P0161)
Anti-Rabbit/HRP	Goat	1:2000	Dako (P0448)

*Table 2: List of primary and HRP-conjugated secondary antibodies used for western blot experiments. The host, working dilution and commercial brand are indicated. *This antibody was kindly provided by Dr. Peter Carmeliet (KU Leuven, Belgium).*

8. RNA isolation

8.1. Primary hippocampal neurons

For the extraction of total mRNA from primary hippocampal neurons in culture, cell culture medium was removed and cells were flash-frozen in liquid nitrogen. Then, 1 mL of TRIzol (Ambion, ThermoFisher Scientific) was added to each well and cells were scraped with a 200µL tip. Samples were incubated at 4°C for 10 min. Then, 200µL of chloroform was added. Samples were vortexed for 15s and incubated at RT for 3 min. Then, they were centrifuged at 12000g for 15 min at 4°C. Supernatant was transferred to a new tube. 500µL of isopropanol and 15µg of GlycoBlue (AM9515, Invitrogen, ThermoFisher Scientific) were added and samples were vortexed again and placed at -20°C for 20 min. Then, they were centrifuged at 14000g for 20 min at 4°C. Supernatant was recovered, 1 mL of 75% ethanol was added and samples were centrifuged at 7500g for 5 min. After a second ethanol wash, supernatant was removed and samples were air-dried at RT for 3 min. Then, samples were resuspended in 20µL of Nuclease-Free water (Nuclease-Free Water, not DEPC-Treated, Ambion, ThermoFisher Scientific). Samples were treated with 1U of DNAse turbo for 15 min at 37°C and the enzyme inactivated and precipitated with the Turbo DNAse inactivation reagent (TURBO DNA-free Kit, AM1907, Ambion, ThermoFisher Scientific).

8.2. Synaptosomes and other subcellular fractions

For total brain homogenates used in experiments involving synaptosomes, an aliquot of 100µL of the initial brain homogenate prepared in Homogenization Buffer (as described in section 3) was mixed with 1mL of TRIzol.

Synaptosomes prepared from these total homogenates were centrifuged at 17500g for 30s and the pellet resuspended in 1 mL of TRIzol. Then, samples were processed as described for primary hippocampal neurons (section 8.1).

8.3. Brain tissue

Dissected hippocampus or cortex from adult mice were homogenized in 1mL of TRIzol using a 1mL dounce tissue grinder (Wheaton). Then, samples were processed as described for primary hippocampal neurons (section 8.1).

9. qRT-PCR

For RT-qPCR, total RNA was isolated with the TRIzol reagent and treated with Turbo-DNase as described in section 8. RNA was quantified using a nanodrop and 1µg was subjected to cDNA synthesis using Revertaid First Strand cDNA Synthesis Kit (ThermoFisher Scientific) in a final volume of 20µL as recommended by the manufacturer. PCR reactions were performed using a 1/4 dilution of the cDNA as a template in a 10µL reaction volume using SYBR Green (Applied Biosystems, ThermoFisher Scientific). The primers used are described in **Table 3**.

Gene	Forward primer	Reverse Primer
Arc	AGCCAGGAGAATGACACCAG	GTGATGCCCTTTCCAGACA
CamKII	GCAATGGAGACTTTGAGTCCTAC	CAAAATAGAATCGATGAAAGTCCA
Cpeb1	CCTCCTCTGCCCTTTCTTTC	TCCAAGAAGGTCCCAAGATG
Cpeb4	TTGTTTCCGATGGAAGATGG	TCAATATCAGGAGGCAATCCA
tPA	GAGCAGCTCTGTTGGCACT	CCGGTCAGAGAAGAATGGAG
Hprt	GGCCAGACTTTGTTGGATTTG	TGCGCTCATCTTAGGCTTTGT

Table 3: List of primers used for qRT-PCR experiments, ordered from 5' to 3'.

10. Rapid Amplification of cDNA Ends (3'-RACE)

3' Rapid Amplification of cDNA Ends (3'-RACE) was performed by using the SMARTer RACE cDNA amplification Kit (Clontech) following the manufacturer's recommendations. In brief, 500ng of synaptosomal total mRNA was retrotranscribed into cDNA using the specific primer sequence AAGCAGTGGTATCAACGCAGA GTAC(T)$_{30}$VN (being V = A, C or G and N = A, T, C or G). This primer contains an anchor sequence, a repetition of 30 thymidines, and two random nucleotides, which ensure that the primer will anneal right at

the beginning of the poly(A) tail. The resulting cDNA was amplified using the Advantage 2 PCR Kit (Clontech), using specific forward primers annealing in the 3'UTR of the genes to study and a mix of two reverse primers designed to anneal in the anchor sequence (provided as part of the kit). The forward primers used for tPA amplification were RACE_Fwd1 (GGCTACGGCAAGCA TGAGGCATCGTCTCC) and RACE_Fwd2 (AGGGGAGGGGGGTCTTTGGGAGCAGA TGTAGCA). The obtained products were run in an agarose gel, cut out of the gel and purified with the Illustra GFX PCR DNA and Gel Band purification Kit (GE healthcare). The purified sequences were cloned into p-GEM-T-Easy vector (Promega). Positive clones were sequenced as described in section 16.

11. Poly(A) tail length (PAT) assay

Measurement of poly(A) tail length was performed by using the Poly(A) Tail-Length Assay Kit (Affymetrix) following the manufacturer's recommendations. In brief, 1μg of synaptosomal mRNA was tailed in the 3'-end with a G/I anchor sequence and retrotranscribed using anchor-specific primers. Then, the tailed cDNA was diluted to a final volume of 40μL and 5μL per target were PCR-amplified using a pair of 3'-end-specific primers (a forward primer annealing at approximately 150-300 nucleotides far from the beginning of the poly(A) tail, and a universal reverse primer complementary to the G/I anchor sequence). To ensure the specificity of the forward primers and to equilibrate cDNA amounts, an additional PCR was performed using the same gene-specific forward primers, and a gene-specific reverse primer annealing right before the beginning of the poly(A) tail. The primers used were: tPA_PAT_Fw1 (CCTCCACGAGAAGGAAGGGGTATCT), tPA_PAT_Fw2 (CCTCCACGAGAAGGAAGG GGTATCT) and CPEB4_PAT_Fw (AAAAGAGTTCATTTGTTGAAGTGCTAGTG). The specific reverse primers were tPA_PAT_Rv1 (GGAAAAGTGTGAAAAATACCT CTGAATTTATTATTT), tPA_PAT_Rv2 (GGTTGGGAGAACTGTATGATTTTAATAA) and CPEB4_PAT_Rev (CTGAGTTAAAAGTTTTATTCATTCAACATCTC).

12. Plasmid construction and mutagenesis

The DNA corresponding to the full-length 3'-UTR of tPA (according to NM_008872.3) was cloned downstream the ORF of the firefly luciferase in pLuc plasmid (Piqué et al., 2006). In brief, total RNA from DIV15 primary hippocampal neurons in culture was obtained and retrotranscribed as described in section 9. The full-length 3'-UTR of tPA (NM_008872.3) was amplified (Accuprime Taq DNA Polymerase High Fidelity, Invitrogen, Thermofisher Scientific) using the specific forward primer **AGATCT**CAAAGAAAGCCCAGCTCCTTC containing a BglII restriction site (marked in bold) and the reverse primer **GGATCC**AAAGTGTGAAAAATACCTCTGAATTTA, which contains a BamHI restriction site (marked in bold). The PCR product was ligated into pGEM-T-Easy vector (Promega) according to the manufacturer's recommendations. pLuc was digested with BamHI and BglII and dephosphorylated using 1U of Calf Intestinal Phosphatase (CIP, New England Biolabs) at 37°C for 30 min. The 3'-UTR insert was released from T-Vector and ligated into pLuc (Piqué et al., 2006) using BamHI and BglII restriction sites and T4 RNA ligase (New England Biolabs) according to the manufacturer's recommendations.

The mutation of the PAS of the full-length 3'-UTR of tPA was performed with the QuickChange II Site-Directed mutagenesis Kit (Stratagene) using the mutagenesis primers CTTTGTATTATACTGTACTTAAA**GGGG**AAATTCAGAGGTAT TTTTCACAC and GTGTGAAAAATACCTCTGAATTT**CCCC**TTTAAGTACAGTATAATA CAAAG (the mutagenic sequences are marked in bold) using the manufacturer's recommendations. These primers replace the PAS sequence AA**TAAT**AAA by AA**GGGG**AAA.

The shorter variant of the 3'-UTR of tPA described by 3'-RACE (pLuc-3'UTRShort) and its positive control (pLuc-tPA3UTRShortPAS+) were cloned using as template pLuc-tPAFull3UTR. The plasmid was amplified using the

specific fwd primer **AGATCT**CAAAGAAAGCCCAGCTCCTTC, containing a BglII restriction site (marked in bold), and the reverse primers **GGATCC**GCTGTTGAGACATGATCTTGTGGTTC for pLuc-3'UTRShort and **GGATCC**G CTTTATTGCTGTTGAGACATGATCTTGTGGTTC for pLuc3'-UTRShortPAS+ (both containing BamHI restriction sites, marked in bold). The PCR products were ligated into pGEM-T-Easy vector, digested and cloned into pLuc as described for the full-length construct.

The plasmids pLuc-Cyclin B1, pLuc-CyclinB1_CPE123- (with the 3 CPEs mutated), and the normalizing plasmid pRenilla have been previously described (Piqué et al., 2006).

13. *In vitro* transcription

15µg of the pLuc constructs containing the different variants of tPA 3'-UTR, and the normalizing pRenilla described above were linearized with BamHI (or Ecl132II for pRenilla) and purified with the Illustra GFX PCR DNA and gel Band Purification kit (GE Healthcare), following the manufacturer's recommendations. 1µg of the linearized plasmids were transcribed *in vitro* using the mMESSAGE mMACHINE T3 Kit (Ambion) following the manufacturer's guidelines. The resulting mRNA was precipitated with LiCl (provided as part of the kit) and resuspended in nuclease-free water.

14. mRNA transfection into N2A cells

Prior to its transfection into cells, *in vitro* transcribed mRNAs were equilibrated in an agarose gel to ensure equal mRNA amounts. Then, they were mixed with pRenilla using a molar ratio vectors:renilla 3:1 and the levels were checked again in an agarose gel.

N2A cells were plated in a 24-well plate at a cell density of 10^6 cells/well. 16h later, the medium was replaced with 500µL of fresh medium. 4h later, cells

were transfected in triplicates with 500ng of each construct:renilla mix using Lipofectamine MessengerMAX transfection reagent (Life Technologies), following the manufacturer's protocol. 16h post-transfection, medium was removed and cells were flash-frozen in liquid nitrogen and stored at -80°C until they were processed.

For the monitorization of the mRNA transfection efficiency, one control well transfected with 500ng of EGFP mRNA (TriLink Biotechnologies) was included.

15. Dual luciferase assay

Translation efficiency was measured using the Dual-Luciferase Reporter Assay System (Promega). Cells frozen at -80°C were directly lysed with 120µL of passive lysis buffer 1x (included in the kit as a 5x concentrate) for 30 min at RT in shaker. 20µL of the extracts were transferred in triplicate into 96 well plates and measured with an Orion II Microplate Luminometer (Titertek Berthold), using the Simplicity 4.2 Software and the standard Dual Luciferase Reporter Assay System (DLR) program recommended by Promega. The ratio firefly/renilla was obtained for all the samples, and translation efficiency was normalized respect tPA3'UTRFull-length construct.

16. DNA purification and sequencing

For small-scale purification, plasmid DNA containing the target sequences was obtained from bacteria using the Wizard Plus SV Miniprep Purification Kit (Promega), following the manufacturer's instructions.

For the sequencing, 500ng of vector per reaction was used as a template for a Sequencing PCR, using 2µL of Big-Dye terminator 3.0 reagent (Applied Biosystems) and 3.2pmol of sequencing primer (AGGAGTTGTGTTTGTGGACG for pLuc sequence validation and TAATACGACTCACTATAGGG for Tvector insert sequencing) in a final volume of 10µL. The PCR conditions included an initial

denaturation step at 94°C for 4 min and 35 cycles of denaturation at 95°C for 30s, annealing at 55°C for 30s and extension at 60°C for 4 min. Samples were precipitated with EDTA/NaOAc/ethanol precipitation, air-dried and sent to the Genomic Sequencing Service of the Universitat Pompeu Fabra for Sanger sequencing.

17. Statistical analysis

Data shown represents the mean ± SD or mean ± SEM. Results were analyzed with parametric statistical procedures (Student's t test, 2-tailed). Significance was accepted at $p < 0.05$. This significance was shown in the graphs with an asterisk (*). When lower p values were obtained, it was shown with additional asterisks. Accordingly, $p < 0.01$ was shown with two (**) and $p < 0.001$ with three (***).

RESULTS

1. Aβ induces tPA expression in the mouse hippocampus

As reviewed in the introduction, it is known that tPA is induced by Aβ. However, in the majority of cases, this induction has been only reported at the level of mRNA or catalytic activity (by zymography), and sometimes by using cell lines or cortical neurons.

Therefore, and in order to gain an insight about tPA kinetics our experimental conditions, we first wanted to determine whether an increase of tPA protein levels could be detected in mouse hippocampal neurons. To this aim, we prepared primary cultures of mouse hippocampal neurons. They were differentiated for 15 days *in vitro* (DIV15), and then treated with aggregated $Aβ_{1-40}$ peptide (Aβ from now on for simplification). In response to Aβ treatment, we detected that tPA was overexpressed at the protein level. This overexpression starts to be detectable after 3 hours of exposure and sustained up to 16h (**Figure 20**). This demonstrates that the primary hippocampal neurons respond to aggregated Aβ peptide and that our conditions of aggregation work.
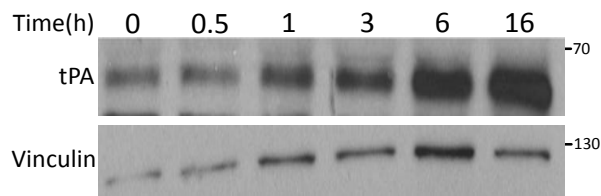
Figure 20. Aβ induces the expression of tPA protein in primary cultures of DIV15 mouse hippocampal neurons. *Western blot of DIV15 mouse primary hippocampal neurons treated with aggregated Aβ peptide for different periods of time. Vinculin was used as a housekeeping protein.*

2. The induction of tPA expression in response to Aβ is regulated by translational control

The next unresolved question we wanted to answer was whether the overexpression of tPA in response to Aβ treatment is regulated by translational control. To this aim, we prepared cultures of primary mouse hippocampal neurons and treated them with Aβ in the presence of different pharmacological inhibitors: actinomycin D (ActD), which blocks transcription; cordycepin (CD) which blocks polyadenylation; and cycloheximide (CHX), an inhibitor of protein synthesis.

Compared with the vehicle-treated neurons, after 8h of treatment, neurons that were treated with Aβ alone produced a 2.7-fold increase in the expression of tPA (**Figures 21A and 21B**). Neurons treated with Aβ in the presence of ActD showed similar increase in tPA expression than those treated with Aβ alone, indicating that the overexpression of tPA after 8h is independent of new transcription. In contrast, the co-treatment with Aβ and CD only showed a 1.9-fold increase of tPA protein in comparison to Aβ alone (**Figures 21A and 21B**). This means that polyadenylation of the pre-existing tPA mRNA is required for the efficient Aβ-induced overexpression of tPA. Finally, Aβ treatment combined with CHX completely abolished the increased tPA protein synthesis (**Figures 21A and 21B**). At the RNA level, whereas Aβ alone or Aβ combined with ActD or CD did not show significant changes in tPA mRNA levels, CHX produced a 10-fold increase (**Figure 21C**).

Overall, these results demonstrate that translational control is important for the overexpression of tPA in response to Aβ. Moreover, they prove that polyadenylation is an important event for the regulation of this process.

A
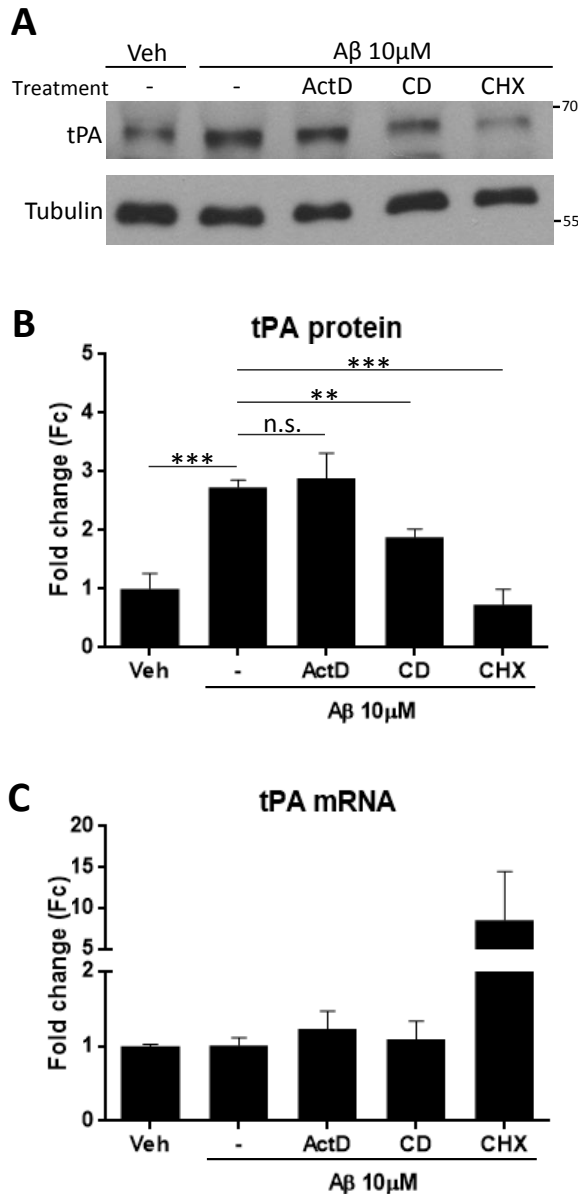
Figure 21. Aβ-induced overexpression of tPA is controlled by translational regulation. *(A, B) Representative western blot and quantification of three independent experiments. DIV15 mouse primary hippocampal neurons were treated for 8h with Vehicle (Veh) or Aβ alone or combined with the inhibitors actinomycin D (ActD), cordycepin (CD) and cycloheximide (CHX). α-Tubulin was used as loading control. Inhibition of transcription (ActD) did not affect Aβ-induced tPA overexpression, whereas inhibition of polyadenylation (CD) or of protein synthesis (CHX) induced a significant decrease of tPA protein levels after Aβ treatment. (C) qRT-PCR showing tPA mRNA levels relative to HPRT of primary neurons treated as in A. tPA mRNA levels were unchanged in all the treatments except for CHX, which resulted in a significant increase. In all the experiments, error bars represent the SD of 3 independent experiments. **p<0.01, ***p<0.001, n.s.: non-statistically significant.*

3. CPEB4 controls tPA basal levels in the mouse hippocampus *in vivo*

It has been previously shown that tPA mRNA is targeted by both CPEB1 and CPEB4 (Ortiz-Zapater et al., 2011; Shin et al., 2004), suggesting that these two proteins can be involved in tPA translational regulation. This led us to hypothesize that CPEB1 and CPEB4 might be involved in the translational control responsible for the observed Aβ-induced overexpression of tPA in neurons.

To investigate this hypothesis, we first compared the expression levels of tPA in the cortex (CX) and hippocampus (HP) of WT, *Cpeb1* KO and *Cpeb4* KO mice. These areas have been shown to regulate the expression and activity of tPA (Baranes et al., 1998; Fiumelli et al., 1999; Huang et al., 1996; Madani et al., 1999; Mataga et al., 2002; Qian et al., 1993), to contain both CPEB1 and CPEB4 (Huang et al., 2006; Tsai et al., 2013; Wu et al., 1998) and to be highly affected by AD pathology (reviewed in Serrano-Pozo et al., 2011).

Our results showed that the expression of tPA protein is lower in the cortex compared to the hippocampus in all the genotypes (**Figures 22A and 22D**). Interestingly, *Cpeb4* KO mice showed a significant downregulation of tPA protein specifically in the hippocampus (**Figures 22D and 22E**). However, when we checked tPA mRNA levels, we did not find statistically significant differences between WT and KO mice neither in the cortex nor in the hippocampus (**Figures 22C and 22F**). These results indicate that tPA mRNA translation is controlled *in vivo* by CPEB4 in the adult hippocampus in basal conditions.

Additionally, we performed a hematoxylin-eosyn staining on brain slices of WT, *Cpeb1* KO and *Cpeb4* KO mice in order to prove that the differences observed were not produced by morphological alterations in the KO mice. Depletion of CPEB1 (**Figure 23c, d**) or CPEB4 (**Figure 23e, f**) does not affect the morphology

of the cortex or hippocampus, which demonstrates that the observed altered expression of tPA in the hippocampus is not related to morphological changes.
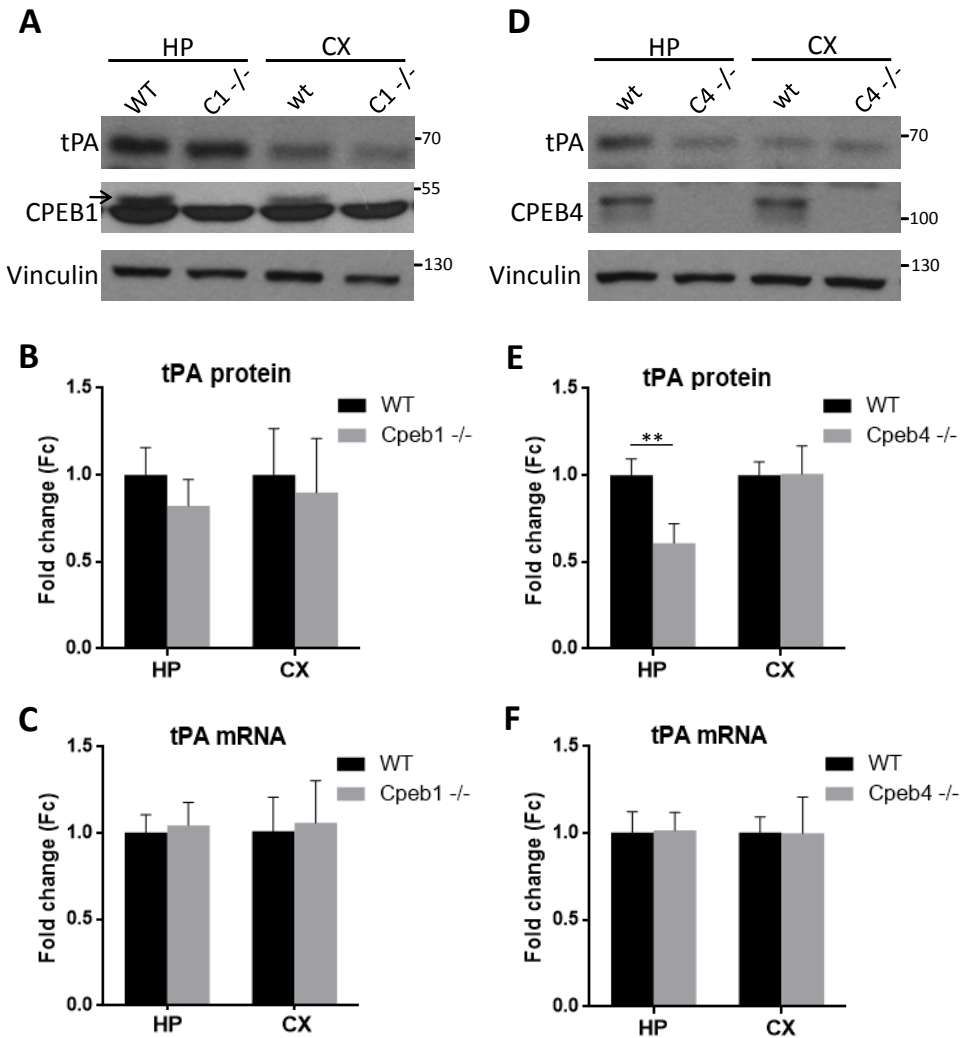
*Figure 22. CPEB4 controls the expression of tPA under basal conditions. Analysis of the mRNA and protein levels of tPA in the cortex (CX) and hippocampus (HP) of WT, Cpeb1 KO (A-C) and Cpeb4 KO (D-F) mice. Western blot (A, D) and tPA protein quantification relative to vinculin (B, E). A reduction in tPA protein levels can be detected specifically in the hippocampus of Cpeb4 KO mice (D, E). In all cases, we did not find statistically significant differences in the mRNA levels of tPA (C, F), thus suggesting that CPEB4 controls tPA levels specifically in the hippocampus at the translational level. C1 -/- is an abbreviated form of Cpeb1 KO and C4 -/- of Cpeb4 KO. In all the experiments, error bars represent the SD of 3 independent mice. ** p<0.01.*

	Hippocampus	Cortex
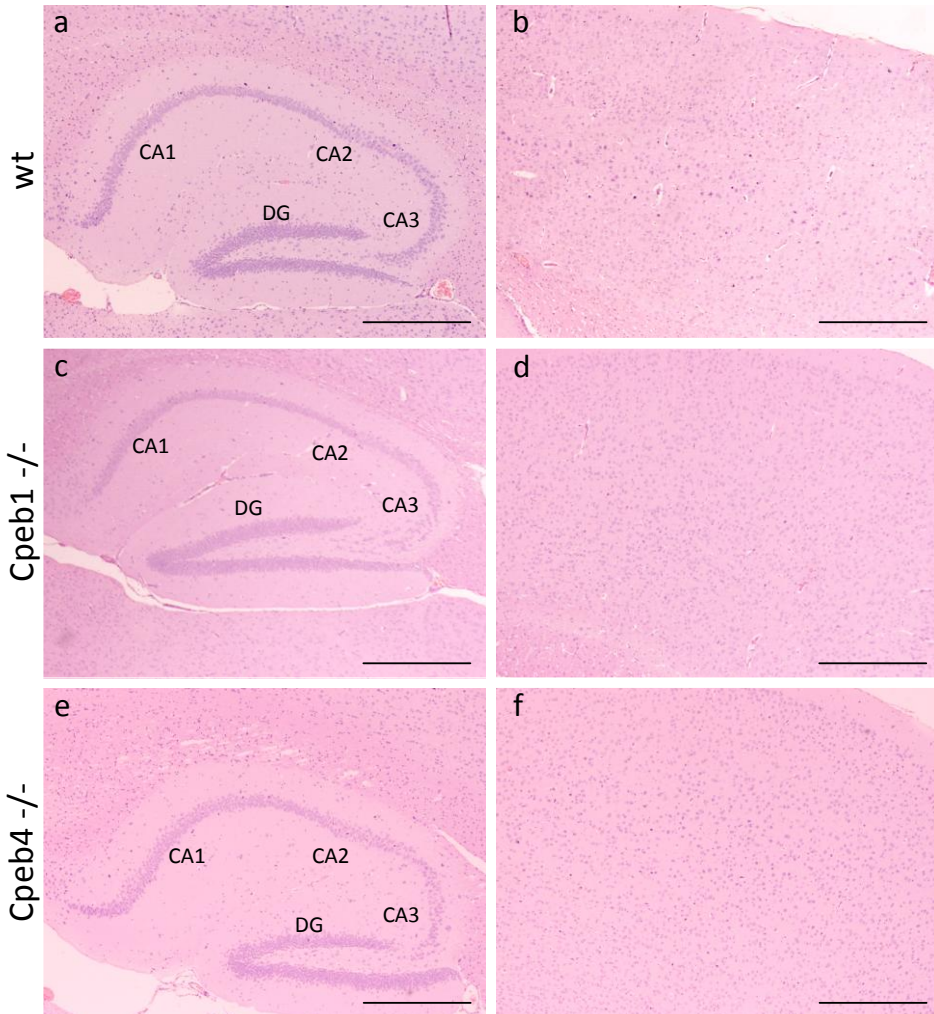
Figure 23. Cpeb1 and Cpeb4 KO mice show normal hippocampus and cortex morphology.
Hematoxylin-eosyn staining of the hippocampus and cortex of WT (a, b), Cpeb1 KO (c, d) and
Cpeb4 KO (e, f) mice. The Cornu Ammonis areas (CA1, CA2, CA3) and the Dentate Gyrus (DG) of
the hippocampus are shown. CPEB1 or CPEB4 depletion does not affect the main morphology of
these structures. Scale bars = 500µm.

We then aimed to study whether the reduced tPA levels observed in *Cpeb4* KO
mice were produced due to a general reduction in translation or mediated by
changes in the subcellular localization or the cells expressing tPA. To this aim,
we performed a double Immunohistofluorescence (IHF) against CPEB4 and tPA
in the hippocampus of WT (**Figure 24a-c**) and *Cpeb4* KO mice (**Figure 24d-f**).
Samples from *tPA* KO mice were used as a control for tPA antibody

(**Figure 24g-i**). As previously reported for WT mice, we found tPA exclusively in the mossy fiber pathway (Salles and Strickland, 2002). The same distribution was found in *Cpeb4* KO mice, suggesting that the cells expressing tPA are not changing in the absence of CPEB4 (**Figure 24, a-f**). Moreover, tPA protein is not detected in the soma of the neurons of the dentate gyrus, which are the source of the mossy fiber axons, suggesting that the subcellular distribution is also maintained in the absence of CPEB4 (**Figure 24, a-f**). We could not detect significant changes in tPA staining (**Figure 24, a-f**), even when we used thicker sections and more magnification (**Fig 25, a-f**).
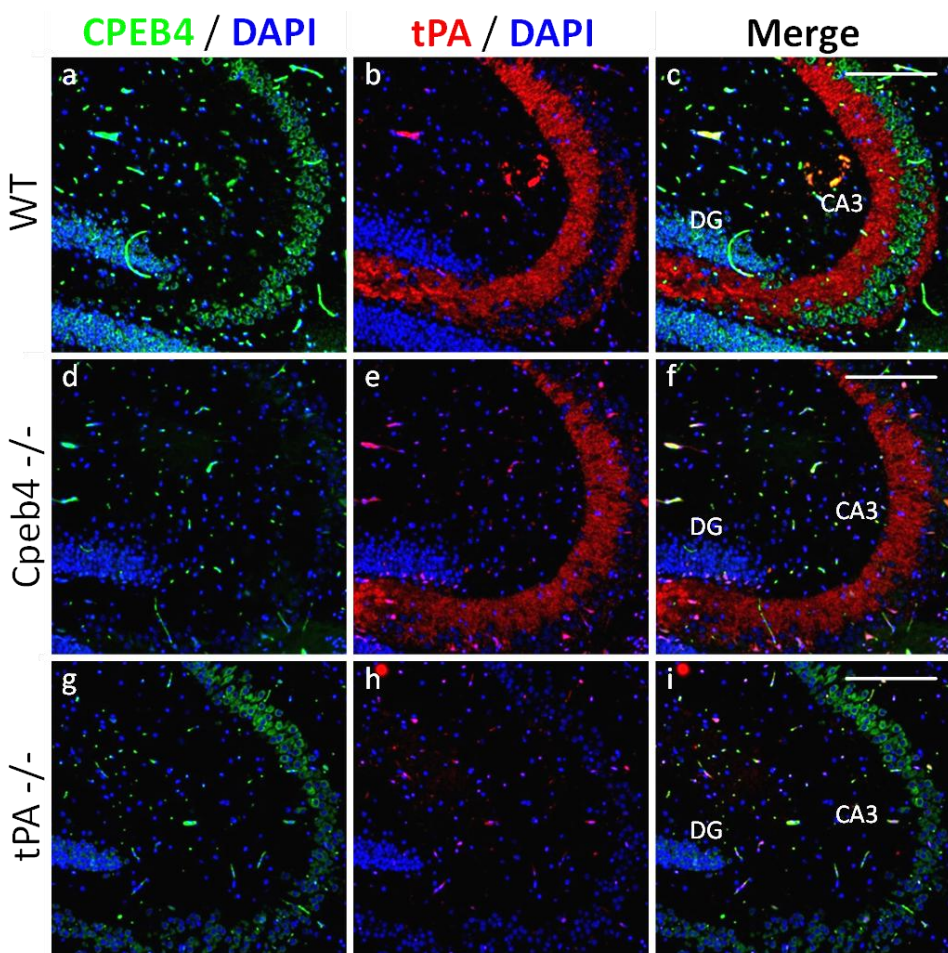
Figure 24. The general distribution of tPA in the hippocampus is not altered in the absence of CPEB4. Immunohistofluorescence of formalin-fixed, paraffin-embedded mouse sagittal brain slices from WT (a-c), Cpeb4 -/- (d-f) and tPA -/- (g-i) mice stained with antibodies against CPEB4 (green) and tPA (red). Nuclei were counterstained with DAPI. Scale bars = 200µm.

Finally, we analyzed tPA extracellular expression to exclude that the decrease of tPA levels observed by western blot in *Cpeb4 KO* mice are not produced by increased secretion of tPA that can be lost during the processing of the samples. To this aim, we performed a double IHF against tPA and MAP2 (a dendritic marker) in hippocampal sections from WT and *Cpeb4* KO mice. We found that synaptic tPA was found mainly surrounding CA3 dendrites, suggesting that it is present in the mossy fiber pathway, probably associated to the axons and in close contact with the dendrites, and a small fraction could also be extracellular (**Figure 26a-c**). This expression pattern was similar in the absence of CPEB4 (**Figure 26d-f**) indicating that tPA secretion is not affected in these mice.

On the other hand, we have found high CPEB4 expression levels in the soma of CA3 pyramidal neurons and in the granular cell layer of the dentate gyrus (**Figure 24a-c**), even though using thicker sections and more magnification we also found it in the dendrites of CA3 neurons (**Figure 25a-c**), as it has been previously reported *in vitro* using rat primary cultures of hippocampal neurons (Huang et al., 2006). The fact that CPEB4 is detected both in the soma and the dendrites of CA3 neurons led us to think that CPEB4 could control the translation of tPA mRNA both in the soma and the post-synaptic compartment.

Altogether, these results indicate that tPA expression in the mouse hippocampus is controlled by CPEB4 in basal conditions and that genetic inhibition of CPEB4 results in a decrease of tPA expression in the hippocampus without affecting tissue morphology, cell types producing tPA or the subcellular localization or secretion of this protein.
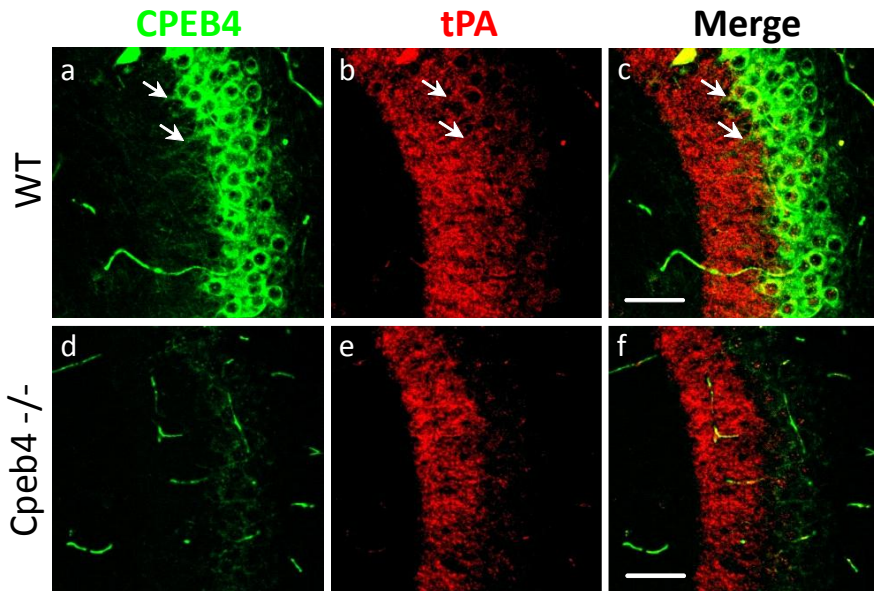
Figure 25. In CA3, Cpeb4 is present both in the soma and the dendrites. *Immunohistofluorescence for CPEB4 (green) and tPA (red) in the CA3 region of formalin-fixed, paraffin-embedded thick tissue sections from WT (a-c) and Cpeb4 KO mice (c-f). CPEB4 is detected in the dendrites of CA3 neurons (arrows in a-c). Scale bars = 50μm.*
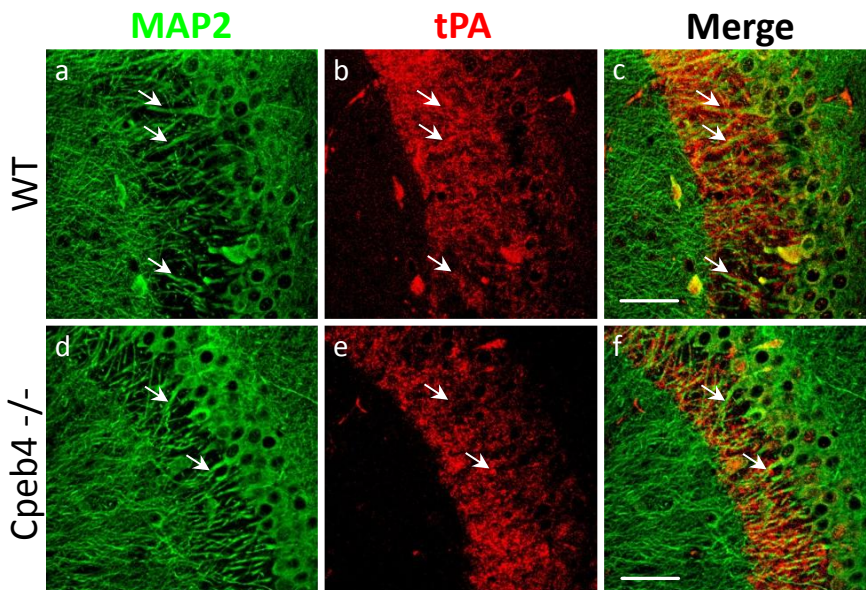
Figure 26. tPA expression pattern in the mossy fiber pathway is not altered in the absence of CPEB4. *Immunohistofluorescence for the dendritic marker MAP2 (green) and tPA (red) in the CA3 region of thick formalin-fixed, paraffin-embedded tissue sections. In WT (a-c) and Cpeb4 KO mice (d-f), tPA is present surrounding the dendrites in close contact with them, but not co-localizing (white arrows), meaning that part of it is associated to the axons and part is extracellular. In Cpeb4 KO mice, this pattern is not changing. Scale bars = 50μm.*

4. CPEB1 and CPEB4 control synaptic tPA overexpression in response to aggregated Aβ

Once we demonstrated that CPEB4 is involved in the translational control of tPA in basal conditions, and considering that both CPEB1 and CPEB4 have been reported to target tPA mRNA (Ortiz-Zapater et al., 2011; Shin et al., 2004), we studied if the absence of CPEB1 or CPEB4 could affect Aβ-induced expression of tPA. To this aim, we established primary cultures of hippocampal neurons derived from WT, *Cpeb1* KO mice or *Cpeb4* KO mice, and treated them with Aβ at DIV15.

Our results showed that Aβ induced a similar increase of tPA expression in WT and *Cpeb1* or *Cpeb4* KO neurons (**Figures 27A, 27B, 27D and 27E**). Additionally, we did not detect statistically significant changes in tPA mRNA levels after Aβ treatment (**Figures 27C and 27F**). This suggests that even though the Aβ-induced control of tPA expression in the hippocampus is under translational regulation and requires polyadenylation, CPEB1 and CPEB4 seem not to be involved in this process, at least in total cell extracts from hippocampal neurons.

Considering that tPA protein has been described to be present in synaptic vesicles in the post-synaptic compartment (Wu et al., 2015), its mRNA is localized in the pre-synaptic compartment (Shin et al., 2004), and that similarly to tPA, CPEB1 and CPEB4 have also been proposed as important mediators of memory formation and other neuronal functions (Berger-Sweeney et al., 2006; Kan et al., 2010; Shin et al., 2016) and are able to target tPA mRNA (Ortiz-Zapater et al., 2011; Shin et al., 2004), we aimed to evaluate if CPEB1 and/or CPEB4 control the Aβ-mediated overexpression of tPA in the synaptic terminals. To this aim, we analyzed the effects of Aβ on tPA expression using adult mouse purified synaptosomes. Synaptosomes are synaptic vesicles purified from nervous tissue after an initial homogenization followed by different procedures

depending on the protocol, such as centrifugation in gradients or filtration using membranes with different pore sizes. In this work, we followed the protocol of differential centrifugation and centrifugation in gradients. A full diagram of the process and the different fractions obtained is available on **Figure 28A** and the whole protocol is fully detailed in materials and methods (section 3).
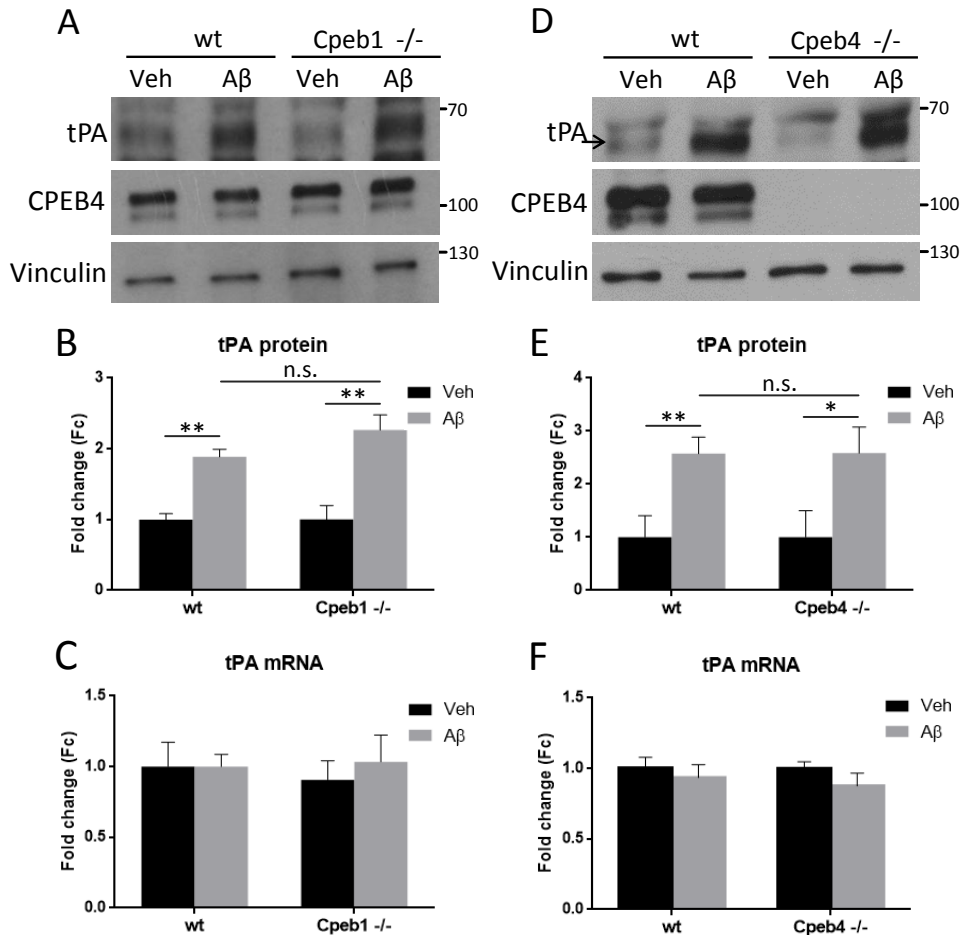
Figure 27. Cpeb1 and Cpeb4 depletion does not affect the Aβ-induced overexpression of tPA in primary hippocampal neurons*. (A,D) Western blot of WT, Cpeb1 KO and Cpeb4 KO primary hippocampal neurons treated with vehicle (Veh) or Aβ (Aβ), showing that depletion of Cpeb1 or Cpeb4 proteins does not impair the Aβ-mediated overexpression in total cell extracts. (C,F) qRT-PCR of WT, Cpeb1 KO and Cpeb4 KO primary hippocampal neurons treated with vehicle (Veh) or Aβ (Aβ) that demonstrates that tPA mRNA levels do not change after Aβ treatment. Error bars represent the SD of 3 independent biological samples. *p<0.05, **p<0.01, n.s.: non-statistically significant.*

A

B   **C**
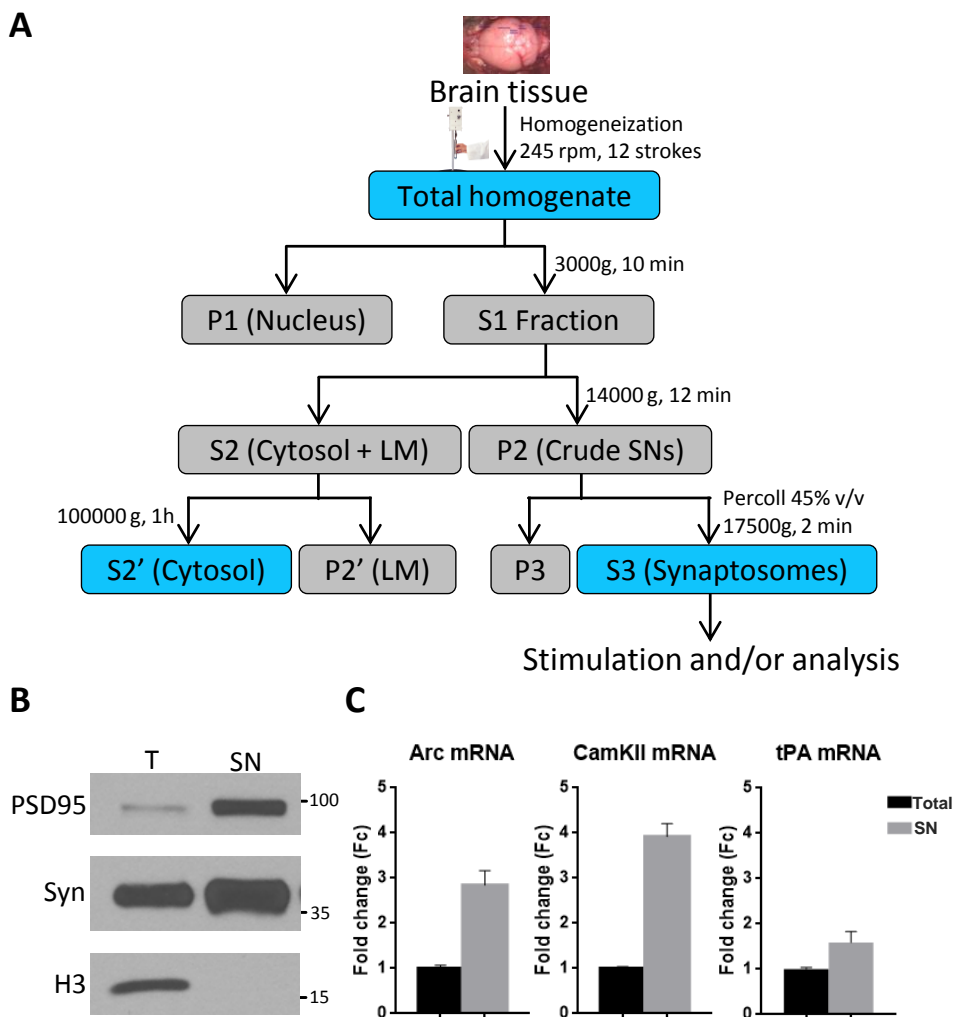
Figure 28. Evaluation of the protocol for the preparation of functional synaptosomes. (A) Flow chart showing the general steps for the preparation of functional synaptosomes. The fractions generally used during this work are shown in blue. (B) Western blot showing the enrichment of the postsynaptic density protein PSD95 and the presynaptic protein Synaptophysin (Syn), as well as the absence of Histone H3 in the synaptosomal fractions (SN). (C) qRT-PCR showing the enrichment of the mRNA of Arc, CaMKII and tPA in the synaptosomal fraction. HPRT was used as a housekeeping gene. LM = light membranes; T= Total extract; SN = Synaptosomal Extract.

After isolation, the synaptosomes, which consist on the presynaptic and postsynaptic terminals bound together, remain active. This happens because they contain mRNA, translation machinery, ATP, neurotransmitters,

mitochondria, etc, and consequently they are able to respond to stimuli. This means that when new protein synthesis or degradation, and even mRNA processing are detected after the stimulation of synaptosomes, it can be concluded that these events took place independently of the cell soma or nucleus, (i.e. independently of new transcription or mRNA translation in the somatic compartment).

As a first approach, we set up the protocol for evaluating the purity of the synaptosomes that we have prepared throughout this work. To this aim, we compared total brain homogenates and synaptosomal fractions at the mRNA and protein levels using different markers. We detected an enrichment in the synaptosomal fraction of the presynaptic protein synaptophysin (Syn) and the postsynaptic density protein 95 (PSD95) and a complete absence of the nuclear marker Histone H3 (whose presence would show a contamination from the nuclear fraction of the initial homogenate) (**Figure 28B**). At the mRNA level, we demonstrated the enrichment in the synaptosomal fraction of dendritically targeted mRNAs, such as Arc, CaMKII, and even tPA (**Figure 28C**). This shows that our protocol for preparing synaptosomes is working properly.

Therefore, we prepared synaptosomes from WT, *Cpeb1* KO and *Cpeb4* KO mice and stimulated them with Aβ. Our results showed that tPA protein is overexpressed in WT synaptosomes in response to Aβ. However, when we used *Cpeb1* KO (**Figure 29A**) or *Cpeb4* KO (**Figure 29B**) synaptosomes, this overexpression was impaired. This means that both CPEB1 and CPEB4 are necessary proteins for the correct synaptic overexpression of tPA in response to Aβ. In addition, we found that *Cpeb1* KO synaptosomes contained lower tPA mRNA levels compared to WT and CPEB4 KO synaptosomes (**Figures 29C and 29G**). These results show that besides its potential role in mediating tPA mRNA translation, CPEB1 may also be involved in the dendritic localization of tPA mRNA.
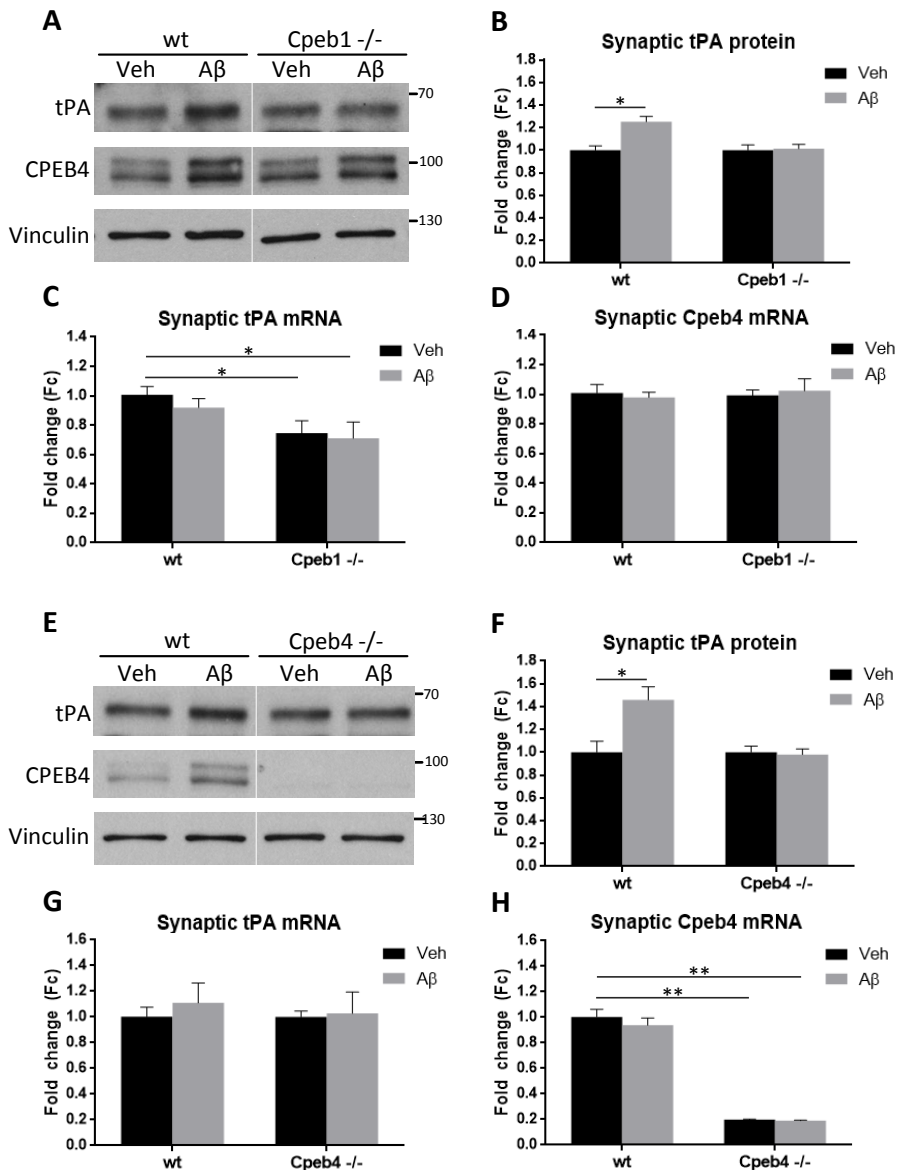
Figure 29. Aβ treatment induces the overexpression of tPA in the synaptic compartment, a mechanism which requires both CPEB1 and CPEB4 proteins. *(A, B) Western blot and quantification relative to Vinculin for the induction of tPA in WT and Cpeb1 KO synaptosomes. The treatment induces the overexpression of tPA and CPEB4 in WT synaptosomes. This effect is impaired in Cpeb1 KO synaptosomes. (C, D) qRT-PCR for tPA and Cpeb4 mRNAs, using HPRT as a housekeeping gene and normalized to WT-Veh. CPEB4 mRNA level does not change, but Cpeb1 KO mice contain reduced levels of tPA mRNA. (E, F) Western blot and quantification relative to Vinculin for the induction of tPA in WT and Cpeb4 KO synaptosomes. In WT synaptosomes, tPA and CPEB4 are induced. This effect is impaired in Cpeb4 KO synaptosomes. (G, H) qRT-PCR for tPA and CPEB4 mRNAs, using HPRT as a housekeeping gene and normalized to WT-Veh. tPA mRNA level does not change with the treatment or between WT and KO synaptosomes. Cpeb4 mRNA reduction is detected in Cpeb4 KO mice. In all cases, error bars represent the SEM of 3 independent biological samples. *p<0,05; **p<0,01.*

We also validated that after the induction with Aβ, mRNA levels are not changing in WT, *Cpeb1* KO and *Cpeb4* KO synaptosomes (**Figures 29C and 29G**), demonstrating that the effect observed is not produced by tPA mRNA degradation.

Surprisingly, we also found that following Aβ stimulation, not only tPA expression is induced, but also CPEB4 (**Figures 29A and 29E**). In contrast to what happens with tPA, CPEB4 overexpression was found not to depend on CPEB1, as Aβ-stimulated *Cpeb1* KO synaptosomes are able to induce CPEB4 expression (**Figure 29A**). We also found that WT and *Cpeb1* KO synaptosomes contained the same levels of *Cpeb4* mRNA. Moreover, these levels do not change after Aβ stimulation (**Figures 29D and 29H**). This means that CPEB1 does not affect the synaptic localization of CPEB4 mRNA, which is in agreement with the fact that CPEB4 overexpression is not dependent on CPEB1. Moreover, it shows that *Cpeb4* mRNA is not being degraded during the treatment (**Figure 29G**).

To summarize, these results indicate that, in the synaptic compartment, tPA overexpression in response to Aβ requires both CPEB1 and CPEB4, while CPEB4 overexpression is independent on CPEB1. Moreover, these data suggest that CPEB4 may regulate tPA mRNA translation, while CPEB1, besides controlling mRNA translation, may be required for tPA mRNA localization in the dendrites.

5. tPA mRNA is cleaved in the dendrites in response to Aβ

In order to go one step further, we aimed to explore which is the molecular mechanism by which the local synaptic overexpression of tPA can be explained. Therefore, taking into consideration that CPEBs control mRNA translation mainly through cytoplasmic or synaptic polyadenylation, we first analyzed if the mRNAs of tPA and CPEB4 are polyadenylated in the synaptic compartment in response to Aβ treatment. To this aim, we performed a poly(A) tail length (PAT) assay in vehicle-treated or Aβ-treated WT, *Cpeb1* KO and *Cpeb4* KO synaptosomes.

We performed the PAT assay using primers directed against the end of the longest 3'-UTR isoform described for tPA mRNA (NM_008872.3) (**Figure 30A**). We found that following Aβ treatment, this tPA mRNA isoform appeared to be slightly less polyadenylated. At the same time, we detected additional lower bands that showed polyadenylation. Interestingly, the intensity of these shorter bands was lower in *Cpeb1* KO and *Cpeb4* KO synaptosomes (**Figure 30B**). We validated the same results using an additional set of primers (**Figures 30A and 30C**). This suggests that, after synaptic stimulation, tPA mRNA is cleaved into a shorter 3'-UTR variant that is then polyadenylated, and that CPEBs may be involved in such process. Importantly, the process of alternative cleavage and polyadenylation in general, and specifically mediated by CPEB1, has only been reported to take place in the nucleus (Bava et al., 2013), and the majority of factors involved have been reported to be nuclear.

In order to gain insights regarding the processing of tPA mRNA into a shorter form, we performed 3'-RACE, which, unlike the PAT assay, produces sharp bands and is more suitable for the detection of 3'-UTR variants. We used a forward primer located at the end of the CDS of tPA mRNA in order to cover its complete 3'-UTR (**Figure 31A**). The results showed that, following Aβ treatment, there is an enrichment in an isoform of tPA mRNA that is shorter compared to

the full-length isoform, as in Aβ-treated WT synaptosomes we detected at the same time a reduction in the levels of the longer isoform and an increase of the shorter one (**Figure 31B**). More interestingly, we found that this increase was not produced in Aβ-stimulated *Cpeb4* KO synaptosomes, even though small levels of the shorter isoform were still detected. The shorter band was cut out of the gel, cloned and sequenced, and turned out to be a shorter variant of tPA lacking 386 nucleotides (**Figure 31D**). The same results were obtained using a second primer (**Figures 31A and 31C**). Similarly to CPEB4, the absence of CPEB1 was also found to hamper the formation of the shorter isoform (**Figure 31C**).

Surprisingly, these results demonstrated that the functional synapses are able to perform mRNA cleavage, a mechanism that had only been previously demonstrated to take place inside the nucleus, but never in the cytosol or the synapses.
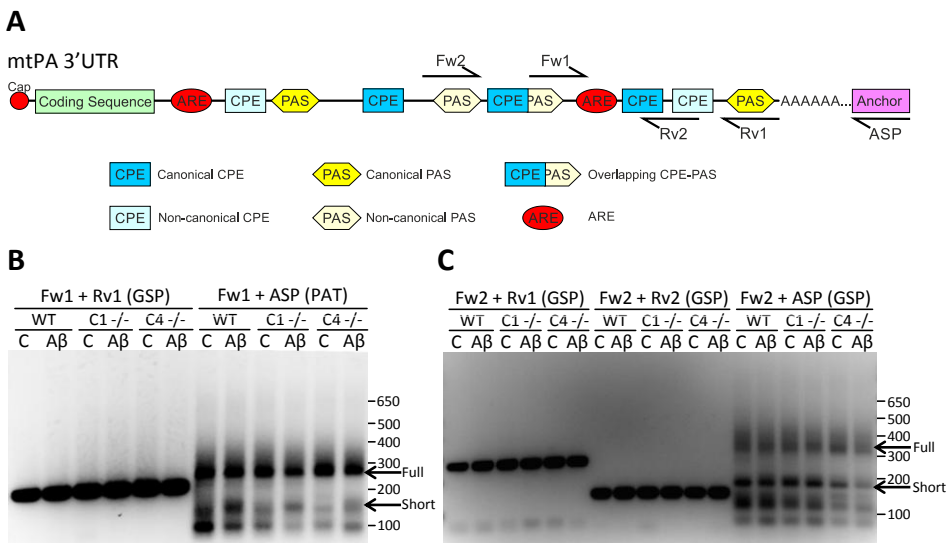
Figure 30. tPA mRNA is cleaved and polyadenylated in the synapses in response to Aβ stimulation. (A) *Representative diagram of the structure of the mRNA of tPA and Cpeb4. The 5'-UTR and the coding sequence were simplified to focus on the functional domains of the 3'-UTR. The forward primers and reverse primers used in B and C are shown. Moreover, in the 3' end, the (G/I)n anchor ligated to the mRNA end prior to the RT (pink box) and the anchor specific primer used in the PAT assay (ASP) are shown. (B) PAT assay for tPA mRNA of WT, Cpeb1 KO (C1 -/-) or Cpeb4 (C4 -/-) synaptosomes treated with Vehicle (C) or Aβ (Aβ) using the combination of primers Fwd1+Rev (gene-specific PCR) and Fwd1+ASP (PAT assay). (C) PAT assay for tPA mRNA with the same samples used in B but using Fwd2 + Rev (Gene-specific PCR) or Fwd2 + ASP (PAT).*
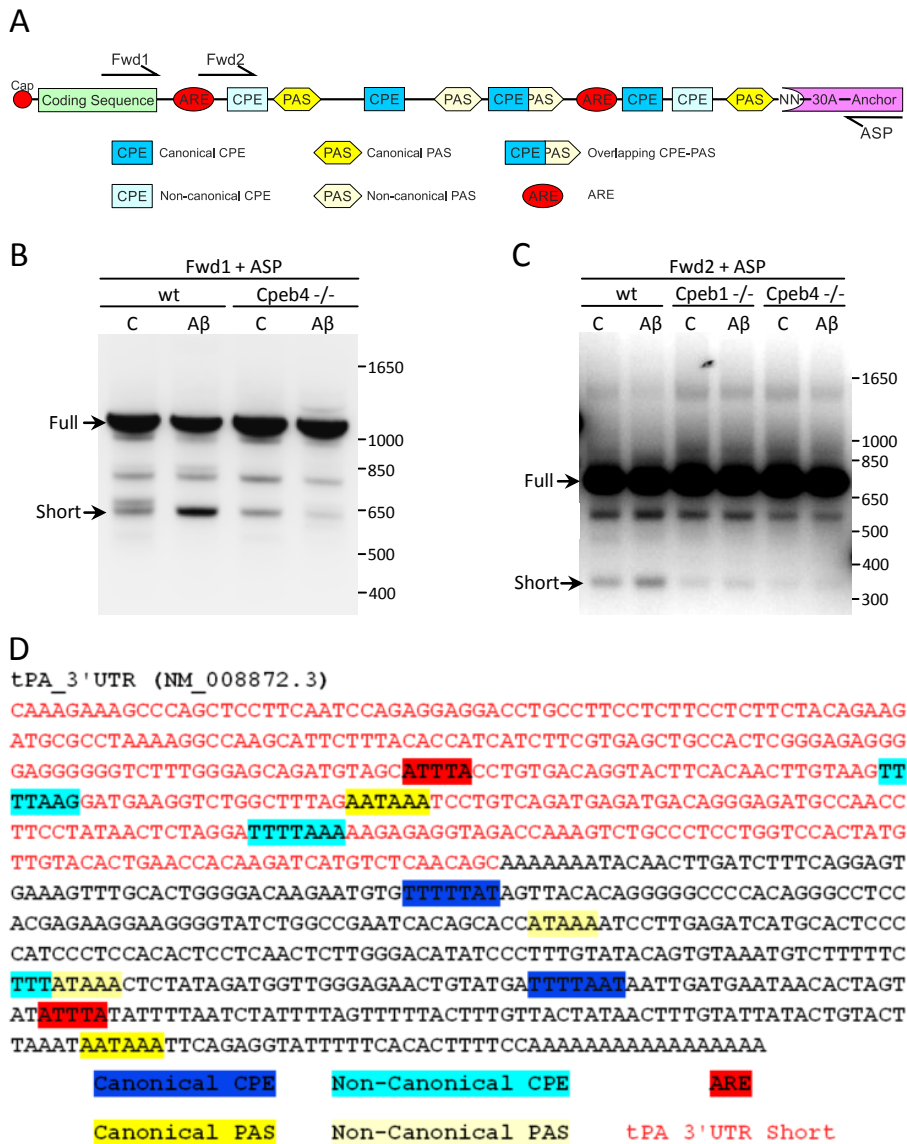
Figure 31. The mRNA of tPA is cleaved in response to Aβ, a mechanism that is impaired in Cpeb1 and Cpeb4 KO synaptosomes. *(A) Representative diagram of the structure of tPA mRNA. The 5'-UTR and the CDS were simplified to focus on the 3'-UTR. The forward primers (Fwd1, Fwd2) and reverse anchor-specific primer (ASP) are shown. (B) RACE analysis of purified mouse synaptosomes from WT and Cpeb4 KO mice treated with vehicle (C) or Aβ (Aβ) using Fwd1+ASP primers. In treated WT synaptosomes there is an enrichment in a shorter variant of the mRNA of tPA ("Short" arrow), but not in the KO synaptosomes. (C) RACE analysis of purified mouse synaptosomes from WT, Cpeb1 KO and Cpeb4 KO mice using Fwd2+ASP primers. The enrichment in a shorter form of the 3'-UTR is impaired in Cpeb1 and Cpeb4 KO synaptosomes. (D) Sequence of tPA Full 3'-UTR and the shorter 3'-UTR based on the cloning and sequencing of the bands obtained in B ("Full" and "Short" arrows, respectively) The functional domains of tPA 3'-UTR are highlighted as shown in the figure. The shorter form of the 3'-UTR is marked in red.*

Moreover, we demonstrated that the longest isoform described of *Cpeb4* mRNA (NM_026252.4) (**Figure 32A**) is polyadenylated in response to Aβ treatment both in WT and *Cpeb1* KO synaptosomes (**Figure 32B**).
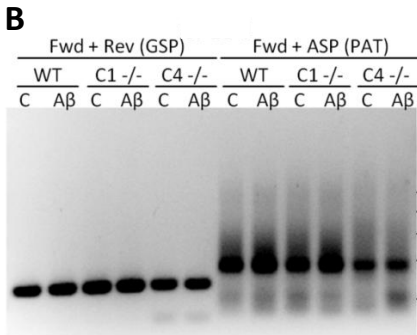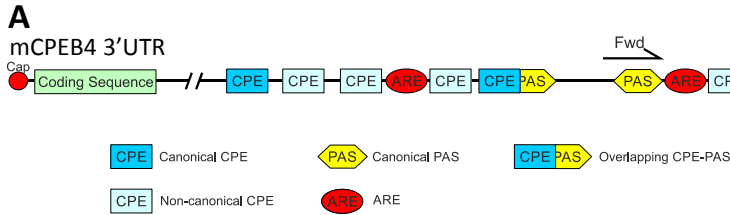
Figure 32. CPEB4 mRNA is polyadenylated in the synapses in response to Aβ stimulation. (A) *Simplified **r**epresentation of the structure of CPEB4 mRNA. 5'-UTR, CDS and part of the 3'-UTR were simplified to focus on the functional domains of the end of its 3'-UTR. The forward (Fwd) and reverse (Rev, ASP) primers used are shown. The (G/I)$_n$ anchor ligated to the mRNA 3'-end prior to the RT is shown as a pink box. (B) CPEB4 mRNA PAT assay of WT, Cpeb1 KO (C1 -/-) or Cpeb4 KO (C4 -/-) synaptosomes treated with Vehicle (C) or Aβ (Aβ) using the combination of primers Fwd+Rev (gene specific primer PCR) and Fwd+ASP (PAT assay).*

6. The cleavage and polyadenylation machinery is present at the neuronal dendrites

The fact that our data suggests that tPA mRNA is processed into a shorter form specifically in the synapses in response to Aβ opens new biological questions. It is known that the CPSF complex, the polymerase Gld2, maskin and PABP are present both in cytoplasm and dendrites. However, there is no information available regarding other members of the cleavage and polyadenylation machinery.

In order to answer this issue, we aimed to determine if besides members of the CPSF complex, other members of the 3'-end formation machinery, such as members of the CSTF complex or the RNA Pol II, are present in the synaptic terminals. Our first approach was to perform a proteomic study using a protein extract obtained from mouse synaptosomes (**Supplementary Table S1**). Before starting the analysis, we first demonstrated that our synaptosomes were pure by analyzing the same protein markers as in **Figure 28B** (data not shown). As additional controls, in the proteome obtained, and considering a false discovery rate (FDR) of 1%, we did not find any Histone proteins (**Supplementary Table S1**). Using this proteomic approach, we could demonstrate that CSTF64 is present in the synaptic terminals. However, it is important to highlight that the synaptic proteome contains so many proteins that the system gets saturated and thus only the most abundant proteins could be detected. Consequently we were unable to detect other *bona fide* synaptic candidates, such as CPEB1, CPEB2, CPEB3, CPEB4 or tPA (**Supplementary Table S1**).

In view that the proteomic analysis, even though being useful for detecting CSTF64, appeared not to be the best option for the detection of other interesting candidates, we decided to proceed analyzing one by one the presence of selected candidates through Immunofluorescence analysis of DIV15 mouse primary hippocampal neurons with antibodies directed against

108

the different factors. As markers, we used anti-PSD95 for the detection of the post-synaptic compartments and anti-MAP2 for the detection of the dendrites and to exclude the axons. Our results demonstrated that not only CPSF30, CPSF59, CPSF68 and CPSF73, but also all the members of the CSTF complex (CSTF50, CSTF64 and CSTF77) were also present in the dendrites (very close to the post-synaptic densities), showing a pattern very similar to the members of CPSF complex (**Figure 33**). Interestingly, we found that RNA Pol II was also present in the dendrites (**Figure 33**).

Furthermore, the presence of some of these complexes was further demonstrated by western blot following the fractionation process described in **Figure 28A**, and then comparing total mouse brain homogenate with the cytosolic and synaptosomal fractions produced from this initial homogenate (**Figure 34A**). In addition, we found that the RNA Pol II containing the specific phosphorylation of its CTD (PSer2), which makes it able to be recognized by the 3'-end formation machinery, is present in the nucleus, the cytosol and, more surprisingly, in the synaptosomes. This suggests that the RNA Pol II CTD could also serve as a loading platform for all the APA factors in the dendrites. Nevertheless, this form corresponded to a hypophosphorylated form of RNA Pol II, as the majority of hyperphosphorylated RNA Pol II containing the PSer2 phosphorylation was present in the nucleus or in the cytosolic compartment, whereas the synaptic PSer2 RNA Pol II is hypophosphorylated. To prove this, we used three different antibodies: N20 (which recognizes the NTD of RNA Pol II and detects both the hyperphosphorylated and hypophosphorylated forms of its CTD), 8WG16 (which recognizes specific phosphorylations of the CTD), and a CTD PSer2-specific antibody (**Figure 34B**). The remarkable differences in the phosphorylation state of the CTD in the cytosol and the synapses suggests that the detected synaptic form is not produced from a contamination coming from the soma.
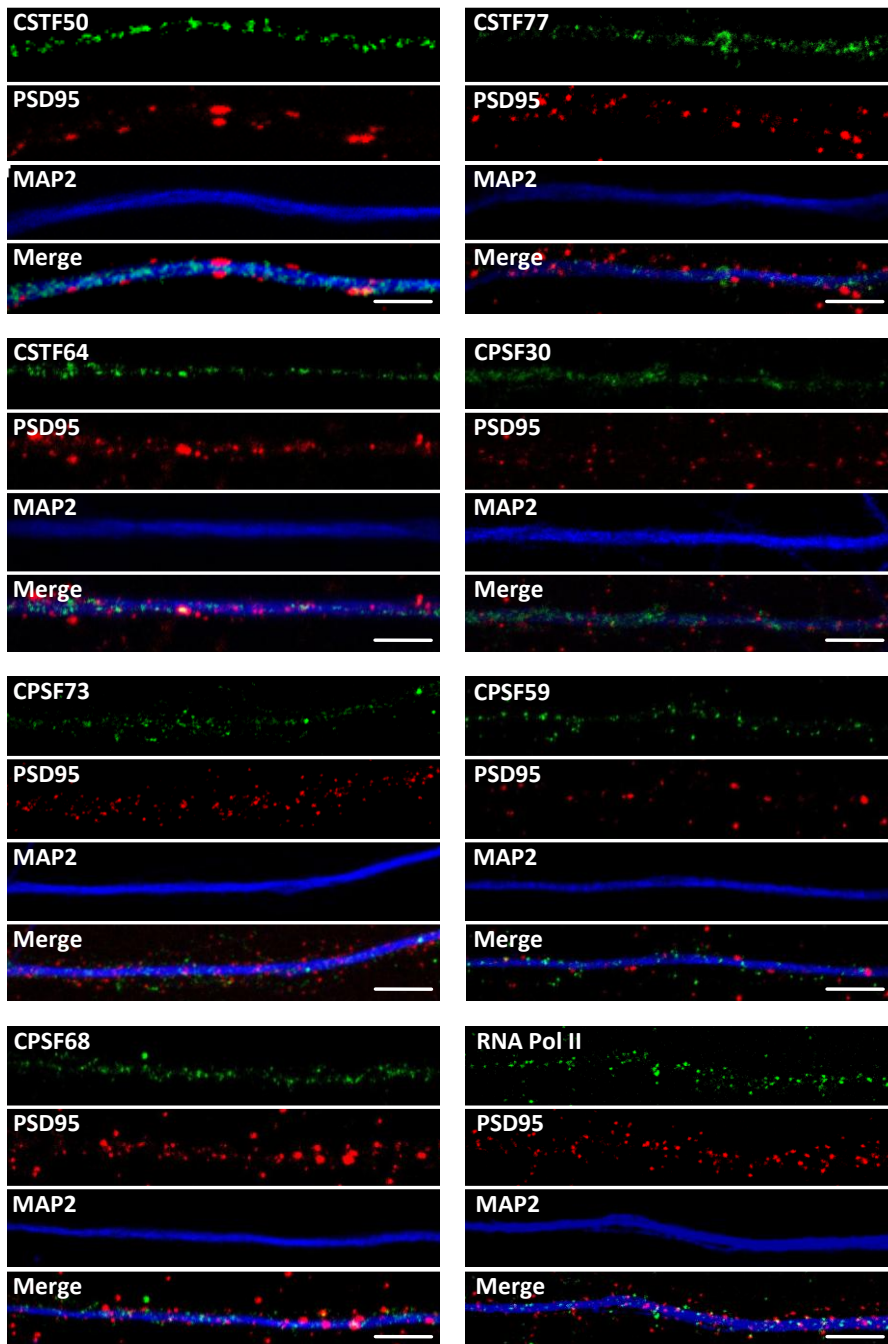
Figure 33. 3'-End processing factors and the RNA Pol II are present in the dendrites of mouse primary hippocampal neurons. *Immunofluorescence of DIV15 mouse primary hippocampal neurons stained with different antibodies against the different members of the cleavage and polyadenylation machinery (in green) and counterstained with the synaptic marker PSD95 (in red) and the dendritic marker MAP2 (in blue). Even though they do not co-localize with PSD95, it can be seen that the different cleavage factors are present in the dendrites, near the synapses. Scale bars = 5μm.*
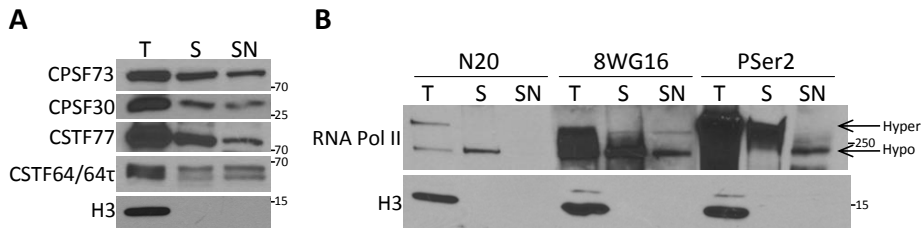
Figure 34. Presence of the cleavage machinery and the P-Ser2 phosphorylated RNA Pol II in purified mouse synaptosomes. *(A) Western blot showing the presence of some of the factors previously identified by IF. (B) Western blot showing the phosphorylation status of the RNA Pol II present in the dendrites. N20 recognizes the RNA Pol II NTD and therefore all the phosphorylations of its CTD. 8WG16 recognizes the CTD. PSer2 recognizes specifically the PSer2 Phosphorylations of the CTD. In contrast to the nuclear or cytoplasmic RNA Pol II, it can be seen that the majority of PSer2 RNA Pol II present in the dendrites is hypophosphorylated. T: Total homogenate, S: Somatic (cytosolic) fraction, SN: Synaptosomal fraction. Hyper: Hyperphosphorylated form of the RNA Pol II, Hypo: hypophosphorylated form of the RNA Pol II.*

7. Evaluation of the translation efficiency of the different tPA 3'-UTR isoforms

Finally, considering that we have identified a new isoform of tPA mRNA, we finally aimed to determine whether it has a physiological role. Considering the literature reviewed in the introduction, we speculated that shorter versions of the 3'-UTR of tPA would display higher translational efficiency compared to the full-length form. To test this, we generated chimeric constructs containing the firefly luciferase ORF under the control of the T3 promoter and a 3'-UTR containing different tPA 3'-UTR isoforms (short and full-length) (**Figure 35A**). As negative control, we generated the full-length 3'-UTR with the last PAS mutated (Full PAS mut, **Figure 35A**). Additionally, considering that the end of the shorter isoform was detected at more than 50 nucleotides of distance from the closest upstream canonical PAS, we generated an additional construct containing the shorter 3'-UTR containing an additional artificial PAS at the end of the sequence (Short PAS+, **Figure 35A**). This approach allowed us to test whether the upstream canonical PAS is usable by means of comparing ratios of translation efficiency between both Short and Short PAS+ constructs (**Figure 35A**). Finally, we used a construct containing Renilla luciferase ORF and a poly(A) tail under the control of the T3 promoter for normalization.

These constructs were linearized, transcribed *in vitro* and the resulting mRNAs co-transfected with the Renilla construct into a Neuro2A. 16h after transfection, cells were processed for the dual luciferase assay. Of note, before processing the samples to perform the luciferase assay, we estimated the transfection efficiency of N2A cells transfected with EGFP mRNA for 16h. This efficiency was estimated to be close to 100% (**Figure 35B**).

Our results showed that the mutation of the PAS in the full-length 3'-UTR reduced ~20% the translation efficiency. The shorter version of the mRNA showed a similar reduction in the translation efficiency. However, when we

analyzed the ShortPAS+ construct, we recovered the translation efficiency, which was even higher than the translation efficiency of the full-length form (**Figure 35C**). Considering that the shorter 3'-UTR form contains less CPEs and AREs, this shorter isoform might be originated with the aim of increasing mRNA stability and the loss of CPE-mediated repression, which could lead to lower but sustained tPA translation.
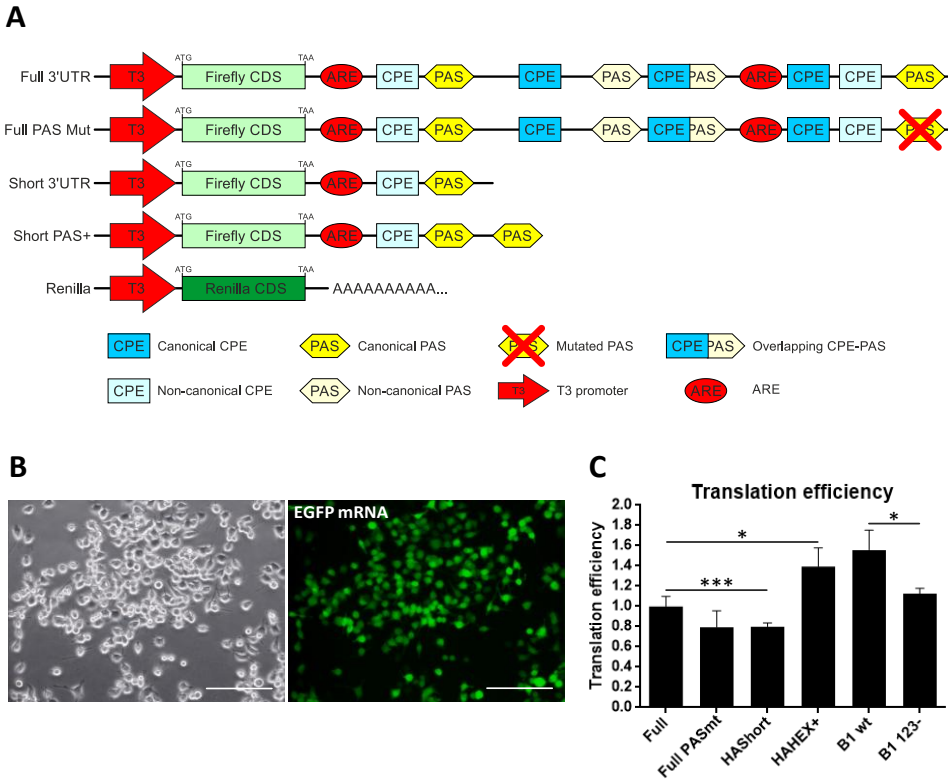
Figure 35. Translation efficiency of the long and short isoforms of tPA. (A) Diagram of the constructs used in the transfection experiments. All the variants of the 3'-UTR of tPA were inserted in reporter vectors containing the coding sequence (CDS) of the firefly luciferase under the control of the T3 promoter. A construct containing the CDS of Renilla followed by a 73A tail was used for normalization. All the constructs were transcribed in vitro, mixed in a 3:1 molar ratio with Renilla and transfected in N2A cells. (B) Evaluation of the translation efficiency in N2A cells that were transfected for 16h with a polyadenylated mRNA construct containing the CDS of enhanced GFP (EGFP). The mRNA transfection efficiency is close to 100%. (C) Translation efficiency of each of the constructs tested. The firefly-to-Renilla chemiluminescence produced was measured for each one and compared considering as 100% the full-length plasmid. B1 WT and Cyclin B1 123- were used as positive and negative controls, respectively. Error bars are the SD. *p<0.05; ***p<0.001.

8. CPEB4 is potentially involved in Alzheimer's disease pathology

Taking into consideration the functions of CPEBs in memory and CNS disorders (Kan et al., 2010; Shin et al., 2016; Udagawa et al., 2013), tPA role in AD (Ledesma et al., 2000; Medina et al., 2005; Tucker et al., 2000) and our data supporting that Aβ-treated synaptic terminals produced the overexpression of CPEB4 independently of the presence or absence of CPEB1, we hypothesized that CPEB4 could be upregulated and possess important roles in AD.

To explore this hypothesis, we first analyzed the expression of CPEB4 in formalin-fixed, paraffin-embedded brain sections of human AD patients with advanced AD (Braak Stages V and VI) and healthy controls of the same age. For the detection of the amyloidogenic areas, we co-stained with an anti-Aβ antibody. Compared to controls, we observed that the brain of AD patients (**Figure 36g-l**) contains higher levels of CPEB4 (**Figure 36a-f**), which usually localizes in the vicinity of senile plaques. These data indicate that CPEB4 is overexpressed during AD progression, thus suggesting CPEB4 to have a role in AD pathology, in which its overexpression would affect the translation efficiency of other mRNAs, as it happens with tPA.

Next, considering that aberrant Tau phosphorylation is a major hallmark of AD, we explored CPEB4 expression in phospho-Tau positive neurons. To this aim, we performed a double Immunofluorescence against hyperphosphorylated Tau (Tau-P) and CPEB4 on brain tissue samples from patients with advanced AD. Similar levels of CPEB4 were detected when we analyzed individual cells expressing somatic Tau-P in comparison to neurons not expressing somatic Tau-P (**Figure 37**). In some cases, we even detected less CPEB4 in Tau-P containing neurons, which could be explained by these cells entering into apoptosis (**Figure 37**).

Overall, this suggests that Tau hyperphosphorylation and CPEB4 overexpression during AD could be independent processes or that CPEB4 overexpression precedes Tau hyperphosphorylation.
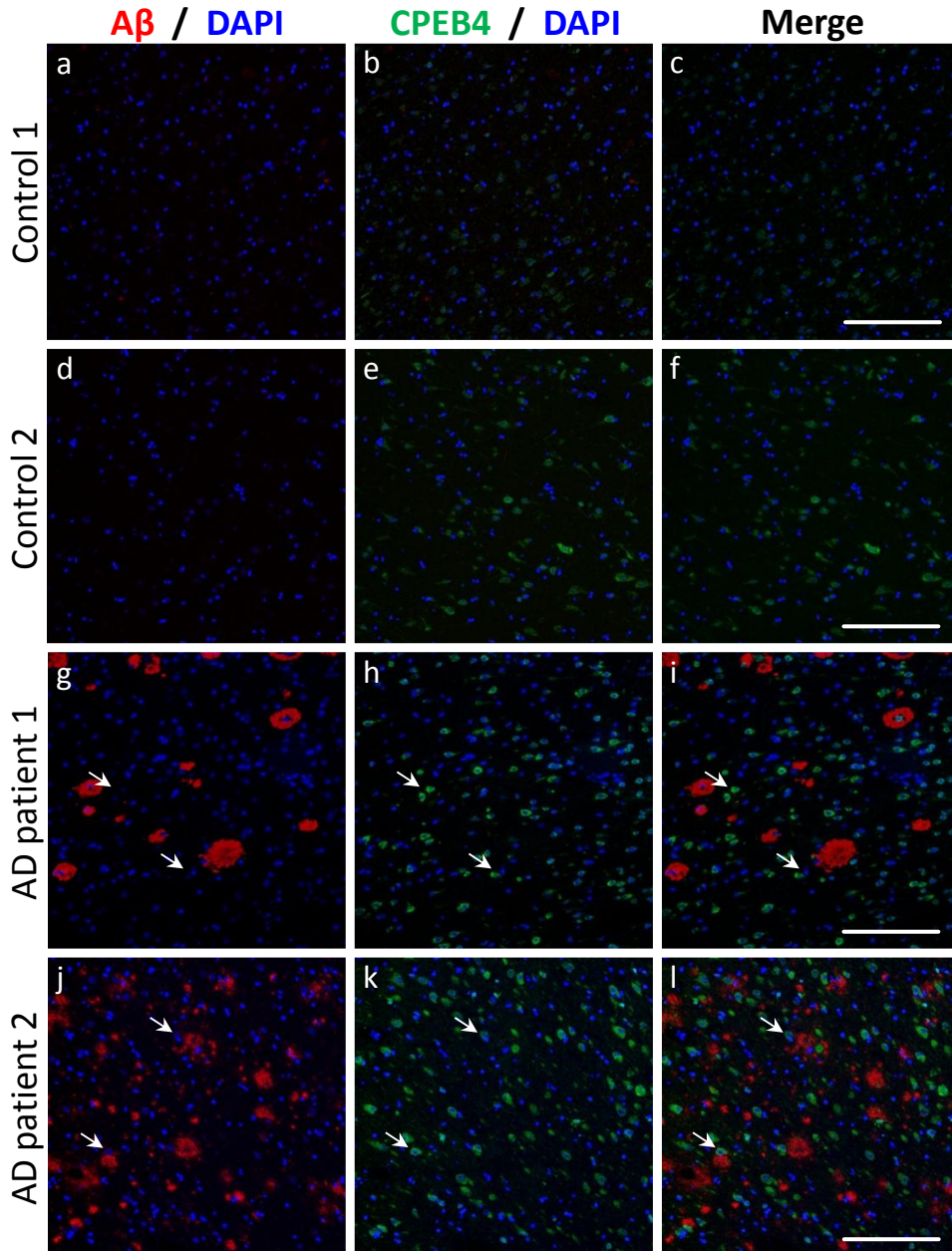
Figure 36. CPEB4 is overexpressed in the brain of human AD patients. *Immunohistofluorescence of human brain tissue from healthy controls (a-f) and AD patients (g-i) showing the expression of Aβ (in red) and CPEB4 (in green). Nuclei were counterstained using DAPI. CPEB4 is overexpressed in the amyloid-containing areas in AD patients, usually near the senile plaques (white arrows). Scale bars = 200μm.*
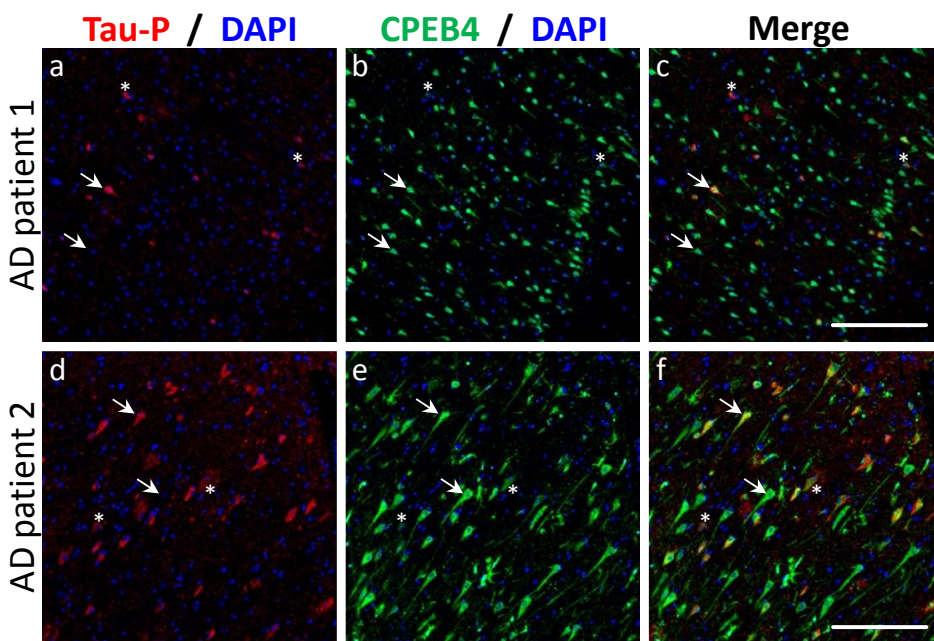
Figure 37. Tau hyperphosphorylation does not correlate with high CPEB4 expression in human AD patients. *Immunohistofluorescence of the hippocampus of two human AD patients (patient 1 from a to c and patient 2 from d to f) showing the expression of hyperphosphorylated Tau (in red) and CPEB4 (in green). Nuclei were counterstained using DAPI. For the majority of cells clearly containing Tau-P in the soma, the same levels of CPEB4 are detected when they are compared to the ones not containing somatic Tau-P (white arrows showing both examples). In some cases, lower levels of CPEB4 are present in cells containing somatic Tau-P (white asterisks), probably because these cells are entering into apoptosis or dead. Scale bars = 250 um.*

The overexpression of CPEB4 in AD samples and the fact that both CPEB1 and CPEB4 control the synaptic expression of tPA, led us to evaluate the effects of CPEB1 or CPEB4 depletion in Aβ-induced neurotoxicity.

To this aim, primary cultures of mouse primary hippocampal neurons from WT, *Cpeb1* KO or *Cpeb4* KO mouse embryos were stimulated with Aβ for 48h and percentage of survival was determined using an MTT assay. Our results showed that Aβ induced a ~50% decrease in cell viability in WT and *Cpeb1* or *Cpeb4* KO neurons (**Figure 38**), thus indicating that these two proteins do not possess a critical role in Aβ-induced toxicity in mouse embryonic primary hippocampal neurons, an effect that was expected considering that both Aβ-induced *Cpeb1*

and *Cpeb4* KO primary neurons overexpress tPA, which is considered the main mediator of Aβ toxicity. An *in vivo* model, such as the Aβ injection model (Eisele et al., 2009; Jean et al., 2015; McLarnon and Ryu, 2008; Tsukuda et al., 2009) will be necessary for the evaluation of these effects in a system containing all the cellular types present in the CNS and for analysis concerning longer periods of Aβ treatment.
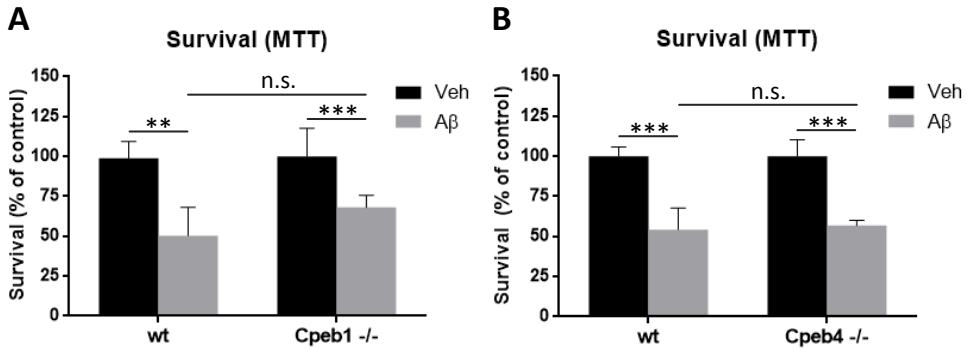
*Figure 38. Removal of Cpeb1 or Cpeb4 does not affect the survival of primary cultures of hippocampal neurons. MTT assay of DIV10 mouse primary hippocampal neurons from WT, CPEB1 KO (A) or Cpeb4 KO (B) E17.5 mouse embryos treated for 48h with Aβ. In both cases, Aβ induces a significant reduction of cell viability of ~50%. However, there are not statistically significant differences between WT and KO animals. Error bars represent the SD. **p<0,001; ***p<0,0001. In both cases, n=4 independent biological samples.*

DISCUSSION

1. The importance of translational control in Alzheimer's disease

Memory loss is one of the key clinical symptoms of Alzheimer's disease. Therefore, the understanding of the molecular mechanisms that regulate this process during ageing and Alzheimer's disease will help us to better understand the pathology and hence provide us clues to prevent its progression.

The hippocampus is one major region of the brain involved in memory acquisition (Squire and Zola-Morgan, 1991). It is precisely in this area where one of the major forms of memory establishment and storage based on the activity-dependent enhancement of synaptic transmission, LTP, takes place (Nicoll and Malenka, 1995). In this regard, tPA has been proved to be an essential protein for neuronal LTP. This protein is widely expressed in the CNS, where its levels are tightly controlled in physiological conditions. In addition, tPA has been identified as an early-immediate gene in the hippocampus (Qian et al., 1993) whose transcription is known to be induced by activity in hippocampal neurons. In fact, *tPA* KO mice show L-LTP deficits (Carmeliet et al., 1994; Frey et al., 1996; Huang et al., 1996) and impaired hippocampal-dependent tasks (Pawlak et al., 2002); whereas mice overexpressing tPA or inoculated with tPA display enhanced LTP and memory (Baranes et al., 1998; Madani et al., 1999). Moreover, tPA mRNA has been shown to be present in the synaptic compartment where it is translated in response to mGluR activation (Shin et al., 2004). Overall, these studies demonstrate that tPA is an important mediator of memory establishment in the hippocampus.

In addition to its physiological roles, tPA has been shown to be linked to AD pathology. However, its role during AD progression is still poorly understood. Our group and others have reported that aggregated Aβ (one of the major hallmarks of AD) induces an overexpression of tPA that can play a dual role in Alzheimer's disease pathology. On the one hand, tPA can exert a protective role

preventing Aβ aggregates accumulation by inducing their degradation in a catalytic-dependent manner through plasmin generation (Ledesma et al., 2000; Melchor et al., 2003; Oh et al., 2014). In fact, tPA can bind to Aβ as a substitute for fibrin, which induces its activity and catalyzes the degradation of Aβ (Kingston et al., 1995). On the other hand, other lines of evidence have shown that tPA can trigger a catalytic-independent cell signaling cascade that leads to neuronal apoptosis and glial inflammation, exacerbating the disease (Medina et al., 2005; Pineda et al., 2012; Siao and Tsirka, 2002). The balance between beneficial or detrimental tPA effects requires the efficient catalytic activity of tPA (linked to the presence of tPA inhibitors or cell membrane lipid raft alterations) as well as the tPA doses reached in response to Aβ generation (Tucker et al., 2000). Although the induction of tPA expression in response to Aβ has been clearly demonstrated in several reports, the underlying molecular mechanisms have not been fully elucidated yet.

In the current study, we have presented several lines of evidence indicating that translational control mediated by the CPEB family of RNA-binding proteins is important for the regulation of tPA expression, both in response to Aβ aggregates and in basal conditions, thus suggesting a role for these proteins in memory loss during Alzheimer's disease.

DISCUSSION

2. tPA expression in the mouse hippocampus in response to Aβ is mediated by translational control

Previous studies showed that aggregated Aβ stimulates the transcriptional expression of tPA (Tucker et al., 2000). However, the role of other mechanisms controlling gene expression have not been explored yet. Our results using inhibitors of transcription, translation or protein synthesis show that tPA expression in response to Aβ is mediated by translational control and requires mRNA polyadenylation. Indeed, the increase in tPA protein levels was similar in hippocampal neurons treated with Aβ alone or in the presence of the transcriptional inhibitor actinomycin D, indicating that transcription is not the major determinant for tPA induction. In contrast, inhibition of translation using the inhibitor of mRNA polyadenylation cordycepin abolished tPA induction in response to Aβ, showing that translational control is required. Accordingly, tPA mRNA levels were similar in the presence of these inhibitors, confirming that transcription or mRNA stability are not involved in this event and that the pre-existing mRNA is sufficient to mediate new tPA synthesis after Aβ treatment. Interestingly, treatment of neurons with the inhibitor of protein synthesis cycloheximide produced a 10-fold increase in tPA mRNA levels. However, since tPA protein levels remained unchanged after CHX treatment, this effect could probably be produced as a side-effect associated to protein synthesis inhibition. Of note, the transcriptional induction previously reported (Tucker et al., 2000), was observed to begin at 12h of treatment, which can explain the discrepancy with our data. Indeed, we presume that translation regulation of tPA synthesis is one of the first steps of gene expression regulation but it is likely that transcription is also required for long term expression of tPA.

3. CPEB4 controls the translation efficiency of tPA in the hippocampus under basal conditions

Once demonstrated that tPA mRNA translation is a key regulatory mechanism required for its expression in response to Aβ, we explored whether CPEBs are involved in this event. Indeed, CPEB1 has been already proposed to mediate tPA synthesis in neurons after glutamate stimulation (Shin et al., 2004) and CPEB4 induces tPA expression in cancer (Ortiz-Zapater et al., 2011).

In this work, we have demonstrated by WB analysis that tPA levels in basal conditions are reduced in the hippocampus of *Cpeb4* KO mice, but not in *Cpeb1* KO mice. We have validated that the differences are not caused by morphological alterations in the hippocampus, as this structure is unaffected in *Cpeb4* KO mice. Moreover, using IHF we observed that the distribution pattern of tPA in the hippocampus is the same in WT and *Cpeb4* KO mice. tPA is present in the axons of the mossy fiber pathway and absent from the soma of the dentate gyrus or CA3 neurons, and this distribution is not changing in *Cpeb4* KO mice. This means that the identity of the cells expressing tPA and the subcellular distribution of tPA in the hippocampus are similar in WT and *Cpeb4* KO mice. In our study we only detect the decrease in tPA levels by WB and not by IHF, which could be explained by the fact that IHF is not a quantitative technique and thus the observed decrease in tPA levels may probably be under the limit of detection.

Our results suggest that in the hippocampus, as described before, tPA protein is expressed in the somatic compartment of DG granule cells and transported to the axons of the mossy fiber pathway, where it will be stored (Lochner et al., 1998; Salles and Strickland, 2002). CPEB4 controls the somatic translation of tPA mRNA, probably through the regulation of its translation efficiency. In *Cpeb4* KO mice, the translational control of tPA is lost. As a result, less tPA

protein will be produced in the soma, which will negatively affect the levels of tPA present in the mossy fiber axons.

4. tPA translational control induced by Aβ is differentially regulated in the somatic and the synaptic compartments

Our results showed that there is reduced tPA translation in the hippocampus of *Cpeb4* KO mice. Moreover, CPEB4 is able to target tPA mRNA (Ortiz-Zapater et al., 2011). This led us to hypothesize that CPEB4 could also control tPA mRNA translation in response to Aβ. Interestingly, we found that CPEBs might play different roles in the somatic and synaptosomal compartments. On the one hand, we observed that depletion of CPEB1 or CPEB4 in mouse primary neurons has no effect on the overexpression of tPA in response to Aβ. In contrast, synaptosomal fractions from *Cpeb1* or *Cpeb4* KO mice treated with Aβ showed a significant reduction of tPA upregulation, meaning that both CPEBs are necessary for ensuring the proper translation of tPA in the synapses in response to Aβ.

Our results using total extracts from hippocampal neurons suggest that CPEB4 probably controls the basal tPA translation in the soma of hippocampal neurons by modulating the translation efficiency of tPA mRNA. However, when Aβ is added to the neurons, other pathways, acting independently of CPEB1 or CPEB4, or even in parallel to them, could have more impact in the translation efficiency of tPA mRNA. Alternatively, it is also possible that for the control of the overexpression of tPA, other CPEBs could compensate for the lack of CPEB4. Future work using neurons lacking CPEB4 in combination with depletion of other CPEBs is required to further understand this possible compensatory effect. Alternatively, neurons containing lower levels of CPEB4 (*i.e. Cpeb4 +/-* neurons isolated from heterozygous mice or even neurons transduced with a *Cpeb4* shRNA) could be used. Finally, CPEB4 protein expressing only the CTD (containing the RRM domains) could be used. This form of CPEB4 would allow RNA binding, but it would lack the regulatory, NTD.

Finally, another possible explanation for the discrepancy in the effects on tPA expression in *Cpeb4* KO mice in basal conditions or after Aβ-treatment would be that we used an *in vivo* model (total extracts from the mouse hippocampus) for studying basal tPA levels, whereas for the study of the response to Aβ, we used an *ex vivo* model (primary cultures of hippocampal neurons), which can potentially respond differently to the stimuli. Indeed we cannot exclude the possibility that neuronal crosstalk with other cells present only in the *in vivo* scenario (astrocytes, microglia, endothelium) may influence regulation of tPA expression by CPEBs.

Whereas control of tPA expression in response to Aβ in the somatic compartment of hippocampal neurons seems to require alternative pathways, we found that Aβ-mediated tPA expression in synapses is dependent on CPEBs. In fact, tPA upregulation after Aβ treatment was impaired in synaptosomes lacking either CPEB1 or CPEB4, meaning that both CPEBs are necessary for ensuring the proper translation of tPA. However, we speculate that each CPEB can work in different ways: CPEB1 has been proposed to control cytoplasmic polyadenylation in the post-synaptic compartment as well as CPE-containing mRNA transport to the dendrites (Huang et al., 2003), while the role of CPEB4 is not yet fully understood. Actually, we found that synaptosomes isolated from *Cpeb1* KO mice contained lower levels of tPA mRNA compared to synaptosomes isolated from WT or *Cpeb4* KO mice. This means that CPEB1 mainly acts localizing tPA mRNA to the dendrites. Additionally, based on previous reports and our own results, it might be in charge of the activation of tPA translation (Shin et al., 2004), probably triggered by its phosphorylation by CamKII (Atkins et al., 2004) or Aurora A (Atkins et al., 2004; Mendez et al., 2000) as reported in response to glutamate stimulation, or even by a non-identified candidate specifically activated by Aβ. The expected mechanism by which CPEB1 regulates tPA mRNA translation is through polyadenylation and/or alternative cleavage and polyadenylation, as it will be discussed in section 5.

127

Like CPEB1, the most probable mechanism by which CPEB4 controls tPA translation is through polyadenylation and alternative cleavage and polyadenylation of tPA mRNA, as it will be discussed in section 5. In this regard, CPEB4 may act in parallel or even sequentially to CPEB1, as has been described previously in the nucleus (Calderone et al., 2015). This would explain why CPEB4 genetic depletion results in an inefficient translation of tPA mRNA in synaptosomes. It is important to mention that up to date, kinases able to phosphorylate CPEB4 in neurons have not been described. We discarded the possibility that CPEB4 participates in tPA mRNA transport into dendrites, as in contrast to *Cpeb1* KO synaptosomes, tPA mRNA levels were similar in WT and *Cpeb4* KO synaptosomes.

Another possible explanation to the decrease of tPA expression in *Cpeb4* KO synaptosomes is an indirect mechanism through alterations in the synapses, as it has been reported that even though *Cpeb4* KO mice are normal, their hippocampal neurons contain abnormally enlarged spines (Tsai et al., 2013). To better understand whether synaptic dysfunction can contribute to the effects observed for tPA expression in *Cpeb4* KO synaptosomes, an inducible *Cpeb4* KO mouse model would be required. Moreover, identification of other *bona fide* candidates controlled by CPEB4 that can be induced by Aβ treatment will help to rule out that effects of CPEB4 depletion in synaptosomes are not an indirect effect derived from synaptic maturation deficits.

Unexpectedly, we found that treatment with Aβ in WT synaptosomes also results in CPEB4 overexpression. Importantly, upregulation of CPEB4 levels in response to Aβ can result in increased translation of its target mRNAs, such as tPA, leading to aberrant neuronal gene reprogramming that can contribute to Alzheimer's disease (see section 5 for further discussion). These data point to an important role for CPEB4 in neuronal degeneration. In this regard, generation of a transgenic mouse model overexpressing CPEB4 in the

hippocampus could help to elucidate the contribution of this protein to an AD-like phenotype. Future work will be required to decipher the underlying molecular mechanism responsible for CPEB4 upregulation in response to Aβ. Previous data in oocytes have reported regulation of CPEB4 mRNA expression by translational control through CPEB1 (Igea and Méndez, 2010). However, we observe similar CPEB4 mRNA polyadenylation and protein upregulation after Aβ treatment in WT or *Cpeb1* KO synaptosomes, suggesting that CPEB1 is not involved in the regulation of Aβ-induced CPEB4 expression in synaptosomes, and that probably, CPEB4 controls its own translation, as has been reported during liver disease (Calderone et al., 2015) .

DISCUSSION

5. Aβ-induced translational control of tPA is regulated by polyadenylation and cleavage and polyadenylation in the synapses

In this work, we have demonstrated that CPEB1 and CPEB4 can control the synapse-specific tPA response to Aβ. Based on what we know for CPEB1 (Bava et al., 2013; Calderone et al., 2015), the expected mechanism by which this process can be controlled would be polyadenylation or cleavage and polyadenylation. Nevertheless, the last event is a process that has only been described to take place in the nucleus.

By analyzing tPA mRNA polyadenylation in Aβ-stimulated synaptosomes, we first detected two different isoforms of tPA mRNA in the synaptic compartment. After cloning and sequencing them, we demonstrated that one of them corresponded to tPA full-length 3'-UTR, and the other to a shorter version of it. More interestingly, we found that, in response to Aβ stimulation, synaptosomes treated with Aβ presented slightly less polyadenylation in the longest isoform, while at the same time, the shorter isoform presented polyadenylation. In addition, we found that synaptosomes prepared from *Cpeb1* or *Cpeb4* KO synaptosomes had the shorter isoform less represented, pointing to the requirement of both CPEB1 and CPEB4 to mediate this process.

When we analyzed this event by 3'-RACE, we found that tPA mRNA is cleaved after the induction with Aβ, a process which was abolished in *Cpeb1* and *Cpeb4* KO synaptosomes. This means that CPEB1 and CPEB4 directly participate in this process by regulating tPA mRNA cleavage or indirectly by co-operating with other CPEBs or RPBs in the process, as both CPEB1 and CPEB4 are necessary for the appropriate tPA response to Aβ. However, as it was discussed in the previous section, even though it is unlikely, we cannot exclude that some of these effects are due to synaptic abnormalities in the *Cpeb4* KO mice.

The shorter isoform that we described contains less ARE sequences, which usually destabilize the mRNA. In addition, the newly generated shorter 3'-UTR lacks the CPE-PAS 3'-UTR organization in repression (2 CPEs in tandem near the PAS), and also is shorter and hence less likely to be targeted by other RBPs or miRNAs. Consequently, we expected this shorter isoform to be more translationally active. However, when we evaluated its translation efficiency in a neuron-like cell line, we found that its translation efficiency was slightly lower, and equivalent to the mutation of the last (distal) PAS of the full-length 3'-UTR. One possible explanation is that, as the shorter 3'-UTR lacks ARE sequences and several repressive sequences, it could yield slightly lower tPA levels, but with a more sustained expression in time. More experiments will be required to determine the stability of this shorter mRNA.

These results indicate that, as a regulatory mechanism, neurons are able to cleave and polyadenylate tPA mRNA (and probably other mRNAs) specifically in the synapses. It is important to highlight that this is a process that has only been reported to take place in the nucleus. Among all the factors involved in 3'-end processing, it is known that the members of the CPSF complex, the poly(A) polymerase Gld2, maskin and PABP are present both in the cytosol and the neuronal dendrites. Contrarily, there is no information available regarding the other members, specifically the CSTF complex and the RNA Pol II.

Our results demonstrate that all the members of the CSTF complex, as well as the RNA Pol II, are present in the dendrites, which show that cleavage and polyadenylation is biological process that can take place at the neuronal synapses. In addition, based on what it is known for the nuclear 3'-end processing, the phosphorylation state of the RNA Pol II CTD found in synaptosomes makes it able to be recognized by the 3'-end machinery. This molecular mechanism represents a new biological function for mRNA cleavage, no longer being restricted to nuclear RNA processing machinery but also

happening in synaptic terminals, possibly to ensure fast protein synthesis in response to external stimuli.

6. *In vivo*, CPEB4 is overexpressed in AD patients, which can affect the translation of hundreds of mRNAs

Our results show that Aβ synaptic stimulation leads to CPEB4 overexpression. Taking into consideration the mounting evidence of a link between Aβ aggregation and AD onset and progression, we decided to evaluate CPEB4 levels in people affected by this pathology. We found by IHF that, in comparison to healthy controls, these patients displayed elevated levels of CPEB4 in the hippocampus, mainly in areas where high amounts of aggregated Aβ are present. This data fit with our *in vitro* results showing increased CPEB4 levels in synaptosomes treated with Aβ and suggest that this peptide, directly or indirectly, can also induce the overexpression of CPEB4 *in vivo* during AD pathology.

We also analyzed whether Tau hyperphosphorylation, another major hallmark of AD pathogenesis, could play a role in the CPEB4 overexpression detected in AD patients. However, in contrast with Aβ data, we did not find a positive correlation between neurons expressing hyperphosphorylated Tau and CPEB4 levels. This suggests that the hyperphosphorylation of Tau and the overexpression of CPEB4 could be completely independent processes or that CPEB4 overexpression takes place before Tau hyperphosphorylation. However, considering that our analysis was performed using slices from human AD brain sections, we cannot exclude that Tau hyperphosphorylation was present in other Z planes containing parts of the neurons present in the slices analyzed. Indeed it has been reported that Tau hyperphosphorylation affects neuronal microtubule network, making more difficult to evaluate this staining by IHF.

Further investigation is required for a better understanding of the molecular mechanism underlying upregulation of CPEB4 in response to Aβ during AD pathology. Our *in vitro* results using synaptosomes suggest that AD pathology would start in the synaptic compartment, in agreement with previous

publications (Selkoe, 2002). During aging, chronic exposure to Aβ and retrograde signaling from the synapses could lead to altered expression of CPEB4 in the soma (either transcriptional or translational), which would result in AD. Then, similarly to what we have reported in cancer (Ortiz-Zapater et al., 2011) synaptic CPEB4 overexpression could affect the translation of hundreds of mRNAs, including tPA, that could mediate AD pathology initiation and/or progression. Regulation of gene expression by CPEBs in neurons is a complex process that can play different roles in physiological or pathological scenarios. The fact that in adult somatic cells CPEBs expression is almost restricted to neurons, suggests a key role for these proteins in neuronal physiology. Generation of KO mice has helped to better understand the role of the different CPEB members in CNS. *Cpeb1* KO mice display deficits of hippocampal-related memory and synaptic plasticity (Berger-Sweeney et al., 2006). In contrast, *Cpeb4* KO mice display normal hippocampus-related synaptic plasticity and memory (Shin et al., 2016; Tsai et al., 2013). However, little is known about the role of CPEBs in CNS disorders. Only a role for CPEB1 has been reported in a mouse model of Fragile X syndrome, where genetic depletion of CPEB1 rescues memory deficits (Udagawa et al., 2013).

Here, we provide data showing that CPEB4 is upregulated *in vitro* in the synapses in response to Aβ, and *in vivo* in AD patients. Moreover, we found that CPEB1 and CPEB4 are required for Aβ-mediated tPA overexpression which, in turn, can lead to beneficial or detrimental effects depending on the balance of catalytic-dependent or independent tPA functions (Ledesma et al., 2000; Medina et al., 2005; Melchor et al., 2003; Oh et al., 2014; Pineda et al., 2012; Siao and Tsirka, 2002). In this context, it is uncertain whether inhibition of CPEBs (and the subsequent abolishment of the expression of their mRNA targets, including tPA) would result in neuroprotection or neuronal damage.

134

To answer this question, we analyzed the effects of Aβ treatment on neuronal survival in primary cultures of *Cpeb1* KO or *Cpeb4* KO hippocampal neurons. However, we did not observe neither enhancing cell death nor conferring protection against Aβ after depletion of CPEB1 or CPEB4 in these cells. One possible explanation to this lack of effect in cultured neurons could be that crosstalk with other cell types present in the *in vivo* situation (astrocytes, microglial cells, endothelial cells) might be required for a CPEB-mediated phenotype in response to Aβ. Future experiments injecting Aβ directly in the hippocampus of *Cpeb1* or *Cpeb4* mice will be necessary to confirm this hypothesis.

7. Final remarks

This is one of the first studies linking members of the CPEB family of RNA-binding proteins and neurodegeneration. The results presented here show that CPEB1 and CPEB4 are important mediators of tPA mRNA localization to the dendrites and its translation in response to Aβ. This work and the previously published literature allowed us to propose a preliminary model for the synaptic roles of these two proteins during AD (**Figure 39**). According to it, Aβ triggers a synaptic signaling cascade that leads to CPEB4 activation (presumably by phosphorylation). The kinase involved in this process has not been determined yet. However, one interesting candidate could be CaMKII.

The cell signaling cascade activated by Aβ leads to CPEB4-mediated translation of its own mRNA, generating a positive feedback loop that leads to the overexpression of CPEB4 protein, as observed during liver disease (Calderone et al., 2015). CPEB4 overexpression would subsequently positively affect the translation efficiency of CPEB4, tPA, and probably of other CPE-containing mRNAs. The mechanism by which tPA is overexpressed is presumably through CPEB1 and CPEB4-mediated polyadenylation and translation of its full-length 3'-UTR (previously localized in the synaptic terminals in a repressed state by CPEB1), as well as by its cleavage into a mRNA with a shorter 3'-UTR and its subsequent polyadenylation. The reason why tPA mRNA is cleaved into this form is not yet understood, but one of the reasons could be the generation of a mRNA with less CPEs and AREs, which would result in a higher translation efficiency and/or longer stability that ensures sustained tPA translation.

These results and the fact that CPEB4 is overexpressed in human AD samples means that this protein may have broader roles during AD onset and progression through translational regulation of other mRNAs besides tPA. This means CPEB4 would be an interesting target for the design of pharmacological inhibitors with potential benefits to block or slow down AD progression.
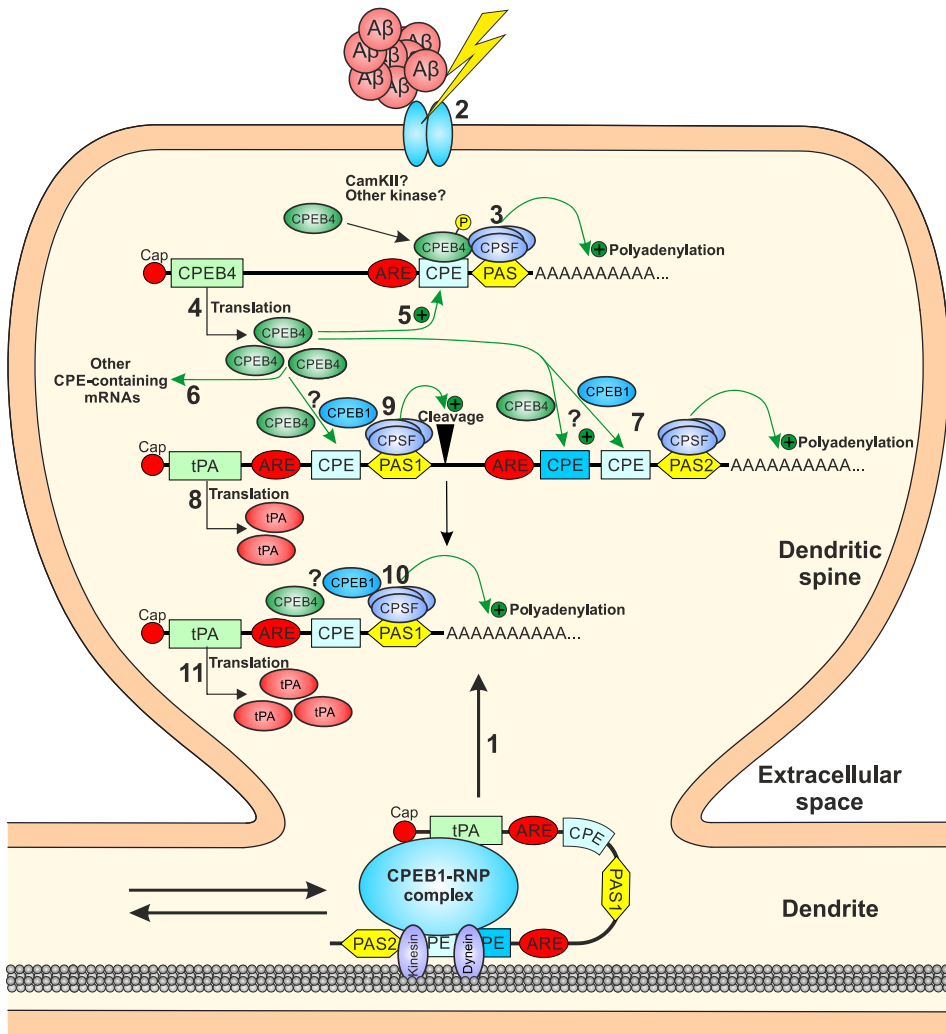
Figure 39. Proposed preliminary model for the regulation of tPA overexpression in the synaptic compartment during Alzheimer's disease pathology. (1) CPEB1 targets the longest isoform of tPA mRNA in the somatic compartment and mediates its synaptic localization (for simplicity, the repression complex is shown as CPEB1-RNP complex). (2) Aβ stimulation triggers a cell signaling cascade that leads to phosphorylation of CPEB4, which promotes polyadenylation (3) and translation (4) of CPEB4 mRNA. The potential kinase involved in the activation of CPEB4 has not been yet characterized. The overexpression of CPEB4 leads to a positive feedback that promotes more CPEB4 mRNA translation (4), as well as the translational control of other CPE-containing mRNAs (6). One of these mRNAs, tPA, will be polyadenylated (7) and translated (8) in a process involving both CPEB1 and CPEB4 (we still do not understand how both CPEBs crosstalk in the process). Part of tPA mRNA, probably in a time-dependent manner, will be cleaved (9) into a mRNA with a shorter 3'-UTR that is then polyadenylated (10) and translated (11) in a CPEB1 and CPEB4-dependent manner. The generation of this shorter mRNA could be a mechanism for producing a mRNA containing less repressive CPEs (2CPE in tandem near PAS2) and AREs, thus generating an mRNA with higher translation efficiency and/or increased stability that may produce sustained tPA translation.

CONCLUSIONS

CONCLUSIONS

The present study shows that CPEB1 and CPEB4 are important regulators of tPA translation in the synaptic compartment during AD pathology. The main conclusions are the following:

1. tPA expression is controlled at the post-transcriptional level in basal conditions in the mouse hippocampus.

2. tPA overexpression in total hippocampal neurons in response to Aβ is controlled by translational regulation. However, CPEB1 and CPEB4 contribution appears to be minor in the process.

3. tPA is overexpressed in the synaptic compartment in response to Aβ and both CPEB1 and CPEB4 are necessary proteins for the regulation of this process.

4. CPEB1 participates in tPA mRNA localization to the synaptic compartment.

5. Both CPEB1 and CPEB4 participate directly or indirectly in cleavage and polyadenylation of tPA mRNA in the synaptic terminals in response to aggregated Aβ.

6. All the members of the 3'-end processing machinery required for the process of mRNA cleavage and polyadenylation is present in the synaptic terminals.

7. Similarly to tPA, CPEB4 is overexpressed *in vitro* in Aβ-stimulated synaptosomes and *in vivo* in amyloidogenic areas of the hippocampus of AD patients, which means that CPEB4 may have important roles in the disease through translational control of tPA and other mRNA targets.

SUPPLEMENTARY INFORMATION

Supplementary table S1: Proteomic analysis of mouse primary synaptosomes.

Accession	Description	Σ Cover.	Σ# Prot.	Σ# Unique Pept.	Σ# Pept.	Σ# PSM
O55042	Alpha-synuclein OS=Mus musculus GN=Snca PE=1 SV=2 - [SYUA_MOUSE]	85,71	1	5	8	29
P26645	Myristoylated alanine-rich C-kinase substrate OS=Mus musculus GN=Marcks PE=1 SV=2 - [MARCS_MOUSE]	66,99	2	10	10	85
Q91XV3	Brain acid soluble protein 1 OS=Mus musculus GN=Basp1 PE=1 SV=3 - [BASP1_MOUSE]	65,04	1	9	9	149
P60879	Synaptosomal-associated protein 25 OS=Mus musculus GN=Snap25 PE=1 SV=1 - [SNP25_MOUSE]	59,71	2	11	11	69
P63044	Vesicle-associated membrane protein 2 OS=Mus musculus GN=Vamp2 PE=1 SV=2 - [VAMP2_MOUSE]	59,48	1	2	4	23
P06837	Neuromodulin OS=Mus musculus GN=Gap43 PE=1 SV=1 - [NEUM_MOUSE]	59,03	1	11	11	104
P63213	Guanine nucleotide-binding protein G(I)/G(S)/G(O) subunit gamma-2 OS=Mus musculus GN=Gng2 PE=1 SV=2 - [GBG2_MOUSE]	57,75	2	3	4	14
Q64433	10 kDa heat shock protein, mitochondrial OS=Mus musculus GN=Hspe1 PE=1 SV=2 - [CH10_MOUSE]	55,88	1	6	6	16
P62259	14-3-3 protein epsilon OS=Mus musculus GN=Ywhae PE=1 SV=1 - [1433E_MOUSE]	50,59	1	11	13	82
Q61016	Guanine nucleotide-binding protein G(I)/G(S)/G(O) subunit gamma-7 OS=Mus musculus GN=Gng7 PE=2 SV=2 - [GBG7_MOUSE]	48,53	1	3	3	9
Q9WTT4	V-type proton ATPase subunit G 2 OS=Mus musculus GN=Atp6v1g2 PE=2 SV=1 - [VATG2_MOUSE]	48,31	1	4	4	23
Q6W8Q3	Purkinje cell protein 4-like protein 1 OS=Mus musculus GN=Pcp4l1 PE=1 SV=1 - [PC4L1_MOUSE]	47,06	1	2	2	5
P63101	14-3-3 protein zeta/delta OS=Mus musculus GN=Ywhaz PE=1 SV=1 - [1433Z_MOUSE]	46,12	4	8	10	56
P28184	Metallothionein-3 OS=Mus musculus GN=Mt3 PE=1 SV=1 - [MT3_MOUSE]	45,59	1	2	2	6
P0CG49	Polyubiquitin-B OS=Mus musculus GN=Ubb PE=1 SV=1 - [UBB_MOUSE]	44,59	5	3	3	13
P61982	14-3-3 protein gamma OS=Mus musculus GN=Ywhag PE=1 SV=2 - [1433G_MOUSE]	42,91	2	8	11	58
P68510	14-3-3 protein eta OS=Mus musculus GN=Ywhah PE=1 SV=2 - [1433F_MOUSE]	42,28	2	7	10	57
P62204	Calmodulin OS=Mus musculus GN=Calm1 PE=1 SV=2 - [CALM_MOUSE]	41,61	3	7	7	45
Q9CQV8	14-3-3 protein beta/alpha OS=Mus musculus GN=Ywhab PE=1 SV=3 - [1433B_MOUSE]	41,06	3	5	8	53
P60710	Actin, cytoplasmic 1 OS=Mus musculus GN=Actb PE=1 SV=1 - [ACTB_MOUSE]	40,80	7	1	14	116
P63260	Actin, cytoplasmic 2 OS=Mus musculus GN=Actg1 PE=1 SV=1 - [ACTG_MOUSE]	40,80	7	1	14	107
P63024	Vesicle-associated membrane protein 3 OS=Mus musculus GN=Vamp3 PE=1 SV=1 - [VAMP3_MOUSE]	38,83	1	1	3	12
Q6PIC6	Sodium/potassium-transporting ATPase subunit alpha-3 OS=Mus musculus GN=Atp1a3 PE=1 SV=1 - [AT1A3_MOUSE]	38,80	4	22	36	240
P62821	Ras-related protein Rab-1A OS=Mus musculus GN=Rab1A PE=1 SV=3 - [RAB1A_MOUSE]	38,05	11	4	8	14
P17182	Alpha-enolase OS=Mus musculus GN=Eno1 PE=1 SV=3 - [ENOA_MOUSE]	37,79	5	10	13	62
P05064	Fructose-bisphosphate aldolase A OS=Mus musculus GN=Aldoa PE=1 SV=2 - [ALDOA_MOUSE]	37,64	3	9	11	47
P63168	Dynein light chain 1, cytoplasmic OS=Mus musculus GN=Dynll1 PE=1 SV=1 - [DYL1_MOUSE]	37,08	1	1	2	14
Q9D0M5	Dynein light chain 2, cytoplasmic OS=Mus musculus GN=Dynll2 PE=1 SV=1 - [DYL2_MOUSE]	37,08	1	1	2	46
Q9CPQ1	Cytochrome c oxidase subunit 6C OS=Mus musculus GN=Cox6c PE=1 SV=3 - [COX6C_MOUSE]	36,84	1	4	4	11
P17742	Peptidyl-prolyl cis-trans isomerase A OS=Mus musculus GN=Ppia PE=1 SV=2 - [PPIA_MOUSE]	36,59	4	5	6	21
P62823	Ras-related protein Rab-3C OS=Mus musculus GN=Rab3c PE=1 SV=1 - [RAB3C_MOUSE]	36,12	12	4	8	39
Q03265	ATP synthase subunit alpha, mitochondrial OS=Mus musculus GN=Atp5a1 PE=1 SV=1 - [ATPA_MOUSE]	35,99	1	20	20	98
P63017	Heat shock cognate 71 kDa protein OS=Mus musculus GN=Hspa8 PE=1 SV=1 - [HSP7C_MOUSE]	35,91	6	10	17	54
Q91ZZ3	Beta-synuclein OS=Mus musculus GN=Sncb PE=1 SV=1 - [SYUB_MOUSE]	35,34	2	2	5	22
P08249	Malate dehydrogenase, mitochondrial OS=Mus musculus GN=Mdh2 PE=1 SV=3 - [MDHM_MOUSE]	34,91	1	11	11	40
Q7TSJ2	Microtubule-associated protein 6 OS=Mus musculus GN=Map6 PE=1 SV=2 - [MAP6_MOUSE]	34,55	1	25	25	58
P05063	Fructose-bisphosphate aldolase C OS=Mus musculus GN=Aldoc PE=1 SV=4 - [ALDOC_MOUSE]	34,44	3	8	10	34
Q04447	Creatine kinase B-type OS=Mus musculus GN=Ckb PE=1 SV=1 - [KCRB_MOUSE]	34,38	1	10	10	40
Q9CQZ1	Heat shock factor-binding protein 1 OS=Mus musculus GN=Hsbp1 PE=2 SV=1 - [HSBP1_MOUSE]	34,21	1	2	2	6
Q62442	Vesicle-associated membrane protein 1 OS=Mus musculus GN=Vamp1 PE=1 SV=1 - [VAMP1_MOUSE]	33,90	1	2	3	15
Q9WV98	Mitochondrial import inner membrane translocase subunit Tim9 OS=Mus musculus GN=Timm9 PE=1 SV=1 - [TIM9_MOUSE]	33,71	1	3	3	4
P63011	Ras-related protein Rab-3A OS=Mus musculus GN=Rab3a PE=1 SV=1 - [RAB3A_MOUSE]	33,64	12	4	8	64
Q8VDN2	Sodium/potassium-transporting ATPase subunit alpha-1 OS=Mus musculus GN=Atp1a1 PE=1 SV=1 - [AT1A1_MOUSE]	33,24	2	15	28	155
P52480	Pyruvate kinase isozymes M1/M2 OS=Mus musculus GN=Pkm PE=1 SV=4 - [KPYM_MOUSE]	33,15	3	16	16	63
P61264	Syntaxin-1B OS=Mus musculus GN=Stx1b PE=1 SV=1 - [STX1B_MOUSE]	32,99	2	8	9	61
Q9Z0P4	Paralemmin-1 OS=Mus musculus GN=Palm PE=1 SV=1 - [PALM_MOUSE]	32,90	2	10	10	41
P48962	ADP/ATP translocase 1 OS=Mus musculus GN=Slc25a4 PE=1 SV=4 - [ADT1_MOUSE]	32,89	2	7	10	53
P18872	Guanine nucleotide-binding protein G(o) subunit alpha OS=Mus musculus GN=Gnao1 PE=1 SV=3 - [GNAO_MOUSE]	32,49	1	9	10	69
Q06185	ATP synthase subunit e, mitochondrial OS=Mus musculus GN=Atp5i PE=1 SV=2 - [ATP5I_MOUSE]	32,39	1	2	2	6
P50396	Rab GDP dissociation inhibitor alpha OS=Mus musculus GN=Gdi1 PE=1 SV=3 - [GDIA_MOUSE]	31,99	2	9	12	37
Q6PIE5	Sodium/potassium-transporting ATPase subunit alpha-2 OS=Mus musculus GN=Atp1a2 PE=1 SV=1 - [AT1A2_MOUSE]	31,96	2	13	27	186
P68254	14-3-3 protein theta OS=Mus musculus GN=Ywhaq PE=1 SV=1 - [1433T_MOUSE]	31,84	3	4	7	42
Q6ZWY8	Thymosin beta-10 OS=Mus musculus GN=Tmsb10 PE=2 SV=3 - [TYB10_MOUSE]	31,82	1	1	1	6
P19536	Cytochrome c oxidase subunit 5B, mitochondrial OS=Mus musculus GN=Cox5b PE=1 SV=1 - [COX5B_MOUSE]	31,25	1	4	4	18
O09111	NADH dehydrogenase [ubiquinone] 1 beta subcomplex subunit 11, mitochondrial OS=Mus musculus GN=Ndufb11 PE=1 SV=2 - [NDUBB_MOUSE]	31,13	1	3	3	6
Q61644	Protein kinase C and casein kinase substrate in neurons protein 1 OS=Mus musculus GN=Pacsin1 PE=1 SV=1 - [PACN1_MOUSE]	31,07	1	10	11	39
P28667	MARCKS-related protein OS=Mus musculus GN=Marcksl1 PE=1 SV=2 - [MRP_MOUSE]	31,00	1	3	3	8

Accession	Description	Σ Cover.	Σ# Prot.	Σ# Unique Pept.	Σ# Pept.	Σ# PSM
Q60932	Voltage-dependent anion-selective channel protein 1 OS=Mus musculus GN=Vdac1 PE=1 SV=3 - [VDAC1_MOUSE]	29,73	1	7	7	33
O08553	Dihydropyrimidinase-related protein 2 OS=Mus musculus GN=Dpysl2 PE=1 SV=2 - [DPYL2_MOUSE]	29,20	1	9	13	80
P51881	ADP/ATP translocase 2 OS=Mus musculus GN=Slc25a5 PE=1 SV=3 - [ADT2_MOUSE]	28,86	2	5	9	45
P16125	L-lactate dehydrogenase B chain OS=Mus musculus GN=Ldhb PE=1 SV=2 - [LDHB_MOUSE]	28,74	2	8	9	23
Q9CQR4	Acyl-coenzyme A thioesterase 13 OS=Mus musculus GN=Acot13 PE=1 SV=1 - [ACO13_MOUSE]	28,57	1	3	3	10
O35526	Syntaxin-1A OS=Mus musculus GN=Stx1a PE=1 SV=3 - [STX1A_MOUSE]	28,47	2	7	8	32
P09411	Phosphoglycerate kinase 1 OS=Mus musculus GN=Pgk1 PE=1 SV=4 - [PGK1_MOUSE]	28,30	2	12	12	41
P17183	Gamma-enolase OS=Mus musculus GN=Eno2 PE=1 SV=2 - [ENOG_MOUSE]	28,11	3	7	10	36
P61027	Ras-related protein Rab-10 OS=Mus musculus GN=Rab10 PE=1 SV=1 - [RAB10_MOUSE]	28,00	11	4	5	17
Q61171	Peroxiredoxin-2 OS=Mus musculus GN=Prdx2 PE=1 SV=3 - [PRDX2_MOUSE]	27,27	1	5	5	14
P63038	60 kDa heat shock protein, mitochondrial OS=Mus musculus GN=Hspd1 PE=1 SV=1 - [CH60_MOUSE]	27,05	1	12	12	147
P46460	Vesicle-fusing ATPase OS=Mus musculus GN=Nsf PE=1 SV=2 - [NSF_MOUSE]	26,88	1	18	18	76
Q9JMF3	Guanine nucleotide-binding protein G(I)/G(S)/G(O) subunit gamma-13 OS=Mus musculus GN=Gng13 PE=3 SV=1 - [GBG13_MOUSE]	26,87	1	2	2	3
P97450	ATP synthase-coupling factor 6, mitochondrial OS=Mus musculus GN=Atp5j PE=1 SV=1 - [ATP5J_MOUSE]	26,85	1	2	2	9
Q9Z1P6	NADH dehydrogenase [ubiquinone] 1 alpha subcomplex subunit 7 OS=Mus musculus GN=Ndufa7 PE=1 SV=3 - [NDUA7_MOUSE]	26,55	1	3	3	10
O08599	Syntaxin-binding protein 1 OS=Mus musculus GN=Stxbp1 PE=1 SV=2 - [STXB1_MOUSE]	26,43	2	15	15	130
P26443	Glutamate dehydrogenase 1, mitochondrial OS=Mus musculus GN=Glud1 PE=1 SV=1 - [DHE3_MOUSE]	26,34	2	13	13	42
P04370	Myelin basic protein OS=Mus musculus GN=Mbp PE=1 SV=2 - [MBP_MOUSE]	26,00	1	7	7	24
Q78IK2	Up-regulated during skeletal muscle growth protein 5 OS=Mus musculus GN=Usmg5 PE=1 SV=1 - [USMG5_MOUSE]	25,86	1	1	1	7
P63054	Purkinje cell protein 4 OS=Mus musculus GN=Pcp4 PE=2 SV=2 - [PCP4_MOUSE]	25,81	1	1	1	11
Q9JKC6	Cell cycle exit and neuronal differentiation protein 1 OS=Mus musculus GN=Cend1 PE=1 SV=1 - [CEND_MOUSE]	25,50	1	3	3	22
Q8CAQ8	Mitochondrial inner membrane protein OS=Mus musculus GN=Immt PE=1 SV=1 - [IMMT_MOUSE]	25,50	1	17	17	54
Q99PT1	Rho GDP-dissociation inhibitor 1 OS=Mus musculus GN=Arhgdia PE=1 SV=3 - [GDIR1_MOUSE]	25,49	1	4	4	15
P16330	2',3'-cyclic-nucleotide 3'-phosphodiesterase OS=Mus musculus GN=Cnp PE=1 SV=3 - [CN37_MOUSE]	25,48	1	11	11	77
P38647	Stress-70 protein, mitochondrial OS=Mus musculus GN=Hspa9 PE=1 SV=3 - [GRP75_MOUSE]	25,18	1	13	13	44
CON_0071 60132	SWISS-PROT:P60661-2| Bos taurus Gene_Symbol=MYL6 Isoform Smooth muscle of Myosin light polypeptide 6	25,17	3	3	3	6
CON_0069 89162	SWISS-PROT:P18203| Bos taurus Gene_Symbol=FKBP1A Peptidyl-prolyl cis-trans isomerase FKBP1A	25,00	2	2	2	6
CON_0069 11372	SWISS-PROT:P62326| Bos taurus Gene_Symbol=TMSB4X Thymosin beta-4	25,00	1	1	1	9
Q9CXP8	Guanine nucleotide-binding protein G(I)/G(S)/G(O) subunit gamma-10 OS=Mus musculus GN=Gng10 PE=3 SV=1 - [GBG10_MOUSE]	25,00	2	1	2	5
Q9DAS9	Guanine nucleotide-binding protein G(I)/G(S)/G(O) subunit gamma-12 OS=Mus musculus GN=Gng12 PE=1 SV=3 - [GBG12_MOUSE]	25,00	1	2	2	5
P16858	Glyceraldehyde-3-phosphate dehydrogenase OS=Mus musculus GN=Gapdh PE=1 SV=2 - [G3P_MOUSE]	24,92	3	8	8	27
P19783	Cytochrome c oxidase subunit 4 isoform 1, mitochondrial OS=Mus musculus GN=Cox4i1 PE=1 SV=2 - [COX41_MOUSE]	24,85	1	4	4	9
Q7TQD2	Tubulin polymerization-promoting protein OS=Mus musculus GN=Tppp PE=1 SV=1 - [TPPP_MOUSE]	24,77	1	6	6	19
Q9CZT8	Ras-related protein Rab-3B OS=Mus musculus GN=Rab3b PE=1 SV=1 - [RAB3B_MOUSE]	24,66	12	3	5	19
P84096	Rho-related GTP-binding protein RhoG OS=Mus musculus GN=Rhog PE=2 SV=1 - [RHOG_MOUSE]	24,61	3	2	3	16
Q99KI0	Aconitate hydratase, mitochondrial OS=Mus musculus GN=Aco2 PE=1 SV=1 - [ACON_MOUSE]	24,49	1	17	17	57
P35802	Neuronal membrane glycoprotein M6-a OS=Mus musculus GN=Gpm6a PE=1 SV=1 - [GPM6A_MOUSE]	24,10	1	6	6	63
Q99PJ0	Neurotrimin OS=Mus musculus GN=Ntm PE=2 SV=2 - [NTRI_MOUSE]	23,84	1	8	8	20
CON_0071 44053	SWISS-PROT:Q5KR47-2| Bos taurus Gene_Symbol=TPM3 Isoform 2 of Tropomyosin alpha-3 chain	23,79	6	3	6	16
Q9D8Y0	EF-hand domain-containing protein D2 OS=Mus musculus GN=Efhd2 PE=1 SV=1 - [EFHD2_MOUSE]	23,75	1	5	5	6
P68368	Tubulin alpha-4A chain OS=Mus musculus GN=Tuba4a PE=1 SV=1 - [TBA4A_MOUSE]	23,66	3	4	9	52
P14152	Malate dehydrogenase, cytoplasmic OS=Mus musculus GN=Mdh1 PE=1 SV=3 - [MDHC_MOUSE]	23,65	1	8	8	30
Q8C0M9	Isoaspartyl peptidase/L-asparaginase OS=Mus musculus GN=Asrgl1 PE=1 SV=1 - [ASGL1_MOUSE]	23,62	1	7	7	18
Q8QZT1	Acetyl-CoA acetyltransferase, mitochondrial OS=Mus musculus GN=Acat1 PE=1 SV=1 - [THIL_MOUSE]	23,58	1	8	8	36
Q9D164	FXYD domain-containing ion transport regulator 6 OS=Mus musculus GN=Fxyd6 PE=1 SV=2 - [FXYD6_MOUSE]	23,40	1	1	1	1
P62835	Ras-related protein Rap-1A OS=Mus musculus GN=Rap1a PE=2 SV=1 - [RAP1A_MOUSE]	23,37	1	1	5	7
Q99JI6	Ras-related protein Rap-1b OS=Mus musculus GN=Rap1b PE=2 SV=2 - [RAP1B_MOUSE]	23,37	1	1	5	8
Q9Z1G3	V-type proton ATPase subunit C 1 OS=Mus musculus GN=Atp6v1c1 PE=1 SV=4 - [VATC1_MOUSE]	23,30	1	9	9	13
Q9QXV0	ProSAAS OS=Mus musculus GN=Pcsk1n PE=1 SV=2 - [PCSK1_MOUSE]	23,26	1	4	4	17
Q9CPQ3	Mitochondrial import receptor subunit TOM22 homolog OS=Mus musculus GN=Tomm22 PE=2 SV=3 - [TOM22_MOUSE]	23,24	1	2	2	5
Q9CQ75	NADH dehydrogenase [ubiquinone] 1 alpha subcomplex subunit 2 OS=Mus musculus GN=Ndufa2 PE=1 SV=3 - [NDUA2_MOUSE]	23,23	1	2	2	2
O88935	Synapsin-1 OS=Mus musculus GN=Syn1 PE=1 SV=2 - [SYN1_MOUSE]	23,09	1	11	12	85
Q9Z2Q6	Septin-5 OS=Mus musculus GN=Sept5 PE=1 SV=2 - [SEPT5_MOUSE]	23,04	2	8	8	25
P16546	Spectrin alpha chain, non-erythrocytic 1 OS=Mus musculus GN=Sptan1 PE=1 SV=4 - [SPTN1_MOUSE]	22,94	2	51	51	119

Accession	Description	Σ Cover.	Σ# Prot.	Σ# Unique Pept.	Σ# Pept.	Σ# PSM
P56480	ATP synthase subunit beta, mitochondrial OS=Mus musculus GN=Atp5b PE=1 SV=2 - [ATPB_MOUSE]	22,87	1	10	10	61
E9PUL5	Proline-rich transmembrane protein 2 OS=Mus musculus GN=Prrt2 PE=1 SV=1 - [PRRT2_MOUSE]	22,54	1	5	5	16
Q9CPW4	Actin-related protein 2/3 complex subunit 5 OS=Mus musculus GN=Arpc5 PE=2 SV=3 - [ARPC5_MOUSE]	22,52	1	2	2	4
Q9CRB9	Coiled-coil-helix-coiled-coil-helix domain-containing protein 3, mitochondrial OS=Mus musculus GN=Chchd3 PE=1 SV=1 - [CHCH3_MOUSE]	22,47	1	5	5	10
Q9R0P9	Ubiquitin carboxyl-terminal hydrolase isozyme L1 OS=Mus musculus GN=Uchl1 PE=1 SV=1 - [UCHL1_MOUSE]	22,42	3	5	5	12
Q9WUC3	Lymphocyte antigen 6H OS=Mus musculus GN=Ly6h PE=2 SV=2 - [LY6H_MOUSE]	22,30	1	3	3	17
Q9D6J6	NADH dehydrogenase [ubiquinone] flavoprotein 2, mitochondrial OS=Mus musculus GN=Ndufv2 PE=1 SV=2 - [NDUV2_MOUSE]	22,18	1	4	4	17
P62774	Myotrophin OS=Mus musculus GN=Mtpn PE=1 SV=2 - [MTPN_MOUSE]	22,03	2	2	2	5
Q9CR51	V-type proton ATPase subunit G 1 OS=Mus musculus GN=Atp6v1g1 PE=2 SV=3 - [VATG1_MOUSE]	22,03	1	2	2	3
Q62425	NADH dehydrogenase [ubiquinone] 1 alpha subcomplex subunit 4 OS=Mus musculus GN=Ndufa4 PE=1 SV=2 - [NDUA4_MOUSE]	21,95	1	2	2	15
Q9D1G1	Ras-related protein Rab-1B OS=Mus musculus GN=Rab1b PE=1 SV=1 - [RAB1B_MOUSE]	21,89	11	1	5	6
Q9CQJ8	NADH dehydrogenase [ubiquinone] 1 beta subcomplex subunit 9 OS=Mus musculus GN=Ndufb9 PE=1 SV=3 - [NDUB9_MOUSE]	21,79	1	3	3	8
P97315	Cysteine and glycine-rich protein 1 OS=Mus musculus GN=Csrp1 PE=1 SV=3 - [CSRP1_MOUSE]	21,76	2	4	4	12
P08551	Neurofilament light polypeptide OS=Mus musculus GN=Nefl PE=1 SV=5 - [NFL_MOUSE]	21,73	4	9	11	43
Q9D2M8	Ubiquitin-conjugating enzyme E2 variant 2 OS=Mus musculus GN=Ube2v2 PE=2 SV=4 - [UB2V2_MOUSE]	21,38	3	3	3	7
P11798	Calcium/calmodulin-dependent protein kinase type II subunit alpha OS=Mus musculus GN=Camk2a PE=1 SV=2 - [KCC2A_MOUSE]	21,34	1	6	8	55
CON_0069 96223	SWISS-PROT:Q76LV2| Bos taurus Gene_Symbol=HSPCA Heat shock protein HSP 90-alpha	21,28	3	7	14	50
P11499	Heat shock protein HSP 90-beta OS=Mus musculus GN=Hsp90ab1 PE=1 SV=3 - [HS90B_MOUSE]	21,27	2	6	14	45
P12787	Cytochrome c oxidase subunit 5A, mitochondrial OS=Mus musculus GN=Cox5a PE=1 SV=2 - [COX5A_MOUSE]	21,23	1	3	3	13
Q9CR61	NADH dehydrogenase [ubiquinone] 1 beta subcomplex subunit 7 OS=Mus musculus GN=Ndufb7 PE=1 SV=3 - [NDUB7_MOUSE]	21,17	1	2	2	6
Q91VR2	ATP synthase subunit gamma, mitochondrial OS=Mus musculus GN=Atp5c1 PE=1 SV=1 - [ATPG_MOUSE]	21,14	1	6	6	18
Q9CWF2	Tubulin beta-2B chain OS=Mus musculus GN=Tubb2b PE=1 SV=1 - [TBB2B_MOUSE]	21,12	1	1	8	154
Q7TMM9	Tubulin beta-2A chain OS=Mus musculus GN=Tubb2a PE=1 SV=1 - [TBB2A_MOUSE]	21,12	1	1	8	157
Q61316	Heat shock 70 kDa protein 4 OS=Mus musculus GN=Hspa4 PE=1 SV=1 - [HSP74_MOUSE]	21,05	1	13	13	53
Q9R0K7	Plasma membrane calcium-transporting ATPase 2 OS=Mus musculus GN=Atp2b2 PE=1 SV=2 - [AT2B2_MOUSE]	20,95	1	22	22	86
P10639	Thioredoxin OS=Mus musculus GN=Txn PE=1 SV=3 - [THIO_MOUSE]	20,95	2	2	2	7
P68373	Tubulin alpha-1C chain OS=Mus musculus GN=Tuba1c PE=1 SV=1 - [TBA1C_MOUSE]	20,94	7	3	8	63
P60202	Myelin proteolipid protein OS=Mus musculus GN=Plp1 PE=1 SV=2 - [MYPR_MOUSE]	20,94	1	6	6	27
P50518	V-type proton ATPase subunit E 1 OS=Mus musculus GN=Atp6v1e1 PE=1 SV=2 - [VATE1_MOUSE]	20,80	2	6	6	26
Q9D6R2	Isocitrate dehydrogenase [NAD] subunit alpha, mitochondrial OS=Mus musculus GN=Idh3a PE=1 SV=1 - [IDH3A_MOUSE]	20,77	1	8	8	30
Q9Z2I9	Succinyl-CoA ligase [ADP-forming] subunit beta, mitochondrial OS=Mus musculus GN=Sucla2 PE=1 SV=2 - [SUCB1_MOUSE]	20,73	1	9	9	31
P20029	78 kDa glucose-regulated protein OS=Mus musculus GN=Hspa5 PE=1 SV=3 - [GRP78_MOUSE]	20,61	1	8	10	30
Q8BLK3	Limbic system-associated membrane protein OS=Mus musculus GN=Lsamp PE=1 SV=1 - [LSAMP_MOUSE]	20,53	1	6	6	13
O55143	Sarcoplasmic/endoplasmic reticulum calcium ATPase 2 OS=Mus musculus GN=Atp2a2 PE=1 SV=2 - [AT2A2_MOUSE]	20,50	3	17	17	35
O55131	Septin-7 OS=Mus musculus GN=Sept7 PE=1 SV=1 - [SEPT7_MOUSE]	20,41	1	8	8	52
Q60930	Voltage-dependent anion-selective channel protein 2 OS=Mus musculus GN=Vdac2 PE=1 SV=2 - [VDAC2_MOUSE]	20,34	1	5	5	39
Q80UU9	Membrane-associated progesterone receptor component 2 OS=Mus musculus GN=Pgrmc2 PE=1 SV=2 - [PGRC2_MOUSE]	20,28	1	2	2	2
Q9DB20	ATP synthase subunit O, mitochondrial OS=Mus musculus GN=Atp5o PE=1 SV=1 - [ATPO_MOUSE]	20,19	1	5	5	10
P46660	Alpha-internexin OS=Mus musculus GN=Ina PE=1 SV=3 - [AINX_MOUSE]	20,16	4	9	12	26
P14094	Sodium/potassium-transporting ATPase subunit beta-1 OS=Mus musculus GN=Atp1b1 PE=1 SV=1 - [AT1B1_MOUSE]	20,07	1	5	5	53
P63216	Guanine nucleotide-binding protein G(I)/G(S)/G(O) subunit gamma-3 OS=Mus musculus GN=Gng3 PE=1 SV=1 - [GBG3_MOUSE]	20,00	1	1	1	7
Q9JJV2	Profilin-2 OS=Mus musculus GN=Pfn2 PE=1 SV=3 - [PROF2_MOUSE]	20,00	1	2	2	14
Q9CWS0	N(G),N(G)-dimethylarginine dimethylaminohydrolase 1 OS=Mus musculus GN=Ddah1 PE=1 SV=3 - [DDAH1_MOUSE]	20,00	1	5	5	8
P50153	Guanine nucleotide-binding protein G(I)/G(S)/G(O) subunit gamma-4 OS=Mus musculus GN=Gng4 PE=2 SV=1 - [GBG4_MOUSE]	20,00	1	1	1	1
Q7TQI3	Ubiquitin thioesterase OTUB1 OS=Mus musculus GN=Otub1 PE=1 SV=2 - [OTUB1_MOUSE]	19,93	1	4	4	12
P52503	NADH dehydrogenase [ubiquinone] iron-sulfur protein 6, mitochondrial OS=Mus musculus GN=Ndufs6 PE=1 SV=2 - [NDUS6_MOUSE]	19,83	1	2	2	2
P28663	Beta-soluble NSF attachment protein OS=Mus musculus GN=Napb PE=1 SV=2 - [SNAB_MOUSE]	19,80	1	5	5	29
P63248	cAMP-dependent protein kinase inhibitor alpha OS=Mus musculus GN=Pkia PE=1 SV=2 - [IPKA_MOUSE]	19,74	1	1	1	1
Q9WTX5	S-phase kinase-associated protein 1 OS=Mus musculus GN=Skp1 PE=1 SV=3 - [SKP1_MOUSE]	19,63	1	3	3	9
Q9Z239	Phospholemman OS=Mus musculus GN=Fxyd1 PE=1 SV=1 - [PLM_MOUSE]	19,57	1	2	2	3
P08752	Guanine nucleotide-binding protein G(i) subunit alpha-2 OS=Mus musculus GN=Gnai2 PE=1 SV=5 - [GNAI2_MOUSE]	19,44	4	3	6	15
P03930	ATP synthase protein 8 OS=Mus musculus GN=Mtatp8 PE=1 SV=1 - [ATP8_MOUSE]	19,40	1	1	1	3
Q9D6F9	Tubulin beta-4A chain OS=Mus musculus GN=Tubb4a PE=1 SV=3 - [TBB4A_MOUSE]	19,37	1	2	7	108

Accession	Description	Σ Cover.	Σ# Prot.	Σ# Unique Pept.	Σ# Pept.	Σ# PSM
Q91VW3	SH3 domain-binding glutamic acid-rich-like protein 3 OS=Mus musculus GN=Sh3bgrl3 PE=1 SV=1 - [SH3L3_MOUSE]	19,35	1	2	2	3
P53994	Ras-related protein Rab-2A OS=Mus musculus GN=Rab2a PE=1 SV=1 - [RAB2A_MOUSE]	19,34	2	3	3	6
Q3UHX2	28 kDa heat- and acid-stable phosphoprotein OS=Mus musculus GN=Pdap1 PE=1 SV=1 - [HAP28_MOUSE]	19,34	1	2	2	5
P61028	Ras-related protein Rab-8B OS=Mus musculus GN=Rab8b PE=1 SV=1 - [RAB8B_MOUSE]	19,32	13	1	4	6
P39053	Dynamin-1 OS=Mus musculus GN=Dnm1 PE=1 SV=2 - [DYN1_MOUSE]	19,26	2	13	15	49
P62874	Guanine nucleotide-binding protein G(I)/G(S)/G(T) subunit beta-1 OS=Mus musculus GN=Gnb1 PE=1 SV=3 - [GBB1_MOUSE]	19,12	3	4	6	23
Q91V41	Ras-related protein Rab-14 OS=Mus musculus GN=Rab14 PE=1 SV=3 - [RAB14_MOUSE]	19,07	11	3	4	9
Q56A07	Sodium channel subunit beta-2 OS=Mus musculus GN=Scn2b PE=1 SV=1 - [SCN2B_MOUSE]	19,07	1	3	3	18
Q99LX0	Protein DJ-1 OS=Mus musculus GN=Park7 PE=1 SV=1 - [PARK7_MOUSE]	19,05	1	3	3	8
P0C913	Overexpressed in colon carcinoma 1 protein homolog OS=Mus musculus PE=3 SV=1 - [OCC1_MOUSE]	19,05	1	1	1	1
Q8BGD8	Cytochrome c oxidase assembly factor 6 homolog OS=Mus musculus GN=Coa6 PE=1 SV=1 - [COA6_MOUSE]	18,99	1	1	1	1
Q9JLR9	HIG1 domain family member 1A, mitochondrial OS=Mus musculus GN=Higd1a PE=2 SV=1 - [HIG1A_MOUSE]	18,95	1	1	1	3
Q9CQN3	Mitochondrial import receptor subunit TOM6 homolog OS=Mus musculus GN=Tomm6 PE=3 SV=1 - [TOM6_MOUSE]	18,92	1	1	1	4
P47754	F-actin-capping protein subunit alpha-2 OS=Mus musculus GN=Capza2 PE=1 SV=3 - [CAZA2_MOUSE]	18,88	1	3	3	9
Q9R0P5	Destrin OS=Mus musculus GN=Dstn PE=1 SV=3 - [DEST_MOUSE]	18,79	2	3	3	5
P67778	Prohibitin OS=Mus musculus GN=Phb PE=1 SV=1 - [PHB_MOUSE]	18,75	1	5	5	13
Q91V61	Sideroflexin-3 OS=Mus musculus GN=Sfxn3 PE=1 SV=1 - [SFXN3_MOUSE]	18,69	1	4	4	16
CON_006941072	SWISS-PROT:P02584 Bos taurus Profilin-1	18,57	2	2	2	4
P03903	NADH-ubiquinone oxidoreductase chain 4L OS=Mus musculus GN=Mtnd4l PE=3 SV=1 - [NU4LM_MOUSE]	18,56	1	1	1	2
Q62261	Spectrin beta chain, non-erythrocytic 1 OS=Mus musculus GN=Sptbn1 PE=1 SV=2 - [SPTB2_MOUSE]	18,45	2	36	36	127
Q9CPQ8	ATP synthase subunit g, mitochondrial OS=Mus musculus GN=Atp5l PE=1 SV=1 - [ATP5L_MOUSE]	18,45	1	1	1	3
P68372	Tubulin beta-4B chain OS=Mus musculus GN=Tubb4b PE=1 SV=1 - [TBB4B_MOUSE]	18,43	1	1	7	150
P12960	Contactin-1 OS=Mus musculus GN=Cntn1 PE=1 SV=1 - [CNTN1_MOUSE]	18,43	2	14	14	57
O08709	Peroxiredoxin-6 OS=Mus musculus GN=Prdx6 PE=1 SV=3 - [PRDX6_MOUSE]	18,30	1	3	3	16
Q9D6J5	NADH dehydrogenase [ubiquinone] 1 beta subcomplex subunit 8, mitochondrial OS=Mus musculus GN=Ndufb8 PE=1 SV=1 - [NDUB8_MOUSE]	18,28	1	2	2	3
P84075	Neuron-specific calcium-binding protein hippocalcin OS=Mus musculus GN=Hpca PE=1 SV=2 - [HPCA_MOUSE]	18,13	2	2	3	11
P54227	Stathmin OS=Mus musculus GN=Stmn1 PE=1 SV=2 - [STMN1_MOUSE]	18,12	2	3	3	6
Q9ERS2	NADH dehydrogenase [ubiquinone] 1 alpha subcomplex subunit 13 OS=Mus musculus GN=Ndufa13 PE=1 SV=3 - [NDUAD_MOUSE]	18,06	1	2	2	14
Q9DCX2	ATP synthase subunit d, mitochondrial OS=Mus musculus GN=Atp5h PE=1 SV=3 - [ATP5H_MOUSE]	18,01	1	3	3	23
P60761	Neurogranin OS=Mus musculus GN=Nrgn PE=1 SV=1 - [NEUG_MOUSE]	17,95	1	1	1	10
Q7TMF3	NADH dehydrogenase [ubiquinone] 1 alpha subcomplex subunit 12 OS=Mus musculus GN=Ndufa12 PE=1 SV=2 - [NDUAC_MOUSE]	17,93	1	2	2	5
Q8VDQ8	NAD-dependent protein deacetylase sirtuin-2 OS=Mus musculus GN=Sirt2 PE=1 SV=2 - [SIR2_MOUSE]	17,74	1	6	6	20
P47757	F-actin-capping protein subunit beta OS=Mus musculus GN=Capzb PE=1 SV=3 - [CAPZB_MOUSE]	17,69	1	4	4	16
P43006	Excitatory amino acid transporter 2 OS=Mus musculus GN=Slc1a2 PE=1 SV=1 - [EAA2_MOUSE]	17,66	1	9	9	119
P35700	Peroxiredoxin-1 OS=Mus musculus GN=Prdx1 PE=1 SV=1 - [PRDX1_MOUSE]	17,59	1	3	3	6
O35685	Nuclear migration protein nudC OS=Mus musculus GN=Nudc PE=1 SV=1 - [NUDC_MOUSE]	17,47	1	5	5	6
P70441	Na(+)/H(+) exchange regulatory cofactor NHE-RF1 OS=Mus musculus GN=Slc9a3r1 PE=1 SV=3 - [NHRF1_MOUSE]	17,46	1	5	5	11
P70349	Histidine triad nucleotide-binding protein 1 OS=Mus musculus GN=Hint1 PE=1 SV=3 - [HINT1_MOUSE]	17,46	1	2	2	4
P12961	Neuroendocrine protein 7B2 OS=Mus musculus GN=Scg5 PE=1 SV=1 - [7B2_MOUSE]	17,45	1	2	2	3
Q9D3D9	ATP synthase subunit delta, mitochondrial OS=Mus musculus GN=Atp5d PE=1 SV=1 - [ATPD_MOUSE]	17,26	2	3	3	19
Q9EPJ9	ADP-ribosylation factor GTPase-activating protein 1 OS=Mus musculus GN=Arfgap1 PE=1 SV=2 - [ARFG1_MOUSE]	17,15	1	5	5	13
P17751	Triosephosphate isomerase OS=Mus musculus GN=Tpi1 PE=1 SV=4 - [TPIS_MOUSE]	17,06	2	4	4	30
Q9DCS9	NADH dehydrogenase [ubiquinone] 1 beta subcomplex subunit 10 OS=Mus musculus GN=Ndufb10 PE=1 SV=3 - [NDUBA_MOUSE]	17,05	1	3	3	5
P84091	AP-2 complex subunit mu OS=Mus musculus GN=Ap2m1 PE=1 SV=1 - [AP2M1_MOUSE]	17,01	1	7	7	24
Q9QYG0	Protein NDRG2 OS=Mus musculus GN=Ndrg2 PE=1 SV=1 - [NDRG2_MOUSE]	16,98	1	4	4	11
Q91VD9	NADH-ubiquinone oxidoreductase 75 kDa subunit, mitochondrial OS=Mus musculus GN=Ndufs1 PE=1 SV=2 - [NDUS1_MOUSE]	16,92	1	9	9	30
Q61598	Rab GDP dissociation inhibitor beta OS=Mus musculus GN=Gdi2 PE=1 SV=1 - [GDIB_MOUSE]	16,85	1	4	7	19
P99028	Cytochrome b-c1 complex subunit 6, mitochondrial OS=Mus musculus GN=Uqcrh PE=1 SV=2 - [QCR6_MOUSE]	16,85	1	1	1	1
P62075	Mitochondrial import inner membrane translocase subunit Tim13 OS=Mus musculus GN=Timm13 PE=1 SV=1 - [TIM13_MOUSE]	16,84	1	1	1	3
Q9WV92	Band 4.1-like protein 3 OS=Mus musculus GN=Epb41l3 PE=1 SV=1 - [E41L3_MOUSE]	16,68	2	9	11	34
P63323	40S ribosomal protein S12 OS=Mus musculus GN=Rps12 PE=1 SV=2 - [RS12_MOUSE]	16,67	1	1	1	1
P62878	E3 ubiquitin-protein ligase RBX1 OS=Mus musculus GN=Rbx1 PE=1 SV=1 - [RBX1_MOUSE]	16,67	1	1	1	3
Q5PR73	GTP-binding protein Di-Ras2 OS=Mus musculus GN=Diras2 PE=2 SV=1 - [DIRA2_MOUSE]	16,58	2	3	3	7
P06151	L-lactate dehydrogenase A chain OS=Mus musculus GN=Ldha PE=1 SV=3 - [LDHA_MOUSE]	16,57	3	4	5	18
Q8K021	Secretory carrier-associated membrane protein 1 OS=Mus musculus GN=Scamp1 PE=1 SV=1 - [SCAM1_MOUSE]	16,57	1	4	4	14
P50516	V-type proton ATPase catalytic subunit A OS=Mus musculus GN=Atp6v1a PE=1 SV=2 - [VATA_MOUSE]	16,53	1	9	9	21
CON_Trypsin	SWISS-PROT:P00761 TRYP_PIG Trypsin - Sus scrofa Pig	16,45	1	3	3	22
P84086	Complexin-2 OS=Mus musculus GN=Cplx2 PE=1 SV=1 - [CPLX2_MOUSE]	16,42	2	2	3	8

Accession	Description	Σ Cover.	Σ# Prot.	Σ# Unique Pept.	Σ# Pept.	Σ# PSM
Q61792	LIM and SH3 domain protein 1 OS=Mus musculus GN=Lasp1 PE=1 SV=1 - [LASP1_MOUSE]	16,35	1	4	4	9
Q9QYC0	Alpha-adducin OS=Mus musculus GN=Add1 PE=1 SV=2 - [ADDA_MOUSE]	16,33	1	9	9	30
Q60931	Voltage-dependent anion-selective channel protein 3 OS=Mus musculus GN=Vdac3 PE=1 SV=1 - [VDAC3_MOUSE]	16,25	1	4	4	19
P59648	FXYD domain-containing ion transport regulator 7 OS=Mus musculus GN=Fxyd7 PE=1 SV=1 - [FXYD7_MOUSE]	16,25	1	1	1	4
Q9D172	ES1 protein homolog, mitochondrial OS=Mus musculus GN=D10Jhu81e PE=1 SV=1 - [ES1_MOUSE]	16,17	1	4	4	8
Q8R191	Synaptogyrin-3 OS=Mus musculus GN=Syngr3 PE=1 SV=1 - [SNG3_MOUSE]	16,16	1	3	3	21
O70439	Syntaxin-7 OS=Mus musculus GN=Stx7 PE=1 SV=3 - [STX7_MOUSE]	16,09	1	3	3	11
P05202	Aspartate aminotransferase, mitochondrial OS=Mus musculus GN=Got2 PE=1 SV=1 - [AATM_MOUSE]	16,05	1	7	7	44
Q8K386	Ras-related protein Rab-15 OS=Mus musculus GN=Rab15 PE=1 SV=1 - [RAB15_MOUSE]	16,04	11	2	3	7
Q9R0Y5	Adenylate kinase isoenzyme 1 OS=Mus musculus GN=Ak1 PE=1 SV=1 - [KAD1_MOUSE]	15,98	1	3	3	6
Q9CYZ2	Tumor protein D54 OS=Mus musculus GN=Tpd52l2 PE=1 SV=1 - [TPD54_MOUSE]	15,91	1	3	3	8
Q3UHL1	CaM kinase-like vesicle-associated protein OS=Mus musculus GN=Camkv PE=1 SV=2 - [CAMKV_MOUSE]	15,82	1	8	8	16
P57746	V-type proton ATPase subunit D OS=Mus musculus GN=Atp6v1d PE=1 SV=1 - [VATD_MOUSE]	15,79	1	3	3	9
Q9CQX2	Cytochrome b5 type B OS=Mus musculus GN=Cyb5b PE=1 SV=1 - [CYB5B_MOUSE]	15,75	1	2	2	6
P23819	Glutamate receptor 2 OS=Mus musculus GN=Gria2 PE=1 SV=3 - [GRIA2_MOUSE]	15,74	1	8	12	30
P56395	Cytochrome b5 OS=Mus musculus GN=Cyb5a PE=1 SV=2 - [CYB5_MOUSE]	15,67	1	1	1	1
Q9ERD7	Tubulin beta-3 chain OS=Mus musculus GN=Tubb3 PE=1 SV=1 - [TBB3_MOUSE]	15,56	4	2	6	58
P28652	Calcium/calmodulin-dependent protein kinase type II subunit beta OS=Mus musculus GN=Camk2b PE=1 SV=1 - [KCC2B_MOUSE]	15,50	1	5	6	28
Q6PHN9	Ras-related protein Rab-35 OS=Mus musculus GN=Rab35 PE=1 SV=1 - [RAB35_MOUSE]	15,42	11	2	3	7
Q3UNH4	G protein-regulated inducer of neurite outgrowth 1 OS=Mus musculus GN=Gprin1 PE=1 SV=2 - [GRIN1_MOUSE]	15,34	1	12	12	22
Q6IRU5	Clathrin light chain B OS=Mus musculus GN=Cltb PE=2 SV=1 - [CLCB_MOUSE]	15,28	1	4	4	7
Q8BLQ9	Cell adhesion molecule 2 OS=Mus musculus GN=Cadm2 PE=1 SV=2 - [CADM2_MOUSE]	15,17	1	4	4	15
P99024	Tubulin beta-5 chain OS=Mus musculus GN=Tubb5 PE=1 SV=1 - [TBB5_MOUSE]	15,09	1	1	6	147
P08553	Neurofilament medium polypeptide OS=Mus musculus GN=Nefm PE=1 SV=4 - [NFM_MOUSE]	15,09	4	8	11	33
Q9R1Q8	Transgelin-3 OS=Mus musculus GN=Tagln3 PE=1 SV=1 - [TAGL3_MOUSE]	15,08	1	3	3	11
Q62420	Endophilin-A1 OS=Mus musculus GN=Sh3gl2 PE=1 SV=2 - [SH3G2_MOUSE]	15,06	2	5	5	27
O35129	Prohibitin-2 OS=Mus musculus GN=Phb2 PE=1 SV=1 - [PHB2_MOUSE]	15,05	1	5	5	16
Q9Z2I0	LETM1 and EF-hand domain-containing protein 1, mitochondrial OS=Mus musculus GN=Letm1 PE=2 SV=1 - [LETM1_MOUSE]	15,04	1	9	9	21
P62880	Guanine nucleotide-binding protein G(I)/G(S)/G(T) subunit beta-2 OS=Mus musculus GN=Gnb2 PE=1 SV=3 - [GBB2_MOUSE]	15,00	2	2	4	19
D3Z7P3	Glutaminase kidney isoform, mitochondrial OS=Mus musculus GN=Gls PE=1 SV=1 - [GLSK_MOUSE]	14,99	1	6	6	31
Q8BR63	Protein FAM177A1 OS=Mus musculus GN=Fam177a1 PE=2 SV=1 - [F177A_MOUSE]	14,98	1	2	2	3
Q76MZ3	Serine/threonine-protein phosphatase 2A 65 kDa regulatory subunit A alpha isoform OS=Mus musculus GN=Ppp2r1a PE=1 SV=3 - [2AAA_MOUSE]	14,94	2	9	9	30
Q62188	Dihydropyrimidinase-related protein 3 OS=Mus musculus GN=Dpysl3 PE=1 SV=1 - [DPYL3_MOUSE]	14,91	1	4	7	37
Q8BGD9	Eukaryotic translation initiation factor 4B OS=Mus musculus GN=Eif4b PE=1 SV=1 - [IF4B_MOUSE]	14,89	1	6	6	13
P27773	Protein disulfide-isomerase A3 OS=Mus musculus GN=Pdia3 PE=1 SV=2 - [PDIA3_MOUSE]	14,85	1	6	6	18
Q80YN3	Breast carcinoma-amplified sequence 1 homolog OS=Mus musculus GN=Bcas1 PE=1 SV=3 - [BCAS1_MOUSE]	14,85	1	7	7	24
P62492	Ras-related protein Rab-11A OS=Mus musculus GN=Rab11a PE=1 SV=3 - [RB11A_MOUSE]	14,81	2	3	3	9
P01831	Thy-1 membrane glycoprotein OS=Mus musculus GN=Thy1 PE=1 SV=1 - [THY1_MOUSE]	14,81	1	2	2	9
Q80SZ7	Guanine nucleotide-binding protein G(I)/G(S)/G(O) subunit gamma-5 OS=Mus musculus GN=Gng5 PE=2 SV=2 - [GBG5_MOUSE]	14,71	1	1	1	1
Q99LC5	Electron transfer flavoprotein subunit alpha, mitochondrial OS=Mus musculus GN=Etfa PE=1 SV=2 - [ETFA_MOUSE]	14,71	1	4	4	9
Q9DC51	Guanine nucleotide-binding protein G(k) subunit alpha OS=Mus musculus GN=Gnai3 PE=1 SV=3 - [GNAI3_MOUSE]	14,69	4	2	5	12
P97300	Neuroplastin OS=Mus musculus GN=Nptn PE=1 SV=3 - [NPTN_MOUSE]	14,61	1	6	6	31
P60764	Ras-related C3 botulinum toxin substrate 3 OS=Mus musculus GN=Rac3 PE=1 SV=1 - [RAC3_MOUSE]	14,58	6	2	3	10
O55100	Synaptogyrin-1 OS=Mus musculus GN=Syngr1 PE=1 SV=2 - [SNG1_MOUSE]	14,53	1	3	3	20
P97427	Dihydropyrimidinase-related protein 1 OS=Mus musculus GN=Crmp1 PE=1 SV=1 - [DPYL1_MOUSE]	14,51	1	4	7	38
Q60634	Flotillin-2 OS=Mus musculus GN=Flot2 PE=1 SV=2 - [FLOT2_MOUSE]	14,49	1	6	6	10
P62073	Mitochondrial import inner membrane translocase subunit Tim10 OS=Mus musculus GN=Timm10 PE=1 SV=1 - [TIM10_MOUSE]	14,44	1	1	1	7
Q9CWZ7	Gamma-soluble NSF attachment protein OS=Mus musculus GN=Napg PE=1 SV=1 - [SNAG_MOUSE]	14,42	1	5	5	10
P35282	Ras-related protein Rab-21 OS=Mus musculus GN=Rab21 PE=1 SV=4 - [RAB21_MOUSE]	14,41	1	2	2	4
CON_0082 48621	Bos taurus Gene_Symbol=LOC785421 similar to ADP-ribosylation factor 1 isoform 1	14,36	5	1	2	12
Q8BIF0	CD99 antigen-like protein 2 OS=Mus musculus GN=Cd99l2 PE=1 SV=1 - [C99L2_MOUSE]	14,35	1	2	2	5
Q8VEM8	Phosphate carrier protein, mitochondrial OS=Mus musculus GN=Slc25a3 PE=1 SV=1 - [MPCP_MOUSE]	14,29	1	6	6	16
Q8BVE3	V-type proton ATPase subunit H OS=Mus musculus GN=Atp6v1h PE=1 SV=1 - [VATH_MOUSE]	14,29	1	5	5	14
P17665	Cytochrome c oxidase subunit 7C, mitochondrial OS=Mus musculus GN=Cox7c PE=1 SV=1 - [COX7C_MOUSE]	14,29	1	1	1	3
Q9DC70	NADH dehydrogenase [ubiquinone] iron-sulfur protein 7, mitochondrial OS=Mus musculus GN=Ndufs7 PE=1 SV=1 - [NDUS7_MOUSE]	14,29	1	3	3	11
Q3UZP4	Small VCP/p97-interacting protein OS=Mus musculus GN=Svip PE=2 SV=1 - [SVIP_MOUSE]	14,29	1	1	1	1
P15105	Glutamine synthetase OS=Mus musculus GN=Glul PE=1 SV=6 - [GLNA_MOUSE]	14,21	1	6	6	25
Q8BVI4	Dihydropteridine reductase OS=Mus musculus GN=Qdpr PE=1 SV=2 - [DHPR_MOUSE]	14,11	1	2	2	10
P13595	Neural cell adhesion molecule 1 OS=Mus musculus GN=Ncam1 PE=1 SV=3 - [NCAM1_MOUSE]	14,08	1	8	13	87
Q9Z1Z2	Serine-threonine kinase receptor-associated protein OS=Mus musculus GN=Strap PE=1 SV=2 - [STRAP_MOUSE]	14,00	1	3	3	8

Accession	Description	Σ Cover.	Σ# Prot.	Σ# Unique Pept.	Σ# Pept.	Σ# PSM
Q68FD5	Clathrin heavy chain 1 OS=Mus musculus GN=Cltc PE=1 SV=3 - [CLH1_MOUSE]	13,97	1	19	19	67
Q9D6M3	Mitochondrial glutamate carrier 1 OS=Mus musculus GN=Slc25a22 PE=1 SV=1 - [GHC1_MOUSE]	13,93	2	4	4	16
Q60829	Protein phosphatase 1 regulatory subunit 1B OS=Mus musculus GN=Ppp1r1b PE=2 SV=2 - [PPR1B_MOUSE]	13,92	1	2	2	3
Q01853	Transitional endoplasmic reticulum ATPase OS=Mus musculus GN=Vcp PE=1 SV=4 - [TERA_MOUSE]	13,90	1	7	7	22
CON_0069 97002	SWISS-PROT:Q5E9F7| Bos taurus Gene_Symbol=CFL1 Cofilin-1	13,86	3	2	2	9
P56565	Protein S100-A1 OS=Mus musculus GN=S100a1 PE=1 SV=2 - [S10A1_MOUSE]	13,83	1	1	1	4
CON_0090 39634	Bos taurus Gene_Symbol=UBE2N Ubiquitin carrier protein	13,82	2	2	2	8
Q80TL4	Protein KIAA1045 OS=Mus musculus GN=Kiaa1045 PE=1 SV=2 - [K1045_MOUSE]	13,75	1	6	6	20
P17156	Heat shock-related 70 kDa protein 2 OS=Mus musculus GN=Hspa2 PE=1 SV=2 - [HSP72_MOUSE]	13,74	2	1	8	20
B1AXP6	Mitochondrial import receptor subunit TOM5 homolog OS=Mus musculus GN=Tomm5 PE=3 SV=1 - [TOM5_MOUSE]	13,73	1	1	1	1
Q91VM9	Inorganic pyrophosphatase 2, mitochondrial OS=Mus musculus GN=Ppa2 PE=2 SV=1 - [IPYR2_MOUSE]	13,64	1	3	3	9
O08585	Clathrin light chain A OS=Mus musculus GN=Clta PE=1 SV=2 - [CLCA_MOUSE]	13,62	1	4	4	11
Q91YT0	NADH dehydrogenase [ubiquinone] flavoprotein 1, mitochondrial OS=Mus musculus GN=Ndufv1 PE=1 SV=1 - [NDUV1_MOUSE]	13,58	1	6	6	15
P10852	4F2 cell-surface antigen heavy chain OS=Mus musculus GN=Slc3a2 PE=1 SV=1 - [4F2_MOUSE]	13,50	1	7	7	29
Q9DCR2	AP-3 complex subunit sigma-1 OS=Mus musculus GN=Ap3s1 PE=1 SV=2 - [AP3S1_MOUSE]	13,47	1	2	2	2
P97807	Fumarate hydratase, mitochondrial OS=Mus musculus GN=Fh PE=1 SV=3 - [FUMH_MOUSE]	13,41	2	5	5	15
P21279	Guanine nucleotide-binding protein G(q) subunit alpha OS=Mus musculus GN=Gnaq PE=1 SV=4 - [GNAQ_MOUSE]	13,37	4	3	4	12
P62897	Cytochrome c, somatic OS=Mus musculus GN=Cycs PE=1 SV=2 - [CYC_MOUSE]	13,33	1	1	1	2
P99029	Peroxiredoxin-5, mitochondrial OS=Mus musculus GN=Prdx5 PE=1 SV=2 - [PRDX5_MOUSE]	13,33	1	2	2	5
Q61753	D-3-phosphoglycerate dehydrogenase OS=Mus musculus GN=Phgdh PE=1 SV=3 - [SERA_MOUSE]	13,32	1	6	6	12
P62814	V-type proton ATPase subunit B, brain isoform OS=Mus musculus GN=Atp6v1b2 PE=1 SV=1 - [VATB2_MOUSE]	13,31	1	7	7	35
Q9CQQ7	ATP synthase subunit b, mitochondrial OS=Mus musculus GN=Atp5f1 PE=1 SV=1 - [AT5F1_MOUSE]	13,28	1	4	4	25
P00405	Cytochrome c oxidase subunit 2 OS=Mus musculus GN=Mtco2 PE=1 SV=1 - [COX2_MOUSE]	13,22	1	3	3	18
Q9D328	Transmembrane protein 35 OS=Mus musculus GN=Tmem35 PE=2 SV=1 - [TMM35_MOUSE]	13,17	1	2	2	9
Q8BH59	Calcium-binding mitochondrial carrier protein Aralar1 OS=Mus musculus GN=Slc25a12 PE=1 SV=1 - [CMC1_MOUSE]	13,15	2	8	8	19
P02798	Metallothionein-2 OS=Mus musculus GN=Mt2 PE=1 SV=2 - [MT2_MOUSE]	13,11	1	1	1	1
P14231	Sodium/potassium-transporting ATPase subunit beta-2 OS=Mus musculus GN=Atp1b2 PE=1 SV=2 - [AT1B2_MOUSE]	13,10	1	3	3	9
P51150	Ras-related protein Rab-7a OS=Mus musculus GN=Rab7a PE=1 SV=2 - [RAB7A_MOUSE]	13,04	1	2	2	5
P03899	NADH-ubiquinone oxidoreductase chain 3 OS=Mus musculus GN=Mtnd3 PE=3 SV=3 - [NU3M_MOUSE]	13,04	1	1	1	4
Q61885	Myelin-oligodendrocyte glycoprotein OS=Mus musculus GN=Mog PE=1 SV=1 - [MOG_MOUSE]	13,01	1	3	3	18
CON_0069 85893	SWISS-PROT:Q3SZ62| Bos taurus Gene_Symbol=PGAM1 Phosphoglycerate mutase 1	12,99	3	3	3	10
P08228	Superoxide dismutase [Cu-Zn] OS=Mus musculus GN=Sod1 PE=1 SV=2 - [SODC_MOUSE]	12,99	1	2	2	13
Q9D8W7	OCIA domain-containing protein 2 OS=Mus musculus GN=Ociad2 PE=2 SV=1 - [OCAD2_MOUSE]	12,99	1	2	2	2
P10637	Microtubule-associated protein tau OS=Mus musculus GN=Mapt PE=1 SV=3 - [TAU_MOUSE]	12,96	1	7	7	34
P48453	Serine/threonine-protein phosphatase 2B catalytic subunit beta isoform OS=Mus musculus GN=Ppp3cb PE=2 SV=2 - [PP2BB_MOUSE]	12,95	2	3	6	9
P35486	Pyruvate dehydrogenase E1 component subunit alpha, somatic form, mitochondrial OS=Mus musculus GN=Pdha1 PE=1 SV=1 - [ODPA_MOUSE]	12,82	2	5	5	23
Q9DB77	Cytochrome b-c1 complex subunit 2, mitochondrial OS=Mus musculus GN=Uqcrc2 PE=1 SV=1 - [QCR2_MOUSE]	12,80	1	4	4	18
P56391	Cytochrome c oxidase subunit 6B1 OS=Mus musculus GN=Cox6b1 PE=1 SV=2 - [CX6B1_MOUSE]	12,79	1	1	1	3
P11404	Fatty acid-binding protein, heart OS=Mus musculus GN=Fabp3 PE=1 SV=5 - [FABPH_MOUSE]	12,78	1	2	2	2
O08749	Dihydrolipoyl dehydrogenase, mitochondrial OS=Mus musculus GN=Dld PE=1 SV=2 - [DLDH_MOUSE]	12,77	1	6	6	21
P14211	Calreticulin OS=Mus musculus GN=Calr PE=1 SV=1 - [CALR_MOUSE]	12,74	1	4	4	8
Q8K3J1	NADH dehydrogenase [ubiquinone] iron-sulfur protein 8, mitochondrial OS=Mus musculus GN=Ndufs8 PE=1 SV=1 - [NDUS8_MOUSE]	12,74	1	2	2	13
Q8K0T0	Reticulon-1 OS=Mus musculus GN=Rtn1 PE=1 SV=1 - [RTN1_MOUSE]	12,69	1	6	7	14
P26350	Prothymosin alpha OS=Mus musculus GN=Ptma PE=1 SV=2 - [PTMA_MOUSE]	12,61	1	1	1	1
Q9D051	Pyruvate dehydrogenase E1 component subunit beta, mitochondrial OS=Mus musculus GN=Pdhb PE=1 SV=1 - [ODPB_MOUSE]	12,53	1	4	4	15
P56212	cAMP-regulated phosphoprotein 19 OS=Mus musculus GN=Arpp19 PE=1 SV=2 - [ARP19_MOUSE]	12,50	1	1	1	1
Q80XI4	Phosphatidylinositol 5-phosphate 4-kinase type-2 beta OS=Mus musculus GN=Pip4k2b PE=1 SV=1 - [PI42B_MOUSE]	12,50	1	4	4	7
Q9DBG3	AP-2 complex subunit beta OS=Mus musculus GN=Ap2b1 PE=1 SV=1 - [AP2B1_MOUSE]	12,49	1	4	11	23
Q80SW1	Putative adenosylhomocysteinase 2 OS=Mus musculus GN=Ahcyl1 PE=1 SV=1 - [SAHH2_MOUSE]	12,45	2	3	6	12
P61161	Actin-related protein 2 OS=Mus musculus GN=Actr2 PE=1 SV=1 - [ARP2_MOUSE]	12,44	1	5	5	13
B2RSH2	Guanine nucleotide-binding protein G(i) subunit alpha-1 OS=Mus musculus GN=Gnai1 PE=2 SV=1 - [GNAI1_MOUSE]	12,43	4	1	4	11
P48024	Eukaryotic translation initiation factor 1 OS=Mus musculus GN=Eif1 PE=2 SV=2 - [EIF1_MOUSE]	12,39	2	1	1	1
Q8BKX1	Brain-specific angiogenesis inhibitor 1-associated protein 2 OS=Mus musculus GN=Baiap2 PE=1 SV=2 - [BAIP2_MOUSE]	12,34	1	6	6	11
P62715	Serine/threonine-protein phosphatase 2A catalytic subunit beta isoform OS=Mus musculus GN=Ppp2cb PE=1 SV=1 - [PP2AB_MOUSE]	12,30	2	3	3	9
Q9DCZ4	Apolipoprotein O OS=Mus musculus GN=Apoo PE=2 SV=1 - [APOO_MOUSE]	12,26	1	2	2	6

Accession	Description	Σ Cover.	Σ# Prot.	Σ# Unique Pept.	Σ# Pept.	Σ# PSM
Q91VC7	Protein phosphatase 1 regulatory subunit 14A OS=Mus musculus GN=Ppp1r14a PE=2 SV=1 - [PP14A_MOUSE]	12,24	1	1	1	1
P61164	Alpha-centractin OS=Mus musculus GN=Actr1a PE=2 SV=1 - [ACTZ_MOUSE]	12,23	2	4	4	8
P08113	Endoplasmin OS=Mus musculus GN=Hsp90b1 PE=1 SV=2 - [ENPL_MOUSE]	12,22	1	6	7	28
D3YVF0	A-kinase anchor protein 5 OS=Mus musculus GN=Akap5 PE=2 SV=2 - [AKAP5_MOUSE]	12,21	1	2	2	3
P63005	Platelet-activating factor acetylhydrolase IB subunit alpha OS=Mus musculus GN=Pafah1b1 PE=1 SV=2 - [LIS1_MOUSE]	12,20	1	4	4	12
P35564	Calnexin OS=Mus musculus GN=Canx PE=1 SV=1 - [CALX_MOUSE]	12,18	1	8	8	19
Q9QUR7	Peptidyl-prolyl cis-trans isomerase NIMA-interacting 1 OS=Mus musculus GN=Pin1 PE=1 SV=1 - [PIN1_MOUSE]	12,12	1	1	1	1
P63328	Serine/threonine-protein phosphatase 2B catalytic subunit alpha isoform OS=Mus musculus GN=Ppp3ca PE=1 SV=1 - [PP2BA_MOUSE]	12,09	2	3	6	12
Q0VBF8	Uncharacterized membrane protein C1orf95 homolog OS=Mus musculus PE=2 SV=1 - [CA095_MOUSE]	12,06	1	1	1	1
P48771	Cytochrome c oxidase subunit 7A2, mitochondrial OS=Mus musculus GN=Cox7a2 PE=1 SV=2 - [CX7A2_MOUSE]	12,05	1	1	1	4
P40124	Adenylyl cyclase-associated protein 1 OS=Mus musculus GN=Cap1 PE=1 SV=4 - [CAP1_MOUSE]	12,03	2	5	5	10
Q8R1B5	Complexin-3 OS=Mus musculus GN=Cplx3 PE=1 SV=1 - [CPLX3_MOUSE]	12,03	1	1	1	1
Q9CXZ1	NADH dehydrogenase [ubiquinone] iron-sulfur protein 4, mitochondrial OS=Mus musculus GN=Ndufs4 PE=1 SV=3 - [NDUS4_MOUSE]	12,00	1	2	2	6
Q91VR8	Protein BRICK1 OS=Mus musculus GN=Brk1 PE=2 SV=1 - [BRK1_MOUSE]	12,00	1	1	1	1
Q62418	Drebrin-like protein OS=Mus musculus GN=Dbnl PE=1 SV=2 - [DBNL_MOUSE]	11,93	1	4	4	9
P21107	Tropomyosin alpha-3 chain OS=Mus musculus GN=Tpm3 PE=1 SV=3 - [TPM3_MOUSE]	11,93	6	1	4	9
O54901	OX-2 membrane glycoprotein OS=Mus musculus GN=Cd200 PE=1 SV=1 - [OX2G_MOUSE]	11,87	1	3	3	5
P35762	CD81 antigen OS=Mus musculus GN=Cd81 PE=1 SV=2 - [CD81_MOUSE]	11,86	1	2	2	9
Q9CZU6	Citrate synthase, mitochondrial OS=Mus musculus GN=Cs PE=1 SV=1 - [CISY_MOUSE]	11,85	1	5	5	29
P52760	Ribonuclease UK114 OS=Mus musculus GN=Hrsp12 PE=1 SV=3 - [UK114_MOUSE]	11,85	1	1	1	1
Q9CZC8	Secernin-1 OS=Mus musculus GN=Scrn1 PE=1 SV=1 - [SCRN1_MOUSE]	11,84	1	4	4	10
O54983	Thiomorpholine-carboxylate dehydrogenase OS=Mus musculus GN=Crym PE=1 SV=1 - [CRYM_MOUSE]	11,82	1	4	4	17
Q7TQF7	Amphiphysin OS=Mus musculus GN=Amph PE=1 SV=1 - [AMPH_MOUSE]	11,81	1	7	7	22
P60335	Poly(rC)-binding protein 1 OS=Mus musculus GN=Pcbp1 PE=1 SV=1 - [PCBP1_MOUSE]	11,80	3	3	3	11
O08532	Voltage-dependent calcium channel subunit alpha-2/delta-1 OS=Mus musculus GN=Cacna2d1 PE=1 SV=1 - [CA2D1_MOUSE]	11,79	1	10	10	19
O55022	Membrane-associated progesterone receptor component 1 OS=Mus musculus GN=Pgrmc1 PE=1 SV=4 - [PGRC1_MOUSE]	11,79	1	2	2	16
Q91WK5	Glycine cleavage system H protein, mitochondrial OS=Mus musculus GN=Gcsh PE=1 SV=2 - [GCSH_MOUSE]	11,76	1	1	1	2
P47708	Rabphilin-3A OS=Mus musculus GN=Rph3a PE=1 SV=2 - [RP3A_MOUSE]	11,75	3	8	8	13
Q3UIU2	NADH dehydrogenase [ubiquinone] 1 beta subcomplex subunit 6 OS=Mus musculus GN=Ndufb6 PE=2 SV=3 - [NDUB6_MOUSE]	11,72	1	2	2	2
P80315	T-complex protein 1 subunit delta OS=Mus musculus GN=Cct4 PE=1 SV=3 - [TCPD_MOUSE]	11,69	1	5	5	9
P05132	cAMP-dependent protein kinase catalytic subunit alpha OS=Mus musculus GN=Prkaca PE=1 SV=3 - [KAPCA_MOUSE]	11,68	1	2	3	3
P84084	ADP-ribosylation factor 5 OS=Mus musculus GN=Arf5 PE=2 SV=2 - [ARF5_MOUSE]	11,67	2	1	2	3
Q9CVB6	Actin-related protein 2/3 complex subunit 2 OS=Mus musculus GN=Arpc2 PE=1 SV=3 - [ARPC2_MOUSE]	11,67	1	4	4	6
Q8K097	Protein lifeguard 2 OS=Mus musculus GN=Faim2 PE=2 SV=1 - [LFG2_MOUSE]	11,67	1	2	2	5
P60840	Alpha-endosulfine OS=Mus musculus GN=Ensa PE=1 SV=1 - [ENSA_MOUSE]	11,57	1	1	1	13
Q99LC3	NADH dehydrogenase [ubiquinone] 1 alpha subcomplex subunit 10, mitochondrial OS=Mus musculus GN=Ndufa10 PE=1 SV=1 - [NDUAA_MOUSE]	11,55	1	4	4	9
Q61301	Catenin alpha-2 OS=Mus musculus GN=Ctnna2 PE=1 SV=3 - [CTNA2_MOUSE]	11,54	1	7	9	24
P10649	Glutathione S-transferase Mu 1 OS=Mus musculus GN=Gstm1 PE=1 SV=2 - [GSTM1_MOUSE]	11,47	1	2	2	9
P00493	Hypoxanthine-guanine phosphoribosyltransferase OS=Mus musculus GN=Hprt1 PE=1 SV=3 - [HPRT_MOUSE]	11,47	1	2	2	3
Q9CQZ5	NADH dehydrogenase [ubiquinone] 1 alpha subcomplex subunit 6 OS=Mus musculus GN=Ndufa6 PE=1 SV=1 - [NDUA6_MOUSE]	11,45	1	2	2	5
Q91X97	Neurocalcin-delta OS=Mus musculus GN=Ncald PE=1 SV=4 - [NCALD_MOUSE]	11,40	1	1	2	12
P46096	Synaptotagmin-1 OS=Mus musculus GN=Syt1 PE=1 SV=1 - [SYT1_MOUSE]	11,40	3	4	4	50
P47738	Aldehyde dehydrogenase, mitochondrial OS=Mus musculus GN=Aldh2 PE=1 SV=1 - [ALDH2_MOUSE]	11,37	1	4	4	15
O88892	Small EDRK-rich factor 1 OS=Mus musculus GN=Serf1 PE=2 SV=1 - [SERF1_MOUSE]	11,29	1	1	1	1
P35803	Neuronal membrane glycoprotein M6-b OS=Mus musculus GN=Gpm6b PE=1 SV=2 - [GPM6B_MOUSE]	11,28	1	3	3	18
CON_0069 01214	SWISS-PROT:P60984| Bos taurus Gene_Symbol=GMFB Glia maturation factor beta	11,27	2	1	1	3
Q3UHJ0	AP2-associated protein kinase 1 OS=Mus musculus GN=Aak1 PE=1 SV=2 - [AAK1_MOUSE]	11,26	1	7	7	23
P70296	Phosphatidylethanolamine-binding protein 1 OS=Mus musculus GN=Pebp1 PE=1 SV=3 - [PEBP1_MOUSE]	11,23	2	2	2	5
Q99KJ8	Dynactin subunit 2 OS=Mus musculus GN=Dctn2 PE=1 SV=3 - [DCTN2_MOUSE]	11,19	1	3	3	5
Q9Z1S5	Neuronal-specific septin-3 OS=Mus musculus GN=Sept3 PE=1 SV=2 - [SEPT3_MOUSE]	11,14	1	4	4	12
Q9DC07	LIM zinc-binding domain-containing Nebulette OS=Mus musculus GN=Nebl PE=2 SV=1 - [LNEBL_MOUSE]	11,11	1	2	2	2
P35278	Ras-related protein Rab-5C OS=Mus musculus GN=Rab5c PE=1 SV=2 - [RAB5C_MOUSE]	11,11	1	2	2	6
P51863	V-type proton ATPase subunit d 1 OS=Mus musculus GN=Atp6v0d1 PE=1 SV=2 - [VA0D1_MOUSE]	11,11	1	4	4	16
Q9R1V6	Disintegrin and metalloproteinase domain-containing protein 22 OS=Mus musculus GN=Adam22 PE=1 SV=2 - [ADA22_MOUSE]	11,06	1	7	7	16
P30275	Creatine kinase U-type, mitochondrial OS=Mus musculus GN=Ckmt1 PE=1 SV=1 - [KCRU_MOUSE]	11,00	3	3	4	8
P62761	Visinin-like protein 1 OS=Mus musculus GN=Vsnl1 PE=1 SV=2 - [VISL1_MOUSE]	10,99	1	2	2	21
Q8BGZ1	Hippocalcin-like protein 4 OS=Mus musculus GN=Hpcal4 PE=2 SV=3 - [HPCL4_MOUSE]	10,99	1	2	2	6
Q91VN4	Coiled-coil-helix-coiled-coil-helix domain-containing protein 6, mitochondrial OS=Mus musculus GN=Chchd6 PE=2 SV=2 - [CHCH6_MOUSE]	10,99	1	2	2	8
Q9CQ69	Cytochrome b-c1 complex subunit 8 OS=Mus musculus GN=Uqcrq PE=1 SV=3 - [QCR8_MOUSE]	10,98	1	1	1	5
Q9D6U8	Protein FAM162A OS=Mus musculus GN=Fam162a PE=2 SV=1 - [F162A_MOUSE]	10,97	1	1	1	2

Accession	Description	Σ Cover.	Σ# Prot.	Σ# Unique Pept.	Σ# Pept.	Σ# PSM
Q9CR68	Cytochrome b-c1 complex subunit Rieske, mitochondrial OS=Mus musculus GN=Uqcrfs1 PE=1 SV=1 - [UCRI_MOUSE]	10,95	1	3	3	10
Q9Z2Y3	Homer protein homolog 1 OS=Mus musculus GN=Homer1 PE=1 SV=2 - [HOME1_MOUSE]	10,93	1	4	4	4
Q9QWI6	SRC kinase signaling inhibitor 1 OS=Mus musculus GN=Srcin1 PE=1 SV=2 - [SRCN1_MOUSE]	10,88	1	9	9	30
Q8BFR5	Elongation factor Tu, mitochondrial OS=Mus musculus GN=Tufm PE=1 SV=1 - [EFTU_MOUSE]	10,84	1	5	5	20
Q9JKK7	Tropomodulin-2 OS=Mus musculus GN=Tmod2 PE=1 SV=2 - [TMOD2_MOUSE]	10,83	2	3	4	8
Q9CZ13	Cytochrome b-c1 complex subunit 1, mitochondrial OS=Mus musculus GN=Uqcrc1 PE=1 SV=2 - [QCR1_MOUSE]	10,83	2	5	5	24
Q9JIS5	Synaptic vesicle glycoprotein 2A OS=Mus musculus GN=Sv2a PE=1 SV=1 - [SV2A_MOUSE]	10,78	1	7	8	34
Q8BMF4	Dihydrolipoyllysine-residue acetyltransferase component of pyruvate dehydrogenase complex, mitochondrial OS=Mus musculus GN=Dlat PE=1 SV=2 - [ODP2_MOUSE]	10,75	1	5	6	13
Q9Z1G4	V-type proton ATPase 116 kDa subunit a isoform 1 OS=Mus musculus GN=Atp6v0a1 PE=1 SV=3 - [VPP1_MOUSE]	10,73	2	8	8	44
P23242	Gap junction alpha-1 protein OS=Mus musculus GN=Gja1 PE=1 SV=2 - [CXA1_MOUSE]	10,73	1	3	3	14
CON_0070 83981	SWISS-PROT:P02769 Bos taurus Bovine serum albumin precursor	10,71	2	5	5	12
Q8BWF0	Succinate-semialdehyde dehydrogenase, mitochondrial OS=Mus musculus GN=Aldh5a1 PE=1 SV=1 - [SSDH_MOUSE]	10,71	1	4	4	9
P63321	Ras-related protein Ral-A OS=Mus musculus GN=Rala PE=1 SV=1 - [RALA_MOUSE]	10,68	1	2	2	2
Q9R1P4	Proteasome subunit alpha type-1 OS=Mus musculus GN=Psma1 PE=1 SV=1 - [PSA1_MOUSE]	10,65	1	2	2	9
Q8BP92	Reticulocalbin-2 OS=Mus musculus GN=Rcn2 PE=2 SV=1 - [RCN2_MOUSE]	10,63	1	2	2	4
Q9R1T4	Septin-6 OS=Mus musculus GN=Sept6 PE=1 SV=4 - [SEPT6_MOUSE]	10,60	1	2	4	15
Q9DCW4	Electron transfer flavoprotein subunit beta OS=Mus musculus GN=Etfb PE=1 SV=3 - [ETFB_MOUSE]	10,59	1	2	2	4
P31324	cAMP-dependent protein kinase type II-beta regulatory subunit OS=Mus musculus GN=Prkar2b PE=1 SV=3 - [KAP3_MOUSE]	10,58	1	3	3	10
Q8BK30	NADH dehydrogenase [ubiquinone] flavoprotein 3, mitochondrial OS=Mus musculus GN=Ndufv3 PE=2 SV=1 - [NDUV3_MOUSE]	10,58	1	1	1	9
Q9CQZ6	NADH dehydrogenase [ubiquinone] 1 beta subcomplex subunit 3 OS=Mus musculus GN=Ndufb3 PE=1 SV=1 - [NDUB3_MOUSE]	10,58	1	1	1	1
P17710	Hexokinase-1 OS=Mus musculus GN=Hk1 PE=1 SV=3 - [HXK1_MOUSE]	10,57	1	10	10	33
Q8CFV4	Neuritin OS=Mus musculus GN=Nrn1 PE=1 SV=1 - [NRN1_MOUSE]	10,56	1	1	1	8
Q7TNS2	Mitochondrial inner membrane organizing system protein 1 OS=Mus musculus GN=Minos1 PE=2 SV=1 - [MOS1_MOUSE]	10,53	1	1	1	1
O08917	Flotillin-1 OS=Mus musculus GN=Flot1 PE=1 SV=1 - [FLOT1_MOUSE]	10,51	1	3	3	12
Q9DBC7	cAMP-dependent protein kinase type I-alpha regulatory subunit OS=Mus musculus GN=Prkar1a PE=1 SV=3 - [KAP0_MOUSE]	10,50	1	3	3	4
Q80UW2	F-box only protein 2 OS=Mus musculus GN=Fbxo2 PE=1 SV=1 - [FBX2_MOUSE]	10,44	1	2	2	3
Q9CQS8	Protein transport protein Sec61 subunit beta OS=Mus musculus GN=Sec61b PE=1 SV=3 - [SC61B_MOUSE]	10,42	1	1	1	2
O35643	AP-1 complex subunit beta-1 OS=Mus musculus GN=Ap1b1 PE=1 SV=2 - [AP1B1_MOUSE]	10,39	1	2	9	16
Q4KMM3	Oxidation resistance protein 1 OS=Mus musculus GN=Oxr1 PE=1 SV=3 - [OXR1_MOUSE]	10,39	1	7	7	15
P48722	Heat shock 70 kDa protein 4L OS=Mus musculus GN=Hspa4l PE=1 SV=2 - [HS74L_MOUSE]	10,38	1	7	7	12
Q9JMA1	Ubiquitin carboxyl-terminal hydrolase 14 OS=Mus musculus GN=Usp14 PE=1 SV=3 - [UBP14_MOUSE]	10,34	1	4	4	4
Q9D8B7	Junctional adhesion molecule C OS=Mus musculus GN=Jam3 PE=1 SV=2 - [JAM3_MOUSE]	10,32	1	2	2	6
P68404	Protein kinase C beta type OS=Mus musculus GN=Prkcb PE=1 SV=4 - [KPCB_MOUSE]	10,28	4	4	6	19
Q6PHZ2	Calcium/calmodulin-dependent protein kinase type II subunit delta OS=Mus musculus GN=Camk2d PE=1 SV=1 - [KCC2D_MOUSE]	10,22	1	2	4	24
P62827	GTP-binding nuclear protein Ran OS=Mus musculus GN=Ran PE=1 SV=3 - [RAN_MOUSE]	10,19	2	2	2	4
Q99L13	3-hydroxyisobutyrate dehydrogenase, mitochondrial OS=Mus musculus GN=Hibadh PE=2 SV=1 - [3HIDH_MOUSE]	10,15	1	2	2	11
Q9D0F9	Phosphoglucomutase-1 OS=Mus musculus GN=Pgm1 PE=1 SV=4 - [PGM1_MOUSE]	10,14	1	4	4	13
Q3TDK6	Protein rogdi homolog OS=Mus musculus GN=Rogdi PE=2 SV=1 - [ROGDI_MOUSE]	10,10	1	2	2	4
P40336	Vacuolar protein sorting-associated protein 26A OS=Mus musculus GN=Vps26a PE=2 SV=1 - [VP26A_MOUSE]	10,09	1	2	2	6
Q9JL62	Glycolipid transfer protein OS=Mus musculus GN=Gltp PE=2 SV=3 - [GLTP_MOUSE]	10,05	1	2	2	10
Q62283	Tetraspanin-7 OS=Mus musculus GN=Tspan7 PE=2 SV=2 - [TSN7_MOUSE]	10,04	1	2	2	25
P45878	Peptidyl-prolyl cis-trans isomerase FKBP2 OS=Mus musculus GN=Fkbp2 PE=1 SV=1 - [FKBP2_MOUSE]	10,00	1	1	1	2
Q8C1B7	Septin-11 OS=Mus musculus GN=Sept11 PE=1 SV=4 - [SEP11_MOUSE]	9,98	1	2	4	10
P60766	Cell division control protein 42 homolog OS=Mus musculus GN=Cdc42 PE=1 SV=2 - [CDC42_MOUSE]	9,95	3	1	2	9
Q8K2B3	Succinate dehydrogenase [ubiquinone] flavoprotein subunit, mitochondrial OS=Mus musculus GN=Sdha PE=1 SV=1 - [DHSA_MOUSE]	9,94	1	6	6	21
Q8K0U4	Heat shock 70 kDa protein 12A OS=Mus musculus GN=Hspa12a PE=1 SV=1 - [HS12A_MOUSE]	9,93	1	5	5	19
Q9D855	Cytochrome b-c1 complex subunit 7 OS=Mus musculus GN=Uqcrb PE=1 SV=3 - [QCR7_MOUSE]	9,91	1	1	1	5
Q8JZS0	Protein lin-7 homolog A OS=Mus musculus GN=Lin7a PE=1 SV=2 - [LIN7A_MOUSE]	9,87	3	2	2	4
Q62465	Synaptic vesicle membrane protein VAT-1 homolog OS=Mus musculus GN=Vat1 PE=1 SV=3 - [VAT1_MOUSE]	9,85	1	3	3	6
Q923T9	Calcium/calmodulin-dependent protein kinase type II subunit gamma OS=Mus musculus GN=Camk2g PE=1 SV=1 - [KCC2G_MOUSE]	9,83	1	3	4	14
Q8R464	Cell adhesion molecule 4 OS=Mus musculus GN=Cadm4 PE=1 SV=1 - [CADM4_MOUSE]	9,79	1	2	2	5
Q6PEB6	MOB-like protein phocein OS=Mus musculus GN=Mob4 PE=1 SV=1 - [PHOCN_MOUSE]	9,78	1	2	2	3
Q5M8N0	CB1 cannabinoid receptor-interacting protein 1 OS=Mus musculus GN=Cnrip1 PE=1 SV=1 - [CNRP1_MOUSE]	9,76	1	1	1	2
P20108	Thioredoxin-dependent peroxide reductase, mitochondrial OS=Mus musculus GN=Prdx3 PE=1 SV=1 - [PRDX3_MOUSE]	9,73	1	3	3	4
Q9CYN2	Signal peptidase complex subunit 2 OS=Mus musculus GN=Spcs2 PE=1 SV=1 - [SPCS2_MOUSE]	9,73	1	1	1	2
P35979	60S ribosomal protein L12 OS=Mus musculus GN=Rpl12 PE=1 SV=2 - [RL12_MOUSE]	9,70	1	1	1	1
CON_LysC	SWISS-PROT:P15636 Protease I precursor Lysyl endopeptidase Achromobacter lyticus	9,65	1	4	4	57
Q9QXS6	Drebrin OS=Mus musculus GN=Dbn1 PE=1 SV=4 - [DREB_MOUSE]	9,63	1	5	5	12
Q8C8R3	Ankyrin-2 OS=Mus musculus GN=Ank2 PE=1 SV=2 - [ANK2_MOUSE]	9,62	1	27	27	69
Q61879	Myosin-10 OS=Mus musculus GN=Myh10 PE=1 SV=2 - [MYH10_MOUSE]	9,62	2	14	15	28

152

Accession	Description	Σ Cover.	Σ# Prot.	Σ# Unique Pept.	Σ# Pept.	Σ# PSM
Q9DB75	Cell death-inducing p53-target protein 1 OS=Mus musculus GN=Cdip1 PE=2 SV=1 - [CDIP1_MOUSE]	9,62	1	1	1	1
Q810U3	Neurofascin OS=Mus musculus GN=Nfasc PE=1 SV=1 - [NFASC_MOUSE]	9,60	1	9	9	21
Q8K1Z0	Ubiquinone biosynthesis protein COQ9, mitochondrial OS=Mus musculus GN=Coq9 PE=1 SV=1 - [COQ9_MOUSE]	9,58	1	2	2	2
Q9CQ86	Migration and invasion enhancer 1 OS=Mus musculus GN=Mien1 PE=1 SV=1 - [MIEN1_MOUSE]	9,57	1	1	1	1
Q9CQY6	Ubiquinol-cytochrome-c reductase complex assembly factor 2 OS=Mus musculus GN=Uqcc2 PE=1 SV=1 - [UQCC2_MOUSE]	9,56	1	1	1	1
Q9CY64	Biliverdin reductase A OS=Mus musculus GN=Blvra PE=2 SV=1 - [BIEA_MOUSE]	9,49	1	2	2	3
P60041	Somatostatin OS=Mus musculus GN=Sst PE=2 SV=1 - [SMS_MOUSE]	9,48	1	1	1	2
Q922Q1	MOSC domain-containing protein 2, mitochondrial OS=Mus musculus GN=Marc2 PE=1 SV=1 - [MOSC2_MOUSE]	9,47	2	3	3	3
Q9R111	Guanine deaminase OS=Mus musculus GN=Gda PE=1 SV=1 - [GUAD_MOUSE]	9,47	1	4	4	10
Q9DBF1	Alpha-aminoadipic semialdehyde dehydrogenase OS=Mus musculus GN=Aldh7a1 PE=1 SV=4 - [AL7A1_MOUSE]	9,46	1	3	3	3
P05201	Aspartate aminotransferase, cytoplasmic OS=Mus musculus GN=Got1 PE=1 SV=3 - [AATC_MOUSE]	9,44	1	4	4	7
P60521	Gamma-aminobutyric acid receptor-associated protein-like 2 OS=Mus musculus GN=Gabarapl2 PE=1 SV=1 - [GBRL2_MOUSE]	9,40	1	1	1	2
Q8CHC4	Synaptojanin-1 OS=Mus musculus GN=Synj1 PE=1 SV=3 - [SYNJ1_MOUSE]	9,28	1	13	13	31
O88737	Protein bassoon OS=Mus musculus GN=Bsn PE=1 SV=4 - [BSN_MOUSE]	9,23	1	28	29	74
Q99K85	Phosphoserine aminotransferase OS=Mus musculus GN=Psat1 PE=1 SV=1 - [SERC_MOUSE]	9,19	1	3	3	4
Q9D7X3	Dual specificity protein phosphatase 3 OS=Mus musculus GN=Dusp3 PE=1 SV=1 - [DUS3_MOUSE]	9,19	1	1	1	2
Q9CQU3	Protein RER1 OS=Mus musculus GN=Rer1 PE=1 SV=1 - [RER1_MOUSE]	9,18	1	1	1	1
P60904	DnaJ homolog subfamily C member 5 OS=Mus musculus GN=Dnajc5 PE=1 SV=1 - [DNJC5_MOUSE]	9,09	1	2	2	7
Q99N28	Cell adhesion molecule 3 OS=Mus musculus GN=Cadm3 PE=1 SV=1 - [CADM3_MOUSE]	9,09	1	2	2	10
P51880	Fatty acid-binding protein, brain OS=Mus musculus GN=Fabp7 PE=1 SV=2 - [FABP7_MOUSE]	9,09	1	1	1	1
Q8VEK0	Cell cycle control protein 50A OS=Mus musculus GN=Tmem30a PE=1 SV=1 - [CC50A_MOUSE]	9,07	1	2	2	8
P58281	Dynamin-like 120 kDa protein, mitochondrial OS=Mus musculus GN=Opa1 PE=1 SV=1 - [OPA1_MOUSE]	9,06	1	8	8	12
Q8R1Q8	Cytoplasmic dynein 1 light intermediate chain 1 OS=Mus musculus GN=Dync1li1 PE=1 SV=1 - [DC1L1_MOUSE]	8,99	1	3	3	3
Q921H8	3-ketoacyl-CoA thiolase A, peroxisomal OS=Mus musculus GN=Acaa1a PE=2 SV=1 - [THIKA_MOUSE]	8,96	2	2	2	2
Q6ZQI3	Malectin OS=Mus musculus GN=Mlec PE=2 SV=2 - [MLEC_MOUSE]	8,93	1	2	2	5
Q9CRD0	OCIA domain-containing protein 1 OS=Mus musculus GN=Ociad1 PE=1 SV=1 - [OCAD1_MOUSE]	8,91	1	1	1	3
Q60692	Proteasome subunit beta type-6 OS=Mus musculus GN=Psmb6 PE=1 SV=3 - [PSB6_MOUSE]	8,82	1	2	2	2
Q9D2G2	Dihydrolipoyllysine-residue succinyltransferase component of 2-oxoglutarate dehydrogenase complex, mitochondrial OS=Mus musculus GN=Dlst PE=1 SV=1 - [ODO2_MOUSE]	8,81	1	3	3	14
O88643	Serine/threonine-protein kinase PAK 1 OS=Mus musculus GN=Pak1 PE=1 SV=1 - [PAK1_MOUSE]	8,81	1	3	4	10
Q9QXT0	Protein canopy homolog 2 OS=Mus musculus GN=Cnpy2 PE=2 SV=1 - [CNPY2_MOUSE]	8,79	1	1	1	2
Q9DCU2	Plasmolipin OS=Mus musculus GN=Pllp PE=2 SV=1 - [PLLP_MOUSE]	8,79	1	1	1	3
Q99JB2	Stomatin-like protein 2, mitochondrial OS=Mus musculus GN=Stoml2 PE=1 SV=1 - [STML2_MOUSE]	8,78	1	2	2	3
P61226	Ras-related protein Rap-2b OS=Mus musculus GN=Rap2b PE=1 SV=1 - [RAP2B_MOUSE]	8,74	1	1	1	2
Q9QYB1	Chloride intracellular channel protein 4 OS=Mus musculus GN=Clic4 PE=1 SV=3 - [CLIC4_MOUSE]	8,70	1	1	1	1
P84099	60S ribosomal protein L19 OS=Mus musculus GN=Rpl19 PE=1 SV=1 - [RL19_MOUSE]	8,67	1	1	1	2
O88487	Cytoplasmic dynein 1 intermediate chain 2 OS=Mus musculus GN=Dync1i2 PE=2 SV=1 - [DC1I2_MOUSE]	8,66	1	3	3	6
Q9QYI5	DnaJ homolog subfamily B member 2 OS=Mus musculus GN=Dnajb2 PE=2 SV=2 - [DNJB2_MOUSE]	8,66	1	2	2	4
P35279	Ras-related protein Rab-6A OS=Mus musculus GN=Rab6a PE=1 SV=4 - [RAB6A_MOUSE]	8,65	12	1	2	4
Q921M7	Protein FAM49B OS=Mus musculus GN=Fam49b PE=1 SV=1 - [FA49B_MOUSE]	8,64	1	1	2	11
O08530	Sphingosine 1-phosphate receptor 1 OS=Mus musculus GN=S1pr1 PE=2 SV=3 - [S1PR1_MOUSE]	8,64	1	2	2	6
Q99L04	Dehydrogenase/reductase SDR family member 1 OS=Mus musculus GN=Dhrs1 PE=2 SV=1 - [DHRS1_MOUSE]	8,63	1	2	2	4
P62264	40S ribosomal protein S14 OS=Mus musculus GN=Rps14 PE=2 SV=3 - [RS14_MOUSE]	8,61	1	1	1	2
Q9D892	Inosine triphosphate pyrophosphatase OS=Mus musculus GN=Itpa PE=1 SV=2 - [ITPA_MOUSE]	8,59	1	1	1	6
Q61735	Leukocyte surface antigen CD47 OS=Mus musculus GN=Cd47 PE=1 SV=2 - [CD47_MOUSE]	8,58	1	3	3	8
P19157	Glutathione S-transferase P 1 OS=Mus musculus GN=Gstp1 PE=1 SV=2 - [GSTP1_MOUSE]	8,57	1	2	2	20
P62812	Gamma-aminobutyric acid receptor subunit alpha-1 OS=Mus musculus GN=Gabra1 PE=1 SV=1 - [GBRA1_MOUSE]	8,57	2	3	3	6
Q61548	Clathrin coat assembly protein AP180 OS=Mus musculus GN=Snap91 PE=1 SV=1 - [AP180_MOUSE]	8,55	2	8	10	25
Q9WUB3	Glycogen phosphorylase, muscle form OS=Mus musculus GN=Pygm PE=1 SV=3 - [PYGM_MOUSE]	8,55	3	5	6	8
Q64010	Adapter molecule crk OS=Mus musculus GN=Crk PE=1 SV=1 - [CRK_MOUSE]	8,55	1	2	2	2
Q8CI94	Glycogen phosphorylase, brain form OS=Mus musculus GN=Pygb PE=1 SV=3 - [PYGB_MOUSE]	8,54	2	7	8	19
Q64521	Glycerol-3-phosphate dehydrogenase, mitochondrial OS=Mus musculus GN=Gpd2 PE=1 SV=2 - [GPDM_MOUSE]	8,53	1	6	6	19
Q61081	Hsp90 co-chaperone Cdc37 OS=Mus musculus GN=Cdc37 PE=2 SV=1 - [CDC37_MOUSE]	8,44	1	3	3	3
Q8CHH9	Septin-8 OS=Mus musculus GN=Sept8 PE=1 SV=4 - [SEPT8_MOUSE]	8,39	1	3	4	10
Q64332	Synapsin-2 OS=Mus musculus GN=Syn2 PE=1 SV=2 - [SYN2_MOUSE]	8,36	1	3	4	29
O35295	Transcriptional activator protein Pur-beta OS=Mus musculus GN=Purb PE=1 SV=3 - [PURB_MOUSE]	8,33	2	1	2	2
Q9D6G9	CKLF-like MARVEL transmembrane domain-containing protein 5 OS=Mus musculus GN=Cmtm5 PE=1 SV=1 - [CKLF5_MOUSE]	8,33	1	1	1	5
Q91WS0	CDGSH iron-sulfur domain-containing protein 1 OS=Mus musculus GN=Cisd1 PE=1 SV=1 - [CISD1_MOUSE]	8,33	1	1	1	1

153

Accession	Description	Σ Cover.	Σ# Prot.	Σ# Unique Pept.	Σ# Pept.	Σ# PSM
Q8R4N0	Citrate lyase subunit beta-like protein, mitochondrial OS=Mus musculus GN=Clybl PE=2 SV=2 - [CLYBL_MOUSE]	8,28	1	2	2	6
Q8BGT8	Phytanoyl-CoA hydroxylase-interacting protein-like OS=Mus musculus GN=Phyhipl PE=2 SV=1 - [PHIPL_MOUSE]	8,27	1	2	3	4
P04925	Major prion protein OS=Mus musculus GN=Prnp PE=1 SV=2 - [PRIO_MOUSE]	8,27	1	2	2	10
Q3ULJ0	Glycerol-3-phosphate dehydrogenase 1-like protein OS=Mus musculus GN=Gpd1l PE=1 SV=2 - [GPD1L_MOUSE]	8,26	1	2	2	5
Q6PH08	ERC protein 2 OS=Mus musculus GN=Erc2 PE=1 SV=2 - [ERC2_MOUSE]	8,25	1	8	8	12
P09528	Ferritin heavy chain OS=Mus musculus GN=Fth1 PE=1 SV=2 - [FRIH_MOUSE]	8,24	1	1	1	3
Q8BL86	Metallo-beta-lactamase domain-containing protein 2 OS=Mus musculus GN=Mblac2 PE=2 SV=2 - [MBLC2_MOUSE]	8,24	1	2	2	2
Q8K1M6	Dynamin-1-like protein OS=Mus musculus GN=Dnm1l PE=1 SV=2 - [DNM1L_MOUSE]	8,22	1	5	5	11
Q91WD5	NADH dehydrogenase [ubiquinone] iron-sulfur protein 2, mitochondrial OS=Mus musculus GN=Ndufs2 PE=1 SV=1 - [NDUS2_MOUSE]	8,21	1	3	3	13
Q5EBJ4	Ermin OS=Mus musculus GN=Ermn PE=1 SV=1 - [ERMIN_MOUSE]	8,19	1	2	2	7
P57776	Elongation factor 1-delta OS=Mus musculus GN=Eef1d PE=1 SV=3 - [EF1D_MOUSE]	8,19	2	2	2	3
Q8BKZ9	Pyruvate dehydrogenase protein X component, mitochondrial OS=Mus musculus GN=Pdhx PE=2 SV=1 - [ODPX_MOUSE]	8,18	1	3	3	6
Q7TPR4	Alpha-actinin-1 OS=Mus musculus GN=Actn1 PE=1 SV=1 - [ACTN1_MOUSE]	8,18	3	5	5	14
P23818	Glutamate receptor 1 OS=Mus musculus GN=Gria1 PE=1 SV=1 - [GRIA1_MOUSE]	8,16	1	3	7	15
O08539	Myc box-dependent-interacting protein 1 OS=Mus musculus GN=Bin1 PE=1 SV=1 - [BIN1_MOUSE]	8,16	1	4	4	12
Q91V12	Cytosolic acyl coenzyme A thioester hydrolase OS=Mus musculus GN=Acot7 PE=1 SV=2 - [BACH_MOUSE]	8,14	1	2	2	4
O55125	Protein NipSnap homolog 1 OS=Mus musculus GN=Nipsnap1 PE=1 SV=1 - [NIPS1_MOUSE]	8,10	1	2	2	4
O88342	WD repeat-containing protein 1 OS=Mus musculus GN=Wdr1 PE=1 SV=3 - [WDR1_MOUSE]	8,09	1	3	4	5
Q9JKD3	Secretory carrier-associated membrane protein 5 OS=Mus musculus GN=Scamp5 PE=2 SV=1 - [SCAM5_MOUSE]	8,09	1	2	2	6
Q9JJK2	LanC-like protein 2 OS=Mus musculus GN=Lancl2 PE=1 SV=1 - [LANC2_MOUSE]	8,00	1	3	3	5
Q9ES97	Reticulon-3 OS=Mus musculus GN=Rtn3 PE=1 SV=2 - [RTN3_MOUSE]	7,99	1	7	8	12
F6SEU4	Ras GTPase-activating protein SynGAP OS=Mus musculus GN=Syngap1 PE=3 SV=2 - [SYGP1_MOUSE]	7,99	1	8	8	25
CON_0071 05152	SWISS-PROT:P31836| Bos taurus Gene_Symbol=NCAM1 Neural cell adhesion molecule 1	7,97	1	1	6	37
Q922S4	cGMP-dependent 3',5'-cyclic phosphodiesterase OS=Mus musculus GN=Pde2a PE=1 SV=3 - [PDE2A_MOUSE]	7,97	1	6	6	11
Q9CRB6	Tubulin polymerization-promoting protein family member 3 OS=Mus musculus GN=Tppp3 PE=1 SV=1 - [TPPP3_MOUSE]	7,95	1	1	1	2
P20357	Microtubule-associated protein 2 OS=Mus musculus GN=Map2 PE=1 SV=2 - [MAP2_MOUSE]	7,93	1	11	11	21
Q8VE22	28S ribosomal protein S23, mitochondrial OS=Mus musculus GN=Mrps23 PE=2 SV=1 - [RT23_MOUSE]	7,91	1	1	1	2
O70318	Band 4.1-like protein 2 OS=Mus musculus GN=Epb41l2 PE=1 SV=2 - [E41L2_MOUSE]	7,89	2	6	8	15
Q9CQ92	Mitochondrial fission 1 protein OS=Mus musculus GN=Fis1 PE=1 SV=1 - [FIS1_MOUSE]	7,89	1	1	1	3
Q640R3	Hepatocyte cell adhesion molecule OS=Mus musculus GN=Hepacam PE=1 SV=2 - [HECAM_MOUSE]	7,89	1	2	2	18
Q62433	Protein NDRG1 OS=Mus musculus GN=Ndrg1 PE=1 SV=1 - [NDRG1_MOUSE]	7,87	1	2	2	4
Q3UJU9	Regulator of microtubule dynamics protein 3 OS=Mus musculus GN=Rmdn3 PE=1 SV=2 - [RMD3_MOUSE]	7,87	1	2	2	2
Q9WVL0	Maleylacetoacetate isomerase OS=Mus musculus GN=Gstz1 PE=1 SV=1 - [MAAI_MOUSE]	7,87	1	1	1	2
Q99104	Unconventional myosin-Va OS=Mus musculus GN=Myo5a PE=1 SV=2 - [MYO5A_MOUSE]	7,83	2	13	13	31
Q9WUM4	Coronin-1C OS=Mus musculus GN=Coro1c PE=1 SV=2 - [COR1C_MOUSE]	7,81	1	4	4	7
O35682	Myeloid-associated differentiation marker OS=Mus musculus GN=Myadm PE=2 SV=2 - [MYADM_MOUSE]	7,81	1	2	2	13
Q9DB05	Alpha-soluble NSF attachment protein OS=Mus musculus GN=Napa PE=1 SV=1 - [SNAA_MOUSE]	7,80	1	2	2	3
P10126	Elongation factor 1-alpha 1 OS=Mus musculus GN=Eef1a1 PE=1 SV=3 - [EF1A1_MOUSE]	7,79	1	3	4	21
Q9DCB8	Iron-sulfur cluster assembly 2 homolog, mitochondrial OS=Mus musculus GN=Isca2 PE=2 SV=2 - [ISCA2_MOUSE]	7,79	1	1	1	1
Q9CPP6	NADH dehydrogenase [ubiquinone] 1 alpha subcomplex subunit 5 OS=Mus musculus GN=Ndufa5 PE=1 SV=3 - [NDUA5_MOUSE]	7,76	1	1	1	6
Q60771	Claudin-11 OS=Mus musculus GN=Cldn11 PE=1 SV=1 - [CLD11_MOUSE]	7,73	1	2	2	23
P06745	Glucose-6-phosphate isomerase OS=Mus musculus GN=Gpi PE=1 SV=4 - [G6PI_MOUSE]	7,71	2	5	5	23
P18572	Basigin OS=Mus musculus GN=Bsg PE=1 SV=2 - [BASI_MOUSE]	7,71	1	3	3	11
O35465	Peptidyl-prolyl cis-trans isomerase FKBP8 OS=Mus musculus GN=Fkbp8 PE=1 SV=2 - [FKBP8_MOUSE]	7,71	1	2	2	4
Q62048	Astrocytic phosphoprotein PEA-15 OS=Mus musculus GN=Pea15 PE=1 SV=1 - [PEA15_MOUSE]	7,69	1	1	1	3
Q9R0N7	Synaptotagmin-7 OS=Mus musculus GN=Syt7 PE=1 SV=1 - [SYT7_MOUSE]	7,69	1	3	3	7
CON_0069 37762	SWISS-PROT:Q0VFX8| Bos taurus Gene_Symbol=CRIP2 Cysteine-rich protein 2	7,69	2	1	1	5
Q80U23	Syntaphilin OS=Mus musculus GN=Snph PE=1 SV=3 - [SNPH_MOUSE]	7,68	1	3	3	5
Q02053	Ubiquitin-like modifier-activating enzyme 1 OS=Mus musculus GN=Uba1 PE=1 SV=1 - [UBA1_MOUSE]	7,66	1	6	6	22
Q924S8	Sprouty-related, EVH1 domain-containing protein 1 OS=Mus musculus GN=Spred1 PE=1 SV=1 - [SPRE1_MOUSE]	7,66	1	2	2	4
P62869	Transcription elongation factor B polypeptide 2 OS=Mus musculus GN=Tceb2 PE=1 SV=1 - [ELOB_MOUSE]	7,63	1	1	1	1
O70443	Guanine nucleotide-binding protein G(z) subunit alpha OS=Mus musculus GN=Gnaz PE=2 SV=4 - [GNAZ_MOUSE]	7,61	3	2	3	11
O89053	Coronin-1A OS=Mus musculus GN=Coro1a PE=1 SV=5 - [COR1A_MOUSE]	7,59	1	3	3	14
Q80XN0	D-beta-hydroxybutyrate dehydrogenase, mitochondrial OS=Mus musculus GN=Bdh1 PE=1 SV=2 - [BDH_MOUSE]	7,58	2	3	3	5
P99026	Proteasome subunit beta type-4 OS=Mus musculus GN=Psmb4 PE=1 SV=1 - [PSB4_MOUSE]	7,58	1	1	1	4
P17426	AP-2 complex subunit alpha-1 OS=Mus musculus GN=Ap2a1 PE=1 SV=1 - [AP2A1_MOUSE]	7,57	1	5	7	14
Q9D1K2	V-type proton ATPase subunit F OS=Mus musculus GN=Atp6v1f PE=1 SV=2 - [VATF_MOUSE]	7,56	1	1	1	1
Q02248	Catenin beta-1 OS=Mus musculus GN=Ctnnb1 PE=1 SV=1 - [CTNB1_MOUSE]	7,55	3	5	5	15
Q60597	2-oxoglutarate dehydrogenase, mitochondrial OS=Mus musculus GN=Ogdh PE=1 SV=3 - [ODO1_MOUSE]	7,53	1	7	7	29

Accession	Description	Σ Cover.	Σ# Prot.	Σ# Unique Pept.	Σ# Pept.	Σ# PSM
Q8R366	Immunoglobulin superfamily member 8 OS=Mus musculus GN=Igsf8 PE=1 SV=2 - [IGSF8_MOUSE]	7,53	1	3	3	12
Q68FL4	Putative adenosylhomocysteinase 3 OS=Mus musculus GN=Ahcyl2 PE=1 SV=1 - [SAHH3_MOUSE]	7,50	2	1	4	7
Q99P72	Reticulon-4 OS=Mus musculus GN=Rtn4 PE=1 SV=2 - [RTN4_MOUSE]	7,49	1	5	5	14
P80314	T-complex protein 1 subunit beta OS=Mus musculus GN=Cct2 PE=1 SV=4 - [TCPB_MOUSE]	7,48	1	4	4	6
Q9JJY3	Sphingomyelin phosphodiesterase 3 OS=Mus musculus GN=Smpd3 PE=1 SV=1 - [NSMA2_MOUSE]	7,48	1	3	3	6
Q8R5M8	Cell adhesion molecule 1 OS=Mus musculus GN=Cadm1 PE=1 SV=2 - [CADM1_MOUSE]	7,46	1	2	2	8
Q9JKK1	Syntaxin-6 OS=Mus musculus GN=Stx6 PE=1 SV=1 - [STX6_MOUSE]	7,45	1	1	1	1
P20444	Protein kinase C alpha type OS=Mus musculus GN=Prkca PE=1 SV=3 - [KPCA_MOUSE]	7,44	4	2	4	12
O88998	Noelin OS=Mus musculus GN=Olfm1 PE=1 SV=1 - [NOE1_MOUSE]	7,42	1	2	2	3
Q05816	Fatty acid-binding protein, epidermal OS=Mus musculus GN=Fabp5 PE=1 SV=3 - [FABP5_MOUSE]	7,41	1	1	1	1
P61922	4-aminobutyrate aminotransferase, mitochondrial OS=Mus musculus GN=Abat PE=1 SV=1 - [GABT_MOUSE]	7,40	1	3	3	16
Q9D0M3	Cytochrome c1, heme protein, mitochondrial OS=Mus musculus GN=Cyc1 PE=1 SV=1 - [CY1_MOUSE]	7,38	1	1	1	1
P63094	Guanine nucleotide-binding protein G(s) subunit alpha isoforms short OS=Mus musculus GN=Gnas PE=1 SV=1 - [GNAS2_MOUSE]	7,36	2	2	2	9
P26040	Ezrin OS=Mus musculus GN=Ezr PE=1 SV=3 - [EZRI_MOUSE]	7,34	2	1	3	5
P63030	Mitochondrial pyruvate carrier 1 OS=Mus musculus GN=Mpc1 PE=1 SV=1 - [MPC1_MOUSE]	7,34	1	1	1	6
Q9CR62	Mitochondrial 2-oxoglutarate/malate carrier protein OS=Mus musculus GN=Slc25a11 PE=1 SV=3 - [M2OM_MOUSE]	7,32	1	3	3	3
O70252	Heme oxygenase 2 OS=Mus musculus GN=Hmox2 PE=2 SV=1 - [HMOX2_MOUSE]	7,30	1	2	2	2
P35293	Ras-related protein Rab-18 OS=Mus musculus GN=Rab18 PE=2 SV=2 - [RAB18_MOUSE]	7,28	1	1	1	3
Q9D6K8	FUN14 domain-containing protein 2 OS=Mus musculus GN=Fundc2 PE=2 SV=1 - [FUND2_MOUSE]	7,28	1	1	1	1
O70161	Phosphatidylinositol 4-phosphate 5-kinase type-1 gamma OS=Mus musculus GN=Pip5k1c PE=1 SV=2 - [PI51C_MOUSE]	7,26	1	4	4	7
Q8R570	Synaptosomal-associated protein 47 OS=Mus musculus GN=Snap47 PE=1 SV=1 - [SNP47_MOUSE]	7,26	1	2	2	5
O35678	Monoglyceride lipase OS=Mus musculus GN=Mgll PE=1 SV=1 - [MGLL_MOUSE]	7,26	1	2	2	5
Q8C419	Probable G-protein coupled receptor 158 OS=Mus musculus GN=Gpr158 PE=1 SV=2 - [GP158_MOUSE]	7,25	1	6	6	20
Q9WUM5	Succinyl-CoA ligase [ADP/GDP-forming] subunit alpha, mitochondrial OS=Mus musculus GN=Suclg1 PE=1 SV=4 - [SUCA_MOUSE]	7,23	1	2	2	7
P40142	Transketolase OS=Mus musculus GN=Tkt PE=1 SV=1 - [TKT_MOUSE]	7,22	1	4	4	10
Q924T2	28S ribosomal protein S2, mitochondrial OS=Mus musculus GN=Mrps2 PE=2 SV=1 - [RT02_MOUSE]	7,22	1	1	1	1
P31650	Sodium- and chloride-dependent GABA transporter 3 OS=Mus musculus GN=Slc6a11 PE=1 SV=2 - [S6A11_MOUSE]	7,18	1	4	4	17
P63318	Protein kinase C gamma type OS=Mus musculus GN=Prkcg PE=1 SV=1 - [KPCG_MOUSE]	7,17	1	4	4	24
Q9QZ88	Vacuolar protein sorting-associated protein 29 OS=Mus musculus GN=Vps29 PE=1 SV=1 - [VPS29_MOUSE]	7,14	1	1	1	2
Q9CY58	Plasminogen activator inhibitor 1 RNA-binding protein OS=Mus musculus GN=Serbp1 PE=1 SV=2 - [PAIRB_MOUSE]	7,13	1	2	2	2
Q8BHZ0	Protein FAM49A OS=Mus musculus GN=Fam49a PE=2 SV=1 - [FA49A_MOUSE]	7,12	1	1	2	4
Q9QYB5	Gamma-adducin OS=Mus musculus GN=Add3 PE=1 SV=2 - [ADDG_MOUSE]	7,08	1	3	3	9
Q9WV34	MAGUK p55 subfamily member 2 OS=Mus musculus GN=Mpp2 PE=1 SV=1 - [MPP2_MOUSE]	7,07	1	3	3	4
Q99PU5	Long-chain-fatty-acid--CoA ligase ACSBG1 OS=Mus musculus GN=Acsbg1 PE=1 SV=1 - [ACBG1_MOUSE]	7,07	1	4	4	6
Q99JY8	Lipid phosphate phosphohydrolase 3 OS=Mus musculus GN=Ppap2b PE=1 SV=1 - [LPP3_MOUSE]	7,05	1	2	2	2
P17427	AP-2 complex subunit alpha-2 OS=Mus musculus GN=Ap2a2 PE=1 SV=2 - [AP2A2_MOUSE]	7,04	1	4	6	15
P62743	AP-2 complex subunit sigma OS=Mus musculus GN=Ap2s1 PE=1 SV=1 - [AP2S1_MOUSE]	7,04	1	1	1	1
Q9CZ44	NSFL1 cofactor p47 OS=Mus musculus GN=Nsfl1c PE=1 SV=1 - [NSF1C_MOUSE]	7,03	1	2	2	2
P57780	Alpha-actinin-4 OS=Mus musculus GN=Actn4 PE=1 SV=1 - [ACTN4_MOUSE]	7,02	1	4	4	12
Q9WUM3	Coronin-1B OS=Mus musculus GN=Coro1b PE=1 SV=1 - [COR1B_MOUSE]	7,02	1	2	2	4
P53810	Phosphatidylinositol transfer protein alpha isoform OS=Mus musculus GN=Pitpna PE=1 SV=2 - [PIPNA_MOUSE]	7,01	1	1	1	6
CON_0070 18861	SWISS-PROT:P04815 Bos taurus Gene_Symbol=LOC404103 Spleen trypsin inhibitor I	7,00	1	1	1	1
Q9Z1B3	1-phosphatidylinositol 4,5-bisphosphate phosphodiesterase beta-1 OS=Mus musculus GN=Plcb1 PE=1 SV=2 - [PLCB1_MOUSE]	6,99	1	7	7	25
Q9Z2W9	Glutamate receptor 3 OS=Mus musculus GN=Gria3 PE=1 SV=2 - [GRIA3_MOUSE]	6,98	2	3	6	17
P03995	Glial fibrillary acidic protein OS=Mus musculus GN=Gfap PE=1 SV=4 - [GFAP_MOUSE]	6,98	1	3	3	3
Q99L43	Phosphatidate cytidylyltransferase 2 OS=Mus musculus GN=Cds2 PE=1 SV=1 - [CDS2_MOUSE]	6,98	1	2	2	7
Q62011	Podoplanin OS=Mus musculus GN=Pdpn PE=1 SV=2 - [PDPN_MOUSE]	6,98	1	1	1	1
Q9D358	Low molecular weight phosphotyrosine protein phosphatase OS=Mus musculus GN=Acp1 PE=1 SV=3 - [PPAC_MOUSE]	6,96	1	1	1	2
P97441	Zinc transporter 3 OS=Mus musculus GN=Slc30a3 PE=1 SV=1 - [ZNT3_MOUSE]	6,96	1	2	2	3
Q99JY9	Actin-related protein 3 OS=Mus musculus GN=Actr3 PE=1 SV=3 - [ARP3_MOUSE]	6,94	1	2	3	3
Q80TJ1	Calcium-dependent secretion activator 1 OS=Mus musculus GN=Cadps PE=1 SV=3 - [CAPS1_MOUSE]	6,94	2	7	7	15
P14869	60S acidic ribosomal protein P0 OS=Mus musculus GN=Rplp0 PE=1 SV=3 - [RLA0_MOUSE]	6,94	1	1	1	1
P42932	T-complex protein 1 subunit theta OS=Mus musculus GN=Cct8 PE=1 SV=3 - [TCPQ_MOUSE]	6,93	1	4	4	8
P00920	Carbonic anhydrase 2 OS=Mus musculus GN=Ca2 PE=1 SV=4 - [CAH2_MOUSE]	6,92	1	2	2	3
P08556	GTPase NRas OS=Mus musculus GN=Nras PE=2 SV=1 - [RASN_MOUSE]	6,88	2	1	1	2
Q8C0L0	Thioredoxin-related transmembrane protein 4 OS=Mus musculus GN=Tmx4 PE=2 SV=2 - [TMX4_MOUSE]	6,87	1	1	1	4
P48758	Carbonyl reductase [NADPH] 1 OS=Mus musculus GN=Cbr1 PE=1 SV=3 - [CBR1_MOUSE]	6,86	1	2	2	5
P68181	cAMP-dependent protein kinase catalytic subunit beta OS=Mus musculus GN=Prkacb PE=1 SV=2 - [KAPCB_MOUSE]	6,84	1	1	2	4
Q9D8B6	Protein FAM210B OS=Mus musculus GN=Fam210b PE=2 SV=3 - [F210B_MOUSE]	6,84	1	1	1	1
Q9JIA1	Leucine-rich glioma-inactivated protein 1 OS=Mus musculus GN=Lgi1 PE=1 SV=1 - [LGI1_MOUSE]	6,82	1	4	4	6
O54829	Regulator of G-protein signaling 7 OS=Mus musculus GN=Rgs7 PE=1 SV=2 - [RGS7_MOUSE]	6,82	2	3	3	5

Accession	Description	Σ Cover.	Σ# Prot.	Σ# Unique Pept.	Σ# Pept.	Σ# PSM
Q3TXX4	Vesicular glutamate transporter 1 OS=Mus musculus GN=Slc17a7 PE=2 SV=2 - [VGLU1_MOUSE]	6,79	1	3	3	9
P35288	Ras-related protein Rab-23 OS=Mus musculus GN=Rab23 PE=1 SV=2 - [RAB23_MOUSE]	6,75	1	1	1	4
Q9D0K2	Succinyl-CoA:3-ketoacid coenzyme A transferase 1, mitochondrial OS=Mus musculus GN=Oxct1 PE=1 SV=1 - [SCOT1_MOUSE]	6,73	1	3	3	6
O08788	Dynactin subunit 1 OS=Mus musculus GN=Dctn1 PE=1 SV=3 - [DCTN1_MOUSE]	6,71	1	8	8	13
Q91Z53	Glyoxylate reductase/hydroxypyruvate reductase OS=Mus musculus GN=Grhpr PE=1 SV=1 - [GRHPR_MOUSE]	6,71	1	1	1	1
P53986	Monocarboxylate transporter 1 OS=Mus musculus GN=Slc16a1 PE=1 SV=1 - [MOT1_MOUSE]	6,69	1	2	2	3
CON_0022 03273	SWISS-PROT:P04264 Tax_Id=9606 Gene_Symbol=KRT1 Keratin, type II cytoskeletal 1	6,68	2	4	4	4
P56399	Ubiquitin carboxyl-terminal hydrolase 5 OS=Mus musculus GN=Usp5 PE=1 SV=1 - [UBP5_MOUSE]	6,64	1	5	5	8
Q6PAM0	5'-AMP-activated protein kinase subunit beta-2 OS=Mus musculus GN=Prkab2 PE=1 SV=1 - [AAKB2_MOUSE]	6,64	1	1	1	1
P80317	T-complex protein 1 subunit zeta OS=Mus musculus GN=Cct6a PE=1 SV=3 - [TCPZ_MOUSE]	6,59	1	3	3	4
Q91XM9	Disks large homolog 2 OS=Mus musculus GN=Dlg2 PE=1 SV=2 - [DLG2_MOUSE]	6,57	1	4	4	10
Q9CQJ6	Density-regulated protein OS=Mus musculus GN=Denr PE=2 SV=1 - [DENR_MOUSE]	6,57	1	1	1	1
Q8C0E2	Vacuolar protein sorting-associated protein 26B OS=Mus musculus GN=Vps26b PE=1 SV=1 - [VP26B_MOUSE]	6,55	1	2	2	3
P14873	Microtubule-associated protein 1B OS=Mus musculus GN=Map1b PE=1 SV=2 - [MAP1B_MOUSE]	6,53	1	12	12	34
O08756	3-hydroxyacyl-CoA dehydrogenase type-2 OS=Mus musculus GN=Hsd17b10 PE=1 SV=4 - [HCD2_MOUSE]	6,51	1	1	1	14
P31648	Sodium- and chloride-dependent GABA transporter 1 OS=Mus musculus GN=Slc6a1 PE=1 SV=2 - [SC6A1_MOUSE]	6,51	1	2	2	2
O08547	Vesicle-trafficking protein SEC22b OS=Mus musculus GN=Sec22b PE=1 SV=3 - [SC22B_MOUSE]	6,51	1	1	1	4
P0C0A3	Charged multivesicular body protein 6 OS=Mus musculus GN=Chmp6 PE=2 SV=2 - [CHMP6_MOUSE]	6,50	1	1	1	6
Q03137	Ephrin type-A receptor 4 OS=Mus musculus GN=Epha4 PE=1 SV=2 - [EPHA4_MOUSE]	6,49	3	4	4	7
Q8CBE3	WD repeat-containing protein 37 OS=Mus musculus GN=Wdr37 PE=2 SV=1 - [WDR37_MOUSE]	6,45	1	2	2	3
Q6PER3	Microtubule-associated protein RP/EB family member 3 OS=Mus musculus GN=Mapre3 PE=1 SV=1 - [MARE3_MOUSE]	6,41	1	1	1	6
Q3THE2	Myosin regulatory light chain 12B OS=Mus musculus GN=Myl12b PE=1 SV=2 - [ML12B_MOUSE]	6,40	1	1	1	1
Q8R0A7	Uncharacterized protein KIAA0513 OS=Mus musculus GN=Kiaa0513 PE=2 SV=1 - [K0513_MOUSE]	6,39	1	2	2	6
Q80UG5	Septin-9 OS=Mus musculus GN=Sept9 PE=1 SV=1 - [SEPT9_MOUSE]	6,35	1	3	3	6
Q3TY60	Protein FAM131B OS=Mus musculus GN=Fam131b PE=1 SV=1 - [F131B_MOUSE]	6,33	1	1	1	2
P09671	Superoxide dismutase [Mn], mitochondrial OS=Mus musculus GN=Sod2 PE=1 SV=3 - [SODM_MOUSE]	6,31	1	1	1	5
Q99KR7	Peptidyl-prolyl cis-trans isomerase F, mitochondrial OS=Mus musculus GN=Ppif PE=1 SV=1 - [PPIF_MOUSE]	6,31	4	1	2	6
Q9CR29	Coiled-coil domain-containing protein 43 OS=Mus musculus GN=Ccdc43 PE=1 SV=1 - [CCD43_MOUSE]	6,31	1	1	1	1
P13707	Glycerol-3-phosphate dehydrogenase [NAD(+)], cytoplasmic OS=Mus musculus GN=Gpd1 PE=1 SV=3 - [GPDA_MOUSE]	6,30	1	2	2	2
Q61553	Fascin OS=Mus musculus GN=Fscn1 PE=1 SV=4 - [FSCN1_MOUSE]	6,29	1	3	3	3
Q8VD57	Vesicle transport protein SFT2B OS=Mus musculus GN=Sft2d2 PE=1 SV=1 - [SFT2B_MOUSE]	6,29	1	1	1	1
Q60864	Stress-induced-phosphoprotein 1 OS=Mus musculus GN=Stip1 PE=1 SV=1 - [STIP1_MOUSE]	6,26	1	3	3	7
Q9Z2H5	Band 4.1-like protein 1 OS=Mus musculus GN=Epb41l1 PE=1 SV=2 - [E41L1_MOUSE]	6,26	1	4	4	14
O35089	Protein cornichon homolog 2 OS=Mus musculus GN=Cnih2 PE=1 SV=2 - [CNIH2_MOUSE]	6,25	1	1	1	2
P16054	Protein kinase C epsilon type OS=Mus musculus GN=Prkce PE=1 SV=1 - [KPCE_MOUSE]	6,24	4	2	4	8
Q8BVQ5	Protein phosphatase methylesterase 1 OS=Mus musculus GN=Ppme1 PE=1 SV=5 - [PPME1_MOUSE]	6,22	1	2	2	2
Q9JJ57	Kv channel-interacting protein 1 OS=Mus musculus GN=Kcnip1 PE=2 SV=2 - [KCIP1_MOUSE]	6,17	2	1	1	1
Q03517	Secretogranin-2 OS=Mus musculus GN=Scg2 PE=1 SV=1 - [SCG2_MOUSE]	6,16	1	3	3	4
Q8BRT1	CLIP-associating protein 2 OS=Mus musculus GN=Clasp2 PE=1 SV=1 - [CLAP2_MOUSE]	6,14	1	5	5	13
Q8R001	Microtubule-associated protein RP/EB family member 2 OS=Mus musculus GN=Mapre2 PE=1 SV=1 - [MARE2_MOUSE]	6,13	1	1	1	1
Q9DBP5	UMP-CMP kinase OS=Mus musculus GN=Cmpk1 PE=1 SV=1 - [KCY_MOUSE]	6,12	1	1	1	2
O35136	Neural cell adhesion molecule 2 OS=Mus musculus GN=Ncam2 PE=1 SV=1 - [NCAM2_MOUSE]	6,09	1	5	5	9
CON_0070 57494	SWISS-PROT:Q2TBG8| Bos taurus Gene_Symbol=UCHL3 Ubiquitin carboxyl-terminal hydrolase isozyme L3	6,09	3	1	1	2
Q9ERR1	Nuclear distribution protein nudE-like 1 OS=Mus musculus GN=Ndel1 PE=1 SV=2 - [NDEL1_MOUSE]	6,09	1	2	2	2
P34884	Macrophage migration inhibitory factor OS=Mus musculus GN=Mif PE=1 SV=2 - [MIF_MOUSE]	6,09	1	1	1	2
Q62108	Disks large homolog 4 OS=Mus musculus GN=Dlg4 PE=1 SV=1 - [DLG4_MOUSE]	6,08	1	4	4	9
Q9JJG6	Transmembrane protein 47 OS=Mus musculus GN=Tmem47 PE=1 SV=1 - [TMM47_MOUSE]	6,08	1	1	1	1
Q6ZWV3	60S ribosomal protein L10 OS=Mus musculus GN=Rpl10 PE=2 SV=3 - [RL10_MOUSE]	6,07	1	1	1	2
Q9QYB8	Beta-adducin OS=Mus musculus GN=Add2 PE=1 SV=1 - [ADDB_MOUSE]	6,07	1	3	3	3
Q8K0S0	Phytanoyl-CoA hydroxylase-interacting protein OS=Mus musculus GN=Phyhip PE=1 SV=1 - [PHYIP_MOUSE]	6,06	1	2	2	3
Q9Z2U0	Proteasome subunit alpha type-7 OS=Mus musculus GN=Psma7 PE=1 SV=1 - [PSA7_MOUSE]	6,05	1	1	1	6
Q9QZB9	Dynactin subunit 5 OS=Mus musculus GN=Dctn5 PE=1 SV=1 - [DCTN5_MOUSE]	6,04	1	1	1	1
O89051	Integral membrane protein 2B OS=Mus musculus GN=Itm2b PE=1 SV=1 - [ITM2B_MOUSE]	6,02	1	1	1	1
Q91YR1	Twinfilin-1 OS=Mus musculus GN=Twf1 PE=1 SV=2 - [TWF1_MOUSE]	6,00	1	2	2	5
P26043	Radixin OS=Mus musculus GN=Rdx PE=1 SV=3 - [RADI_MOUSE]	6,00	2	1	3	5
P47802	Metaxin-1 OS=Mus musculus GN=Mtx1 PE=1 SV=1 - [MTX1_MOUSE]	5,99	1	2	2	5
P63046	Sulfotransferase 4A1 OS=Mus musculus GN=Sult4a1 PE=2 SV=1 - [ST4A1_MOUSE]	5,99	1	1	1	3
P28738	Kinesin heavy chain isoform 5C OS=Mus musculus GN=Kif5c PE=1 SV=3 - [KIF5C_MOUSE]	5,96	2	3	4	11
Q60902	Epidermal growth factor receptor substrate 15-like 1 OS=Mus musculus GN=Eps15l1 PE=1 SV=3 - [EP15R_MOUSE]	5,95	1	3	3	4
Q9JKL4	NADH dehydrogenase [ubiquinone] 1 alpha subcomplex assembly factor 3 OS=Mus musculus GN=Ndufaf3 PE=2 SV=1 - [NDUF3_MOUSE]	5,95	1	1	1	1

Accession	Description	Σ Cover.	Σ# Prot.	Σ# Unique Pept.	Σ# Pept.	Σ# PSM
Q8CHP8	Phosphoglycolate phosphatase OS=Mus musculus GN=Pgp PE=2 SV=1 - [PGP_MOUSE]	5,92	1	2	2	2
P50571	Gamma-aminobutyric acid receptor subunit beta-1 OS=Mus musculus GN=Gabrb1 PE=1 SV=1 - [GBRB1_MOUSE]	5,91	1	2	2	4
P62071	Ras-related protein R-Ras2 OS=Mus musculus GN=Rras2 PE=1 SV=1 - [RRAS2_MOUSE]	5,88	1	1	1	1
Q63810	Calcineurin subunit B type 1 OS=Mus musculus GN=Ppp3r1 PE=1 SV=3 - [CANB1_MOUSE]	5,88	1	1	1	4
Q8R0Y6	Cytosolic 10-formyltetrahydrofolate dehydrogenase OS=Mus musculus GN=Aldh1l1 PE=1 SV=1 - [AL1L1_MOUSE]	5,88	1	3	3	5
Q9JLJ2	4-trimethylaminobutyraldehyde dehydrogenase OS=Mus musculus GN=Aldh9a1 PE=1 SV=1 - [AL9A1_MOUSE]	5,87	1	2	2	4
P68037	Ubiquitin-conjugating enzyme E2 L3 OS=Mus musculus GN=Ube2l3 PE=2 SV=1 - [UB2L3_MOUSE]	5,84	1	1	1	1
P60487	Pyridoxal phosphate phosphatase OS=Mus musculus GN=Pdxp PE=1 SV=1 - [PLPP_MOUSE]	5,82	1	1	1	1
P63037	DnaJ homolog subfamily A member 1 OS=Mus musculus GN=Dnaja1 PE=1 SV=1 - [DNJA1_MOUSE]	5,79	1	2	2	2
Q91VR7	Microtubule-associated proteins 1A/1B light chain 3A OS=Mus musculus GN=Map1lc3a PE=1 SV=1 - [MLP3A_MOUSE]	5,79	2	1	1	4
Q9EQ20	Methylmalonate-semialdehyde dehydrogenase [acylating], mitochondrial OS=Mus musculus GN=Aldh6a1 PE=1 SV=1 - [MMSA_MOUSE]	5,79	1	2	2	4
CON_0001 93593	SWISS-PROT:P35527 Tax_Id=9606 Gene_Symbol=KRT9 Keratin, type I cytoskeletal 9	5,78	1	3	3	4
P20352	Tissue factor OS=Mus musculus GN=F3 PE=1 SV=2 - [TF_MOUSE]	5,78	1	1	1	1
O35927	Catenin delta-2 OS=Mus musculus GN=Ctnnd2 PE=1 SV=1 - [CTND2_MOUSE]	5,77	1	5	5	13
Q8K183	Pyridoxal kinase OS=Mus musculus GN=Pdxk PE=1 SV=1 - [PDXK_MOUSE]	5,77	1	2	2	3
P10518	Delta-aminolevulinic acid dehydratase OS=Mus musculus GN=Alad PE=1 SV=1 - [HEM2_MOUSE]	5,76	1	1	1	1
P54071	Isocitrate dehydrogenase [NADP], mitochondrial OS=Mus musculus GN=Idh2 PE=1 SV=3 - [IDHP_MOUSE]	5,75	1	2	2	2
P60469	Liprin-alpha-3 OS=Mus musculus GN=Ppfia3 PE=1 SV=1 - [LIPA3_MOUSE]	5,75	1	4	4	7
Q80Z24	Neuronal growth regulator 1 OS=Mus musculus GN=Negr1 PE=1 SV=1 - [NEGR1_MOUSE]	5,75	1	1	1	2
Q925I1	ATPase family AAA domain-containing protein 3 OS=Mus musculus GN=Atad3 PE=1 SV=1 - [ATAD3_MOUSE]	5,75	1	2	2	4
Q62277	Synaptophysin OS=Mus musculus GN=Syp PE=1 SV=2 - [SYPH_MOUSE]	5,73	1	2	2	18
Q8BSZ2	AP-3 complex subunit sigma-2 OS=Mus musculus GN=Ap3s2 PE=1 SV=1 - [AP3S2_MOUSE]	5,70	1	1	1	1
Q8BLE7	Vesicular glutamate transporter 2 OS=Mus musculus GN=Slc17a6 PE=1 SV=1 - [VGLU2_MOUSE]	5,67	1	2	2	8
Q78IK4	Apolipoprotein O-like OS=Mus musculus GN=Apool PE=2 SV=1 - [APOOL_MOUSE]	5,66	1	1	1	3
Q9CQI6	Coactosin-like protein OS=Mus musculus GN=Cotl1 PE=1 SV=3 - [COTL1_MOUSE]	5,63	1	1	1	2
Q921H9	Sel1 repeat-containing protein 1 OS=Mus musculus GN=Selrc1 PE=2 SV=1 - [SELR1_MOUSE]	5,63	1	1	1	2
Q9Z0S6	Claudin-10 OS=Mus musculus GN=Cldn10 PE=1 SV=2 - [CLD10_MOUSE]	5,63	1	1	1	3
Q99JR1	Sideroflexin-1 OS=Mus musculus GN=Sfxn1 PE=1 SV=3 - [SFXN1_MOUSE]	5,59	1	1	1	3
Q9CQD1	Ras-related protein Rab-5A OS=Mus musculus GN=Rab5a PE=1 SV=1 - [RAB5A_MOUSE]	5,58	1	1	1	4
Q9QYJ0	DnaJ homolog subfamily A member 2 OS=Mus musculus GN=Dnaja2 PE=1 SV=1 - [DNJA2_MOUSE]	5,58	1	2	2	2
Q8BG39	Synaptic vesicle glycoprotein 2B OS=Mus musculus GN=Sv2b PE=1 SV=1 - [SV2B_MOUSE]	5,56	1	3	4	22
Q9QYA2	Mitochondrial import receptor subunit TOM40 homolog OS=Mus musculus GN=Tomm40 PE=1 SV=3 - [TOM40_MOUSE]	5,54	1	2	2	2
O35857	Mitochondrial import inner membrane translocase subunit TIM44 OS=Mus musculus GN=Timm44 PE=2 SV=2 - [TIM44_MOUSE]	5,53	1	2	3	5
P61255	60S ribosomal protein L26 OS=Mus musculus GN=Rpl26 PE=2 SV=1 - [RL26_MOUSE]	5,52	1	1	1	1
O35633	Vesicular inhibitory amino acid transporter OS=Mus musculus GN=Slc32a1 PE=1 SV=3 - [VIAAT_MOUSE]	5,52	2	1	2	4
Q6R891	Neurabin-2 OS=Mus musculus GN=Ppp1r9b PE=1 SV=1 - [NEB2_MOUSE]	5,51	1	3	3	4
O88696	Putative ATP-dependent Clp protease proteolytic subunit, mitochondrial OS=Mus musculus GN=Clpp PE=2 SV=1 - [CLPP_MOUSE]	5,51	1	1	1	3
P09103	Protein disulfide-isomerase OS=Mus musculus GN=P4hb PE=1 SV=2 - [PDIA1_MOUSE]	5,50	1	2	2	5
Q9WUA3	6-phosphofructokinase type C OS=Mus musculus GN=Pfkp PE=1 SV=1 - [K6PP_MOUSE]	5,48	2	3	3	11
Q5FWK3	Rho GTPase-activating protein 1 OS=Mus musculus GN=Arhgap1 PE=1 SV=1 - [RHG01_MOUSE]	5,47	1	1	1	1
Q922J6	Tetraspanin-2 OS=Mus musculus GN=Tspan2 PE=1 SV=1 - [TSN2_MOUSE]	5,43	1	1	1	8
Q9JHI5	Isovaleryl-CoA dehydrogenase, mitochondrial OS=Mus musculus GN=Ivd PE=1 SV=1 - [IVD_MOUSE]	5,42	1	2	2	3
O35658	Complement component 1 Q subcomponent-binding protein, mitochondrial OS=Mus musculus GN=C1qbp PE=1 SV=1 - [C1QBP_MOUSE]	5,40	1	1	1	1
P39688	Tyrosine-protein kinase Fyn OS=Mus musculus GN=Fyn PE=1 SV=4 - [FYN_MOUSE]	5,40	5	3	3	3
Q8VHI6	Wiskott-Aldrich syndrome protein family member 3 OS=Mus musculus GN=Wasf3 PE=2 SV=1 - [WASF3_MOUSE]	5,39	1	1	2	7
CON_0070 61422	SWISS-PROT:A7MBJ5| Bos taurus Gene_Symbol=CAND1 Cullin-associated NEDD8-dissociated protein 1	5,37	2	6	6	8
Q60737	Casein kinase II subunit alpha OS=Mus musculus GN=Csnk2a1 PE=1 SV=2 - [CSK21_MOUSE]	5,37	3	1	2	2
P14824	Annexin A6 OS=Mus musculus GN=Anxa6 PE=1 SV=3 - [ANXA6_MOUSE]	5,35	1	3	3	5
O35621	Phosphomannomutase 1 OS=Mus musculus GN=Pmm1 PE=1 SV=1 - [PMM1_MOUSE]	5,34	1	1	1	3
Q91YJ2	Sorting nexin-4 OS=Mus musculus GN=Snx4 PE=2 SV=1 - [SNX4_MOUSE]	5,33	1	2	2	3
Q9R0P3	S-formylglutathione hydrolase OS=Mus musculus GN=Esd PE=2 SV=1 - [ESTD_MOUSE]	5,32	1	1	1	3
Q61768	Kinesin-1 heavy chain OS=Mus musculus GN=Kif5b PE=1 SV=3 - [KINH_MOUSE]	5,30	2	3	4	9
Q9D1M0	Protein SEC13 homolog OS=Mus musculus GN=Sec13 PE=2 SV=3 - [SEC13_MOUSE]	5,28	1	1	1	1
Q8BGN8	Synaptoporin OS=Mus musculus GN=Synpr PE=1 SV=1 - [SYNPR_MOUSE]	5,28	1	1	1	2
P63137	Gamma-aminobutyric acid receptor subunit beta-2 OS=Mus musculus GN=Gabrb2 PE=1 SV=2 - [GBRB2_MOUSE]	5,27	1	2	2	3
Q9Z127	Large neutral amino acids transporter small subunit 1 OS=Mus musculus GN=Slc7a5 PE=1 SV=2 - [LAT1_MOUSE]	5,27	1	2	2	5
P47753	F-actin-capping protein subunit alpha-1 OS=Mus musculus GN=Capza1 PE=1 SV=4 - [CAZA1_MOUSE]	5,24	1	1	1	1
Q9WUK2	Eukaryotic translation initiation factor 4H OS=Mus musculus GN=Eif4h PE=1 SV=3 - [IF4H_MOUSE]	5,24	1	1	1	2
Q8BJI1	Sodium-dependent neutral amino acid transporter SLC6A17 OS=Mus musculus GN=Slc6a17 PE=1 SV=1 - [S6A17_MOUSE]	5,23	1	3	3	6
Q9QYR6	Microtubule-associated protein 1A OS=Mus musculus GN=Map1a PE=1 SV=2 - [MAP1A_MOUSE]	5,22	1	10	10	17

Accession	Description	Σ Cover.	Σ# Prot.	Σ# Unique Pept.	Σ# Pept.	Σ# PSM
Q9Z218	Dipeptidyl aminopeptidase-like protein 6 OS=Mus musculus GN=Dpp6 PE=1 SV=1 - [DPP6_MOUSE]	5,22	1	2	3	3
Q9D819	Inorganic pyrophosphatase OS=Mus musculus GN=Ppa1 PE=1 SV=1 - [IPYR_MOUSE]	5,19	1	1	1	4
Q61036	Serine/threonine-protein kinase PAK 3 OS=Mus musculus GN=Pak3 PE=1 SV=2 - [PAK3_MOUSE]	5,19	1	1	2	3
Q6NZL0	Protein SOGA3 OS=Mus musculus GN=Soga3 PE=2 SV=2 - [SOGA3_MOUSE]	5,19	3	4	4	4
Q8CDN6	Thioredoxin-like protein 1 OS=Mus musculus GN=Txnl1 PE=1 SV=3 - [TXNL1_MOUSE]	5,19	1	1	1	1
Q9QYX7	Protein piccolo OS=Mus musculus GN=Pclo PE=1 SV=4 - [PCLO_MOUSE]	5,19	1	21	22	35
Q9QUI0	Transforming protein RhoA OS=Mus musculus GN=Rhoa PE=1 SV=1 - [RHOA_MOUSE]	5,18	1	1	1	2
Q8BH58	TIP41-like protein OS=Mus musculus GN=Tiprl PE=2 SV=1 - [TIPRL_MOUSE]	5,17	1	1	1	1
P80313	T-complex protein 1 subunit eta OS=Mus musculus GN=Cct7 PE=1 SV=1 - [TCPH_MOUSE]	5,15	1	2	2	4
Q61490	CD166 antigen OS=Mus musculus GN=Alcam PE=1 SV=3 - [CD166_MOUSE]	5,15	1	3	3	6
Q9CR84	ATP synthase lipid-binding protein, mitochondrial OS=Mus musculus GN=Atp5g1 PE=2 SV=1 - [AT5G1_MOUSE]	5,15	3	1	1	4
Q8R0S2	IQ motif and SEC7 domain-containing protein 1 OS=Mus musculus GN=Iqsec1 PE=1 SV=2 - [IQEC1_MOUSE]	5,10	1	3	3	4
Q91V14	Solute carrier family 12 member 5 OS=Mus musculus GN=Slc12a5 PE=1 SV=2 - [S12A5_MOUSE]	5,10	3	5	5	14
Q5U3K5	Rab-like protein 6 OS=Mus musculus GN=Rabl6 PE=1 SV=2 - [RABL6_MOUSE]	5,10	1	3	3	5
Q9ERI6	Retinol dehydrogenase 14 OS=Mus musculus GN=Rdh14 PE=1 SV=1 - [RDH14_MOUSE]	5,09	1	1	1	1
O70325	Phospholipid hydroperoxide glutathione peroxidase, mitochondrial OS=Mus musculus GN=Gpx4 PE=1 SV=4 - [GPX41_MOUSE]	5,08	2	1	1	1
Q9CZW5	Mitochondrial import receptor subunit TOM70 OS=Mus musculus GN=Tomm70a PE=1 SV=2 - [TOM70_MOUSE]	5,07	1	4	4	5
Q9CR98	Protein FAM136A OS=Mus musculus GN=Fam136a PE=1 SV=1 - [F136A_MOUSE]	5,07	1	1	1	4
P32037	Solute carrier family 2, facilitated glucose transporter member 3 OS=Mus musculus GN=Slc2a3 PE=1 SV=1 - [GTR3_MOUSE]	5,07	1	2	2	6
P16388	Potassium voltage-gated channel subfamily A member 1 OS=Mus musculus GN=Kcna1 PE=1 SV=1 - [KCNA1_MOUSE]	5,05	1	2	2	2
Q9JHU4	Cytoplasmic dynein 1 heavy chain 1 OS=Mus musculus GN=Dync1h1 PE=1 SV=2 - [DYHC1_MOUSE]	5,00	1	18	18	39
Q8BW75	Amine oxidase [flavin-containing] B OS=Mus musculus GN=Maob PE=1 SV=4 - [AOFB_MOUSE]	5,00	1	2	2	3
P12367	cAMP-dependent protein kinase type II-alpha regulatory subunit OS=Mus musculus GN=Prkar2a PE=1 SV=2 - [KAP2_MOUSE]	4,99	1	1	1	2
O55126	Protein NipSnap homolog 2 OS=Mus musculus GN=Gbas PE=2 SV=1 - [NIPS2_MOUSE]	4,98	1	1	1	4
P42669	Transcriptional activator protein Pur-alpha OS=Mus musculus GN=Pura PE=1 SV=1 - [PURA_MOUSE]	4,98	2	1	2	2
P56564	Excitatory amino acid transporter 1 OS=Mus musculus GN=Slc1a3 PE=1 SV=2 - [EAA1_MOUSE]	4,97	2	3	3	31
Q91ZA3	Propionyl-CoA carboxylase alpha chain, mitochondrial OS=Mus musculus GN=Pcca PE=2 SV=2 - [PCCA_MOUSE]	4,97	1	2	2	3
Q9CZ42	ATP-dependent (S)-NAD(P)H-hydrate dehydratase OS=Mus musculus GN=Carkd PE=1 SV=1 - [NNRD_MOUSE]	4,96	1	1	1	2
P62702	40S ribosomal protein S4, X isoform OS=Mus musculus GN=Rps4x PE=2 SV=2 - [RS4X_MOUSE]	4,94	1	1	1	1
Q9Z0E0	Neurochondrin OS=Mus musculus GN=Ncdn PE=1 SV=1 - [NCDN_MOUSE]	4,94	1	4	4	6
Q9QY76	Vesicle-associated membrane protein-associated protein B OS=Mus musculus GN=Vapb PE=2 SV=3 - [VAPB_MOUSE]	4,94	1	1	1	1
Q8C4Q6	Axin interactor, dorsalization-associated protein OS=Mus musculus GN=Aida PE=1 SV=1 - [AIDA_MOUSE]	4,92	1	1	1	1
P48774	Glutathione S-transferase Mu 5 OS=Mus musculus GN=Gstm5 PE=1 SV=1 - [GSTM5_MOUSE]	4,91	1	1	1	3
Q62393	Tumor protein D52 OS=Mus musculus GN=Tpd52 PE=1 SV=2 - [TPD52_MOUSE]	4,91	1	1	1	2
P12970	60S ribosomal protein L7a OS=Mus musculus GN=Rpl7a PE=2 SV=2 - [RL7A_MOUSE]	4,89	1	1	1	1
P08003	Protein disulfide-isomerase A4 OS=Mus musculus GN=Pdia4 PE=1 SV=3 - [PDIA4_MOUSE]	4,86	1	2	2	5
Q9R0Q6	Actin-related protein 2/3 complex subunit 1A OS=Mus musculus GN=Arpc1a PE=1 SV=1 - [ARC1A_MOUSE]	4,86	1	2	2	2
Q8C996	Transmembrane protein 163 OS=Mus musculus GN=Tmem163 PE=1 SV=1 - [TM163_MOUSE]	4,86	1	1	1	2
Q9Z140	Copine-6 OS=Mus musculus GN=Cpne6 PE=1 SV=1 - [CPNE6_MOUSE]	4,85	1	2	2	8
Q6P9K8	Caskin-1 OS=Mus musculus GN=Caskin1 PE=1 SV=2 - [CSKI1_MOUSE]	4,82	1	5	5	17
Q9JME5	AP-3 complex subunit beta-2 OS=Mus musculus GN=Ap3b2 PE=1 SV=2 - [AP3B2_MOUSE]	4,81	1	4	4	11
P80316	T-complex protein 1 subunit epsilon OS=Mus musculus GN=Cct5 PE=1 SV=1 - [TCPE_MOUSE]	4,81	1	2	2	5
Q6PFD5	Disks large-associated protein 3 OS=Mus musculus GN=Dlgap3 PE=1 SV=1 - [DLGP3_MOUSE]	4,81	1	2	3	9
Q9R062	Glycogenin-1 OS=Mus musculus GN=Gyg1 PE=2 SV=3 - [GLYG_MOUSE]	4,80	1	1	1	1
Q9EQF6	Dihydropyrimidinase-related protein 5 OS=Mus musculus GN=Dpysl5 PE=1 SV=1 - [DPYL5_MOUSE]	4,79	1	2	2	3
Q9CQA1	Trafficking protein particle complex subunit 5 OS=Mus musculus GN=Trappc5 PE=1 SV=1 - [TPPC5_MOUSE]	4,79	1	1	1	1
P49615	Cyclin-dependent kinase 5 OS=Mus musculus GN=Cdk5 PE=1 SV=1 - [CDK5_MOUSE]	4,79	1	1	1	2
P53702	Cytochrome c-type heme lyase OS=Mus musculus GN=Hccs PE=1 SV=2 - [CCHL_MOUSE]	4,78	1	1	1	1
Q6NXK7	Inactive dipeptidyl peptidase 10 OS=Mus musculus GN=Dpp10 PE=2 SV=1 - [DPP10_MOUSE]	4,77	1	4	4	6
P63085	Mitogen-activated protein kinase 1 OS=Mus musculus GN=Mapk1 PE=1 SV=3 - [MK01_MOUSE]	4,75	11	2	2	2
P62631	Elongation factor 1-alpha 2 OS=Mus musculus GN=Eef1a2 PE=1 SV=1 - [EF1A2_MOUSE]	4,75	1	1	2	13
P26231	Catenin alpha-1 OS=Mus musculus GN=Ctnna1 PE=1 SV=1 - [CTNA1_MOUSE]	4,75	1	1	3	8
G5E8K5	Ankyrin-3 OS=Mus musculus GN=Ank3 PE=1 SV=1 - [ANK3_MOUSE]	4,74	1	7	7	9
Q61831	Mitogen-activated protein kinase 10 OS=Mus musculus GN=Mapk10 PE=1 SV=2 - [MK10_MOUSE]	4,74	2	2	2	2
Q2PFD7	PH and SEC7 domain-containing protein 3 OS=Mus musculus GN=Psd3 PE=1 SV=2 - [PSD3_MOUSE]	4,73	1	4	4	4
Q9QZX7	Serine racemase OS=Mus musculus GN=Srr PE=1 SV=1 - [SRR_MOUSE]	4,72	1	1	1	4
P49722	Proteasome subunit alpha type-2 OS=Mus musculus GN=Psma2 PE=1 SV=3 - [PSA2_MOUSE]	4,70	1	1	1	1
Q7TNR6	Immunoglobulin superfamily member 21 OS=Mus musculus GN=Igsf21 PE=2 SV=1 - [IGS21_MOUSE]	4,70	1	2	2	2
O55023	Inositol monophosphatase 1 OS=Mus musculus GN=Impa1 PE=1 SV=1 - [IMPA1_MOUSE]	4,69	1	1	1	3
Q8BUV3	Gephyrin OS=Mus musculus GN=Gphn PE=1 SV=2 - [GEPH_MOUSE]	4,68	1	3	3	5

Accession	Description	Σ Cover.	Σ# Prot.	Σ# Unique Pept.	Σ# Pept.	Σ# PSM
P51174	Long-chain specific acyl-CoA dehydrogenase, mitochondrial OS=Mus musculus GN=Acadl PE=2 SV=2 - [ACADL_MOUSE]	4,65	1	1	1	1
Q9DCJ5	NADH dehydrogenase [ubiquinone] 1 alpha subcomplex subunit 8 OS=Mus musculus GN=Ndufa8 PE=1 SV=3 - [NDUA8_MOUSE]	4,65	1	1	1	4
Q99JY0	Trifunctional enzyme subunit beta, mitochondrial OS=Mus musculus GN=Hadhb PE=1 SV=1 - [ECHB_MOUSE]	4,63	1	2	2	5
Q9CYT6	Adenylyl cyclase-associated protein 2 OS=Mus musculus GN=Cap2 PE=1 SV=1 - [CAP2_MOUSE]	4,62	1	2	2	2
Q8BIZ1	Ankyrin repeat and sterile alpha motif domain-containing protein 1B OS=Mus musculus GN=Anks1b PE=1 SV=3 - [ANS1B_MOUSE]	4,61	2	5	5	14
P70336	Rho-associated protein kinase 2 OS=Mus musculus GN=Rock2 PE=1 SV=1 - [ROCK2_MOUSE]	4,61	2	6	6	11
Q99LP6	GrpE protein homolog 1, mitochondrial OS=Mus musculus GN=Grpel1 PE=1 SV=1 - [GRPE1_MOUSE]	4,61	1	1	1	1
P12658	Calbindin OS=Mus musculus GN=Calb1 PE=1 SV=2 - [CALB1_MOUSE]	4,60	1	1	1	1
Q8C437	PEX5-related protein OS=Mus musculus GN=Pex5l PE=1 SV=2 - [PEX5R_MOUSE]	4,59	1	2	2	2
Q6X893	Choline transporter-like protein 1 OS=Mus musculus GN=Slc44a1 PE=1 SV=3 - [CTL1_MOUSE]	4,59	1	3	3	4
Q05920	Pyruvate carboxylase, mitochondrial OS=Mus musculus GN=Pc PE=1 SV=1 - [PYC_MOUSE]	4,58	1	5	5	8
Q8BIG7	Catechol O-methyltransferase domain-containing protein 1 OS=Mus musculus GN=Comtd1 PE=2 SV=1 - [CMTD1_MOUSE]	4,58	1	1	1	3
Q9JM96	Cdc42 effector protein 4 OS=Mus musculus GN=Cdc42ep4 PE=1 SV=1 - [BORG4_MOUSE]	4,58	1	1	1	1
Q80TB8	Synaptic vesicle membrane protein VAT-1 homolog-like OS=Mus musculus GN=Vat1l PE=2 SV=2 - [VAT1L_MOUSE]	4,56	1	2	2	3
P62881	Guanine nucleotide-binding protein subunit beta-5 OS=Mus musculus GN=Gnb5 PE=1 SV=1 - [GBB5_MOUSE]	4,56	1	1	1	4
P62192	26S protease regulatory subunit 4 OS=Mus musculus GN=Psmc1 PE=1 SV=1 - [PRS4_MOUSE]	4,55	1	1	1	1
P28474	Alcohol dehydrogenase class-3 OS=Mus musculus GN=Adh5 PE=1 SV=3 - [ADHX_MOUSE]	4,55	1	1	1	1
Q9CQW1	Synaptobrevin homolog YKT6 OS=Mus musculus GN=Ykt6 PE=2 SV=1 - [YKT6_MOUSE]	4,55	1	1	1	1
Q9CZP5	Mitochondrial chaperone BCS1 OS=Mus musculus GN=Bcs1l PE=1 SV=1 - [BCS1_MOUSE]	4,55	1	2	2	2
Q07076	Annexin A7 OS=Mus musculus GN=Anxa7 PE=2 SV=2 - [ANXA7_MOUSE]	4,54	1	2	2	2
P08226	Apolipoprotein E OS=Mus musculus GN=Apoe PE=1 SV=2 - [APOE_MOUSE]	4,50	1	1	1	3
P0DI97	Neurexin-1-beta OS=Mus musculus GN=Nrxn1 PE=1 SV=1 - [NRX1B_MOUSE]	4,49	2	1	1	2
Q9WUR9	GTP:AMP phosphotransferase AK4, mitochondrial OS=Mus musculus GN=Ak4 PE=2 SV=1 - [KAD4_MOUSE]	4,48	1	1	1	1
Q9R0Q3	Transmembrane emp24 domain-containing protein 2 OS=Mus musculus GN=Tmed2 PE=1 SV=1 - [TMED2_MOUSE]	4,48	1	1	1	1
Q8VD37	SH3-containing GRB2-like protein 3-interacting protein 1 OS=Mus musculus GN=Sgip1 PE=1 SV=1 - [SGIP1_MOUSE]	4,47	1	3	3	6
Q8K212	Phosphofurin acidic cluster sorting protein 1 OS=Mus musculus GN=Pacs1 PE=1 SV=2 - [PACS1_MOUSE]	4,47	1	2	2	5
Q9CXI5	Mesencephalic astrocyte-derived neurotrophic factor OS=Mus musculus GN=Manf PE=1 SV=1 - [MANF_MOUSE]	4,47	1	1	1	1
Q9CX34	Suppressor of G2 allele of SKP1 homolog OS=Mus musculus GN=Sugt1 PE=2 SV=3 - [SUGT1_MOUSE]	4,46	1	1	1	1
Q9R1V7	Disintegrin and metalloproteinase domain-containing protein 23 OS=Mus musculus GN=Adam23 PE=1 SV=1 - [ADA23_MOUSE]	4,46	1	2	2	6
Q921C1	Gap junction gamma-3 protein OS=Mus musculus GN=Gjc3 PE=2 SV=2 - [CXG3_MOUSE]	4,46	1	1	1	3
O35381	Acidic leucine-rich nuclear phosphoprotein 32 family member A OS=Mus musculus GN=Anp32a PE=1 SV=1 - [AN32A_MOUSE]	4,45	1	1	1	3
P07724	Serum albumin OS=Mus musculus GN=Alb PE=1 SV=3 - [ALBU_MOUSE]	4,44	1	2	2	3
O88447	Kinesin light chain 1 OS=Mus musculus GN=Klc1 PE=1 SV=3 - [KLC1_MOUSE]	4,44	1	2	2	4
P70429	Ena/VASP-like protein OS=Mus musculus GN=Evl PE=1 SV=2 - [EVL_MOUSE]	4,35	1	1	1	2
Q8BHN3	Neutral alpha-glucosidase AB OS=Mus musculus GN=Ganab PE=1 SV=1 - [GANAB_MOUSE]	4,34	1	3	3	4
P62242	40S ribosomal protein S8 OS=Mus musculus GN=Rps8 PE=1 SV=2 - [RS8_MOUSE]	4,33	1	1	1	1
P31938	Dual specificity mitogen-activated protein kinase kinase 1 OS=Mus musculus GN=Map2k1 PE=1 SV=2 - [MP2K1_MOUSE]	4,33	1	2	2	2
Q8VCD6	Receptor expression-enhancing protein 2 OS=Mus musculus GN=Reep2 PE=2 SV=2 - [REEP2_MOUSE]	4,33	1	1	1	1
Q8R317	Ubiquilin-1 OS=Mus musculus GN=Ubqln1 PE=1 SV=1 - [UBQL1_MOUSE]	4,30	1	1	1	3
O35459	Delta(3,5)-Delta(2,4)-dienoyl-CoA isomerase, mitochondrial OS=Mus musculus GN=Ech1 PE=2 SV=1 - [ECH1_MOUSE]	4,28	1	1	1	1
Q5RJI5	Serine/threonine-protein kinase BRSK1 OS=Mus musculus GN=Brsk1 PE=1 SV=1 - [BRSK1_MOUSE]	4,24	1	2	2	5
Q9D1T0	Leucine-rich repeat and immunoglobulin-like domain-containing nogo receptor-interacting protein 1 OS=Mus musculus GN=Lingo1 PE=1 SV=1 - [LIGO1_MOUSE]	4,23	1	2	2	3
Q3UGC7	Eukaryotic translation initiation factor 3 subunit J-A OS=Mus musculus GN=Eif3j1 PE=2 SV=1 - [EI3JA_MOUSE]	4,21	2	1	1	2
Q9R257	Heme-binding protein 1 OS=Mus musculus GN=Hebp1 PE=1 SV=2 - [HEBP1_MOUSE]	4,21	1	1	1	1
O88741	Ganglioside-induced differentiation-associated protein 1 OS=Mus musculus GN=Gdap1 PE=1 SV=1 - [GDAP1_MOUSE]	4,19	1	1	1	4
Q9D8W5	26S proteasome non-ATPase regulatory subunit 12 OS=Mus musculus GN=Psmd12 PE=1 SV=4 - [PSD12_MOUSE]	4,17	1	1	1	5
Q9D832	DnaJ homolog subfamily B member 4 OS=Mus musculus GN=Dnajb4 PE=2 SV=1 - [DNJB4_MOUSE]	4,15	1	1	1	1
Q9QZH6	Evolutionarily conserved signaling intermediate in Toll pathway, mitochondrial OS=Mus musculus GN=Ecsit PE=1 SV=2 - [ECSIT_MOUSE]	4,14	1	1	1	1
P11983	T-complex protein 1 subunit alpha OS=Mus musculus GN=Tcp1 PE=1 SV=3 - [TCPA_MOUSE]	4,14	1	2	2	3
P19246	Neurofilament heavy polypeptide OS=Mus musculus GN=Nefh PE=1 SV=3 - [NFH_MOUSE]	4,13	4	3	4	8
Q9D2P8	Myelin-associated oligodendrocyte basic protein OS=Mus musculus GN=Mobp PE=1 SV=1 - [MOBP_MOUSE]	4,12	1	1	1	1
O70589	Peripheral plasma membrane protein CASK OS=Mus musculus GN=Cask PE=1 SV=2 - [CSKP_MOUSE]	4,10	1	3	3	5
Q9QYS2	Metabotropic glutamate receptor 3 OS=Mus musculus GN=Grm3 PE=2 SV=1 - [GRM3_MOUSE]	4,10	2	3	3	6
Q9WTR5	Cadherin-13 OS=Mus musculus GN=Cdh13 PE=1 SV=2 - [CAD13_MOUSE]	4,06	1	2	2	6
P52196	Thiosulfate sulfurtransferase OS=Mus musculus GN=Tst PE=1 SV=3 - [THTR_MOUSE]	4,04	1	1	1	1
P49442	Inositol polyphosphate 1-phosphatase OS=Mus musculus GN=Inpp1 PE=1 SV=2 - [INPP_MOUSE]	4,04	1	1	1	2

Accession	Description	Σ Cover.	Σ# Prot.	Σ# Unique Pept.	Σ# Pept.	Σ# PSM
Q60598	Src substrate cortactin OS=Mus musculus GN=Cttn PE=1 SV=2 - [SRC8_MOUSE]	4,03	1	2	2	4
Q99NE5	Regulating synaptic membrane exocytosis protein 1 OS=Mus musculus GN=Rims1 PE=1 SV=2 - [RIMS1_MOUSE]	4,03	1	4	4	10
P58389	Serine/threonine-protein phosphatase 2A activator OS=Mus musculus GN=Ppp2r4 PE=1 SV=1 - [PTPA_MOUSE]	4,02	1	1	1	1
Q80TA1	Ethanolaminephosphotransferase 1 OS=Mus musculus GN=Ept1 PE=2 SV=3 - [EPT1_MOUSE]	4,02	1	1	1	1
Q8BHK1	Magnesium transporter NIPA1 OS=Mus musculus GN=Nipa1 PE=1 SV=1 - [NIPA1_MOUSE]	4,02	1	1	1	1
Q9CZR8	Elongation factor Ts, mitochondrial OS=Mus musculus GN=Tsfm PE=2 SV=1 - [EFTS_MOUSE]	4,01	1	1	1	1
Q8CGK3	Lon protease homolog, mitochondrial OS=Mus musculus GN=Lonp1 PE=1 SV=2 - [LONM_MOUSE]	4,00	1	3	3	7
Q8R3V5	Endophilin-B2 OS=Mus musculus GN=Sh3glb2 PE=2 SV=2 - [SHLB2_MOUSE]	4,00	2	2	2	11
Q80WM4	Hyaluronan and proteoglycan link protein 4 OS=Mus musculus GN=Hapln4 PE=2 SV=2 - [HPLN4_MOUSE]	4,00	1	1	1	1
Q00493	Carboxypeptidase E OS=Mus musculus GN=Cpe PE=1 SV=2 - [CBPE_MOUSE]	3,99	1	2	2	3
P20917	Myelin-associated glycoprotein OS=Mus musculus GN=Mag PE=1 SV=2 - [MAG_MOUSE]	3,99	1	3	3	3
Q811D0	Disks large homolog 1 OS=Mus musculus GN=Dlg1 PE=1 SV=1 - [DLG1_MOUSE]	3,98	1	3	3	9
P27601	Guanine nucleotide-binding protein subunit alpha-13 OS=Mus musculus GN=Gna13 PE=1 SV=1 - [GNA13_MOUSE]	3,98	3	1	2	5
Q80WJ7	Protein LYRIC OS=Mus musculus GN=Mtdh PE=1 SV=1 - [LYRIC_MOUSE]	3,97	1	2	2	3
O08663	Methionine aminopeptidase 2 OS=Mus musculus GN=Metap2 PE=1 SV=1 - [AMPM2_MOUSE]	3,97	1	1	1	2
Q61699	Heat shock protein 105 kDa OS=Mus musculus GN=Hsph1 PE=1 SV=2 - [HS105_MOUSE]	3,96	1	3	3	5
Q9D8U8	Sorting nexin-5 OS=Mus musculus GN=Snx5 PE=1 SV=1 - [SNX5_MOUSE]	3,96	1	1	1	1
O88704	Potassium/sodium hyperpolarization-activated cyclic nucleotide-gated channel 1 OS=Mus musculus GN=Hcn1 PE=1 SV=1 - [HCN1_MOUSE]	3,96	1	2	2	3
Q8BXZ1	Protein disulfide-isomerase TMX3 OS=Mus musculus GN=Tmx3 PE=1 SV=2 - [TMX3_MOUSE]	3,95	1	1	1	1
P12849	cAMP-dependent protein kinase type I-beta regulatory subunit OS=Mus musculus GN=Prkar1b PE=2 SV=2 - [KAP1_MOUSE]	3,94	1	1	1	1
Q9JM76	Actin-related protein 2/3 complex subunit 3 OS=Mus musculus GN=Arpc3 PE=1 SV=3 - [ARPC3_MOUSE]	3,93	1	1	1	1
Q9JKV1	Proteasomal ubiquitin receptor ADRM1 OS=Mus musculus GN=Adrm1 PE=1 SV=2 - [ADRM1_MOUSE]	3,93	1	1	1	1
P27612	Phospholipase A-2-activating protein OS=Mus musculus GN=Plaa PE=2 SV=4 - [PLAP_MOUSE]	3,90	1	2	2	2
Q80TE7	Leucine-rich repeat-containing protein 7 OS=Mus musculus GN=Lrrc7 PE=1 SV=2 - [LRRC7_MOUSE]	3,89	1	4	4	5
Q8WTY4	Anamorsin OS=Mus musculus GN=Ciapin1 PE=1 SV=1 - [CPIN1_MOUSE]	3,88	1	1	1	1
Q8CAA7	Glucose 1,6-bisphosphate synthase OS=Mus musculus GN=Pgm2l1 PE=1 SV=1 - [PGM2L_MOUSE]	3,86	1	2	2	7
Q922H2	[Pyruvate dehydrogenase (acetyl-transferring)] kinase isozyme 3, mitochondrial OS=Mus musculus GN=Pdk3 PE=2 SV=1 - [PDK3_MOUSE]	3,86	1	1	1	4
Q99JT2	Serine/threonine-protein kinase MST4 OS=Mus musculus GN=Mst4 PE=2 SV=1 - [MST4_MOUSE]	3,85	3	1	1	2
Q91W90	Thioredoxin domain-containing protein 5 OS=Mus musculus GN=Txndc5 PE=1 SV=2 - [TXND5_MOUSE]	3,84	1	1	1	1
Q641P0	Actin-related protein 3B OS=Mus musculus GN=Actr3b PE=2 SV=1 - [ARP3B_MOUSE]	3,83	1	1	2	2
Q80U63	Mitofusin-2 OS=Mus musculus GN=Mfn2 PE=1 SV=3 - [MFN2_MOUSE]	3,83	1	2	2	2
P27546	Microtubule-associated protein 4 OS=Mus musculus GN=Map4 PE=1 SV=3 - [MAP4_MOUSE]	3,82	1	4	4	7
Q8CIN4	Serine/threonine-protein kinase PAK 2 OS=Mus musculus GN=Pak2 PE=1 SV=1 - [PAK2_MOUSE]	3,82	1	1	1	2
P28660	Nck-associated protein 1 OS=Mus musculus GN=Nckap1 PE=1 SV=2 - [NCKP1_MOUSE]	3,81	1	4	4	7
P17563	Selenium-binding protein 1 OS=Mus musculus GN=Selenbp1 PE=1 SV=2 - [SBP1_MOUSE]	3,81	2	1	1	2
Q8BH95	Enoyl-CoA hydratase, mitochondrial OS=Mus musculus GN=Echs1 PE=1 SV=1 - [ECHM_MOUSE]	3,79	1	1	1	1
Q99L47	Hsc70-interacting protein OS=Mus musculus GN=St13 PE=1 SV=1 - [F10A1_MOUSE]	3,77	1	1	1	4
Q9DCS3	Trans-2-enoyl-CoA reductase, mitochondrial OS=Mus musculus GN=Mecr PE=2 SV=2 - [MECR_MOUSE]	3,75	1	1	1	1
B1AXV0	DOMON domain-containing protein FRRS1L OS=Mus musculus GN=Frrs1l PE=1 SV=1 - [FRS1L_MOUSE]	3,75	1	1	1	1
Q8R5J9	PRA1 family protein 3 OS=Mus musculus GN=Arl6ip5 PE=1 SV=2 - [PRAF3_MOUSE]	3,72	1	1	1	1
Q9CYN9	Renin receptor OS=Mus musculus GN=Atp6ap2 PE=2 SV=2 - [RENR_MOUSE]	3,71	1	1	1	4
Q9WVE8	Protein kinase C and casein kinase substrate in neurons protein 2 OS=Mus musculus GN=Pacsin2 PE=1 SV=1 - [PACN2_MOUSE]	3,70	1	1	2	3
Q9JII6	Alcohol dehydrogenase [NADP(+)] OS=Mus musculus GN=Akr1a1 PE=1 SV=3 - [AK1A1_MOUSE]	3,69	1	1	1	1
Q9CYH2	Redox-regulatory protein FAM213A OS=Mus musculus GN=Fam213a PE=1 SV=2 - [F213A_MOUSE]	3,67	1	1	1	1
Q9QWW1	Homer protein homolog 2 OS=Mus musculus GN=Homer2 PE=1 SV=1 - [HOME2_MOUSE]	3,67	1	1	1	1
P70704	Probable phospholipid-transporting ATPase IA OS=Mus musculus GN=Atp8a1 PE=1 SV=1 - [AT8A1_MOUSE]	3,66	2	4	4	6
Q9QXL2	Kinesin-like protein KIF21A OS=Mus musculus GN=Kif21a PE=1 SV=2 - [KI21A_MOUSE]	3,65	2	4	4	5
Q63912	Oligodendrocyte-myelin glycoprotein OS=Mus musculus GN=Omg PE=1 SV=1 - [OMGP_MOUSE]	3,64	1	2	2	5
Q8BGH2	Sorting and assembly machinery component 50 homolog OS=Mus musculus GN=Samm50 PE=1 SV=1 - [SAM50_MOUSE]	3,62	1	1	1	3
P47867	Secretogranin-3 OS=Mus musculus GN=Scg3 PE=1 SV=1 - [SCG3_MOUSE]	3,61	1	1	1	1
Q9JM52	Misshapen-like kinase 1 OS=Mus musculus GN=Mink1 PE=1 SV=3 - [MINK1_MOUSE]	3,59	3	4	4	6
O35449	Proline-rich transmembrane protein 1 OS=Mus musculus GN=Prrt1 PE=1 SV=1 - [PRRT1_MOUSE]	3,59	1	1	1	2
Q8R5H6	Wiskott-Aldrich syndrome protein family member 1 OS=Mus musculus GN=Wasf1 PE=1 SV=2 - [WASF1_MOUSE]	3,58	1	1	2	4
Q91V92	ATP-citrate synthase OS=Mus musculus GN=Acly PE=1 SV=1 - [ACLY_MOUSE]	3,57	1	4	4	8
P97447	Four and a half LIM domains protein 1 OS=Mus musculus GN=Fhl1 PE=1 SV=3 - [FHL1_MOUSE]	3,57	1	1	1	1
P61793	Lysophosphatidic acid receptor 1 OS=Mus musculus GN=Lpar1 PE=1 SV=1 - [LPAR1_MOUSE]	3,57	1	1	1	2
Q60780	Growth arrest-specific protein 7 OS=Mus musculus GN=Gas7 PE=1 SV=1 - [GAS7_MOUSE]	3,56	1	1	1	2
Q9CQA3	Succinate dehydrogenase [ubiquinone] iron-sulfur subunit, mitochondrial OS=Mus musculus GN=Sdhb PE=1 SV=1 - [DHSB_MOUSE]	3,55	1	1	1	1
Q9QXY6	EH domain-containing protein 3 OS=Mus musculus GN=Ehd3 PE=1 SV=2 - [EHD3_MOUSE]	3,55	3	2	2	3

Accession	Description	Σ Cover.	Σ# Prot.	Σ# Unique Pept.	Σ# Pept.	Σ# PSM
O88543	COP9 signalosome complex subunit 3 OS=Mus musculus GN=Cops3 PE=1 SV=3 - [CSN3_MOUSE]	3,55	1	1	1	1
CON_0000 98652	SWISS-PROT:P13645 Tax_Id=9606 Gene_Symbol=KRT10 Keratin, type I cytoskeletal 10	3,54	7	2	2	3
Q61481	Calcium/calmodulin-dependent 3',5'-cyclic nucleotide phosphodiesterase 1A OS=Mus musculus GN=Pde1a PE=2 SV=2 - [PDE1A_MOUSE]	3,54	1	1	1	1
Q8BYI9	Tenascin-R OS=Mus musculus GN=Tnr PE=1 SV=2 - [TENR_MOUSE]	3,53	1	3	3	4
Q8BFZ9	Erlin-2 OS=Mus musculus GN=Erlin2 PE=1 SV=1 - [ERLN2_MOUSE]	3,53	2	1	1	1
P32921	Tryptophan--tRNA ligase, cytoplasmic OS=Mus musculus GN=Wars PE=1 SV=2 - [SYWC_MOUSE]	3,53	1	1	1	4
Q922D8	C-1-tetrahydrofolate synthase, cytoplasmic OS=Mus musculus GN=Mthfd1 PE=1 SV=4 - [C1TC_MOUSE]	3,53	1	3	3	3
Q61249	Immunoglobulin-binding protein 1 OS=Mus musculus GN=Igbp1 PE=1 SV=1 - [IGBP1_MOUSE]	3,53	2	1	1	2
P70414	Sodium/calcium exchanger 1 OS=Mus musculus GN=Slc8a1 PE=1 SV=1 - [NAC1_MOUSE]	3,51	1	3	3	3
Q9Z268	RasGAP-activating-like protein 1 OS=Mus musculus GN=Rasal1 PE=2 SV=2 - [RASL1_MOUSE]	3,50	1	2	2	4
Q8R373	CXADR-like membrane protein OS=Mus musculus GN=Clmp PE=1 SV=1 - [CLMP_MOUSE]	3,49	1	1	1	1
Q62443	Neuronal pentraxin-1 OS=Mus musculus GN=Nptx1 PE=2 SV=1 - [NPTX1_MOUSE]	3,47	1	1	1	7
Q9WV69	Dematin OS=Mus musculus GN=Epb49 PE=1 SV=1 - [DEMA_MOUSE]	3,46	1	1	1	2
O88746	Target of Myb protein 1 OS=Mus musculus GN=Tom1 PE=1 SV=1 - [TOM1_MOUSE]	3,46	1	1	1	1
Q6PDL0	Cytoplasmic dynein 1 light intermediate chain 2 OS=Mus musculus GN=Dync1li2 PE=1 SV=2 - [DC1L2_MOUSE]	3,46	1	1	1	1
O08795	Glucosidase 2 subunit beta OS=Mus musculus GN=Prkcsh PE=1 SV=1 - [GLU2B_MOUSE]	3,45	1	2	2	2
O09117	Synaptophysin-like protein 1 OS=Mus musculus GN=Sypl1 PE=1 SV=2 - [SYPL1_MOUSE]	3,45	1	1	1	2
Q91YQ5	Dolichyl-diphosphooligosaccharide--protein glycosyltransferase subunit 1 OS=Mus musculus GN=Rpn1 PE=2 SV=1 - [RPN1_MOUSE]	3,45	1	2	2	3
Q9D154	Leukocyte elastase inhibitor A OS=Mus musculus GN=Serpinb1a PE=1 SV=1 - [ILEUA_MOUSE]	3,43	1	1	1	1
O55234	Proteasome subunit beta type-5 OS=Mus musculus GN=Psmb5 PE=1 SV=3 - [PSB5_MOUSE]	3,41	1	1	1	2
P51660	Peroxisomal multifunctional enzyme type 2 OS=Mus musculus GN=Hsd17b4 PE=1 SV=3 - [DHB4_MOUSE]	3,40	1	2	2	4
Q11011	Puromycin-sensitive aminopeptidase OS=Mus musculus GN=Npepps PE=1 SV=2 - [PSA_MOUSE]	3,37	1	3	3	6
Q3TDN2	FAS-associated factor 2 OS=Mus musculus GN=Faf2 PE=2 SV=2 - [FAF2_MOUSE]	3,37	1	1	1	3
Q9CPV4	Glyoxalase domain-containing protein 4 OS=Mus musculus GN=Glod4 PE=2 SV=1 - [GLOD4_MOUSE]	3,36	1	1	1	1
O88485	Cytoplasmic dynein 1 intermediate chain 1 OS=Mus musculus GN=Dync1i1 PE=1 SV=2 - [DC1I1_MOUSE]	3,34	1	1	1	2
Q91WC3	Long-chain-fatty-acid--CoA ligase 6 OS=Mus musculus GN=Acsl6 PE=2 SV=1 - [ACSL6_MOUSE]	3,30	1	2	2	5
Q99N89	39S ribosomal protein L43, mitochondrial OS=Mus musculus GN=Mrpl43 PE=2 SV=1 - [RM43_MOUSE]	3,28	1	1	1	1
Q9CR95	Adaptin ear-binding coat-associated protein 1 OS=Mus musculus GN=Necap1 PE=1 SV=2 - [NECP1_MOUSE]	3,27	1	1	1	2
Q5SQX6	Cytoplasmic FMR1-interacting protein 2 OS=Mus musculus GN=Cyfip2 PE=1 SV=2 - [CYFP2_MOUSE]	3,27	1	3	4	12
Q8BWT1	3-ketoacyl-CoA thiolase, mitochondrial OS=Mus musculus GN=Acaa2 PE=1 SV=3 - [THIM_MOUSE]	3,27	1	1	1	1
P70195	Proteasome subunit beta type-7 OS=Mus musculus GN=Psmb7 PE=1 SV=1 - [PSB7_MOUSE]	3,25	1	1	1	1
P26339	Chromogranin-A OS=Mus musculus GN=Chga PE=1 SV=1 - [CMGA_MOUSE]	3,24	1	1	1	2
Q8BP47	Asparagine--tRNA ligase, cytoplasmic OS=Mus musculus GN=Nars PE=1 SV=2 - [SYNC_MOUSE]	3,22	1	1	1	1
Q99P58	Ras-related protein Rab-27B OS=Mus musculus GN=Rab27b PE=1 SV=3 - [RB27B_MOUSE]	3,21	1	1	1	1
P62754	40S ribosomal protein S6 OS=Mus musculus GN=Rps6 PE=1 SV=1 - [RS6_MOUSE]	3,21	1	1	1	1
P62196	26S protease regulatory subunit 8 OS=Mus musculus GN=Psmc5 PE=1 SV=1 - [PRS8_MOUSE]	3,20	1	1	1	1
Q8BPN8	DmX-like protein 2 OS=Mus musculus GN=Dmxl2 PE=1 SV=3 - [DMXL2_MOUSE]	3,20	2	7	7	12
Q99K10	Neuroligin-1 OS=Mus musculus GN=Nlgn1 PE=2 SV=2 - [NLGN1_MOUSE]	3,20	1	2	2	3
P29758	Ornithine aminotransferase, mitochondrial OS=Mus musculus GN=Oat PE=1 SV=1 - [OAT_MOUSE]	3,19	1	1	1	4
Q71M36	Chondroitin sulfate proteoglycan 5 OS=Mus musculus GN=Cspg5 PE=1 SV=2 - [CSPG5_MOUSE]	3,18	1	1	1	1
Q99LD4	COP9 signalosome complex subunit 1 OS=Mus musculus GN=Gps1 PE=1 SV=1 - [CSN1_MOUSE]	3,18	1	1	1	1
Q60854	Serpin B6 OS=Mus musculus GN=Serpinb6 PE=2 SV=1 - [SPB6_MOUSE]	3,17	1	1	1	2
P28658	Ataxin-10 OS=Mus musculus GN=Atxn10 PE=1 SV=2 - [ATX10_MOUSE]	3,16	1	1	1	3
O55091	Protein IMPACT OS=Mus musculus GN=Impact PE=1 SV=2 - [IMPCT_MOUSE]	3,14	1	1	1	2
P28740	Kinesin-like protein KIF2A OS=Mus musculus GN=Kif2a PE=1 SV=2 - [KIF2A_MOUSE]	3,12	1	2	2	3
Q8CBW3	Abl interactor 1 OS=Mus musculus GN=Abi1 PE=1 SV=3 - [ABI1_MOUSE]	3,12	1	1	1	2
Q8QZS1	3-hydroxyisobutyryl-CoA hydrolase, mitochondrial OS=Mus musculus GN=Hibch PE=1 SV=1 - [HIBCH_MOUSE]	3,12	1	1	1	1
P55088	Aquaporin-4 OS=Mus musculus GN=Aqp4 PE=2 SV=2 - [AQP4_MOUSE]	3,10	1	1	1	4
Q6PCP5	Mitochondrial fission factor OS=Mus musculus GN=Mff PE=1 SV=1 - [MFF_MOUSE]	3,09	1	1	1	1
Q9CPY7	Cytosol aminopeptidase OS=Mus musculus GN=Lap3 PE=1 SV=3 - [AMPL_MOUSE]	3,08	1	1	1	4
Q8VHH5	Arf-GAP with GTPase, ANK repeat and PH domain-containing protein 3 OS=Mus musculus GN=Agap3 PE=1 SV=2 - [AGAP3_MOUSE]	3,08	2	2	2	5
Q60612	Adenosine receptor A1 OS=Mus musculus GN=Adora1 PE=2 SV=4 - [AA1R_MOUSE]	3,07	1	1	1	1
O88343	Electrogenic sodium bicarbonate cotransporter 1 OS=Mus musculus GN=Slc4a4 PE=1 SV=2 - [S4A4_MOUSE]	3,06	1	3	3	16
Q2NL51	Glycogen synthase kinase-3 alpha OS=Mus musculus GN=Gsk3a PE=1 SV=2 - [GSK3A_MOUSE]	3,06	1	1	1	2
P62141	Serine/threonine-protein phosphatase PP1-beta catalytic subunit OS=Mus musculus GN=Ppp1cb PE=1 SV=3 - [PP1B_MOUSE]	3,06	1	1	1	1
P58252	Elongation factor 2 OS=Mus musculus GN=Eef2 PE=1 SV=2 - [EF2_MOUSE]	3,03	1	3	3	6
Q8CHU3	Epsin-2 OS=Mus musculus GN=Epn2 PE=1 SV=1 - [EPN2_MOUSE]	3,03	1	1	1	1
O54991	Contactin-associated protein 1 OS=Mus musculus GN=Cntnap1 PE=2 SV=2 - [CNTP1_MOUSE]	3,03	1	3	3	11
Q99MN1	Lysine--tRNA ligase OS=Mus musculus GN=Kars PE=1 SV=1 - [SYK_MOUSE]	3,03	1	1	1	1
Q9CZ16	Transmembrane protein 178A OS=Mus musculus GN=Tmem178a PE=2 SV=3 - [T178A_MOUSE]	3,03	1	1	1	1

Accession	Description	Σ Cover.	Σ# Prot.	Σ# Unique Pept.	Σ# Pept.	Σ# PSM
Q99L45	Eukaryotic translation initiation factor 2 subunit 2 OS=Mus musculus GN=Eif2s2 PE=1 SV=1 - [IF2B_MOUSE]	3,02	1	1	1	1
P14685	26S proteasome non-ATPase regulatory subunit 3 OS=Mus musculus GN=Psmd3 PE=1 SV=3 - [PSMD3_MOUSE]	3,02	1	1	1	3
Q497Q6	Protein FAM228B OS=Mus musculus GN=Fam228b PE=2 SV=1 - [F228B_MOUSE]	3,02	1	1	1	1
Q9DBL1	Short/branched chain specific acyl-CoA dehydrogenase, mitochondrial OS=Mus musculus GN=Acadsb PE=1 SV=1 - [ACDSB_MOUSE]	3,01	1	1	1	1
O35864	COP9 signalosome complex subunit 5 OS=Mus musculus GN=Cops5 PE=1 SV=3 - [CSN5_MOUSE]	2,99	1	1	1	1
O08919	Numb-like protein OS=Mus musculus GN=Numbl PE=1 SV=3 - [NUMBL_MOUSE]	2,98	1	1	1	1
Q93092	Transaldolase OS=Mus musculus GN=Taldo1 PE=1 SV=2 - [TALDO_MOUSE]	2,97	1	1	1	2
Q8C8N2	Protein SCAI OS=Mus musculus GN=Scai PE=1 SV=2 - [SCAI_MOUSE]	2,97	1	1	1	3
Q5SRX1	TOM1-like protein 2 OS=Mus musculus GN=Tom1l2 PE=1 SV=1 - [TM1L2_MOUSE]	2,96	1	1	1	4
Q99MN9	Propionyl-CoA carboxylase beta chain, mitochondrial OS=Mus musculus GN=Pccb PE=1 SV=2 - [PCCB_MOUSE]	2,96	1	1	1	10
Q9Z2W0	Aspartyl aminopeptidase OS=Mus musculus GN=Dnpep PE=2 SV=2 - [DNPEP_MOUSE]	2,96	1	1	1	1
O88544	COP9 signalosome complex subunit 4 OS=Mus musculus GN=Cops4 PE=1 SV=1 - [CSN4_MOUSE]	2,96	1	1	1	1
Q8VDI9	Alpha-1,2-mannosyltransferase ALG9 OS=Mus musculus GN=Alg9 PE=2 SV=1 - [ALG9_MOUSE]	2,95	1	1	1	1
Q8BLF1	Neutral cholesterol ester hydrolase 1 OS=Mus musculus GN=Nceh1 PE=1 SV=1 - [NCEH1_MOUSE]	2,94	1	1	1	2
Q06138	Calcium-binding protein 39 OS=Mus musculus GN=Cab39 PE=1 SV=2 - [CAB39_MOUSE]	2,93	1	1	1	1
Q9Z0S1	3'(2'),5'-bisphosphate nucleotidase 1 OS=Mus musculus GN=Bpnt1 PE=1 SV=2 - [BPNT1_MOUSE]	2,92	1	1	1	1
A2RT62	F-box/LRR-repeat protein 16 OS=Mus musculus GN=Fbxl16 PE=2 SV=1 - [FXL16_MOUSE]	2,92	1	1	1	2
Q8BZ98	Dynamin-3 OS=Mus musculus GN=Dnm3 PE=1 SV=1 - [DYN3_MOUSE]	2,90	1	1	3	10
Q9D7N9	Adipocyte plasma membrane-associated protein OS=Mus musculus GN=Apmap PE=1 SV=1 - [APMAP_MOUSE]	2,89	1	1	1	1
P35438	Glutamate receptor ionotropic, NMDA 1 OS=Mus musculus GN=Grin1 PE=1 SV=1 - [NMDZ1_MOUSE]	2,88	1	3	3	6
Q8C145	Zinc transporter ZIP6 OS=Mus musculus GN=Slc39a6 PE=1 SV=1 - [S39A6_MOUSE]	2,88	1	2	2	2
P40630	Transcription factor A, mitochondrial OS=Mus musculus GN=Tfam PE=1 SV=2 - [TFAM_MOUSE]	2,88	1	1	1	1
Q9CWJ9	Bifunctional purine biosynthesis protein PURH OS=Mus musculus GN=Atic PE=1 SV=2 - [PUR9_MOUSE]	2,87	1	1	1	1
Q4KUS2	Protein unc-13 homolog A OS=Mus musculus GN=Unc13a PE=1 SV=3 - [UN13A_MOUSE]	2,86	2	4	4	9
Q91XU3	Phosphatidylinositol 5-phosphate 4-kinase type-2 gamma OS=Mus musculus GN=Pip4k2c PE=2 SV=1 - [PI42C_MOUSE]	2,85	1	1	1	1
Q6P9R2	Serine/threonine-protein kinase OSR1 OS=Mus musculus GN=Oxsr1 PE=1 SV=1 - [OXSR1_MOUSE]	2,85	1	1	1	1
Q64487	Receptor-type tyrosine-protein phosphatase delta OS=Mus musculus GN=Ptprd PE=1 SV=3 - [PTPRD_MOUSE]	2,82	1	3	3	9
O35098	Dihydropyrimidinase-related protein 4 OS=Mus musculus GN=Dpysl4 PE=1 SV=1 - [DPYL4_MOUSE]	2,80	1	1	1	3
Q9ERZ4	Muscarinic acetylcholine receptor M2 OS=Mus musculus GN=Chrm2 PE=2 SV=2 - [ACM2_MOUSE]	2,79	1	1	1	1
Q922B1	O-acetyl-ADP-ribose deacetylase MACROD1 OS=Mus musculus GN=Macrod1 PE=1 SV=2 - [MACD1_MOUSE]	2,79	1	1	1	1
Q8R361	Rab11 family-interacting protein 5 OS=Mus musculus GN=Rab11fip5 PE=1 SV=2 - [RFIP5_MOUSE]	2,79	1	1	1	1
Q9JMH9	Unconventional myosin-XVIIIa OS=Mus musculus GN=Myo18a PE=1 SV=2 - [MY18A_MOUSE]	2,78	1	4	4	6
Q64514	Tripeptidyl-peptidase 2 OS=Mus musculus GN=Tpp2 PE=2 SV=3 - [TPP2_MOUSE]	2,77	1	2	2	3
Q8VCT3	Aminopeptidase B OS=Mus musculus GN=Rnpep PE=2 SV=2 - [AMPB_MOUSE]	2,77	1	1	1	1
Q9CX00	IST1 homolog OS=Mus musculus GN=Ist1 PE=2 SV=1 - [IST1_MOUSE]	2,76	1	1	1	1
P51830	Adenylate cyclase type 9 OS=Mus musculus GN=Adcy9 PE=1 SV=1 - [ADCY9_MOUSE]	2,73	1	3	3	6
P21995	Embigin OS=Mus musculus GN=Emb PE=1 SV=2 - [EMB_MOUSE]	2,73	1	1	1	3
Q99JP7	Gamma-glutamyltransferase 7 OS=Mus musculus GN=Ggt7 PE=2 SV=2 - [GGT7_MOUSE]	2,72	1	1	1	2
Q9Z1W9	STE20/SPS1-related proline-alanine-rich protein kinase OS=Mus musculus GN=Stk39 PE=1 SV=1 - [STK39_MOUSE]	2,70	1	1	1	1
Q3TDD9	Protein phosphatase 1 regulatory subunit 21 OS=Mus musculus GN=Ppp1r21 PE=2 SV=2 - [PPR21_MOUSE]	2,69	1	2	2	2
Q9CQ62	2,4-dienoyl-CoA reductase, mitochondrial OS=Mus musculus GN=Decr1 PE=1 SV=1 - [DECR_MOUSE]	2,69	1	1	1	1
Q8BGQ7	Alanine--tRNA ligase, cytoplasmic OS=Mus musculus GN=Aars PE=1 SV=1 - [SYAC_MOUSE]	2,69	1	2	2	2
P54822	Adenylosuccinate lyase OS=Mus musculus GN=Adsl PE=2 SV=2 - [PUR8_MOUSE]	2,69	1	1	1	1
Q5U458	DnaJ homolog subfamily C member 11 OS=Mus musculus GN=Dnajc11 PE=2 SV=2 - [DJC11_MOUSE]	2,68	1	1	1	2
Q5SSL4	Active breakpoint cluster region-related protein OS=Mus musculus GN=Abr PE=2 SV=1 - [ABR_MOUSE]	2,68	1	2	2	2
Q9Z0H8	CAP-Gly domain-containing linker protein 2 OS=Mus musculus GN=Clip2 PE=1 SV=2 - [CLIP2_MOUSE]	2,67	1	2	2	2
Q80T41	Gamma-aminobutyric acid type B receptor subunit 2 OS=Mus musculus GN=Gabbr2 PE=2 SV=2 - [GABR2_MOUSE]	2,66	1	2	2	4
Q9WVJ2	26S proteasome non-ATPase regulatory subunit 13 OS=Mus musculus GN=Psmd13 PE=1 SV=1 - [PSD13_MOUSE]	2,66	1	1	1	1
Q8VDD5	Myosin-9 OS=Mus musculus GN=Myh9 PE=1 SV=4 - [MYH9_MOUSE]	2,65	2	3	4	6
Q9DC69	NADH dehydrogenase [ubiquinone] 1 alpha subcomplex subunit 9, mitochondrial OS=Mus musculus GN=Ndufa9 PE=1 SV=2 - [NDUA9_MOUSE]	2,65	1	1	1	2
Q8BGQ1	Spermatogenesis-defective protein 39 homolog OS=Mus musculus GN=Vipas39 PE=1 SV=1 - [SPE39_MOUSE]	2,65	1	1	1	1
P19096	Fatty acid synthase OS=Mus musculus GN=Fasn PE=1 SV=2 - [FAS_MOUSE]	2,64	1	5	5	9
Q791V5	Mitochondrial carrier homolog 2 OS=Mus musculus GN=Mtch2 PE=1 SV=1 - [MTCH2_MOUSE]	2,64	1	1	1	2
Q9ERG2	Striatin-3 OS=Mus musculus GN=Strn3 PE=1 SV=1 - [STRN3_MOUSE]	2,64	1	1	1	2
Q3TMH2	Secernin-3 OS=Mus musculus GN=Scrn3 PE=1 SV=1 - [SCRN3_MOUSE]	2,63	1	1	1	1
O70310	Glycylpeptide N-tetradecanoyltransferase 1 OS=Mus musculus GN=Nmt1 PE=1 SV=1 - [NMT1_MOUSE]	2,62	1	1	1	1
Q61206	Platelet-activating factor acetylhydrolase IB subunit beta OS=Mus musculus GN=Pafah1b2 PE=1 SV=2 - [PA1B2_MOUSE]	2,62	1	1	1	1

Accession	Description	Σ Cover.	Σ# Prot.	Σ# Unique Pept.	Σ# Pept.	Σ# PSM
Q920N7	Synaptotagmin-12 OS=Mus musculus GN=Syt12 PE=2 SV=1 - [SYT12_MOUSE]	2,61	1	1	1	1
Q922D4	Serine/threonine-protein phosphatase 6 regulatory subunit 3 OS=Mus musculus GN=Ppp6r3 PE=1 SV=1 - [PP6R3_MOUSE]	2,61	1	2	2	3
Q7TME0	Lipid phosphate phosphatase-related protein type 4 OS=Mus musculus GN=Lppr4 PE=2 SV=2 - [LPPR4_MOUSE]	2,61	1	1	1	1
Q60676	Serine/threonine-protein phosphatase 5 OS=Mus musculus GN=Ppp5c PE=1 SV=3 - [PPP5_MOUSE]	2,61	1	1	1	1
Q9JKR6	Hypoxia up-regulated protein 1 OS=Mus musculus GN=Hyou1 PE=1 SV=1 - [HYOU1_MOUSE]	2,60	1	2	2	4
Q8BHL5	Engulfment and cell motility protein 2 OS=Mus musculus GN=Elmo2 PE=1 SV=1 - [ELMO2_MOUSE]	2,60	1	1	1	1
Q7TQ95	Protein lunapark OS=Mus musculus GN=Lnp PE=1 SV=1 - [LNP_MOUSE]	2,59	1	1	1	1
Q99MI1	ELKS/Rab6-interacting/CAST family member 1 OS=Mus musculus GN=Erc1 PE=1 SV=1 - [RB6I2_MOUSE]	2,59	1	2	2	2
Q8C522	Endonuclease domain-containing 1 protein OS=Mus musculus GN=Endod1 PE=1 SV=2 - [ENDD1_MOUSE]	2,59	1	1	1	2
Q99JB8	Protein kinase C and casein kinase II substrate protein 3 OS=Mus musculus GN=Pacsin3 PE=1 SV=1 - [PACN3_MOUSE]	2,59	1	1	1	1
Q08331	Calretinin OS=Mus musculus GN=Calb2 PE=1 SV=3 - [CALB2_MOUSE]	2,58	1	1	1	1
Q921I1	Serotransferrin OS=Mus musculus GN=Tf PE=1 SV=1 - [TRFE_MOUSE]	2,58	1	1	1	2
Q7M6Y3	Phosphatidylinositol-binding clathrin assembly protein OS=Mus musculus GN=Picalm PE=1 SV=1 - [PICAL_MOUSE]	2,58	1	1	2	2
Q61151	Serine/threonine-protein phosphatase 2A 56 kDa regulatory subunit epsilon isoform OS=Mus musculus GN=Ppp2r5e PE=2 SV=3 - [2A5E_MOUSE]	2,57	1	1	1	1
Q791T5	Mitochondrial carrier homolog 1 OS=Mus musculus GN=Mtch1 PE=1 SV=1 - [MTCH1_MOUSE]	2,57	1	1	1	5
Q80VQ0	Aldehyde dehydrogenase family 3 member B1 OS=Mus musculus GN=Aldh3b1 PE=2 SV=1 - [AL3B1_MOUSE]	2,56	1	1	1	1
Q9ET30	Transmembrane 9 superfamily member 3 OS=Mus musculus GN=Tm9sf3 PE=1 SV=1 - [TM9S3_MOUSE]	2,56	1	1	1	2
Q61425	Hydroxyacyl-coenzyme A dehydrogenase, mitochondrial OS=Mus musculus GN=Hadh PE=1 SV=2 - [HCDH_MOUSE]	2,55	1	1	1	2
Q810U4	Neuronal cell adhesion molecule OS=Mus musculus GN=Nrcam PE=1 SV=2 - [NRCAM_MOUSE]	2,55	1	3	3	5
Q99N87	28S ribosomal protein S5, mitochondrial OS=Mus musculus GN=Mrps5 PE=2 SV=1 - [RT05_MOUSE]	2,55	1	1	1	1
O35887	Calumenin OS=Mus musculus GN=Calu PE=1 SV=1 - [CALU_MOUSE]	2,54	1	1	1	1
Q9WU78	Programmed cell death 6-interacting protein OS=Mus musculus GN=Pdcd6ip PE=1 SV=3 - [PDC6I_MOUSE]	2,53	1	2	2	3
Q64442	Sorbitol dehydrogenase OS=Mus musculus GN=Sord PE=1 SV=3 - [DHSO_MOUSE]	2,52	1	1	1	1
P35235	Tyrosine-protein phosphatase non-receptor type 11 OS=Mus musculus GN=Ptpn11 PE=1 SV=2 - [PTN11_MOUSE]	2,51	1	1	1	1
O88533	Aromatic-L-amino-acid decarboxylase OS=Mus musculus GN=Ddc PE=2 SV=1 - [DDC_MOUSE]	2,50	1	1	1	2
Q99J08	SEC14-like protein 2 OS=Mus musculus GN=Sec14l2 PE=2 SV=1 - [S14L2_MOUSE]	2,48	1	1	1	3
Q9QXS1	Plectin OS=Mus musculus GN=Plec PE=1 SV=2 - [PLEC_MOUSE]	2,47	1	9	9	18
Q6P1F6	Serine/threonine-protein phosphatase 2A 55 kDa regulatory subunit B alpha isoform OS=Mus musculus GN=Ppp2r2a PE=1 SV=1 - [2ABA_MOUSE]	2,46	1	1	1	1
P70663	SPARC-like protein 1 OS=Mus musculus GN=Sparcl1 PE=1 SV=3 - [SPRL1_MOUSE]	2,46	1	1	1	2
P59823	Interleukin-1 receptor accessory protein-like 1 OS=Mus musculus GN=Il1rapl1 PE=1 SV=1 - [IRPL1_MOUSE]	2,45	1	1	1	2
Q3TFD2	Lysophosphatidylcholine acyltransferase 1 OS=Mus musculus GN=Lpcat1 PE=1 SV=1 - [PCAT1_MOUSE]	2,43	1	1	1	1
Q9D415	Disks large-associated protein 1 OS=Mus musculus GN=Dlgap1 PE=1 SV=3 - [DLGP1_MOUSE]	2,42	1	2	2	3
Q8VE88	Protein FAM114A2 OS=Mus musculus GN=Fam114a2 PE=1 SV=2 - [F1142_MOUSE]	2,41	1	1	1	1
P54728	UV excision repair protein RAD23 homolog B OS=Mus musculus GN=Rad23b PE=1 SV=2 - [RD23B_MOUSE]	2,40	1	1	1	2
Q8CHX7	Raftlin-2 OS=Mus musculus GN=Rftn2 PE=2 SV=3 - [RFTN2_MOUSE]	2,40	1	1	1	1
Q8JZQ2	AFG3-like protein 2 OS=Mus musculus GN=Afg3l2 PE=1 SV=1 - [AFG32_MOUSE]	2,37	1	1	1	3
Q8BG32	26S proteasome non-ATPase regulatory subunit 11 OS=Mus musculus GN=Psmd11 PE=1 SV=3 - [PSD11_MOUSE]	2,37	1	1	1	1
O08842	GDNF family receptor alpha-2 OS=Mus musculus GN=Gfra2 PE=2 SV=2 - [GFRA2_MOUSE]	2,37	1	1	1	2
P47911	60S ribosomal protein L6 OS=Mus musculus GN=Rpl6 PE=1 SV=3 - [RL6_MOUSE]	2,36	1	1	1	1
Q9D6F4	Gamma-aminobutyric acid receptor subunit alpha-4 OS=Mus musculus GN=Gabra4 PE=2 SV=1 - [GBRA4_MOUSE]	2,36	1	1	1	2
Q91VE0	Long-chain fatty acid transport protein 4 OS=Mus musculus GN=Slc27a4 PE=1 SV=1 - [S27A4_MOUSE]	2,33	1	1	1	2
Q8CHK3	Lysophospholipid acyltransferase 7 OS=Mus musculus GN=Mboat7 PE=2 SV=1 - [MBOA7_MOUSE]	2,33	1	1	1	1
Q80W54	CAAX prenyl protease 1 homolog OS=Mus musculus GN=Zmpste24 PE=1 SV=2 - [FACE1_MOUSE]	2,32	1	1	1	1
Q80XA6	RalBP1-associated Eps domain-containing protein 2 OS=Mus musculus GN=Reps2 PE=1 SV=1 - [REPS2_MOUSE]	2,30	1	1	1	1
O35114	Lysosome membrane protein 2 OS=Mus musculus GN=Scarb2 PE=1 SV=3 - [SCRB2_MOUSE]	2,30	1	1	1	1
Q9JLT4	Thioredoxin reductase 2, mitochondrial OS=Mus musculus GN=Txnrd2 PE=1 SV=4 - [TRXR2_MOUSE]	2,29	1	1	1	1
Q9DCT2	NADH dehydrogenase [ubiquinone] iron-sulfur protein 3, mitochondrial OS=Mus musculus GN=Ndufs3 PE=1 SV=2 - [NDUS3_MOUSE]	2,28	1	1	1	1
Q9WV54	Acid ceramidase OS=Mus musculus GN=Asah1 PE=1 SV=1 - [ASAH1_MOUSE]	2,28	1	1	1	1
Q9D880	Mitochondrial import inner membrane translocase subunit TIM50 OS=Mus musculus GN=Timm50 PE=1 SV=1 - [TIM50_MOUSE]	2,27	1	1	1	2
Q9CY27	Very-long-chain enoyl-CoA reductase OS=Mus musculus GN=Tecr PE=1 SV=1 - [TECR_MOUSE]	2,27	1	1	1	2
Q91V09	WD repeat-containing protein 13 OS=Mus musculus GN=Wdr13 PE=1 SV=1 - [WDR13_MOUSE]	2,27	1	1	1	1
P16332	Methylmalonyl-CoA mutase, mitochondrial OS=Mus musculus GN=Mut PE=2 SV=2 - [MUTA_MOUSE]	2,27	1	1	1	1
Q9D5K4	S100P-binding protein OS=Mus musculus GN=S100pbp PE=2 SV=1 - [S1PBP_MOUSE]	2,27	1	1	1	1
Q2M3X8	Phosphatase and actin regulator 1 OS=Mus musculus GN=Phactr1 PE=1 SV=1 - [PHAR1_MOUSE]	2,24	1	1	1	1

Accession	Description	Σ Cover.	Σ# Prot.	Σ# Unique Pept.	Σ# Pept.	Σ# PSM
Q8BMS1	Trifunctional enzyme subunit alpha, mitochondrial OS=Mus musculus GN=Hadha PE=1 SV=1 - [ECHA_MOUSE]	2,23	1	1	1	3
Q11136	Xaa-Pro dipeptidase OS=Mus musculus GN=Pepd PE=2 SV=3 - [PEPD_MOUSE]	2,23	1	1	1	1
P42208	Septin-2 OS=Mus musculus GN=Sept2 PE=1 SV=2 - [SEPT2_MOUSE]	2,22	1	1	1	1
Q3V0K9	Plastin-1 OS=Mus musculus GN=Pls1 PE=2 SV=1 - [PLSI_MOUSE]	2,22	2	1	1	1
P16014	Secretogranin-1 OS=Mus musculus GN=Chgb PE=1 SV=2 - [SCG1_MOUSE]	2,22	1	1	1	1
Q9DBG6	Dolichyl-diphosphooligosaccharide--protein glycosyltransferase subunit 2 OS=Mus musculus GN=Rpn2 PE=2 SV=1 - [RPN2_MOUSE]	2,22	1	1	1	1
Q8K1C0	Protein angel homolog 2 OS=Mus musculus GN=Angel2 PE=2 SV=1 - [ANGE2_MOUSE]	2,21	1	1	1	1
P62482	Voltage-gated potassium channel subunit beta-2 OS=Mus musculus GN=Kcnab2 PE=2 SV=1 - [KCAB2_MOUSE]	2,18	2	1	1	3
P30416	Peptidyl-prolyl cis-trans isomerase FKBP4 OS=Mus musculus GN=Fkbp4 PE=1 SV=5 - [FKBP4_MOUSE]	2,18	1	1	1	1
Q60625	Intercellular adhesion molecule 5 OS=Mus musculus GN=Icam5 PE=1 SV=2 - [ICAM5_MOUSE]	2,18	1	2	2	4
Q8R071	Inositol-trisphosphate 3-kinase A OS=Mus musculus GN=Itpka PE=2 SV=1 - [IP3KA_MOUSE]	2,18	1	1	1	1
O88844	Isocitrate dehydrogenase [NADP] cytoplasmic OS=Mus musculus GN=Idh1 PE=1 SV=2 - [IDHC_MOUSE]	2,17	1	1	1	2
Q80UG2	Plexin-A4 OS=Mus musculus GN=Plxna4 PE=1 SV=3 - [PLXA4_MOUSE]	2,17	3	2	3	3
Q9QY42	Prosaposin receptor GPR37 OS=Mus musculus GN=Gpr37 PE=2 SV=1 - [GPR37_MOUSE]	2,17	1	1	1	1
Q6PB66	Leucine-rich PPR motif-containing protein, mitochondrial OS=Mus musculus GN=Lrpprc PE=1 SV=2 - [LPPRC_MOUSE]	2,16	1	2	2	7
Q9ESN6	Tripartite motif-containing protein 2 OS=Mus musculus GN=Trim2 PE=1 SV=1 - [TRIM2_MOUSE]	2,15	1	1	1	1
B0V2N1	Receptor-type tyrosine-protein phosphatase S OS=Mus musculus GN=Ptprs PE=1 SV=1 - [PTPRS_MOUSE]	2,15	1	3	3	6
Q8C3Q5	Protein shisa-7 OS=Mus musculus GN=Shisa7 PE=1 SV=3 - [SHSA7_MOUSE]	2,15	1	1	1	1
Q9Z307	Inward rectifier potassium channel 16 OS=Mus musculus GN=Kcnj16 PE=2 SV=2 - [IRK16_MOUSE]	2,15	1	1	1	2
P55096	ATP-binding cassette sub-family D member 3 OS=Mus musculus GN=Abcd3 PE=1 SV=2 - [ABCD3_MOUSE]	2,12	1	1	1	4
P21836	Acetylcholinesterase OS=Mus musculus GN=Ache PE=1 SV=1 - [ACES_MOUSE]	2,12	1	1	1	1
Q8CGA3	Large neutral amino acids transporter small subunit 4 OS=Mus musculus GN=Slc43a2 PE=1 SV=1 - [LAT4_MOUSE]	2,11	1	1	1	2
O54865	Guanylate cyclase soluble subunit beta-1 OS=Mus musculus GN=Gucy1b3 PE=2 SV=1 - [GCYB1_MOUSE]	2,10	1	1	1	1
Q78PY7	Staphylococcal nuclease domain-containing protein 1 OS=Mus musculus GN=Snd1 PE=1 SV=1 - [SND1_MOUSE]	2,09	1	2	2	2
Q8VDM4	26S proteasome non-ATPase regulatory subunit 2 OS=Mus musculus GN=Psmd2 PE=1 SV=1 - [PSMD2_MOUSE]	2,09	1	1	1	1
Q7TPB0	Lipid phosphate phosphatase-related protein type 3 OS=Mus musculus GN=Lppr3 PE=2 SV=1 - [LPPR3_MOUSE]	2,09	1	1	1	1
O70311	Glycylpeptide N-tetradecanoyltransferase 2 OS=Mus musculus GN=Nmt2 PE=1 SV=1 - [NMT2_MOUSE]	2,08	1	1	1	1
Q61165	Sodium/hydrogen exchanger 1 OS=Mus musculus GN=Slc9a1 PE=1 SV=1 - [SL9A1_MOUSE]	2,07	1	1	1	4
Q9CPW0	Contactin-associated protein-like 2 OS=Mus musculus GN=Cntnap2 PE=1 SV=2 - [CNTP2_MOUSE]	2,03	1	1	1	3
Q8BH04	Phosphoenolpyruvate carboxykinase [GTP], mitochondrial OS=Mus musculus GN=Pck2 PE=2 SV=1 - [PCKGM_MOUSE]	2,03	1	1	1	1
O89112	LanC-like protein 1 OS=Mus musculus GN=Lancl1 PE=1 SV=1 - [LANC1_MOUSE]	2,01	1	1	1	1
Q80YA3	Phospholipase DDHD1 OS=Mus musculus GN=Ddhd1 PE=2 SV=1 - [DDHD1_MOUSE]	2,01	1	1	1	1
Q80TL0	Protein phosphatase 1E OS=Mus musculus GN=Ppm1e PE=1 SV=2 - [PPM1E_MOUSE]	2,00	1	1	1	1
A7XUX6	Selection and upkeep of intraepithelial T-cells protein 2 OS=Mus musculus GN=Skint2 PE=2 SV=1 - [SKIT2_MOUSE]	2,00	1	1	1	1
Q71LX4	Talin-2 OS=Mus musculus GN=Tln2 PE=1 SV=3 - [TLN2_MOUSE]	1,98	2	4	4	5
Q8K3H0	DCC-interacting protein 13-alpha OS=Mus musculus GN=Appl1 PE=1 SV=1 - [DP13A_MOUSE]	1,98	1	1	1	2
Q99KK9	Probable histidine--tRNA ligase, mitochondrial OS=Mus musculus GN=Hars2 PE=2 SV=1 - [SYHM_MOUSE]	1,98	2	1	1	1
Q80UP8	Sodium-dependent phosphate transporter 2 OS=Mus musculus GN=Slc20a2 PE=1 SV=2 - [S20A2_MOUSE]	1,98	1	1	1	2
Q9EPU5	Tumor necrosis factor receptor superfamily member 21 OS=Mus musculus GN=Tnfrsf21 PE=1 SV=2 - [TNR21_MOUSE]	1,98	1	1	1	1
Q9D9D5	Transmembrane and coiled-coil domain-containing protein 5A OS=Mus musculus GN=Tmco5a PE=2 SV=1 - [TMC5A_MOUSE]	1,98	1	1	1	2
Q61207	Sulfated glycoprotein 1 OS=Mus musculus GN=Psap PE=1 SV=2 - [SAP_MOUSE]	1,97	1	1	1	3
Q5DTL9	Sodium-driven chloride bicarbonate exchanger OS=Mus musculus GN=Slc4a10 PE=1 SV=2 - [S4A10_MOUSE]	1,97	2	2	2	2
P0C192	Leucine-rich repeat-containing protein 4B OS=Mus musculus GN=Lrrc4b PE=1 SV=1 - [LRC4B_MOUSE]	1,97	1	1	1	1
Q3UUG6	TBC1 domain family member 24 OS=Mus musculus GN=Tbc1d24 PE=2 SV=2 - [TBC24_MOUSE]	1,96	1	1	1	1
P26638	Serine--tRNA ligase, cytoplasmic OS=Mus musculus GN=Sars PE=2 SV=3 - [SYSC_MOUSE]	1,95	1	1	1	1
Q5DQR4	Syntaxin-binding protein 5-like OS=Mus musculus GN=Stxbp5l PE=2 SV=1 - [STB5L_MOUSE]	1,94	1	2	2	7
Q9JJG5	SERTA domain-containing protein 2 OS=Mus musculus GN=Sertad2 PE=2 SV=2 - [SRTD2_MOUSE]	1,94	2	1	1	6
Q7TMB8	Cytoplasmic FMR1-interacting protein 1 OS=Mus musculus GN=Cyfip1 PE=1 SV=1 - [CYFP1_MOUSE]	1,92	1	1	2	5
Q8JZP2	Synapsin-3 OS=Mus musculus GN=Syn3 PE=1 SV=2 - [SYN3_MOUSE]	1,90	1	1	1	2
Q8CA95	cAMP and cAMP-inhibited cGMP 3',5'-cyclic phosphodiesterase 10A OS=Mus musculus GN=Pde10a PE=1 SV=2 - [PDE10_MOUSE]	1,90	1	1	1	4
Q64133	Amine oxidase [flavin-containing] A OS=Mus musculus GN=Maoa PE=1 SV=3 - [AOFA_MOUSE]	1,90	1	1	1	1
Q8VE33	Ganglioside-induced differentiation-associated protein 1-like 1 OS=Mus musculus GN=Gdap1l1 PE=2 SV=1 - [GD1L1_MOUSE]	1,89	1	1	1	1
Q5FWH7	Zinc transporter ZIP12 OS=Mus musculus GN=Slc39a12 PE=2 SV=1 - [S39AC_MOUSE]	1,89	1	1	1	2
Q8K2L8	Trafficking protein particle complex subunit 12 OS=Mus musculus GN=Trappc12 PE=1 SV=2 - [TPC12_MOUSE]	1,88	1	1	1	1
Q9R1R2	Tripartite motif-containing protein 3 OS=Mus musculus GN=Trim3 PE=1 SV=1 - [TRIM3_MOUSE]	1,88	1	1	1	1

Accession	Description	Σ Cover.	Σ# Prot.	Σ# Unique Pept.	Σ# Pept.	Σ# PSM
Q7SIG6	Arf-GAP with SH3 domain, ANK repeat and PH domain-containing protein 2 OS=Mus musculus GN=Asap2 PE=1 SV=3 - [ASAP2_MOUSE]	1,88	1	1	1	2
Q9D2N4	Dystrobrevin alpha OS=Mus musculus GN=Dtna PE=1 SV=2 - [DTNA_MOUSE]	1,88	1	1	1	1
Q8R4I7	Neuropilin and tolloid-like protein 1 OS=Mus musculus GN=Neto1 PE=1 SV=2 - [NETO1_MOUSE]	1,88	1	1	1	1
O35551	Rab GTPase-binding effector protein 1 OS=Mus musculus GN=Rabep1 PE=1 SV=2 - [RABE1_MOUSE]	1,86	1	1	1	1
P61222	ATP-binding cassette sub-family E member 1 OS=Mus musculus GN=Abce1 PE=2 SV=1 - [ABCE1_MOUSE]	1,84	1	1	1	1
Q9QUR6	Prolyl endopeptidase OS=Mus musculus GN=Prep PE=2 SV=1 - [PPCE_MOUSE]	1,83	1	1	1	1
Q3UHB1	5'-nucleotidase domain-containing protein 3 OS=Mus musculus GN=Nt5dc3 PE=2 SV=1 - [NT5D3_MOUSE]	1,83	1	1	1	1
Q8BMF3	NADP-dependent malic enzyme, mitochondrial OS=Mus musculus GN=Me3 PE=1 SV=2 - [MAON_MOUSE]	1,82	1	1	1	2
Q922R8	Protein disulfide-isomerase A6 OS=Mus musculus GN=Pdia6 PE=1 SV=3 - [PDIA6_MOUSE]	1,82	1	1	1	1
Q08460	Calcium-activated potassium channel subunit alpha-1 OS=Mus musculus GN=Kcnma1 PE=1 SV=2 - [KCMA1_MOUSE]	1,82	1	1	2	2
Q8BH65	Protein DENND6A OS=Mus musculus GN=Dennd6a PE=2 SV=1 - [DEN6A_MOUSE]	1,82	1	1	1	1
Q9Z0R4	Intersectin-1 OS=Mus musculus GN=Itsn1 PE=1 SV=2 - [ITSN1_MOUSE]	1,81	1	2	2	5
P54763	Ephrin type-B receptor 2 OS=Mus musculus GN=Ephb2 PE=1 SV=2 - [EPHB2_MOUSE]	1,81	1	1	1	1
Q9Z0X1	Apoptosis-inducing factor 1, mitochondrial OS=Mus musculus GN=Aifm1 PE=1 SV=1 - [AIFM1_MOUSE]	1,80	1	1	1	1
Q80ZJ6	Protein zer-1 homolog OS=Mus musculus GN=Zer1 PE=1 SV=1 - [ZER1_MOUSE]	1,80	1	1	1	2
Q921G7	Electron transfer flavoprotein-ubiquinone oxidoreductase, mitochondrial OS=Mus musculus GN=Etfdh PE=1 SV=1 - [ETFD_MOUSE]	1,79	1	1	1	1
Q8VCW8	Acyl-CoA synthetase family member 2, mitochondrial OS=Mus musculus GN=Acsf2 PE=2 SV=1 - [ACSF2_MOUSE]	1,79	1	1	1	1
P28656	Nucleosome assembly protein 1-like 1 OS=Mus musculus GN=Nap1l1 PE=1 SV=2 - [NP1L1_MOUSE]	1,79	1	1	1	1
Q8BH66	Atlastin-1 OS=Mus musculus GN=Atl1 PE=1 SV=1 - [ATLA1_MOUSE]	1,79	1	1	1	2
P70404	Isocitrate dehydrogenase [NAD] subunit gamma 1, mitochondrial OS=Mus musculus GN=Idh3g PE=1 SV=1 - [IDHG1_MOUSE]	1,78	1	1	1	1
Q8K4G5	Actin-binding LIM protein 1 OS=Mus musculus GN=Ablim1 PE=1 SV=1 - [ABLM1_MOUSE]	1,74	1	1	1	1
P27659	60S ribosomal protein L3 OS=Mus musculus GN=Rpl3 PE=2 SV=3 - [RL3_MOUSE]	1,74	1	1	1	1
Q80VP1	Epsin-1 OS=Mus musculus GN=Epn1 PE=1 SV=3 - [EPN1_MOUSE]	1,74	1	1	1	1
Q9JLM8	Serine/threonine-protein kinase DCLK1 OS=Mus musculus GN=Dclk1 PE=1 SV=1 - [DCLK1_MOUSE]	1,72	1	1	1	1
Q8C0P5	Coronin-2A OS=Mus musculus GN=Coro2a PE=2 SV=1 - [COR2A_MOUSE]	1,72	1	1	1	1
Q80YV4	Pantothenate kinase 4 OS=Mus musculus GN=Pank4 PE=1 SV=2 - [PANK4_MOUSE]	1,71	1	1	1	1
P49025	Citron Rho-interacting kinase OS=Mus musculus GN=Cit PE=1 SV=2 - [CTRO_MOUSE]	1,70	1	3	3	4
Q9QXW9	Large neutral amino acids transporter small subunit 2 OS=Mus musculus GN=Slc7a8 PE=1 SV=1 - [LAT2_MOUSE]	1,69	1	1	1	1
Q6PCN3	Tau-tubulin kinase 1 OS=Mus musculus GN=Ttbk1 PE=2 SV=3 - [TTBK1_MOUSE]	1,68	1	2	2	2
Q62095	ATP-dependent RNA helicase DDX3Y OS=Mus musculus GN=Ddx3y PE=1 SV=2 - [DDX3Y_MOUSE]	1,67	3	1	1	1
P70175	Disks large homolog 3 OS=Mus musculus GN=Dlg3 PE=1 SV=1 - [DLG3_MOUSE]	1,65	1	1	1	2
Q8R127	Saccharopine dehydrogenase-like oxidoreductase OS=Mus musculus GN=Sccpdh PE=2 SV=1 - [SCPDL_MOUSE]	1,63	1	1	1	1
P59016	Vacuolar protein sorting-associated protein 33B OS=Mus musculus GN=Vps33b PE=1 SV=1 - [VP33B_MOUSE]	1,62	1	1	1	1
Q8CCN5	Breast carcinoma-amplified sequence 3 homolog OS=Mus musculus GN=Bcas3 PE=1 SV=2 - [BCAS3_MOUSE]	1,62	1	1	1	2
O88712	C-terminal-binding protein 1 OS=Mus musculus GN=Ctbp1 PE=1 SV=2 - [CTBP1_MOUSE]	1,59	2	1	1	2
Q9JK53	Prolargin OS=Mus musculus GN=Prelp PE=1 SV=2 - [PRELP_MOUSE]	1,59	1	1	1	1
Q921Q7	Ras and Rab interactor 1 OS=Mus musculus GN=Rin1 PE=1 SV=1 - [RIN1_MOUSE]	1,57	1	1	1	1
Q9CZS1	Aldehyde dehydrogenase X, mitochondrial OS=Mus musculus GN=Aldh1b1 PE=2 SV=1 - [AL1B1_MOUSE]	1,54	1	1	1	1
P03911	NADH-ubiquinone oxidoreductase chain 4 OS=Mus musculus GN=Mtnd4 PE=1 SV=1 - [NU4M_MOUSE]	1,53	1	1	1	1
Q9EP69	Phosphatidylinositide phosphatase SAC1 OS=Mus musculus GN=Sacm1l PE=2 SV=1 - [SAC1_MOUSE]	1,53	1	1	1	3
F8VPU2	FERM, RhoGEF and pleckstrin domain-containing protein 1 OS=Mus musculus GN=Farp1 PE=1 SV=1 - [FARP1_MOUSE]	1,53	1	1	1	1
Q3UV17	Keratin, type II cytoskeletal 2 oral OS=Mus musculus GN=Krt76 PE=2 SV=1 - [K22O_MOUSE]	1,52	1	1	1	1
Q80U28	MAP kinase-activating death domain protein OS=Mus musculus GN=Madd PE=1 SV=2 - [MADD_MOUSE]	1,52	1	2	2	3
P50544	Very long-chain specific acyl-CoA dehydrogenase, mitochondrial OS=Mus musculus GN=Acadvl PE=1 SV=3 - [ACADV_MOUSE]	1,52	1	1	1	1
P09838	DNA nucleotidylexotransferase OS=Mus musculus GN=Dntt PE=1 SV=3 - [TDT_MOUSE]	1,51	1	1	1	1
Q9Z2C4	Myotubularin-related protein 1 OS=Mus musculus GN=Mtmr1 PE=2 SV=1 - [MTMR1_MOUSE]	1,49	1	1	1	1
Q9D4H8	Cullin-2 OS=Mus musculus GN=Cul2 PE=1 SV=2 - [CUL2_MOUSE]	1,48	1	1	1	1
Q91XL9	Oxysterol-binding protein-related protein 1 OS=Mus musculus GN=Osbpl1a PE=1 SV=2 - [OSBL1_MOUSE]	1,47	1	1	1	1
O08759	Ubiquitin-protein ligase E3A OS=Mus musculus GN=Ube3a PE=1 SV=1 - [UBE3A_MOUSE]	1,47	1	1	1	2
Q07409	Contactin-3 OS=Mus musculus GN=Cntn3 PE=1 SV=2 - [CNTN3_MOUSE]	1,46	1	1	1	1
Q8BPQ7	Small G protein signaling modulator 1 OS=Mus musculus GN=Sgsm1 PE=2 SV=2 - [SGSM1_MOUSE]	1,46	1	1	1	3
P58404	Striatin-4 OS=Mus musculus GN=Strn4 PE=1 SV=2 - [STRN4_MOUSE]	1,45	1	1	1	1
Q8BTN6	Leukocyte receptor cluster member 9 OS=Mus musculus GN=Leng9 PE=2 SV=1 - [LENG9_MOUSE]	1,44	1	1	1	4
Q9QYY0	GRB2-associated-binding protein 1 OS=Mus musculus GN=Gab1 PE=1 SV=2 - [GAB1_MOUSE]	1,44	1	1	1	1
O88444	Adenylate cyclase type 1 OS=Mus musculus GN=Adcy1 PE=2 SV=2 - [ADCY1_MOUSE]	1,43	1	1	1	4
Q3UHD9	Arf-GAP with GTPase, ANK repeat and PH domain-containing protein 2 OS=Mus musculus GN=Agap2 PE=1 SV=1 - [AGAP2_MOUSE]	1,43	1	1	1	2
P47857	6-phosphofructokinase, muscle type OS=Mus musculus GN=Pfkm PE=1 SV=3 - [K6PF_MOUSE]	1,41	1	1	1	1
B0F2B4	Neuroligin 4-like OS=Mus musculus GN=Nlgn4l PE=1 SV=1 - [NLGN4_MOUSE]	1,38	1	1	1	1
Q9DBT5	AMP deaminase 2 OS=Mus musculus GN=Ampd2 PE=1 SV=1 - [AMPD2_MOUSE]	1,38	1	1	1	1
Q9CZD3	Glycine--tRNA ligase OS=Mus musculus GN=Gars PE=1 SV=1 - [SYG_MOUSE]	1,37	1	1	1	1

Accession	Description	Σ Cover.	Σ# Prot.	Σ# Unique Pept.	Σ# Pept.	Σ# PSM
Q3UTJ2	Sorbin and SH3 domain-containing protein 2 OS=Mus musculus GN=Sorbs2 PE=1 SV=2 - [SRBS2_MOUSE]	1,36	1	1	1	1
P98203	Armadillo repeat protein deleted in velo-cardio-facial syndrome homolog OS=Mus musculus GN=Arvcf PE=1 SV=2 - [ARVC_MOUSE]	1,35	1	1	1	1
Q8R307	Vacuolar protein sorting-associated protein 18 homolog OS=Mus musculus GN=Vps18 PE=1 SV=2 - [VPS18_MOUSE]	1,34	1	1	1	1
Q01063	cAMP-specific 3',5'-cyclic phosphodiesterase 4D OS=Mus musculus GN=Pde4d PE=1 SV=2 - [PDE4D_MOUSE]	1,34	1	1	1	1
P37040	NADPH--cytochrome P450 reductase OS=Mus musculus GN=Por PE=1 SV=2 - [NCPR_MOUSE]	1,33	1	1	1	1
Q8BYM5	Neuroligin-3 OS=Mus musculus GN=Nlgn3 PE=1 SV=2 - [NLGN3_MOUSE]	1,33	1	1	1	1
Q8BJ42	Disks large-associated protein 2 OS=Mus musculus GN=Dlgap2 PE=1 SV=2 - [DLGP2_MOUSE]	1,32	1	1	1	2
Q91Z69	SLIT-ROBO Rho GTPase-activating protein 1 OS=Mus musculus GN=Srgap1 PE=1 SV=2 - [SRGP1_MOUSE]	1,32	1	1	1	1
B1AZP2	Disks large-associated protein 4 OS=Mus musculus GN=Dlgap4 PE=1 SV=1 - [DLGP4_MOUSE]	1,31	1	1	1	2
Q6NVE8	WD repeat-containing protein 44 OS=Mus musculus GN=Wdr44 PE=1 SV=1 - [WDR44_MOUSE]	1,31	1	1	1	1
Q80TZ3	Putative tyrosine-protein phosphatase auxilin OS=Mus musculus GN=Dnajc6 PE=2 SV=2 - [AUXI_MOUSE]	1,28	1	1	1	1
P58871	182 kDa tankyrase-1-binding protein OS=Mus musculus GN=Tnks1bp1 PE=1 SV=2 - [TB182_MOUSE]	1,28	1	2	2	2
O55106	Striatin OS=Mus musculus GN=Strn PE=1 SV=2 - [STRN_MOUSE]	1,28	1	1	1	1
O09126	Semaphorin-4D OS=Mus musculus GN=Sema4d PE=1 SV=2 - [SEM4D_MOUSE]	1,28	1	1	1	1
P11627	Neural cell adhesion molecule L1 OS=Mus musculus GN=L1cam PE=1 SV=1 - [L1CAM_MOUSE]	1,27	1	2	2	2
Q6A4J8	Ubiquitin carboxyl-terminal hydrolase 7 OS=Mus musculus GN=Usp7 PE=1 SV=1 - [UBP7_MOUSE]	1,27	1	1	1	1
Q9EQH3	Vacuolar protein sorting-associated protein 35 OS=Mus musculus GN=Vps35 PE=1 SV=1 - [VPS35_MOUSE]	1,26	1	1	1	2
Q6NS60	F-box only protein 41 OS=Mus musculus GN=Fbxo41 PE=1 SV=3 - [FBX41_MOUSE]	1,26	1	1	1	1
Q3UHC7	Disabled homolog 2-interacting protein OS=Mus musculus GN=Dab2ip PE=1 SV=1 - [DAB2P_MOUSE]	1,26	1	1	1	1
Q0GA42	Metal transporter CNNM1 OS=Mus musculus GN=Cnnm1 PE=1 SV=5 - [CNNM1_MOUSE]	1,26	1	1	1	4
P55288	Cadherin-11 OS=Mus musculus GN=Cdh11 PE=1 SV=1 - [CAD11_MOUSE]	1,26	1	1	1	1
Q6URW6	Myosin-14 OS=Mus musculus GN=Myh14 PE=1 SV=1 - [MYH14_MOUSE]	1,25	1	1	2	2
B9EKR1	Receptor-type tyrosine-protein phosphatase zeta OS=Mus musculus GN=Ptprz1 PE=1 SV=1 - [PRPTZ_MOUSE]	1,25	1	2	2	4
Q5GH67	XK-related protein 4 OS=Mus musculus GN=Xkr4 PE=1 SV=1 - [XKR4_MOUSE]	1,24	1	1	1	1
Q8K3E5	Jouberin OS=Mus musculus GN=Ahi1 PE=1 SV=2 - [AHI1_MOUSE]	1,24	1	1	1	1
Q99LG2	Transportin-2 OS=Mus musculus GN=Tnpo2 PE=2 SV=1 - [TNPO2_MOUSE]	1,24	1	1	1	1
Q8BG95	Protein phosphatase 1 regulatory subunit 12B OS=Mus musculus GN=Ppp1r12b PE=1 SV=2 - [MYPT2_MOUSE]	1,23	1	1	1	2
Q5DU25	IQ motif and SEC7 domain-containing protein 2 OS=Mus musculus GN=Iqsec2 PE=1 SV=3 - [IQEC2_MOUSE]	1,22	1	1	1	3
Q3U0M1	Trafficking protein particle complex subunit 9 OS=Mus musculus GN=Trappc9 PE=1 SV=2 - [TPPC9_MOUSE]	1,22	1	1	1	2
Q8CCB4	Vacuolar protein sorting-associated protein 53 homolog OS=Mus musculus GN=Vps53 PE=2 SV=1 - [VPS53_MOUSE]	1,20	1	1	1	2
Q6P5F6	Zinc transporter ZIP10 OS=Mus musculus GN=Slc39a10 PE=1 SV=1 - [S39AA_MOUSE]	1,20	1	1	1	1
Q8CGC7	Bifunctional glutamate/proline--tRNA ligase OS=Mus musculus GN=Eprs PE=1 SV=4 - [SYEP_MOUSE]	1,19	1	1	1	2
Q9Z1L5	Voltage-dependent calcium channel subunit alpha-2/delta-3 OS=Mus musculus GN=Cacna2d3 PE=1 SV=1 - [CA2D3_MOUSE]	1,19	1	1	1	4
Q6KAR6	Exocyst complex component 3 OS=Mus musculus GN=Exoc3 PE=1 SV=2 - [EXOC3_MOUSE]	1,19	1	1	1	1
O35071	Kinesin-like protein KIF1C OS=Mus musculus GN=Kif1c PE=1 SV=2 - [KIF1C_MOUSE]	1,18	3	1	1	1
Q80TQ2	Ubiquitin carboxyl-terminal hydrolase CYLD OS=Mus musculus GN=Cyld PE=1 SV=2 - [CYLD_MOUSE]	1,16	1	1	1	2
Q64096	Guanine nucleotide exchange factor DBS OS=Mus musculus GN=Mcf2l PE=1 SV=2 - [MCF2L_MOUSE]	1,13	1	1	1	1
Q8CE33	Kelch-like protein 11 OS=Mus musculus GN=Klhl11 PE=2 SV=1 - [KLH11_MOUSE]	1,13	1	1	1	1
Q6PE13	Proline-rich transmembrane protein 3 OS=Mus musculus GN=Prrt3 PE=1 SV=1 - [PRRT3_MOUSE]	1,13	1	1	1	1
P62500	TSC22 domain family protein 1 OS=Mus musculus GN=Tsc22d1 PE=2 SV=2 - [T22D1_MOUSE]	1,11	1	1	1	1
Q8BG51	Mitochondrial Rho GTPase 1 OS=Mus musculus GN=Rhot1 PE=2 SV=1 - [MIRO1_MOUSE]	1,11	1	1	1	1
O54774	AP-3 complex subunit delta-1 OS=Mus musculus GN=Ap3d1 PE=1 SV=1 - [AP3D1_MOUSE]	1,08	1	1	1	2
Q5PR69	Uncharacterized protein KIAA1211 OS=Mus musculus GN=Kiaa1211 PE=2 SV=3 - [K1211_MOUSE]	1,08	1	1	1	1
P70206	Plexin-A1 OS=Mus musculus GN=Plxna1 PE=1 SV=1 - [PLXA1_MOUSE]	1,06	3	1	2	3
Q61290	Voltage-dependent R-type calcium channel subunit alpha-1E OS=Mus musculus GN=Cacna1e PE=1 SV=1 - [CAC1E_MOUSE]	1,06	1	2	2	8
Q4ACU6	SH3 and multiple ankyrin repeat domains protein 3 OS=Mus musculus GN=Shank3 PE=1 SV=2 - [SHAN3_MOUSE]	1,05	1	2	2	4
P13020	Gelsolin OS=Mus musculus GN=Gsn PE=1 SV=3 - [GELS_MOUSE]	1,03	1	1	1	1
Q8BIQ5	Cleavage stimulation factor subunit 2 OS=Mus musculus GN=Cstf2 PE=1 SV=2 - [CSTF2_MOUSE]	1,03	2	1	1	1
Q8BKC5	Importin-5 OS=Mus musculus GN=Ipo5 PE=1 SV=3 - [IPO5_MOUSE]	1,00	1	1	1	1
P80560	Receptor-type tyrosine-protein phosphatase N2 OS=Mus musculus GN=Ptprn2 PE=1 SV=2 - [PTPR2_MOUSE]	1,00	1	1	1	1
Q6ZPQ6	Membrane-associated phosphatidylinositol transfer protein 2 OS=Mus musculus GN=Pitpnm2 PE=1 SV=2 - [PITM2_MOUSE]	0,97	1	1	1	3
Q9DC29	ATP-binding cassette sub-family B member 6, mitochondrial OS=Mus musculus GN=Abcb6 PE=1 SV=1 - [ABCB6_MOUSE]	0,95	1	1	1	1
P27671	Ras-specific guanine nucleotide-releasing factor 1 OS=Mus musculus GN=Rasgrf1 PE=1 SV=2 - [RGRF1_MOUSE]	0,95	1	1	1	2
Q61543	Golgi apparatus protein 1 OS=Mus musculus GN=Glg1 PE=1 SV=1 - [GSLG1_MOUSE]	0,94	1	1	1	2
Q60943	Interleukin-17 receptor A OS=Mus musculus GN=Il17ra PE=1 SV=1 - [I17RA_MOUSE]	0,93	1	1	1	1

Accession	Description	Σ Cover.	Σ# Prot.	Σ# Unique Pept.	Σ# Pept.	Σ# PSM
Q6P5F9	Exportin-1 OS=Mus musculus GN=Xpo1 PE=1 SV=1 - [XPO1_MOUSE]	0,93	1	1	1	1
Q58A65	C-Jun-amino-terminal kinase-interacting protein 4 OS=Mus musculus GN=Spag9 PE=1 SV=2 - [JIP4_MOUSE]	0,91	1	1	1	1
Q3UDW8	Heparan-alpha-glucosaminide N-acetyltransferase OS=Mus musculus GN=Hgsnat PE=1 SV=2 - [HGNAT_MOUSE]	0,91	1	1	1	3
Q9ESN9	C-Jun-amino-terminal kinase-interacting protein 3 OS=Mus musculus GN=Mapk8ip3 PE=1 SV=1 - [JIP3_MOUSE]	0,90	1	1	1	1
Q9EQZ6	Rap guanine nucleotide exchange factor 4 OS=Mus musculus GN=Rapgef4 PE=1 SV=1 - [RPGF4_MOUSE]	0,89	1	1	1	1
Q80TK0	Uncharacterized protein KIAA1107 OS=Mus musculus GN=Kiaa1107 PE=2 SV=5 - [K1107_MOUSE]	0,88	1	1	1	1
Q3U1J4	DNA damage-binding protein 1 OS=Mus musculus GN=Ddb1 PE=1 SV=2 - [DDB1_MOUSE]	0,88	1	1	1	1
A2AP18	1-phosphatidylinositol 4,5-bisphosphate phosphodiesterase eta-2 OS=Mus musculus GN=Plch2 PE=1 SV=2 - [PLCH2_MOUSE]	0,87	1	1	1	2
Q80VP0	Tectonin beta-propeller repeat-containing protein 1 OS=Mus musculus GN=Tecpr1 PE=2 SV=1 - [TCPR1_MOUSE]	0,86	1	1	1	2
Q61137	Astrotactin-1 OS=Mus musculus GN=Astn1 PE=1 SV=4 - [ASTN1_MOUSE]	0,84	1	1	1	1
P55012	Solute carrier family 12 member 2 OS=Mus musculus GN=Slc12a2 PE=1 SV=2 - [S12A2_MOUSE]	0,83	1	1	1	2
P35436	Glutamate receptor ionotropic, NMDA 2A OS=Mus musculus GN=Grin2a PE=1 SV=2 - [NMDE1_MOUSE]	0,82	1	1	1	1
Q80XK6	Autophagy-related protein 2 homolog B OS=Mus musculus GN=Atg2b PE=1 SV=3 - [ATG2B_MOUSE]	0,82	1	1	2	5
Q0KL02	Triple functional domain protein OS=Mus musculus GN=Trio PE=1 SV=3 - [TRIO_MOUSE]	0,81	1	2	2	2
Q7TSH8	Uncharacterized protein KIAA0195 OS=Mus musculus GN=Kiaa0195 PE=1 SV=1 - [K0195_MOUSE]	0,81	1	1	1	2
Q5SYD0	Unconventional myosin-Id OS=Mus musculus GN=Myo1d PE=1 SV=1 - [MYO1D_MOUSE]	0,80	1	1	1	1
Q64331	Unconventional myosin-VI OS=Mus musculus GN=Myo6 PE=1 SV=1 - [MYO6_MOUSE]	0,79	1	1	1	1
Q9EQZ7	Regulating synaptic membrane exocytosis protein 2 OS=Mus musculus GN=Rims2 PE=1 SV=1 - [RIMS2_MOUSE]	0,78	1	1	1	3
Q99LI8	Hepatocyte growth factor-regulated tyrosine kinase substrate OS=Mus musculus GN=Hgs PE=1 SV=2 - [HGS_MOUSE]	0,77	1	1	1	1
Q99KY4	Cyclin-G-associated kinase OS=Mus musculus GN=Gak PE=1 SV=2 - [GAK_MOUSE]	0,77	1	1	1	1
Q01341	Adenylate cyclase type 6 OS=Mus musculus GN=Adcy6 PE=1 SV=1 - [ADCY6_MOUSE]	0,77	2	1	1	1
Q6DFV8	von Willebrand factor D and EGF domain-containing protein OS=Mus musculus GN=Vwde PE=2 SV=2 - [VWDE_MOUSE]	0,76	1	1	1	1
Q8C1B1	Calmodulin-regulated spectrin-associated protein 2 OS=Mus musculus GN=Camsap2 PE=1 SV=3 - [CAMP2_MOUSE]	0,75	1	1	1	2
P70232	Neural cell adhesion molecule L1-like protein OS=Mus musculus GN=Chl1 PE=1 SV=2 - [CHL1_MOUSE]	0,74	1	1	1	1
B9EJA2	Cortactin-binding protein 2 OS=Mus musculus GN=Cttnbp2 PE=1 SV=2 - [CTTB2_MOUSE]	0,73	1	1	1	1
A2AGT5	Cytoskeleton-associated protein 5 OS=Mus musculus GN=Ckap5 PE=2 SV=1 - [CKAP5_MOUSE]	0,69	1	1	1	1
Q61361	Brevican core protein OS=Mus musculus GN=Bcan PE=1 SV=2 - [PGCB_MOUSE]	0,68	1	1	1	1
Q7TQG1	Pleckstrin homology domain-containing family A member 6 OS=Mus musculus GN=Plekha6 PE=1 SV=1 - [PKHA6_MOUSE]	0,68	1	1	1	1
Q811P8	Rho GTPase-activating protein 32 OS=Mus musculus GN=Arhgap32 PE=1 SV=2 - [RHG32_MOUSE]	0,67	1	1	1	1
Q9WTU3	Sodium channel protein type 8 subunit alpha OS=Mus musculus GN=Scn8a PE=1 SV=1 - [SCN8A_MOUSE]	0,66	1	1	1	3
D3Z750	Maestro heat-like repeat-containing protein family member 2A OS=Mus musculus GN=Mroh2a PE=2 SV=2 - [MRO2A_MOUSE]	0,66	1	1	1	1
Q80TS3	Latrophilin-3 OS=Mus musculus GN=Lphn3 PE=1 SV=3 - [LPHN3_MOUSE]	0,65	1	1	1	1
Q8BMD7	MORC family CW-type zinc finger protein 4 OS=Mus musculus GN=Morc4 PE=2 SV=2 - [MORC4_MOUSE]	0,65	1	1	1	1
Q3UH66	Serine/threonine-protein kinase WNK2 OS=Mus musculus GN=Wnk2 PE=1 SV=2 - [WNK2_MOUSE]	0,65	1	1	1	1
CON_0070 41182	Bos taurus Gene_Symbol=- 505 kDa protein	0,64	2	2	2	3
Q8C0T5	Signal-induced proliferation-associated 1-like protein 1 OS=Mus musculus GN=Sipa1l1 PE=1 SV=2 - [SI1L1_MOUSE]	0,62	1	1	1	1
Q01097	Glutamate receptor ionotropic, NMDA 2B OS=Mus musculus GN=Grin2b PE=1 SV=3 - [NMDE2_MOUSE]	0,61	1	1	1	1
Q60675	Laminin subunit alpha-2 OS=Mus musculus GN=Lama2 PE=1 SV=2 - [LAMA2_MOUSE]	0,58	1	1	2	3
Q920I9	WD repeat-containing protein 7 OS=Mus musculus GN=Wdr7 PE=1 SV=3 - [WDR7_MOUSE]	0,54	1	1	1	1
P97393	Rho GTPase-activating protein 5 OS=Mus musculus GN=Arhgap5 PE=2 SV=2 - [RHG05_MOUSE]	0,53	1	1	1	1
Q8CC88	von Willebrand factor A domain-containing protein 8 OS=Mus musculus GN=Vwa8 PE=2 SV=2 - [VWA8_MOUSE]	0,52	1	1	1	1
P97445	Voltage-dependent P/Q-type calcium channel subunit alpha-1A OS=Mus musculus GN=Cacna1a PE=1 SV=2 - [CAC1A_MOUSE]	0,51	1	1	1	4
P11881	Inositol 1,4,5-trisphosphate receptor type 1 OS=Mus musculus GN=Itpr1 PE=1 SV=2 - [ITPR1_MOUSE]	0,47	1	1	1	1
A2AQ25	Sickle tail protein OS=Mus musculus GN=Skt PE=1 SV=1 - [SKT_MOUSE]	0,46	1	1	1	1
Q3UHK6	Teneurin-4 OS=Mus musculus GN=Tenm4 PE=1 SV=2 - [TEN4_MOUSE]	0,43	1	1	1	1
Q8K2X1	Probable phospholipid-transporting ATPase VD OS=Mus musculus GN=Atp10d PE=2 SV=2 - [AT10D_MOUSE]	0,42	2	1	1	1

Supplemtary table S1. List of proteins detected in the synaptic terminals of C57BL/6 mice. *Total synaptosomes were prepared and the synaptosomal fraction was analyzed by LC-MS/MS. A false discovery rate (FDR) of 1% was used. The identified candidate protein CSTF2 (CSTF64) is marked in grey.*

REFERENCES

REFERENCES

Akassoglou, K., Kombrinck, K.W., Degen, J.L., and Strickland, S. (2000). Tissue plasminogen activator-mediated fibrinolysis protects against axonal degeneration and demyelination after sciatic nerve injury. J. Cell Biol. *149*, 1157–1166.

Alarcon, J.M., Hodgman, R., Theis, M., Huang, Y.-S., Kandel, E.R., and Richter, J.D. (2004). Selective modulation of some forms of schaffer collateral-CA1 synaptic plasticity in mice with a disruption of the CPEB-1 gene. Learn. Mem. *11*, 318–327.

Alberini, C.M. (2009). Transcription factors in long-term memory and synaptic plasticity. Physiol. Rev. *89*, 121–145.

Alexandrov, I.M., Ivshina, M., Jung, D.Y., Friedline, R., Ko, H.J., Xu, M., O'Sullivan-Murphy, B., Bortell, R., Huang, Y.-T., Urano, F., et al. (2012). Cytoplasmic polyadenylation element binding protein deficiency stimulates PTEN and Stat3 mRNA translation and induces hepatic insulin resistance. PLoS Genet. *8*, e1002457.

Allison, L.A., Moyle, M., Shales, M., and Ingles, C.J. (1985). Extensive homology among the largest subunits of eukaryotic and prokaryotic RNA polymerases. Cell *42*, 599–610.

Alzheimer, A. (1907). Über eine eigenartige Erkrankung der Hirnrinde. Allg. Zeitschrift Fűr Psychiatr. *64*, 146–148.

Andorfer, C., Kress, Y., Espinoza, M., de Silva, R., Tucker, K.L., Barde, Y.-A., Duff, K., and Davies, P. (2003). Hyperphosphorylation and aggregation of tau in mice expressing normal human tau isoforms. J. Neurochem. *86*, 582–590.

Andrei, M.A., Ingelfinger, D., Heintzmann, R., Achsel, T., Rivera-Pomar, R., and Lührmann, R. (2005). A role for eIF4E and eIF4E-transporter in targeting mRNPs to mammalian processing bodies. RNA *11*, 717–727.

Araujo, P.R., Yoon, K., Ko, D., Smith, A.D., Qiao, M., Suresh, U., Burns, S.C., and Penalva, L.O.F. (2012). Before it gets started: Regulating translation at the 5' UTR. Comp. Funct. Genomics *2012*, 475731.

Arvanitakis, Z., Wilson, R.S., Bienias, J.L., Evans, D.A., and Bennett, D.A. (2004). Diabetes mellitus and risk of Alzheimer disease and decline in cognitive function. Arch. Neurol. *61*, 661–666.

Atkins, C.M., Nozaki, N., Shigeri, Y., and Soderling, T.R. (2004). Cytoplasmic polyadenylation element binding protein-dependent protein synthesis is regulated by calcium/calmodulin-dependent protein kinase II. J. Neurosci. *24*, 5193–5201.

Baranes, D., Lederfein, D., Huang, Y.Y., Chen, M., Bailey, C.H., and Kandel, E.R. (1998). Tissue plasminogen activator contributes to the late phase of LTP and to synaptic growth in the hippocampal mossy fiber pathway. Neuron *21*, 813–825.

Barker-Carlson, K., Lawrence, D.A., and Schwartz, B.S. (2002). Acyl-enzyme complexes between tissue-type plasminogen activator and neuroserpin are short-lived in vitro. J. Biol. Chem. *277*, 46852–46857.

Bateman, R.J., Xiong, C., Benzinger, T.L.S., Fagan, A.M., Goate, A., Fox, N.C., Marcus, D.S., Cairns, N.J., Xie, X., Blazey, T.M., et al. (2012). Clinical and biomarker changes in dominantly inherited Alzheimer's disease. N. Engl. J. Med. *367*, 795–804.

Bava, F.-A., Eliscovich, C., Ferreira, P.G., Miñana, B., Ben-Dov, C., Guigó, R., Valcárcel, J., and Méndez, R. (2013). CPEB1 coordinates alternative 3'-UTR formation with translational regulation. Nature *495*, 121–125.

Beaudoing, E., Freier, S., Wyatt, J.R., Claverie, J.M., and Gautheret, D. (2000). Patterns of variant polyadenylation signal usage in human genes. Genome Res. *10*, 1001–1010.

Benoit, P., Papin, C., Kwak, J.E., Wickens, M., and Simonelig, M. (2008). PAP- and GLD-2-type poly(A) polymerases are required sequentially in cytoplasmic polyadenylation and oogenesis in Drosophila. Development *135*, 1969–1979.

Berger-Sweeney, J., Zearfoss, N.R., and Richter, J.D. (2006). Reduced extinction of hippocampal-dependent memories in CPEB knockout mice. Learn. Mem. *13*, 4–7.

Bestman, J.E., and Cline, H.T. (2008). The RNA binding protein CPEB regulates dendrite morphogenesis and neuronal circuit assembly in vivo. Proc. Natl. Acad. Sci. U. S. A. *105*, 20494–20499.

Beydoun, M.A., Beydoun, H.A., and Wang, Y. (2008). Obesity and central obesity as risk factors for incident dementia and its subtypes: a systematic review and meta-analysis. Obes. Rev. *9*, 204–218.

Blasi, F. (1999). Proteolysis, cell adhesion, chemotaxis, and invasiveness are regulated by the u-PA-u-PAR-PAI-1 system. Thromb. Haemost. *82*, 298–304.

Both, G.W., Banerjee, A.K., and Shatkin, A.J. (1975). Methylation-dependent translation of viral messenger RNAs in vitro. Proc. Natl. Acad. Sci. U. S. A. *72*, 1189–1193.

Brown, K.M., and Gilmartin, G.M. (2003). A mechanism for the regulation of pre-mRNA 3' processing by human cleavage factor Im. Mol. Cell *12*, 1467–1476.

Bukhari, N., Torres, L., Robinson, J.K., and Tsirka, S.E. (2011). Axonal regrowth after spinal cord injury via chondroitinase and the tissue plasminogen activator (tPA)/plasmin system. J. Neurosci. *31*, 14931–14943.

Burns, D.M., and Richter, J.D. (2008). CPEB regulation of human cellular senescence, energy metabolism, and p53 mRNA translation. Genes Dev. *22*, 3449–3460.

Burns, D.M., D'Ambrogio, A., Nottrott, S., and Richter, J.D. (2011). CPEB and two poly(A) polymerases control miR-122 stability and p53 mRNA translation. Nature *473*, 105–108.

Cacquevel, M., Launay, S., Castel, H., Benchenane, K., Cheenne, S., Buee, L., Moons, L., Delacourte, A., Carmeliet, P., and Vivien, D. (2007). Ageing and amyloid-beta peptide deposition contribute to an impaired brain tissue plasminogen activator activity by different mechanisms. Neurobiol Dis.

Calderone, V., Gallego, J., Fernandez-Miranda, G., Garcia-Pras, E., Maillo, C., Berzigotti, A., Mejias, M., Bava, F.-A., Angulo-Urarte, A., Graupera, M., et al. (2015). Sequential Functions of CPEB1 and CPEB4 Regulate Pathologic Expression of VEGF and Angiogenesis in Chronic Liver Disease. Gastroenterology *150*, 982–997.e30.

Camoletto, P.G., Vara, H., Morando, L., Connell, E., Marletto, F.P., Giustetto, M., Sassoè-Pognetto, M., Van Veldhoven, P.P., and Ledesma, M.D. (2009). Synaptic vesicle docking: sphingosine regulates syntaxin1 interaction with Munc18. PLoS One *4*, e5310.

Cao, C., Lawrence, D.A., Li, Y., Von Arnim, C.A.F., Herz, J., Su, E.J., Makarova, A., Hyman, B.T., Strickland, D.K., and Zhang, L. (2006). Endocytic receptor LRP together with tPA and PAI-1 coordinates Mac-1-dependent macrophage migration. EMBO J. *25*, 1860–1870.

Cao, Q., Huang, Y.-S., Kan, M.-C., and Richter, J.D. (2005). Amyloid precursor proteins anchor CPEB to membranes and promote polyadenylation-induced translation. Mol. Cell. Biol. *25*, 10930–10939.

Carmeliet, P., Schoonjans, L., Kieckens, L., Ream, B., Degen, J., Bronson, R., De Vos, R., van den Oord, J.J., Collen, D., and Mulligan, R.C. (1994). Physiological consequences of loss of plasminogen activator gene function in mice. Nature *368*, 419–424.

Cataldo, J.K., Prochaska, J.J., and Glantz, S.A. (2010). Cigarette smoking is a risk factor for Alzheimer's Disease: an analysis controlling for tobacco industry affiliation. J. Alzheimers. Dis. *19*, 465–480.

Cesarman, G.M., Guevara, C.A., and Hajjar, K.A. (1994). An endothelial cell receptor for plasminogen/tissue plasminogen activator (t-PA). II. Annexin II-mediated enhancement of t-PA-dependent plasminogen activation. J. Biol. Chem. *269*, 21198–21203.

Chandra, V., Bharucha, N.E., and Schoenberg, B.S. (1986). Conditions associated with Alzheimer's disease at death: case-control study. Neurology *36*, 209–211.

Chang, J.S., Tan, L., and Schedl, P. (1999). The Drosophila CPEB homolog, orb, is required for oskar protein expression in oocytes. Dev. Biol. *215*, 91–106.

Chao, H.-W., Tsai, L.-Y., Lu, Y.-L., Lin, P.-Y., Huang, W.-H., Chou, H.-J., Lu, W.-H., Lin, H.-C., Lee, P.-T., and Huang, Y.-S. (2013). Deletion of CPEB3 enhances hippocampus-dependent memory via increasing expressions of PSD95 and NMDA receptors. J. Neurosci. *33*, 17008–17022.

Chapman, R.D., Heidemann, M., Albert, T.K., Mailhammer, R., Flatley, A., Meisterernst, M., Kremmer, E., and Eick, D. (2007). Transcribing RNA polymerase II is phosphorylated at CTD residue serine-7. Science *318*, 1780–1782.

Charlesworth, A., Meijer, H.A., and De Moor, C.H. (2013). Specificity factors in cytoplasmic polyadenylation. Wiley Interdiscip. Rev. RNA *4*, 437–461.

Chen, Z.L., and Strickland, S. (1997). Neuronal death in the hippocampus is promoted by plasmin-catalyzed degradation of laminin. Cell *91*, 917–925.

Chen, C.S., Lyons-Giordano, B., Lazarus, G.S., and Jensen, P.J. (1993). Differential expression of plasminogen activators and their inhibitors in an organotypic skin coculture system. J. Cell Sci. *106 (Pt 1*, 45–53.

Chen, P.-J., Weng, J.-Y., Hsu, P.-H., Shew, J.-Y., Huang, Y.-S., and Lee, W.-H. (2015). NPGPx modulates CPEB2-controlled HIF-1α RNA translation in response to oxidative stress. Nucleic Acids Res. *43*, 9393–9404.

Chishti, M.A., Yang, D.S., Janus, C., Phinney, A.L., Horne, P., Pearson, J., Strome, R., Zuker, N., Loukides, J., French, J., et al. (2001). Early-onset amyloid deposition and cognitive deficits in transgenic mice expressing a double mutant form of amyloid precursor protein 695. J. Biol. Chem. *276*, 21562–21570.

Cho, E.J., Takagi, T., Moore, C.R., and Buratowski, S. (1997). mRNA capping enzyme is recruited to the transcription complex by phosphorylation of the RNA polymerase II carboxy-terminal domain. Genes Dev. *11*, 3319–3326.

Chou, Z.F., Chen, F., and Wilusz, J. (1994). Sequence and position requirements for uridylate-rich downstream elements of polyadenylation signals. Nucleic Acids Res. *22*, 2525–2531.

Christerson, L.B., and McKearin, D.M. (1994). orb is required for anteroposterior and dorsoventral patterning during Drosophila oogenesis. Genes Dev. *8*, 614–628.

Cinelli, P., Madani, R., Tsuzuki, N., Vallet, P., Arras, M., Zhao, C.N., Osterwalder, T., Rülicke, T., and Sonderegger, P. (2001). Neuroserpin, a neuroprotective factor in focal ischemic stroke. Mol. Cell. Neurosci. *18*, 443–457.

Collen, D. (1976). Identification and some properties of a new fast-reacting plasmin inhibitor in human plasma. Eur. J. Biochem. *69*, 209–216.

Collen, D., and Lijnen, H.R. (1991). Basic and clinical aspects of fibrinolysis and thrombolysis. Blood *78*, 3114–3124.

Cooke, C., and Alwine, J.C. (1996). The cap and the 3′ splice site similarly affect polyadenylation efficiency. Mol. Cell. Biol. *16*, 2579–2584.

Corden, J.L., Cadena, D.L., Ahearn, J.M., and Dahmus, M.E. (1985). A unique structure at the carboxyl terminus of the largest subunit of eukaryotic RNA polymerase II. Proc. Natl. Acad. Sci. U. S. A. *82*, 7934–7938.

Corte, M.D., Vérez, P., Rodríguez, J.C., Roibás, A., Domínguez, M.L., Lamelas, M.L., Vázquez, J., García Muñiz, J.L., Allende, M.T., González, L.O., et al. (2005). Tissue-type plasminogen activator (tPA) in breast cancer: relationship with clinicopathological parameters and prognostic significance. Breast Cancer Res. Treat. *90*, 33–40.

Cummings, J.L. (2004). Alzheimer's disease. N. Engl. J. Med. *351*, 56–67.

Darnell, J.C., Van Driesche, S.J., Zhang, C., Hung, K.Y.S., Mele, A., Fraser, C.E., Stone, E.F., Chen, C., Fak, J.J., Chi, S.W., et al. (2011). FMRP stalls ribosomal translocation on mRNAs linked to synaptic function and autism. Cell *146*, 247–261.

Davies, S.W., Turmaine, M., Cozens, B.A., DiFiglia, M., Sharp, A.H., Ross, C.A., Scherzinger, E., Wanker, E.E., Mangiarini, L., and Bates, G.P. (1997). Formation of neuronal intranuclear inclusions underlies the neurological dysfunction in mice transgenic for the HD mutation. Cell *90*, 537–548.

Davis, H.P., and Squire, L.R. (1984). Protein synthesis and memory: a review. Psychol. Bull. *96*, 518–559.

Deininger, M.H., Trautmann, K., Magdolen, V., Luther, T., Schluesener, H.J., and Meyermann, R. (2002). Cortical neurons of Creutzfeldt-Jakob disease patients express the urokinase-type plasminogen activator receptor. Neurosci. Lett. *324*, 80–82.

Dever, T.E., and Green, R. (2012). The elongation, termination, and recycling phases of translation in eukaryotes. Cold Spring Harb. Perspect. Biol. *4*, a013706.

Díaz, V.M., Planaguma, J., Thomson, T.M., Reventós, J., and Paciucci, R. (2002). Tissue plasminogen activator is required for the growth, invasion, and angiogenesis of pancreatic tumor cells. Gastroenterology *122*, 806–819.

Dickson, K.S., Bilger, A., Ballantyne, S., and Wickens, M.P. (1999). The cleavage and polyadenylation specificity factor in Xenopus laevis oocytes is a cytoplasmic factor involved in regulated polyadenylation. Mol. Cell. Biol. *19*, 5707–5717.

DiFiglia, M., Sapp, E., Chase, K.O., Davies, S.W., Bates, G.P., Vonsattel, J.P., and Aronin, N. (1997). Aggregation of huntingtin in neuronal intranuclear inclusions and dystrophic neurites in brain. Science *277*, 1990–1993.

Dostie, J., Ferraiuolo, M., Pause, A., Adam, S.A., and Sonenberg, N. (2000). A novel shuttling protein, 4E-T, mediates the nuclear import of the mRNA 5' cap-binding protein, eIF4E. EMBO J. *19*, 3142–3156.

Dotti, C.G., Sullivan, C.A., and Banker, G.A. (1988). The establishment of polarity by hippocampal neurons in culture. J. Neurosci. *8*, 1454–1468.

Drisaldi, B., Colnaghi, L., Fioriti, L., Rao, N., Myers, C., Snyder, A.M., Metzger, D.J., Tarasoff, J., Konstantinov, E., Fraser, P.E., et al. (2015). SUMOylation Is an Inhibitory Constraint that Regulates the Prion-like Aggregation and Activity of CPEB3. Cell Rep. 1–9.

East, E., Baker, D., Pryce, G., Lijnen, H.R., Cuzner, M.L., and Gverić, D. (2005). A role for the plasminogen activator system in inflammation and neurodegeneration in the central nervous system during experimental allergic encephalomyelitis. Am. J. Pathol. *167*, 545–554.

Echeverry, R., Wu, J., Haile, W.B., Guzman, J., and Yepes, M. (2010). Tissue-type plasminogen activator is a neuroprotectant in the mouse hippocampus. J. Clin. Invest. *120*, 2194–2205.

Eckman, E.A., Reed, D.K., and Eckman, C.B. (2001). Degradation of the Alzheimer's amyloid beta peptide by endothelin-converting enzyme. J. Biol. Chem. *276*, 24540–24548.

Edery, I., and Sonenberg, N. (1985). Cap-dependent RNA splicing in a HeLa nuclear extract. Proc. Natl. Acad. Sci. U. S. A. *82*, 7590–7594.

Egloff, S., and Murphy, S. (2008). Cracking the RNA polymerase II CTD code. Trends Genet. *24*, 280–288.

Egloff, S., O'Reilly, D., Chapman, R.D., Taylor, A., Tanzhaus, K., Pitts, L., Eick, D., and Murphy, S. (2007). Serine-7 of the RNA polymerase II CTD is specifically required for snRNA gene expression. Science *318*, 1777–1779.

Eisele, Y.S., Bolmont, T., Heikenwalder, M., Langer, F., Jacobson, L.H., Yan, Z.-X., Roth, K., Aguzzi, A., Staufenbiel, M., Walker, L.C., et al. (2009). Induction of cerebral beta-amyloidosis: intracerebral versus systemic Abeta inoculation. Proc. Natl. Acad. Sci. U. S. A. *106*, 12926–12931.

Elkon, R., Ugalde, A.P., and Agami, R. (2013). Alternative cleavage and polyadenylation: extent, regulation and function. Nat. Rev. Genet. *14*, 496–506.

Ellis, V., and Dano, K. (1991). Plasminogen activation by receptor-bound urokinase. Semin. Thromb. Hemost. *17*, 194–200.

Ernoult-Lange, M., Wilczynska, A., Harper, M., Aigueperse, C., Dautry, F., Kress, M., and Weil, D. (2009). Nucleocytoplasmic traffic of CPEB1 and accumulation in Crm1 nucleolar bodies. Mol. Biol. Cell *20*, 176–187.

Esteban-Santillan, C., Praditsuwan, R., Ueda, H., and Geldmacher, D.S. (1998). Clock drawing test in very mild Alzheimer's disease. J. Am. Geriatr. Soc. *46*, 1266–1269.

Fauser, S., Deininger, M.H., Kremsner, P.G., Magdolen, V., Luther, T., Meyermann, R., and Schluesener, H.J. (2000). Lesion associated expression of urokinase-type plasminogen activator receptor (uPAR, CD87) in human cerebral malaria. J. Neuroimmunol. *111*, 234–240.

Fernández-Miranda, G., and Méndez, R. (2012). The CPEB-family of proteins, translational control in senescence and cancer. Ageing Res. Rev. *11*, 460–472.

Fernández-Monreal, M., López-Atalaya, J.P., Benchenane, K., Cacquevel, M., Dulin, F., Le Caer, J.-P., Rossier, J., Jarrige, A.-C., Mackenzie, E.T., Colloc'h, N., et al. (2004). Arginine 260 of the amino-terminal domain of NR1 subunit is critical for tissue-type plasminogen activator-mediated enhancement of N-methyl-D-aspartate receptor signaling. J. Biol. Chem. *279*, 50850–50856.

Ferraiuolo, M.A., Basak, S., Dostie, J., Murray, E.L., Schoenberg, D.R., and Sonenberg, N. (2005). A role for the eIF4E-binding protein 4E-T in P-body formation and mRNA decay. J. Cell Biol. *170*, 913–924.

Ferreira, A., Lu, Q., Orecchio, L., and Kosik, K.S. (1997). Selective phosphorylation of adult tau isoforms in mature hippocampal neurons exposed to fibrillar A beta. Mol. Cell. Neurosci. *9*, 220–234.

Fioriti, L., Myers, C., Huang, Y.-Y., Li, X., Stephan, J.S., Trifilieff, P., Colnaghi, L., Kosmidis, S., Drisaldi, B., Pavlopoulos, E., et al. (2015). The Persistence of Hippocampal-Based Memory Requires Protein Synthesis Mediated by the Prion-like Protein CPEB3. Neuron *86*, 1433–1448.

Fiumelli, H., Jabaudon, D., Magistretti, P.J., and Martin, J.L. (1999). BDNF stimulates expression, activity and release of tissue-type plasminogen activator in mouse cortical neurons. Eur. J. Neurosci. *11*, 1639–1646.

Flaherty, S.M., Fortes, P., Izaurralde, E., Mattaj, I.W., and Gilmartin, G.M. (1997). Participation of the nuclear cap binding complex in pre-mRNA 3' processing. Proc. Natl. Acad. Sci. U. S. A. *94*, 11893–11898.

Fox, C.A., Sheets, M.D., and Wickens, M.P. (1989). Poly(A) addition during maturation of frog oocytes: Distinct nuclear and cytoplasmic activities and regulation by the sequence UUUUUAU. Genes Dev. *3*, 2151–2162.

Frey, U., Müller, M., and Kuhl, D. (1996). A different form of long-lasting potentiation revealed in tissue plasminogen activator mutant mice. J. Neurosci. *16*, 2057–2063.

Fukazawa, Y., Saitoh, Y., Ozawa, F., Ohta, Y., Mizuno, K., and Inokuchi, K. (2003). Hippocampal LTP is accompanied by enhanced F-actin content within the dendritic spine that is essential for late LTP maintenance in vivo. Neuron *38*, 447–460.

Furuichi, Y., LaFiandra, A., and Shatkin, A.J. (1977). 5'-Terminal structure and mRNA stability. Nature *266*, 235–239.

Gabay, C., and Kushner, I. (1999). Acute-phase proteins and other systemic responses to inflammation. N. Engl. J. Med. *340*, 448–454.

Gaberel, T., Macrez, R., Gauberti, M., Montagne, A., Hebert, M., Petersen, K.-U., Touze, E., Agin, V., Emery, E., Ali, C., et al. (2013). Immunotherapy blocking the tissue plasminogen activator-dependent activation of N-methyl-D-aspartate glutamate receptors improves hemorrhagic stroke outcome. Neuropharmacology *67*, 267–271.

Gallie, D.R. (1991). The cap and poly(A) tail function synergistically to regulate mRNA translational efficiency. Genes Dev. *5*, 2108–2116.

Games, D., Adams, D., Alessandrini, R., Barbour, R., Berthelette, P., Blackwell, C., Carr, T., Clemens, J., Donaldson, T., and Gillespie, F. (1995). Alzheimer-type neuropathology in transgenic mice overexpressing V717F beta-amyloid precursor protein. Nature *373*, 523–527.

Ganrot, P.O. (1967). Inhibition of plasmin activity by alpha-2-macroglobulin. Clin. Chim. Acta. *16*, 328–329.

Gardiol, A., Racca, C., and Triller, A. (1999). Dendritic and postsynaptic protein synthetic machinery. J. Neurosci. *19*, 168–179.

Gebauer, F., and Hentze, M.W. (2004). Molecular mechanisms of translational control. Nat.Rev.Mol.Cell Biol. *5*, 827–835.

Gil, A., and Proudfoot, N.J. (1987). Position-dependent sequence elements downstream of AAUAAA are required for efficient rabbit beta-globin mRNA 3' end formation. Cell *49*, 399–406.

Gilmartin, G.M., McDevitt, M.A., and Nevins, J.R. (1988). Multiple factors are required for specific RNA cleavage at a poly(A) addition site. Genes Dev. *2*, 578–587.

Glanzman, D.L. (2013). PKM and the maintenance of memory. F1000 Biol. Rep. *5*, 4.

Glenner, G.G., and Wong, C.W. (1984). Alzheimer's disease: initial report of the purification and characterization of a novel cerebrovascular amyloid protein. Biochem. Biophys. Res. Commun. *120*, 885–890.

Greene, J.D., Baddeley, A.D., and Hodges, J.R. (1996). Analysis of the episodic memory deficit in early Alzheimer's disease: evidence from the doors and people test. Neuropsychologia *34*, 537–551.

Groisman, I., Ivshina, M., Marin, V., Kennedy, N.J., Davis, R.J., and Richter, J.D. (2006). Control of cellular senescence by CPEB. Genes Dev. *20*, 2701–2712.

Groppo, R., and Richter, J.D. (2011). CPEB control of NF-kappaB nuclear localization and interleukin-6 production mediates cellular senescence. Mol. Cell. Biol. *31*, 2707–2714.

Gveric, D., Hanemaaijer, R., Newcombe, J., van Lent, N.A., Sier, C.F., and Cuzner, M.L. (2001). Plasminogen activators in multiple sclerosis lesions: implications for the inflammatory response and axonal damage. Brain *124*, 1978–1988.

Hacke, W., Kaste, M., Bluhmki, E., Brozman, M., Dávalos, A., Guidetti, D., Larrue, V., Lees, K.R., Medeghri, Z., Machnig, T., et al. (2008). Thrombolysis with alteplase 3 to 4.5 hours after acute ischemic stroke. N. Engl. J. Med. *359*, 1317–1329.

Hajjar, K.A., and Acharya, S.S. (2000). Annexin II and regulation of cell surface fibrinolysis. Ann. N. Y. Acad. Sci. *902*, 265–271.

Hajjar, K.A., and Krishnan, S. (1999). Annexin II: a mediator of the plasmin/plasminogen activator system. Trends Cardiovasc. Med. *9*, 128–138.

Hajjar, K.A., Jacovina, A.T., and Chacko, J. (1994). An endothelial cell receptor for plasminogen/tissue plasminogen activator. I. Identity with annexin II. J. Biol. Chem. *269*, 21191–21197.

Hake, L.E., Mendez, R., and Richter, J.D. (1998). Specificity of RNA binding by CPEB: requirement for RNA recognition motifs and a novel zinc finger. Mol. Cell. Biol. *18*, 685–693.

Hamm, J., and Mattaj, I.W. (1990). Monomethylated cap structures facilitate RNA export from the nucleus. Cell *63*, 109–118.

Hardy, J., and Selkoe, D.J. (2002). The amyloid hypothesis of Alzheimer's disease: progress and problems on the road to therapeutics. Science *297*, 353–356.

Hashimoto, K., Horikoshi, T., Nishioka, K., Yoshikawa, K., and Carter, D.M. (1986). Plasminogen activator secreted by cultured human melanocytes. Br. J. Dermatol. *115*, 205–209.

Heinrich, S.U., and Lindquist, S. (2011). Protein-only mechanism induces self-perpetuating changes in the activity of neuronal Aplysia cytoplasmic polyadenylation element binding protein (CPEB). Proc. Natl. Acad. Sci. U. S. A. *108*, 2999–3004.

Herzig, M.C., Winkler, D.T., Burgermeister, P., Pfeifer, M., Kohler, E., Schmidt, S.D., Danner, S., Abramowski, D., Stürchler-Pierrat, C., Bürki, K., et al. (2004). Abeta is targeted to the vasculature in a mouse model of hereditary cerebral hemorrhage with amyloidosis. Nat. Neurosci. *7*, 954–960.

Ho, C.K., Sriskanda, V., McCracken, S., Bentley, D., Schwer, B., and Shuman, S. (1998). The guanylyltransferase domain of mammalian mRNA capping enzyme binds to the phosphorylated carboxyl-terminal domain of RNA polymerase II. J. Biol. Chem. *273*, 9577–9585.

Holcomb, L., Gordon, M.N., McGowan, E., Yu, X., Benkovic, S., Jantzen, P., Wright, K., Saad, I., Mueller, R., Morgan, D., et al. (1998). Accelerated Alzheimer-type phenotype in transgenic mice carrying both mutant amyloid precursor protein and presenilin 1 transgenes. Nat. Med. *4*, 97–100.

Holt, C.E., and Bullock, S.L. (2009). Subcellular mRNA localization in animal cells and why it matters. Science *326*, 1212–1216.

Hsiao, K., Chapman, P., Nilsen, S., Eckman, C., Harigaya, Y., Younkin, S., Yang, F., and Cole, G. (1996). Correlative memory deficits, Abeta elevation, and amyloid plaques in transgenic mice. Science *274*, 99–102.

Hsin, J., and Manley, J.L. (2012). The RNA polymerase II CTD coordinates transcription and RNA processing. Genes Dev. *26*, 2119–2137.

Hu, J., Igarashi, A., Kamata, M., and Nakagawa, H. (2001). Angiotensin-converting enzyme degrades Alzheimer amyloid ß-peptide (Aß), retards Aß aggregation , deposition , fibril formation and inhibits cytotoxicity Jianguo Hu , Akira Igarashi *, Makiko Kamata and Hachiro Nakagawa R & D Center , BML . 1361-1 Matob.

Hu, J., Lutz, C.S., Wilusz, J., and Tian, B. (2005). Bioinformatic identification of candidate cis-regulatory elements involved in human mRNA polyadenylation. RNA *11*, 1485–1493.

Hu, K., Yang, J., Tanaka, S., Gonias, S.L., Mars, W.M., and Liu, Y. (2006). Tissue-type plasminogen activator acts as a cytokine that triggers intracellular signal transduction and induces matrix metalloproteinase-9 gene expression. J. Biol. Chem. *281*, 2120–2127.

Huang, Y., and Carmichael, G.G. (1996). Role of polyadenylation in nucleocytoplasmic transport of mRNA. Mol. Cell. Biol. *16*, 1534–1542.

Huang, Y.-S., Jung, M.-Y., Sarkissian, M., and Richter, J.D. (2002). N-methyl-D-aspartate receptor signaling results in Aurora kinase-catalyzed CPEB phosphorylation and alpha CaMKII mRNA polyadenylation at synapses. EMBO J. *21*, 2139–2148.

Huang, Y.-S., Carson, J.H., Barbarese, E., and Richter, J.D. (2003). Facilitation of dendritic mRNA transport by CPEB. Genes Dev. *17*, 638–653.

Huang, Y.-S., Kan, M.-C., Lin, C.-L., and Richter, J.D. (2006). CPEB3 and CPEB4 in neurons: analysis of RNA-binding specificity and translational control of AMPA receptor GluR2 mRNA. EMBO J. *25*, 4865–4876.

Huang, Y.Y., Bach, M.E., Lipp, H.P., Zhuo, M., Wolfer, D.P., Hawkins, R.D., Schoonjans, L., Kandel, E.R., Godfraind, J.M., Mulligan, R., et al. (1996). Mice lacking the gene encoding tissue-type plasminogen activator show a selective interference with late-phase long-term potentiation in both Schaffer collateral and mossy fiber pathways. Proc. Natl. Acad. Sci. U. S. A. *93*, 8699–8704.

Igea, A., and Méndez, R. (2010). Meiosis requires a translational positive loop where CPEB1 ensues its replacement by CPEB4. EMBO J. *29*, 2182–2193.

Imataka, H., Gradi, A., and Sonenberg, N. (1998). A newly identified N-terminal amino acid sequence of human eIF4G binds poly(A)-binding protein and functions in poly(A)-dependent translation. EMBO J. *17*, 7480–7489.

Inoue, K., Ohno, M., Sakamoto, H., and Shimura, Y. (1989). Effect of the cap structure on pre-mRNA splicing in Xenopus oocyte nuclei. Genes Dev. *3*, 1472–1479.

Iqbal, K., and Grundke-Iqbal, I. (2008). Alzheimer neurofibrillary degeneration: significance, etiopathogenesis, therapeutics and prevention. J. Cell. Mol. Med. *12*, 38–55.

Ivshina, M., Lasko, P., and Richter, J.D. (2014). Cytoplasmic Polyadenylation Element Binding Proteins in Development, Health, and Disease. Annu. Rev. Cell Dev. Biol. *30*, 393–415.

Izaurralde, E., Lewis, J., McGuigan, C., Jankowska, M., Darzynkiewicz, E., and Mattaj, I.W. (1994). A nuclear cap binding protein complex involved in pre-mRNA splicing. Cell *78*, 657–668.

Izaurralde, E., Lewis, J., Gamberi, C., Jarmolowski, A., McGuigan, C., and Mattaj, I.W. (1995). A cap-binding protein complex mediating U snRNA export. Nature *376*, 709–712.

Jackson, R.J., Hellen, C.U.T., and Pestova, T. V (2010). The mechanism of eukaryotic translation initiation and principles of its regulation. Nat. Rev. Mol. Cell Biol. *11*, 113–127.

Jacobs, D., Sano, M., Marder, K., Bell, K., Bylsma, F., Lafleche, G., Albert, M., Brandt, J., and Stern, Y. (1994). Age at onset of Alzheimer's disease: relation to pattern of cognitive dysfunction and rate of decline. Neurology *44*, 1215–1220.

Jean, Y.Y., Baleriola, J., Fà, M., Hengst, U., and Troy, C.M. (2015). Stereotaxic Infusion of Oligomeric Amyloid-beta into the Mouse Hippocampus. J. Vis. Exp. e52805.

Ji, Z., Lee, J.Y., Pan, Z., Jiang, B., and Tian, B. (2009). Progressive lengthening of 3' untranslated regions of mRNAs by alternative polyadenylation during mouse embryonic development. Proc. Natl. Acad. Sci. U. S. A. *106*, 7028–7033.

Jung, M.-Y., Lorenz, L., and Richter, J.D. (2006). Translational control by neuroguidin, a eukaryotic initiation factor 4E and CPEB binding protein. Mol. Cell. Biol. *26*, 4277–4287.

Jurado, A.R., Tan, D., Jiao, X., Kiledjian, M., and Tong, L. (2014). Structure and function of pre-mRNA 5???-end capping quality control and 3???-end processing. Biochemistry *53*, 1882–1898.

Kaech, S., and Banker, G. (2006). Culturing hippocampal neurons. Nat. Protoc. *1*, 2406–2415.

Kan, M.-C., Oruganty-Das, A., Cooper-Morgan, A., Jin, G., Swanger, S.A., Bassell, G.J., Florman, H., van Leyen, K., and Richter, J.D. (2010). CPEB4 is a cell survival protein retained in the nucleus upon ischemia or endoplasmic reticulum calcium depletion. Mol. Cell. Biol. *30*, 5658–5671.

Kandel, E.R. (2001). The molecular biology of memory storage: a dialogue between genes and synapses. Science *294*, 1030–1038.

Kandel, E.R. (2012). The molecular biology of memory: cAMP, PKA, CRE, CREB-1, CREB-2, and CPEB. Mol. Brain *5*, 14.

Kandel, E.R., Schwartz, J.H., Jessell, T.M., Siegelbaum, S.A., and Hudspeth, A. (2013). Principles of neural science, fifth edition (McGraw-Hill).

Kanemitsu, H., Tomiyama, T., and Mori, H. (2003). Human neprilysin is capable of degrading amyloid beta peptide not only in the monomeric form but also the pathological oligomeric form. Neurosci. Lett. *350*, 113–116.

Keleman, K., Krüttner, S., Alenius, M., and Dickson, B.J. (2007). Function of the Drosophila CPEB protein Orb2 in long-term courtship memory. Nat. Neurosci. *10*, 1587–1593.

Kim, J.H., and Richter, J.D. (2006). Opposing polymerase-deadenylase activities regulate cytoplasmic polyadenylation. Mol. Cell *24*, 173–183.

Kim, J.H., and Richter, J.D. (2007). RINGO/cdk1 and CPEB mediate poly(A) tail stabilization and translational regulation by ePAB. Genes Dev. *21*, 2571–2579.

Kingston, I., Castro, M., and Anderson, S. (1995a). In vitro stimulation of tissue-type plasminogen activator by Alzheimer amyloid beta-peptide analogues. Nat Med *1*, 138–142.

Kingston, I.B., Castro, M.J., and Anderson, S. (1995b). In vitro stimulation of tissue-type plasminogen activator by Alzheimer amyloid beta-peptide analogues. Nat. Med. *1*, 138–142.

Kirk, A., and Kertesz, A. (1991). On drawing impairment in Alzheimer's disease. Arch. Neurol. *48*, 73–77.

Konarska, M.M., Padgett, R.A., and Sharp, P.A. (1984). Recognition of cap structure in splicing in vitro of mRNA precursors. Cell *38*, 731–736.

Krichevsky, A.M., and Kosik, K.S. (2001). Neuronal RNA granules: a link between RNA localization and stimulation-dependent translation. Neuron *32*, 683–696.

Krueger, S.R., Ghisu, G.P., Cinelli, P., Gschwend, T.P., Osterwalder, T., Wolfer, D.P., and Sonderegger, P. (1997). Expression of neuroserpin, an inhibitor of tissue plasminogen activator, in the developing and adult nervous system of the mouse. J. Neurosci. *17*, 8984–8996.

Kruithof, E.K., Tran-Thang, C., Ransijn, A., and Bachmann, F. (1984). Demonstration of a fast-acting inhibitor of plasminogen activators in human plasma. Blood *64*, 907–913.

Kruithof, E.K., Baker, M.S., and Bunn, C.L. (1995). Biological and clinical aspects of plasminogen activator inhibitor type 2. Blood *86*, 4007–4024.

Krüttner, S., Stepien, B., Noordermeer, J.N., Mommaas, M.A., Mechtler, K., Dickson, B.J., and Keleman, K. (2012). Drosophila CPEB Orb2A Mediates Memory Independent of Its RNA-Binding Domain. Neuron *76*, 383–395.

Lantz, V., Ambrosio, L., and Schedl, P. (1992). The Drosophila orb gene is predicted to encode sex-specific germline RNA-binding proteins and has localized transcripts in ovaries and early embryos. Development *115*, 75–88.

Lantz, V., Chang, J.S., Horabin, J.I., Bopp, D., and Schedl, P. (1994). The Drosophila orb RNA-binding protein is required for the formation of the egg chamber and establishment of polarity. Genes Dev. *8*, 598–613.

Laybourn, P.J., and Dahmus, M.E. (1989). Transcription-dependent structural changes in the C-terminal domain of mammalian RNA polymerase subunit IIa/o. J. Biol. Chem. *264*, 6693–6698.

Ledesma, M.D., Da Silva, J.S., Crassaerts, K., Delacourte, A., De Strooper, B., and Dotti, C.G. (2000). Brain plasmin enhances APP alpha-cleavage and Abeta degradation and is reduced in Alzheimer's disease brains. EMBO Rep. *1*, 530–535.

Ledesma, M.D., Abad-Rodriguez, J., Galvan, C., Biondi, E., Navarro, P., Delacourte, A., Dingwall, C., and Dotti, C.G. (2003a). Raft disorganization leads to reduced plasmin activity in Alzheimer's disease brains. EMBO Rep. *4*, 1190–1196.

Ledesma, M.D., Da Silva, J.S., Schevchenko, A., Wilm, M., and Dotti, C.G. (2003b). Proteomic characterisation of neuronal sphingolipid-cholesterol microdomains: role in plasminogen activation. Brain Res. *987*, 107–116.

Lee, H.-Y., Hwang, I.-Y., Im, H., Koh, J.-Y., and Kim, Y.-H. (2007a). Non-proteolytic neurotrophic effects of tissue plasminogen activator on cultured mouse cerebrocortical neurons. J. Neurochem. *101*, 1236–1247.

Lee, S.-R., Lok, J., Rosell, A., Kim, H.-Y., Murata, Y., Atochin, D., Huang, P.L., Wang, X., Ayata, C., Moskowitz, M.A., et al. (2007b). Reduction of hippocampal cell death and proteolytic responses in tissue plasminogen activator knockout mice after transient global cerebral ischemia. Neuroscience *150*, 50–57.

Lee, T.W., Tsang, V.W.K., and Birch, N.P. (2015). Physiological and pathological roles of tissue plasminogen activator and its inhibitor neuroserpin in the nervous system. Front. Cell. Neurosci. *9*, 396.

Lee, V.M., Balin, B.J., Otvos, L., and Trojanowski, J.Q. (1991). A68: a major subunit of paired helical filaments and derivatized forms of normal Tau. Science *251*, 675–678.

Levin, E.G., and del Zoppo, G.J. (1994). Localization of tissue plasminogen activator in the endothelium of a limited number of vessels. Am. J. Pathol. *144*, 855–861.

Lewis, J., McGowan, E., Rockwood, J., Melrose, H., Nacharaju, P., Van Slegtenhorst, M., Gwinn-Hardy, K., Paul Murphy, M., Baker, M., Yu, X., et al. (2000). Neurofibrillary tangles, amyotrophy and progressive motor disturbance in mice expressing mutant (P301L) tau protein. Nat. Genet. *25*, 402–405.

Lewis, J., Dickson, D.W., Lin, W.L., Chisholm, L., Corral, A., Jones, G., Yen, S.H., Sahara, N., Skipper, L., Yager, D., et al. (2001). Enhanced neurofibrillary degeneration in transgenic mice expressing mutant tau and APP. Science *293*, 1487–1491.

Lijnen, H.R., and Collen, D. (1991). Strategies for the improvement of thrombolytic agents. Thromb. Haemost. *66*, 88–110.

Lin, C.-L., Evans, V., Shen, S., Xing, Y., and Richter, J.D. (2010). The nuclear experience of CPEB: implications for RNA processing and translational control. RNA *16*, 338–348.

Liu, J., and Schwartz, J.H. (2003). The cytoplasmic polyadenylation element binding protein and polyadenylation of messenger RNA in Aplysia neurons. Brain Res. *959*, 68–76.

Liu, R.-M., van Groen, T., Katre, A., Cao, D., Kadisha, I., Ballinger, C., Wang, L., Carroll, S.L., and Li, L. (2011). Knockout of plasminogen activator inhibitor 1 gene reduces amyloid beta peptide burden in a mouse model of Alzheimer's disease. Neurobiol. Aging *32*, 1079–1089.

Lochner, J.E., Kingma, M., Kuhn, S., Meliza, C.D., Cutler, B., and Scalettar, B. a (1998). Real-time imaging of the axonal transport of granules containing a tissue plasminogen activator/green fluorescent protein hybrid. Mol. Biol. Cell *9*, 2463–2476.

Lochner, J.E., Honigman, L.S., Grant, W.F., Gessford, S.K., Hansen, A.B., Silverman, M.A., and Scalettar, B.A. (2006). Activity-Dependent Release of Tissue Plasminogen Activator from the Dendritic Spines of Hippocampal Neurons Revealed by Live-Cell Imaging Viral Infection of Primary Cultures. 564–577.

Lorenzo, A., and Yankner, B.A. (1994). Beta-amyloid neurotoxicity requires fibril formation and is inhibited by congo red. Proc. Natl. Acad. Sci. U. S. A. *91*, 12243–12247.

Luitjens, C., Gallegos, M., Kraemer, B., Kimble, J., and Wickens, M. (2000). CPEB proteins control two key steps in spermatogenesis in *C. elegans*. Genes Dev. *14*, 2596–2609.

Maccioni, R.B., Farías, G., Morales, I., and Navarrete, L. (2010). The revitalized tau hypothesis on Alzheimer's disease. Arch. Med. Res. *41*, 226–231.

Madani, R., Hulo, S., Toni, N., Madani, H., Steimer, T., Muller, D., and Vassalli, J.D. (1999). Enhanced hippocampal long-term potentiation and learning by increased neuronal expression of tissue-type plasminogen activator in transgenic mice. EMBO J. *18*, 3007–3012.

Mader, S., Lee, H., Pause, A., and Sonenberg, N. (1995). The translation initiation factor eIF-4E binds to a common motif shared by the translation factor eIF-4 gamma and the translational repressors 4E-binding proteins. Mol. Cell. Biol. *15*, 4990–4997.

Majumdar, A., Cesario, W.C., White-Grindley, E., Jiang, H., Ren, F., Khan, M.R., Li, L., Choi, E.M.-L., Kannan, K., Guo, F., et al. (2012). Critical role of amyloid-like oligomers of Drosophila Orb2 in the persistence of memory. Cell *148*, 515–529.

Martin, A.M., Kuhlmann, C., Trossbach, S., Jaeger, S., Waldron, E., Roebroek, A., Luhmann, H.J., Laatsch, A., Weggen, S., Lessmann, V., et al. (2008). The functional role of the second NPXY motif of the LRP1 beta-chain in tissue-type plasminogen activator-mediated activation of N-methyl-D-aspartate receptors. J. Biol. Chem. *283*, 12004–12013.

Martin, K.C., Casadio, A., Zhu, H., Yaping, E., Rose, J.C., Chen, M., Bailey, C.H., and Kandel, E.R. (1997). Synapse-specific, long-term facilitation of aplysia sensory to motor synapses: a function for local protein synthesis in memory storage. Cell *91*, 927–938.

184

Masuda, A., Kobayashi, Y., Kogo, N., Saito, T., Saido, T.C., and Itohara, S. (2016). Cognitive deficits in single App knock-in mouse models. Neurobiol. Learn. Mem. 0–5.

Mataga, N., Nagai, N., and Hensch, T.K. (2002). Permissive proteolytic activity for visual cortical plasticity. Proc. Natl. Acad. Sci. U. S. A. *99*, 7717–7721.

Matoulkova, E., Michalova, E., Vojtesek, B., and Hrstka, R. (2012). The role of the 3' untranslated region in post-transcriptional regulation of protein expression in mammalian cells. RNA Biol. *9*, 563–576.

Mayford, M., Siegelbaum, S.A., and Kandel, E.R. (2012). Synapses and memory storage. Cold Spring Harb. Perspect. Biol. *4*, 1–18.

McCracken, S., Fong, N., Yankulov, K., Ballantyne, S., Pan, G., Greenblatt, J., Patterson, S.D., Wickens, M., and Bentley, D.L. (1997a). The C-terminal domain of RNA polymerase II couples mRNA processing to transcription. Nature *385*, 357–361.

McCracken, S., Fong, N., Rosonina, E., Yankulov, K., Brothers, G., Siderovski, D., Hessel, A., Foster, S., Shuman, S., and Bentley, D.L. (1997b). 5'-Capping enzymes are targeted to pre-mRNA by binding to the phosphorylated carboxy-terminal domain of RNA polymerase II. Genes Dev. *11*, 3306–3318.

McGrew, L.L., Dworkin-Rastl, E., Dworkin, M.B., and Richter, J.D. (1989). Poly(A) elongation during Xenopus oocyte maturation is required for translational recruitment and is mediated by a short sequence element. Genes Dev. *3*, 803–815.

McKhann, G., Drachman, D., Folstein, M., and Katzman, R. (1984). views & reviews Clinical diagnosis of Alzheimer ' s disease : Neurology *34*, 939.

McLarnon, J.G., and Ryu, J.K. (2008). Relevance of abeta1-42 intrahippocampal injection as an animal model of inflamed Alzheimer's disease brain. Curr. Alzheimer Res. *5*, 475–480.

McLauchlan, J., Gaffney, D., Whitton, J.L., and Clements, J.B. (1985). The consensus sequence YGTGTTYY located downstream from the AATAAA signal is required for efficient formation of mRNA 3' termini. Nucleic Acids Res. *13*, 1347–1368.

Medina, M.G., Ledesma, M.D., Domínguez, J.E., Medina, M., Zafra, D., Alameda, F., Dotti, C.G., and Navarro, P. (2005). Tissue plasminogen activator mediates amyloid-induced neurotoxicity via Erk1/2 activation. EMBO J. *24*, 1706–1716.

Melchor, J.P., Pawlak, R., and Strickland, S. (2003). The tissue plasminogen activator-plasminogen proteolytic cascade accelerates amyloid-beta (Abeta) degradation and inhibits Abeta-induced neurodegeneration. J. Neurosci.

Mendez, R., and Richter, J.D. (2001). Translational control by CPEB: a means to the end. Nat. Rev. Mol. Cell Biol. *2*, 521–529.

Mendez, R., Hake, L.E., Andresson, T., Littlepage, L.E., Ruderman, J. V, and Richter, J.D. (2000a). Phosphorylation of CPE binding factor by Eg2 regulates translation of c-mos mRNA. Nature *404*, 302–307.

Mendez, R., Murthy, K.G., Ryan, K., Manley, J.L., and Richter, J.D. (2000b). Phosphorylation of CPEB by Eg2 mediates the recruitment of CPSF into an active cytoplasmic polyadenylation complex. Mol. Cell *6*, 1253–1259.

Mendez, R., Barnard, D., and Richter, J.D. (2002). Differential mRNA translation and meiotic progression require Cdc2-mediated CPEB destruction. EMBO J. *21*, 1833–1844.

Merkel, D.J., Wells, S.B., Hilburn, B.C., Elazzouzi, F., Pérez-Alvarado, G.C., and Lee, B.M. (2013). The C-terminal region of cytoplasmic polyadenylation element binding protein is a ZZ domain with potential for protein-protein interactions. J. Mol. Biol. *425*, 2015–2026.

Miles, L.A., Dahlberg, C.M., Levin, E.G., and Plow, E.F. (1989). Gangliosides interact directly with plasminogen and urokinase and may mediate binding of these fibrinolytic components to cells. Biochemistry *28*, 9337–9343.

Miles, L.A., Dahlberg, C.M., Plescia, J., Felez, J., Kato, K., and Plow, E.F. (1991). Role of cell-surface lysines in plasminogen binding to cells: identification of alpha-enolase as a candidate plasminogen receptor. Biochemistry *30*, 1682–1691.

Miniaci, M.C., Kim, J.-H., Puthanveettil, S. V., Si, K., Zhu, H., Kandel, E.R., and Bailey, C.H. (2008). Sustained CPEB-dependent local protein synthesis is required to stabilize synaptic growth for persistence of long-term facilitation in Aplysia. Neuron *59*, 1024–1036.

Minor, K., Phillips, J., and Seeds, N.W. (2009). Tissue plasminogen activator promotes axonal outgrowth on CNS myelin after conditioned injury. J. Neurochem. *109*, 706–715.

Minshall, N., Reiter, M.H., Weil, D., and Standart, N. (2007). CPEB interacts with an ovary-specific eIF4E and 4E-T in early Xenopus oocytes. J. Biol. Chem. *282*, 37389–37401.

Minshall, N., Kress, M., Weil, D., and Standart, N. (2009). Role of p54 RNA helicase activity and its C-terminal domain in translational repression, P-body localization and assembly. Mol. Biol. Cell *20*, 2464–2472.

Mohandas, E., Rajmohan, V., and Raghunath, B. (2009). Neurobiology of Alzheimer's disease. Indian J. Psychiatry *51*, 55–61.

Moonen, G., Grau-Wagemans, M.P., and Selak, I. (1982). Plasminogen activator-plasmin system and neuronal migration. Nature *298*, 753–755.

Moroi, M., and Aoki, N. (1976). Isolation and characterization of alpha2-plasmin inhibitor from human plasma. A novel proteinase inhibitor which inhibits activator-induced clot lysis. J. Biol. Chem. *251*, 5956–5965.

van Mourik, J.A., Lawrence, D.A., and Loskutoff, D.J. (1984). Purification of an inhibitor of plasminogen activator (antiactivator) synthesized by endothelial cells. J. Biol. Chem. *259*, 14914–14921.

Mucke, L., Masliah, E., Yu, G.Q., Mallory, M., Rockenstein, E.M., Tatsuno, G., Hu, K., Kholodenko, D., Johnson-Wood, K., and McConlogue, L. (2000). High-level neuronal expression of abeta 1-42 in wild-type human amyloid protein precursor transgenic mice: synaptotoxicity without plaque formation. J. Neurosci. *20*, 4050–4058.

Mudher, A., and Lovestone, S. (2002). Alzheimer's disease-do tauists and baptists finally shake hands? Trends Neurosci. *25*, 22–26.

Mukherjee, A., Song, E., Kihiko-Ehmann, M., Goodman, J.P., Pyrek, J.S., Estus, S., and Hersh, L.B. (2000). Insulysin hydrolyzes amyloid beta peptides to products that are neither neurotoxic nor deposit on amyloid plaques. J. Neurosci. *20*, 8745–8749.

Müllertz, S., and Clemmensen, I. (1976). The primary inhibitor of plasmin in human plasma. Biochem. J. *159*, 545–553.

Muthukrishnan, S., Both, G.W., Furuichi, Y., and Shatkin, A.J. (1975). 5'-Terminal 7-methylguanosine in eukaryotic mRNA is required for translation. Nature *255*, 33–37.

Nagaoka, K., Fujii, K., Zhang, H., Usuda, K., Watanabe, G., Ivshina, M., and Richter, J.D. (2016). CPEB1 mediates epithelial-to-mesenchyme transition and breast cancer metastasis. Oncogene *35*, 2893–2901.

Nagy, A., and Delgado-Escueta, A. V (1984). Rapid preparation of synaptosomes from mammalian brain using nontoxic isoosmotic gradient material (Percoll). J. Neurochem. *43*, 1114–1123.

Nassar, T., Akkawi, S., Shina, A., Haj-Yehia, A., Bdeir, K., Tarshis, M., Heyman, S.N., and Higazi, A.A.-R. (2004). In vitro and in vivo effects of tPA and PAI-1 on blood vessel tone. Blood *103*, 897–902.

Ng, K.-S., Leung, H.-W., Wong, P.T.-H., and Low, C.-M. (2012). Cleavage of the NR2B subunit amino terminus of N-methyl-D-aspartate (NMDA) receptor by tissue plasminogen activator: identification of the cleavage site and characterization of ifenprodil and glycine affinities on truncated NMDA receptor. J. Biol. Chem. *287*, 25520–25529.

Nicole, O., Docagne, F., Ali, C., Margaill, I., Carmeliet, P., MacKenzie, E.T., Vivien, D., and Buisson, a (2001). The proteolytic activity of tissue-plasminogen activator enhances NMDA receptor-mediated signaling. Nat. Med. *7*, 59–64.

Nicoll, R.A., and Malenka, R.C. (1995). Contrasting properties of two forms of long-term potentiation in the hippocampus. Nature *377*, 115–118.

Nordt, T.K., and Bode, C. (2003). Thrombolysis: newer thrombolytic agents and their role in clinical medicine. Heart *89*, 1358–1362.

REFERENCES

Norris, E.H., and Strickland, S. (2007). Modulation of NR2B-regulated contextual fear in the hippocampus by the tissue plasminogen activator system. Proc. Natl. Acad. Sci. U. S. A. *104*, 13473–13478.

Novoa, I., Gallego, J., Ferreira, P.G., and Mendez, R. (2010). Mitotic cell-cycle progression is regulated by CPEB1 and CPEB4-dependent translational control. Nat. Cell Biol. *12*, 447–456.

Nürenberg, E., and Tampé, R. (2013). Tying up loose ends: Ribosome recycling in eukaryotes and archaea. Trends Biochem. Sci. *38*, 64–74.

Oakley, H., Cole, S.L., Logan, S., Maus, E., Shao, P., Craft, J., Guillozet-Bongaarts, A., Ohno, M., Disterhoft, J., Van Eldik, L., et al. (2006). Intraneuronal beta-amyloid aggregates, neurodegeneration, and neuron loss in transgenic mice with five familial Alzheimer's disease mutations: potential factors in amyloid plaque formation. J. Neurosci. *26*, 10129–10140.

Obiang, P., Macrez, R., Jullienne, A., Bertrand, T., Lesept, F., Ali, C., Maubert, E., Vivien, D., and Agin, V. (2012). GluN2D subunit-containing NMDA receptors control tissue plasminogen activator-mediated spatial memory. J. Neurosci. *32*, 12726–12734.

Oddo, S., Caccamo, A., Shepherd, J.D., Murphy, M.P., Golde, T.E., Kayed, R., Metherate, R., Mattson, M.P., Akbari, Y., and LaFerla, F.M. (2003). Triple-transgenic model of Alzheimer's disease with plaques and tangles: intracellular Abeta and synaptic dysfunction. Neuron *39*, 409–421.

Oh, S.B., Byun, C.J., Yun, J.-H., Jo, D.-G., Carmeliet, P., Koh, J.-Y., and Lee, J.-Y. (2014). Tissue plasminogen activator arrests Alzheimer's disease pathogenesis. Neurobiol. Aging *35*, 511–519.

Ohno, M., Sakamoto, H., and Shimura, Y. (1987). Preferential excision of the 5' proximal intron from mRNA precursors with two introns as mediated by the cap structure. Proc. Natl. Acad. Sci. U. S. A. *84*, 5187–5191.

Ortiz-Zapater, E., Peiró, S., Roda, O., Corominas, J.M., Aguilar, S., Ampurdanés, C., Real, F.X., and Navarro, P. (2007). Tissue plasminogen activator induces pancreatic cancer cell proliferation by a non-catalytic mechanism that requires extracellular signal-regulated kinase 1/2 activation through epidermal growth factor receptor and annexin A2. Am. J. Pathol. *170*, 1573–1584.

Ortiz-Zapater, E., Pineda, D., Martínez-Bosch, N., Fernández-Miranda, G., Iglesias, M., Alameda, F., Moreno, M., Eliscovich, C., Eyras, E., Real, F.X., et al. (2011). Key contribution of CPEB4-mediated translational control to cancer progression. Nat. Med. *18*, 83–90.

Oruganty-Das, A., Ng, T., Udagawa, T., Goh, E.L.K., and Richter, J.D. (2012). Translational control of mitochondrial energy production mediates neuron morphogenesis. Cell Metab. *16*, 789–800.

Ouyang, Y., Kantor, D., Harris, K.M., Schuman, E.M., and Kennedy, M.B. (1997). Visualization of the distribution of autophosphorylated calcium/calmodulin-dependent protein kinase II after tetanic stimulation in the CA1 area of the hippocampus. J. Neurosci. *17*, 5416–5427.

Paciucci, R., Torà, M., Díaz, V.M., and Real, F.X. (1998). The plasminogen activator system in pancreas cancer: role of t-PA in the invasive potential in vitro. Oncogene *16*, 625–633.

Pang, P.T., Teng, H.K., Zaitsev, E., Woo, N.T., Sakata, K., Zhen, S., Teng, K.K., Yung, W.-H., Hempstead, B.L., and Lu, B. (2004). Cleavage of proBDNF by tPA/plasmin is essential for long-term hippocampal plasticity. Science *306*, 487–491.

Paris, J., Osborne, H.B., Couturier, A., Le Guellec, R., and Philippe, M. (1988). Changes in the polyadenylation of specific stable RNA during the early development of Xenopus laevis. Gene *72*, 169–176.

Parkkinen, J., and Rauvala, H. (1991). Interactions of plasminogen and tissue plasminogen activator (t-PA) with amphoterin. Enhancement of t-PA-catalyzed plasminogen activation by amphoterin. J. Biol. Chem. *266*, 16730–16735.

Parmar, P.K., Coates, L.C., Pearson, J.F., Hill, R.M., and Birch, N.P. (2002). Neuroserpin regulates neurite outgrowth in nerve growth factor-treated PC12 cells. J. Neurochem. *82*, 1406–1415.

Pavlopoulos, E., Trifilieff, P., Chevaleyre, V., Fioriti, L., Zairis, S., Pagano, A., Malleret, G., and Kandel, E.R. (2011). Neuralized1 activates CPEB3: a function for nonproteolytic ubiquitin in synaptic plasticity and memory storage. Cell *147*, 1369–1383.

Pawlak, R., Nagai, N., Urano, T., Napiorkowska-Pawlak, D., Ihara, H., Takada, Y., Collen, D., and Takada, A. (2002). Rapid, specific and active site-catalyzed effect of tissue-plasminogen activator on hippocampus-dependent learning in mice. Neuroscience *113*, 995–1001.

Pawlak, R., Magarinos, A.M., Melchor, J., McEwen, B., and Strickland, S. (2003). Tissue plasminogen activator in the amygdala is critical for stress-induced anxiety-like behavior. Nat. Neurosci. *6*, 168–174.

Pawlak, R., Melchor, J.P., Matys, T., Skrzypiec, A.E., and Strickland, S. (2005). Ethanol-withdrawal seizures are controlled by tissue plasminogen activator via modulation of NR2B-containing NMDA receptors. Proc. Natl. Acad. Sci. U. S. A. *102*, 443–448.

Pennica, D., Holmes, W.E., Kohr, W.J., Harkins, R.N., Vehar, G.A., Ward, C.A., Bennett, W.F., Yelverton, E., Seeburg, P.H., Heyneker, H.L., et al. (1983). Cloning and expression of human tissue-type plasminogen activator cDNA in E. coli. Nature *301*, 214–221.

Pestova, T. V, Kolupaeva, V.G., Lomakin, I.B., Pilipenko, E. V, Shatsky, I.N., Agol, V.I., and Hellen, C.U. (2001). Molecular mechanisms of translation initiation in eukaryotes. Proc. Natl. Acad. Sci. U. S. A. *98*, 7029–7036.

Petersen, P.H., Zou, K., Hwang, J.K., Jan, Y.N., and Zhong, W. (2002). Progenitor cell maintenance requires numb and numblike during mouse neurogenesis. Nature *419*, 929–934.

Phatnani, H.P., and Greenleaf, A.L. (2006). Phosphorylation and functions of the RNA polymerase II CTD. Genes Dev. *20*, 2922–2936.

Pillon, B., Deweer, B., Agid, Y., and Dubois, B. (1993). Explicit memory in Alzheimer's, Huntington's, and Parkinson's diseases. Arch. Neurol. *50*, 374–379.

Pineda, D., Ampurdanés, C., Medina, M.G., Serratosa, J., Tusell, J.M., Saura, J., Planas, A.M., and Navarro, P. (2012). Tissue plasminogen activator induces microglial inflammation via a noncatalytic molecular mechanism involving activation of mitogen-activated protein kinases and Akt signaling pathways and AnnexinA2 and Galectin-1 receptors. Glia *60*, 526–540.

Piqué, M., López, J.M., and Méndez, R. (2006). Cytoplasmic mRNA polyadenylation and translation assays. Methods Mol. Biol. *322*, 183–198.

Piqué, M., López, J.M., Foissac, S., Guigó, R., and Méndez, R. (2008). A combinatorial code for CPE-mediated translational control. Cell *132*, 434–448.

Pittman, R.N., and DiBenedetto, A.J. (1995). PC12 cells overexpressing tissue plasminogen activator regenerate neurites to a greater extent and migrate faster than control cells in complex extracellular matrix. J. Neurochem. *64*, 566–575.

Plow, E.F., Herren, T., Redlitz, A., Miles, L.A., and Hoover-Plow, J.L. (1995). The cell biology of the plasminogen system. FASEB J. *9*, 939–945.

Polavarapu, R., Gongora, M.C., Yi, H., Ranganthan, S., Lawrence, D.A., Strickland, D., and Yepes, M. (2007). Tissue-type plasminogen activator-mediated shedding of astrocytic low-density lipoprotein receptor-related protein increases the permeability of the neurovascular unit. Blood *109*, 3270–3278.

Price, B.H., Gurvit, H., Weintraub, S., Geula, C., Leimkuhler, E., and Mesulam, M. (1993). Neuropsychological patterns and language deficits in 20 consecutive cases of autopsy-confirmed Alzheimer's disease. Arch. Neurol. *50*, 931–937.

Proudfoot, N.J., and Brownlee, G.G. (1976). 3' non-coding region sequences in eukaryotic messenger RNA. Nature *263*, 211–214.

Qian, Z., Gilbert, M.E., Colicos, M.A., Kandel, E.R., and Kuhl, D. (1993). Tissue-plasminogen activator is induced as an immediate-early gene during seizure, kindling and long-term potentiation. Nature *361*, 453–457.

Radde, R., Duma, C., Goedert, M., and Jucker, M. (2008). The value of incomplete mouse models of Alzheimer's disease. Eur. J. Nucl. Med. Mol. Imaging *35 Suppl 1*, S70–S74.

Rasmussen, E.B., and Lis, J.T. (1993). In vivo transcriptional pausing and cap formation on three Drosophila heat shock genes. Proc. Natl. Acad. Sci. U. S. A. *90*, 7923–7927.

Raveendra, B.L., Siemer, A.B., Puthanveettil, S. V, Hendrickson, W.A., Kandel, E.R., and McDermott, A.E. (2013). Characterization of prion-like conformational changes of the neuronal isoform of Aplysia CPEB. Nat. Struct. Mol. Biol. *20*, 495–501.

Raymond, C.S., and Soriano, P. (2007). High-efficiency FLP and PhiC31 site-specific recombination in mammalian cells. PLoS One *2*, e162.

Reverte, C.G., Ahearn, M.D., and Hake, L.E. (2001). CPEB degradation during Xenopus oocyte maturation requires a PEST domain and the 26S proteasome. Dev. Biol. *231*, 447–458.

Rhoads, R.E. (1988). Cap recognition and the entry of mRNA into the protein synthesis initiation cycle. Trends Biochem. Sci. *13*, 52–56.

Richter, J.D., and Coller, J. (2015). Pausing on Polyribosomes: Make Way for Elongation in Translational Control. Cell *163*, 292–300.

Richter, J.D., and Klann, E. (2009). Making synaptic plasticity and memory last: mechanisms of translational regulation. Genes Dev. *23*, 1–11.

Riedel, B.C., Thompson, P.M., and Brinton, R.D. (2016). Age, APOE and sex: Triad of risk of Alzheimer's disease. J. Steroid Biochem. Mol. Biol. *160*, 134–147.

Roda, O., Ortiz-Zapater, E., Martínez-Bosch, N., Gutiérrez-Gallego, R., Vila-Perelló, M., Ampurdanés, C., Gabius, H.-J., André, S., Andreu, D., Real, F.X., et al. (2009). Galectin-1 is a novel functional receptor for tissue plasminogen activator in pancreatic cancer. Gastroenterology *136*, 1379–1390, e1–e5.

Rodier, M., Prigent-Tessier, A., Béjot, Y., Jacquin, A., Mossiat, C., Marie, C., and Garnier, P. (2014). Exogenous t-PA administration increases hippocampal mature BDNF levels. plasmin- or NMDA-dependent mechanism? PLoS One *9*, e92416.

Rodríguez, C.I., Buchholz, F., Galloway, J., Sequerra, R., Kasper, J., Ayala, R., Stewart, A.F., and Dymecki, S.M. (2000). High-efficiency deleter mice show that FLPe is an alternative to Cre-loxP. Nat. Genet. *25*, 139–140.

Rogers, S., Wells, R., and Rechsteiner, M. (1986). Amino acid sequences common to rapidly degraded proteins: the PEST hypothesis. Science *234*, 364–368.

Rogove, a D., Siao, C., Keyt, B., Strickland, S., and Tsirka, S.E. (1999). Activation of microglia reveals a non-proteolytic cytokine function for tissue plasminogen activator in the central nervous system. J. Cell Sci. *112 (Pt 2*, 4007–4016.

Rosenberg, G.A., Navratil, M., Barone, F., and Feuerstein, G. (1996). Proteolytic cascade enzymes increase in focal cerebral ischemia in rat. J. Cereb. Blood Flow Metab. *16*, 360–366.

Ross, J. (1995). mRNA stability in mammalian cells. Microbiol. Rev. *59*, 423–450.

Roth, S., and Schüpbach, T. (1994). The relationship between ovarian and embryonic dorsoventral patterning in Drosophila. Development *120*, 2245–2257.

Sachs, A. (1990). The role of poly(A) in the translation and stability of mRNA. Curr. Opin. Cell Biol. *2*, 1092–1098.

Sacktor, T.C. (2012). Memory maintenance by PKMζ--an evolutionary perspective. Mol. Brain *5*, 31.

Saito, T., Matsuba, Y., Mihira, N., Takano, J., Nilsson, P., Itohara, S., Iwata, N., and Saido, T.C. (2014). Single App knock-in mouse models of Alzheimer's disease. Nat. Neurosci. *17*, 661–663.

Salles, F.J., and Strickland, S. (2002a). Localization and regulation of the tissue plasminogen activator-plasmin system in the hippocampus. J. Neurosci.

Salles, F.J., and Strickland, S. (2002b). Localization and regulation of the tissue plasminogen activator-plasmin system in the hippocampus. J. Neurosci. *22*, 2125–2134.

Samson, A.L., and Medcalf, R.L. (2006). Tissue-Type Plasminogen Activator: A Multifaceted Modulator of Neurotransmission and Synaptic Plasticity. Neuron.

Samson, A.L., Nevin, S.T., Croucher, D., Niego, B., Daniel, P.B., Weiss, T.W., Moreno, E., Monard, D., Lawrence, D.A., and Medcalf, R.L. (2008). Tissue-type plasminogen activator requires a co-receptor to enhance NMDA receptor function. J. Neurochem. *107*, 1091–1101.

Sandberg, R., Neilson, J.R., Sarma, A., Sharp, P. a, and Burge, C.B. (2008). Proliferating cells express mRNAs with shortened 3 UTRs and fewer microRNA target sites. Science (80-.). *320*, 1643–1647.

Santacruz, K., Lewis, J., Spires, T., Paulson, J., Kotilinek, L., Ingelsson, M., Guimaraes, A., DeTure, M., Ramsden, M., McGowan, E., et al. (2005). Tau suppression in a neurodegenerative mouse model improves memory function. Science *309*, 476–481.

Santoro, M.R., Bray, S.M., and Warren, S.T. (2012). Molecular mechanisms of fragile X syndrome: a twenty-year perspective. Annu. Rev. Pathol. *7*, 219–245.

Sappino, A.P., Madani, R., Huarte, J., Belin, D., Kiss, J.Z., Wohlwend, A., and Vassalli, J.D. (1993). Extracellular proteolysis in the adult murine brain. J. Clin. Invest. *92*, 679–685.

Sashindranath, M., Sales, E., Daglas, M., Freeman, R., Samson, A.L., Cops, E.J., Beckham, S., Galle, A., McLean, C., Morganti-Kossmann, C., et al. (2012). The tissue-type plasminogen activator-plasminogen activator inhibitor 1 complex promotes neurovascular injury in brain trauma: evidence from mice and humans. Brain *135*, 3251–3264.

Scherzinger, E., Lurz, R., Turmaine, M., Mangiarini, L., Hollenbach, B., Hasenbank, R., Bates, G.P., Davies, S.W., Lehrach, H., and Wanker, E.E. (1997). Huntingtin-encoded polyglutamine expansions form amyloid-like protein aggregates in vitro and in vivo. Cell *90*, 549–558.

Schmidt, E., Wehr, B., Tabengwa, E.M., Reimer, S., Bröcker, E.-B., and Zillikens, D. (2004). Elevated expression and release of tissue-type, but not urokinase-type, plasminogen activator after binding of autoantibodies to bullous pemphigoid antigen 180 in cultured human keratinocytes. Clin. Exp. Immunol. *135*, 497–504.

Schubert, V., Da Silva, J.S., and Dotti, C.G. (2006). Localized recruitment and activation of RhoA underlies dendritic spine morphology in a glutamate receptor-dependent manner. J. Cell Biol. *172*, 453–467.

Seeds, N.W., Williams, B.L., and Bickford, P.C. (1995). Tissue plasminogen activator induction in Purkinje neurons after cerebellar motor learning. Science *270*, 1992–1994.

Selkoe, D.J. (2002). Alzheimer's disease is a synaptic failure. Science *298*, 789–791.

Serrano-Pozo, A., Frosch, M.P., Masliah, E., and Hyman, B.T. (2011). Neuropathological alterations in Alzheimer disease. Cold Spring Harb. Perspect. Med. *1*, a006189.

Setoyama, D., Yamashita, M., and Sagata, N. (2007). Mechanism of degradation of CPEB during Xenopus oocyte maturation. Proc. Natl. Acad. Sci. *104*, 18001–18006.

Shatkin, A.J. (1985). mRNA cap binding proteins: essential factors for initiating translation. Cell *40*, 223–224.

Shea, T.B., and Beermann, M. Lou (1992). Regulation of neuronal migration and neuritogenesis by distinct surface proteases Relative contribution of plasmin and a thrombin-like protease. FEBS Lett. *307*, 190–194.

Sheets, M.D., Fox, C.A., Hunt, T., Vande Woude, G., and Wickens, M. (1994). The 3'-untranslated regions of c-mos and cyclin mRNAs stimulate translation by regulating cytoplasmic polyadenylation. Genes Dev. *8*, 926–938.

Shepherd, J.D., and Huganir, R.L. (2007). The cell biology of synaptic plasticity: AMPA receptor trafficking. Annu. Rev. Cell Dev. Biol. *23*, 613–643.

Shi, Y., Mantuano, E., Inoue, G., Campana, W.M., and Gonias, S.L. (2009). Ligand binding to LRP1 transactivates Trk receptors by a Src family kinase-dependent pathway. Sci. Signal. *2*, ra18.

Shimotohno, K., Kodama, Y., Hashimoto, J., and Miura, K.I. (1977). Importance of 5'-terminal blocking structure to stabilize mRNA in eukaryotic protein synthesis. Proc. Natl. Acad. Sci. U. S. A. *74*, 2734–2738.

Shin, C.Y., Kundel, M., and Wells, D.G. (2004). Rapid, activity-induced increase in tissue plasminogen activator is mediated by metabotropic glutamate receptor-dependent mRNA translation. J. Neurosci. *24*, 9425–9433.

Shin, J., Salameh, J.S., and Richter, J.D. (2016). Impaired neurodevelopment by the low complexity domain of CPEB4 reveals a convergent pathway with neurodegeneration. Sci. Rep. *6*, 29395.

Shuman, S. (1995). Capping enzyme in eukaryotic mRNA synthesis. Prog. Nucleic Acid Res. Mol. Biol. *50*, 101–129.

Si, K., Lindquist, S., and Kandel, E.R. (2003a). A neuronal isoform of the aplysia CPEB has prion-like properties. Cell *115*, 879–891.

Si, K., Giustetto, M., Etkin, A., Hsu, R., Janisiewicz, A.M., Miniaci, M.C., Kim, J.-H., Zhu, H., and Kandel, E.R. (2003b). A neuronal isoform of CPEB regulates local protein synthesis and stabilizes synapse-specific long-term facilitation in aplysia. Cell *115*, 893–904.

Si, K., Choi, Y.B., White-Grindley, E., Majumdar, A., and Kandel, E.R. (2010). Aplysia CPEB Can Form Prion-like Multimers in Sensory Neurons that Contribute to Long-Term Facilitation. Cell *140*, 421–435.

Siao, C.-J., and Tsirka, S.E. (2002). Tissue plasminogen activator mediates microglial activation via its finger domain through annexin II. J. Neurosci. *22*, 3352–3358.

Siconolfi, L.B., and Seeds, N.W. (2001). Induction of the plasminogen activator system accompanies peripheral nerve regeneration after sciatic nerve crush. J. Neurosci. *21*, 4336–4347.

Sidenius, N., Nebuloni, M., Sala, S., Zerbi, P., Price, R.W., Gisslen, M., Hagberg, L., Vago, L., Lazzarin, A., Blasi, F., et al. (2004). Expression of the urokinase plasminogen activator and its receptor in HIV-1-associated central nervous system disease. J. Neuroimmunol. *157*, 133–139.

Simon, P., Schott, K., Williams, R.W., and Schaeffel, F. (2004). Posttranscriptional regulation of the immediate-early gene EGR1 by light in the mouse retina. Eur. J. Neurosci. *20*, 3371–3377.

Skubal, M., Gielen, G.H., Waha, A., Gessi, M., Seifert, G., Freihoff, D., Freihoff, J., Simon, M., Theis, M., Steinhäuser, C., et al. (2016). Altered splicing leads to reduced activation of CPEB3 in high-grade gliomas.

Small, D.H., Mok, S.S., and Bornstein, J.C. (2001). Alzheimer ' s disease and A β toxicity : from top to bottom. Nat. Rev. Neurosci. *2*, 595–598.

Spence, J., Gali, R.R., Dittmar, G., Sherman, F., Karin, M., and Finley, D. (2000). Cell cycle-regulated modification of the ribosome by a variant multiubiquitin chain. Cell *102*, 67–76.

Squire, L.R., and Zola-Morgan, S. (1991). The medial temporal lobe memory system. Science *253*, 1380–1386.

St Clair, D., Rennie, M., Slorach, E., Norrman, J., Yates, C., and Carothers, A. (1995). Apolipoprotein E epsilon 4 allele is a risk factor for familial and sporadic presenile Alzheimer's disease in both homozygote and heterozygote carriers. J. Med. Genet. *32*, 642–644.

Stebbins-Boaz, B., Cao, Q., de Moor, C.H., Mendez, R., and Richter, J.D. (1999). Maskin is a CPEB-associated factor that transiently interacts with elF-4E. Mol. Cell *4*, 1017–1027.

Stephan, J.S., Fioriti, L., Lamba, N., Colnaghi, L., Karl, K., Derkatch, I.L., and Kandel, E.R. (2015). The CPEB3 Protein Is a Functional Prion that Interacts with the Actin Cytoskeleton. Cell Rep. 1–14.

Steward, O., and Levy, W.B. (1982). Preferential localization of polyribosomes under the base of dendritic spines in granule cells of the dentate gyrus. J. Neurosci. *2*, 284–291.

De Strooper, B., Vassar, R., and Golde, T. (2010). The secretases: enzymes with therapeutic potential in Alzheimer disease. Nat. Rev. Neurol. *6*, 99–107.

Sturchler-Pierrat, C., Abramowski, D., Duke, M., Wiederhold, K.H., Mistl, C., Rothacher, S., Ledermann, B., Bürki, K., Frey, P., Paganetti, P.A., et al. (1997). Two amyloid precursor protein transgenic mouse models with Alzheimer disease-like pathology. Proc. Natl. Acad. Sci. U. S. A. *94*, 13287–13292.

Sutton, M.A., and Schuman, E.M. (2006). Dendritic protein synthesis, synaptic plasticity, and memory. Cell *127*, 49–58.

Swan, A., and Schüpbach, T. (2007). The Cdc20 (Fzy)/Cdh1-related protein, Cort, cooperates with Fzy in cyclin destruction and anaphase progression in meiosis I and II in Drosophila. Development *134*, 891–899.

Swanger, S.A., He, Y.A., Richter, J.D., and Bassell, G.J. (2013). Dendritic GluN2A synthesis mediates activity-induced NMDA receptor insertion. J. Neurosci. *33*, 8898–8908.

Takagaki, Y., Seipelt, R.L., Peterson, M.L., and Manley, J.L. (1996). The polyadenylation factor CstF-64 regulates alternative processing of IgM heavy chain pre-mRNA during B cell differentiation. Cell *87*, 941–952.

Tarun, S.Z., Wells, S.E., Deardorff, J.A., and Sachs, A.B. (1997). Translation initiation factor eIF4G mediates in vitro poly(A) tail-dependent translation. Proc. Natl. Acad. Sci. U. S. A. *94*, 9046–9051.

Tay, J., and Richter, J.D. (2001). Germ cell differentiation and synaptonemal complex formation are disrupted in CPEB knockout mice. Dev. Cell *1*, 201–213.

Tay, J., Hodgman, R., Sarkissian, M., and Richter, J.D. (2003). Regulated CPEB phosphorylation during meiotic progression suggests a mechanism for temporal control of maternal mRNA translation. Genes Dev. *17*, 1457–1462.

Teesalu, T., Kulla, A., Simisker, A., Sirén, V., Lawrence, D.A., Asser, T., and Vaheri, A. (2004). Tissue plasminogen activator and neuroserpin are widely expressed in the human central nervous system. Thromb. Haemost. *92*, 358–368.

The National Institute of Neurological Disorders and Stroke rt-PA Stroke Study Group (1995). Tissue plasminogen activator for acute ischemic stroke. The National Institute of Neurological Disorders and Stroke rt-PA Stroke Study Group. N. Engl. J. Med. *333*, 1581–1587.

Theis, M., Si, K., and Kandel, E.R. (2003). Two previously undescribed members of the mouse CPEB family of genes and their inducible expression in the principal cell layers of the hippocampus. Proc. Natl. Acad. Sci. U. S. A. *100*, 9602–9607.

Torre, E.R., and Steward, O. (1992). Demonstration of local protein synthesis within dendrites using a new cell culture system that permits the isolation of living axons and dendrites from their cell bodies. J. Neurosci. *12*, 762–772.

Tsai, L.-Y., Chang, Y.-W., Lin, P.-Y., Chou, H.-J., Liu, T.-J., Lee, P.-T., Huang, W.-H., Tsou, Y.-L., and Huang, Y.-S. (2013). CPEB4 knockout mice exhibit normal hippocampus-related synaptic plasticity and memory. PLoS One *8*, e84978.

Tsirka, S.E., Gualandris, A., Amaral, D.G., and Strickland, S. (1995). Excitotoxin-induced neuronal degeneration and seizure are mediated by tissue plasminogen activator. Nature *377*, 340–344.

Tsirka, S.E., Rogove, A.D., Bugge, T.H., Degen, J.L., and Strickland, S. (1997). An extracellular proteolytic cascade promotes neuronal degeneration in the mouse hippocampus. J. Neurosci. *17*, 543–552.

Tsukuda, K., Mogi, M., Iwanami, J., Min, L.-J., Sakata, A., Jing, F., Iwai, M., and Horiuchi, M. (2009). Cognitive deficit in amyloid-beta-injected mice was improved by pretreatment with a low dose of telmisartan partly because of peroxisome proliferator-activated receptor-gamma activation. Hypertens. (Dallas, Tex. 1979) *54*, 782–787.

Tucker, H.M., Kihiko, M., Caldwell, J.N., Wright, S., Kawarabayashi, T., Price, D., Walker, D., Scheff, S., McGillis, J.P., Rydel, R.E., et al. (2000a). The plasmin system is induced by and degrades amyloid-beta aggregates. J. Neurosci. *20*, 3937–3946.

Tucker, H.M., Kihiko, M., Caldwell, J.N., Wright, S., Kawarabayashi, T., Price, D., Walker, D., Scheff, S., McGillis, J.P., Rydel, R.E., et al. (2000b). The plasmin system is induced by and degrades amyloid-beta aggregates. J. Neurosci. *20*, 3937–3946.

Turimella, S.L., Bedner, P., Skubal, M., Vangoor, V.R., Kaczmarczyk, L., Karl, K., Zoidl, G., Gieselmann, V., Seifert, G., Steinhäuser, C., et al. (2015). Characterization of cytoplasmic polyadenylation element binding 2 protein expression and its RNA binding activity. Hippocampus *25*, 630–642.

Uchida, N., Hoshino, S. ichi, Imataka, H., Sonenberg, N., and Katada, T. (2002). A novel role of the mammalian GSPT/eRF3 associating with poly(A)-binding protein in cap/poly(A)-dependent translation. J. Biol. Chem. *277*, 50286–50292.

Udagawa, T., Swanger, S.A., Takeuchi, K., Kim, J.H., Nalavadi, V., Shin, J., Lorenz, L.J., Zukin, R.S., Bassell, G.J., and Richter, J.D. (2012). Bidirectional control of mRNA translation and synaptic plasticity by the cytoplasmic polyadenylation complex. Mol. Cell *47*, 253–266.

Udagawa, T., Farny, N.G., Jakovcevski, M., Kaphzan, H., Alarcon, J.M., Anilkumar, S., Ivshina, M., Hurt, J.A., Nagaoka, K., Nalavadi, V.C., et al. (2013). Genetic and acute CPEB1 depletion ameliorate fragile X pathophysiology. Nat. Med. *19*, 1473–1477.

Vassalli, J.D., Huarte, J., Belin, D., Gubler, P., Vassalli, A., O'Connell, M.L., Parton, L.A., Rickles, R.J., and Strickland, S. (1989). Regulated polyadenylation controls mRNA translation during meiotic maturation of mouse oocytes. Genes Dev. *3*, 2163–2171.

Walker, D.G., Lue, L.-F., and Beach, T.G. (2002). Increased expression of the urokinase plasminogen-activator receptor in amyloid beta peptide-treated human brain microglia and in AD brains. Brain Res. *926*, 69–79.

Wang, C.-F., and Huang, Y.-S. (2012). Calpain 2 activated through N-methyl-D-aspartic acid receptor signaling cleaves CPEB3 and abrogates CPEB3-repressed translation in neurons. Mol. Cell. Biol. *32*, 3321–3332.

Wang, X., Lee, S.-R., Arai, K., Lee, S.-R., Tsuji, K., Rebeck, G.W., and Lo, E.H. (2003). Lipoprotein receptor-mediated induction of matrix metalloproteinase by tissue plasminogen activator. Nat. Med. *9*, 1313–1317.

Wang, Y.F., Tsirka, S.E., Strickland, S., Stieg, P.E., Soriano, S.G., and Lipton, S.A. (1998). Tissue plasminogen activator (tPA) increases neuronal damage after focal cerebral ischemia in wild-type and tPA-deficient mice. Nat. Med. *4*, 228–231.

Wells, S.E., Hillner, P.E., Vale, R.D., and Sachs, A.B. (1998). Circularization of mRNA by eukaryotic translation initiation factors. Mol. Cell *2*, 135–140.

Wingo, T.S., Lah, J.J., Levey, A.I., and Cutler, D.J. (2012). Autosomal recessive causes likely in early-onset Alzheimer disease. Arch. Neurol. *69*, 59–64.

Winkler, F., Kastenbauer, S., Koedel, U., and Pfister, H.W. (2002). Role of the urokinase plasminogen activator system in patients with bacterial meningitis. Neurology *59*, 1350–1355.

Wogulis, M., Wright, S., Cunningham, D., Chilcote, T., Powell, K., and Rydel, R.E. (2005). Nucleation-dependent polymerization is an essential component of amyloid-mediated neuronal cell death. J. Neurosci. *25*, 1071–1080.

Wu, F., Torre, E., Cuellar-Giraldo, D., Cheng, L., Yi, H., Bichler, E.K., García, P.S., and Yepes, M. (2015). Tissue-type plasminogen activator triggers the synaptic vesicle cycle in cerebral cortical neurons. J. Cereb. Blood Flow Metab. *35*, 1966–1976.

Wu, L., Wells, D., Tay, J., Mendis, D., Abbott, M.A., Barnitt, A., Quinlan, E., Heynen, A., Fallon, J.R., and Richter, J.D. (1998). CPEB-mediated cytoplasmic polyadenylation and the regulation of experience-dependent translation of alpha-CaMKII mRNA at synapses. Neuron *21*, 1129–1139.

Wu, Y.P., Siao, C.J., Lu, W., Sung, T.C., Frohman, M.A., Milev, P., Bugge, T.H., Degen, J.L., Levine, J.M., Margolis, R.U., et al. (2000). The tissue plasminogen activator (tPA)/plasmin extracellular proteolytic system regulates seizure-induced hippocampal mossy fiber outgrowth through a proteoglycan substrate. J. Cell Biol. *148*, 1295–1304.

Yepes, M., Sandkvist, M., Moore, E.G., Bugge, T.H., Strickland, D.K., and Lawrence, D.A. (2003). Tissue-type plasminogen activator induces opening of the blood-brain barrier via the LDL receptor-related protein. J. Clin. Invest. *112*, 1533–1540.

Zearfoss, N.R., Alarcon, J.M., Trifilieff, P., Kandel, E., and Richter, J.D. (2008). A molecular circuit composed of CPEB-1 and c-Jun controls growth hormone-mediated synaptic plasticity in the mouse hippocampus. J. Neurosci. *28*, 8502–8509.

Zhang, C., An, J., Strickland, D.K., and Yepes, M. (2009). The low-density lipoprotein receptor-related protein 1 mediates tissue-type plasminogen activator-induced microglial activation in the ischemic brain. Am. J. Pathol. *174*, 586–594.

Zimmerman, L., Parr, B., Lendahl, U., Cunningham, M., McKay, R., Gavin, B., Mann, J., Vassileva, G., and McMahon, a (1994). Independent regulatory elements in the nestin gene direct transgene expression to neural stem cells or muscle precursors [published erratum appears in Neuron 1994 Jun;12(6):following 1388]. Neuron *12*, 11–24.

Zou, T., Ling, C., Xiao, Y., Tao, X., Ma, D., Chen, Z.-L., Strickland, S., and Song, H. (2006). Exogenous tissue plasminogen activator enhances peripheral nerve regeneration and functional recovery after injury in mice. J. Neuropathol. Exp. Neurol. *65*, 78–86.